Studies on the structural basis of NCAM functions and on the role of (poly)sialyltransferases and their biosynthetic products in onco- and neurodevelopment

Von der Naturwissenschaftlichen Fakultät

der Gottfried Wilhelm Leibniz Universität Hannover

zur Erlangung des Grades

Doktorin der Naturwissenschaften

Dr. rer. nat.

genehmigte Dissertation

von

Dipl.-Biochem. Katinka Caroline Eggers

geboren am 21.10.1982 in Tübingen

2011

Erklärung zur Dissertation

Hierdurch erkläre ich, dass ich die Dissertation „Studies on the structural basis of NCAM functions and on the role of (poly)sialyltransferases and their biosynthetic products in onco- and neurodevelopment" selbständig verfasst und alle benutzten Hilfmittel sowie evtll. zur Hilfeleistung herangezogene Institutionen vollständig angegeben habe.

Die Dissertation wurde nicht schon als Diplom- oder ähnliche Prüfungsarbeit verwendet.

Hannover, den 15.12.2010

Table of Contents

Zusammenfassung

Ein Charakteristikum der Säugetierzelle ist die Glykokalyx, eine über Proteine und Lipide der Zellmembran verankerte Kohlenhydratschicht, die die Zelle nach außen begrenzt. Als Sialinsäure wird ein aus neun C-Atomen bestehender saurer Zucker bezeichnet, der sich ausschließlich in terminalen (d.h. den nicht reduzierenden) Positionen von Glykokonjugaten befindet. Sialinsäuren sind im Wesentlichen für die negative Ladung der Zelloberfläche verantwortlich und sind entsprechend ihrer exponierten Position entscheidende Kommunikationselemente. Die Embryonalentwicklung der Vertebraten ist essentiell an die Anwesenheit der Sialinsäure (Sia) gebunden. Inaktivierung des Schlüsselenzyms der Sialinsäurebiosynthese führt in der Maus zu embryonaler Letalität. Darüber hinaus hat in der jüngsten Zeit das Auffinden von Mutationen in Enzymen entlang des zellulären Sialylierungsweges im Zusammenhang mit Erbkrankheiten dazu beigetragen die hohe Relevanz dieser Modifikation auch im Menschen zu bestätigen. Weiterhin wurde gezeigt, dass Sia als Bestandteile von Gangliosiden und in polymerer Form (Polysialinsäure; polySia) entscheidend an der Entwicklung und Funktion des Gehirns beteiligt ist.

Der Hauptakzeptor für die PolySia ist das Neurale Zelladhäsionsmolekül (NCAM). Der Transfer der PolySia auf NCAM wird durch zwei Polysialyltransferasen, ST8SiaII und ST8SiaIV, katalysiert. Die hohe Selektivität der Erkennung des NCAMs durch die Polysialyltransferasen ist ein unverstandener Prozess. Eine bedeutende Hürde ist dabei das Fehlen funktioneller rekombinanter Proteine zur Verwendung in einem *in vitro* Testsystem. Beim Versuch ein robustes Expressionssystem für die Herstellung der Interaktionspartner aufzubauen, musste der Tatsache Rechung getragen werden, dass sowohl die Polysialyltransferasen wie auch das NCAM Glykoproteine sind und die Glykosylierung für die Funktion der Proteine von Bedeutung ist. Daher wurde ein Insektenzellsystem für die Herstellung der rekombinanten Proteine aufgebaut. Auf diese Weise wurden funktionelle lösliche Formen beider Proteine hergestellt und begleitet durch funktionelle Testsysteme in sukzessiven Schritten weiter verkürzt bzw. in minimal glykosylierte Formen überführt. Zusätzlich wurde eine Reihe von NCAM-Fragmenten hergestellt, die zur Aufklärung der Beiträge der einzelnen NCAM-Domänen zur Funktion des Moleküls genutzt werden konnten. Alle rekombinanten Proteine konnten mit guter Ausbeute und in hoher Reinheit hergestellt werden und ermöglichen so die Durchführung erster Struktur-Funktionsstudien. Über analytische Ultrazentrifugation konnte gezeigt werden, dass die Ektodomäne des NCAM in Lösung dimerisiert und diese Interaktion im wesentlichen über die Immunglobulin-ähnlichen Domänen 1 und 2 vermittelt ist. Die Anwesenheit der Fibronektin III-ähnlichen Domäne 2 verstärkt die Dimerbildung. Auf dem gleichen Wege durchgeführte

Analysen zur Komplexbildung zwischen NCAM und der Polysialyltransferase ST8SiaII waren bislang nicht aussagekräftig. Da die hergestellten rekombinanten Proteine in Menge und Reinheit jedoch ausreichend waren, konnte zur Beantwortung dieses Fragenkomplexes mit Kristallisationsstudien begonnen werden. Wenngleich auswertbare Kristalle im Rahmen dieser Studie nicht erreicht wurden, so war es doch möglich erste Bedingungen zu finden, die die Ko-Kristallisation der beiden Interaktionspartner erlauben und eine gute Grundlage für zukünftige Studien bilden.

In einer zweiten Studie (Kapitel 3) wurden die hergestellten NCAM-Fragmente eingesetzt, um Einzelbeiträge von NCAM-Domänen und PolySia in der Tumorzellmigration und –adhäsion zu untersuchen. Es konnte gezeigt werden, dass die NCAM-induzierte Stimulierung fokaler Adhäsion die Anwesenheit eines heterophilen, bislang nicht beschriebenen NCAM-Rezeptors voraussetzt jedoch unabhängig von einer FGF-Rezeptor-Aktivierung und ERK 1/2-Phosphorylierung abläuft. Durch Nutzung der NCAM-Fragmente konnte die für die Interaktion mit dem Rezeptor notwendige NCAM-Region auf die Immunglobulin-ähnlichen Domänen 3 und/oder 4 festgelegt werden. Diese Ergebnisse erbringen neue Einsichten in die Funktion von polySia-NCAM und liefern neue Ansatzpunkte für Entwicklung neuer Konzepte für die Krebstherapie.

Obwohl NCAM das Hauptträgermolekül der Polysialinsäure ist, wurde in NCAM-negativen Mäusen ~5% verbleibende Polysialinsäure gefunden. In einem glykoproteomischen Ansatz wurde das Synaptische Zelladhäsionsmolekül 1 (SynCAM 1), ein wichtiger Stimulator der Synapsenbildung, als neues PolySia-Träger im postnatalen Maushirn identifiziert. Die im Rahmen meiner Doktorarbeit hergestellten rekombinanten Polysialyltransferasen wurden genutzt, um ein Testsystem für die *in vitro* Polysialylierung des SynCAM 1 aufzubauen. Dabei konnte gezeigt werden, dass unter den Bedingungen *in vitro* beide Polysialyltransferasen SynCAM 1 als Akzeptor nutzen. Die Polysialylierung interferiert mit der Ausbildung homophiler SynCAM 1 Kontakte. Die Arbeit zeigt darüber hinaus dass die Polysialylierung am N-Glykan des Asn^{116} in der 1. Immunglobulinähnlichen Domäne erfolgt und polysialyliertes SynCAM 1 ausschließlich auf einem spezialisierten Zelltyp mit der Bezeichnung NG-2 vorkommt.

Schließlich konnte ich mit meinen Arbeiten zur molekularen Interpretation des Krankheitsbildes „geistige Behinderung" beitragen. Im Rahmen einer humangenetischen Studie (durchgeführt von Prof. Dr. A. Kuß, Max-Planck-Institut for Molecular Genetics, Berlin) wurde in betroffenen Individuen zweier irakischer Familien Mutationen im Gen für die Sialyltransferase ST3GalIII gefunden. Die im Rahmen meiner Arbeit durchgeführte biochemische Charakterisierung dieser

mutierten Enzyme zeigte, dass beide Mutationen den Transport der Sialyltransferase in den Golgi-Apparat behindern. Eine innerhalb der Transmembrandomäne (TMD) gefundene Mutation verursacht dabei eine Teilrückhaltung im endoplasmatischen Retikulum (ER), während die zweite, nahe dem C-Terminus des Enzyms gelegene Mutation den aus Austritt aus dem ER vollständig verhindert. Durchgeführte Expressionsanalysen weisen darauf hin, dass das Enzyms aufgrund einer Fehlfaltung über das ER assozierte Degradationssystem (ERAD) erkannt und abgebaut wird. Durch forcierte Überexpression konnten kleine Mengen einer löslichen Form der C-terminalen Mutante hergestellt und *in vitro* getestet werden, wobei eine mit der angenommenen Fehlfaltung des Proteins vereinbare drastische Aktivitätsabnahme beobachtet wurde. Mit der Analyse dieser Patienten konnte eindrucksvoll der Beweis geführt werden, dass die Gehirnentwicklung essentiell an die Integrität der Sialylierungsstoffwechselwege gebunden ist.

Abstract

The glycocalyx, a layer of carbohydrates that is bound to proteins and lipids of the cell membrane, is a characteristic of the mammalian cell. Sialic acid is an acidic sugar consisting of nine carbon atoms, exclusively bound in terminal (i.e. the non-reducing) positions of glycoconjugates. Sialic acids are the major constituents determining the negative charge of the cell surface and according to their exposed position, are crucially involved in cellular communication. Vertebrate development essentially depends on the presence of sialic acids. Inactivation of the key enzyme of sialic acid biosynthesis causes embryonic lethality in the mouse. Moreover, the recent discovery that hereditary diseases can be caused by mutations in enzymes in the cellular sialylation pathway, confirmed the high relevance of this modification also in the human organism. Sia as a part of gangliosides and in its polymeric form (polysialic acid, polySia) is crucially involved in brain development and function.

The major acceptor for polySia is the neural cell adhesion molecule NCAM. The transfer of polySia onto NCAM is mediated by two polysialyltransferases (polySTs), ST8SiaII and ST8SiaIV. The high selectivity of NCAM recognition by the polySTs is a poorly understood process, mainly hampered by the lack of recombinant proteins for the use in an *in vitro* test system. With the aim to overcome this limitation, a robust expression system for the production of the interaction partners (NCAM and polySTs) was the major goal of this study. To pursue this goal, it was important to consider that both NCAM and the polySTs are glycoproteins and that the glycan additions had been shown to influence the proteins functions. Here, an insect cell system was established for the production of the recombinant proteins. Functional soluble truncations for both proteins could be produced and, as controlled by functional test systems, could be successively further engineered to generate maximally truncated and minimally glycosylated forms. In addition, a series of NCAM fragments was produced, allowing to analyse the distinct impact of individual NCAM domains. All recombinant proteins were produced in good yields and high purity and thus enabled first investigations on structure-function-relationships. Using analytical ultracentrifugation (AUC), the NCAM ectodomain was shown to dimerise in solution and this interaction was mainly mediated by the immunoglobulin like domain 1 and 2. The presence of the fibronectin III like domain 2 enhanced dimerisation. AUC studies were extended towards analysing complex formation between NCAM and ST8SiaII but did not produce unambiguous results. However, since the produced recombinant proteins were satisfying in terms of yield and purity, crystallisation studies could be initiated to address this question. Although, diffracting crystals have not yet been obtained, the information elaborated on crystallisation conditions will support subsequent studies planed in this area.

In a second study, the produced NCAM fragments were used to dissect the individual impact of the distinct NCAM domains and of polySia in tumour cell migration and adhesion. Thus, NCAM-mediated stimulation of focal adhesions was shown to depend on the presence of a so far unknown heterophilic receptor and to be independant of FGF receptor activation and ERK 1/2 phosphorylation. By using the NCAM fragments, the interaction site for the receptor could be shown to reside in Ig 3 and/or 4 of NCAM. These findings provide new insights into polySia-NCAM function and might lead to new therapeutic approaches in cancer therapy.

Although NCAM is the major scaffold for polySia, NCAM negative mice retain ~5% of total polySia in the brain. Using a glycoproteomics approach, the potent synapse inducing molecule Synaptic Cell Adhesion Molecule 1 (SynCAM 1) was identified as a novel polySia carrier in mouse brain. The recombinant polySTs produced in the course of my thesis were used to establish an *in vitro* test system for SynCAM 1 polysialylation. Thus, it could be demonstrated that both polySTs were able to recognise SynCAM 1 as an acceptor under *in vitro* conditions. Polysialylation was shown to interfere with SynCAM 1 homophilic binding. Moreover, the study demonstrates that polysialylation occurs on the N-glycan residing on Asn^{116} in Ig1 and that polysialylated SynCAM 1 is restricted to a specialised cell type named NG-2.

Finally, I was able to contribute to the molecular interpretation of the disease "Intellectual Disability". In the frame of a genetic study, Prof. Dr. A. Kuß (Max-Planck-Institut for Molecular Genetics, Berlin), identified mutations in the gene encoding the sialyltransferase ST3GalIII in two Iranian families affected by Intellectual Disability. To understand how the identified mutations influence the function of the enzyme, a biochemical characterisation of the mutant enzymes was performed. In chapter 5 of this study, I was able to show that both mutations impacted the transport of the enzyme to the Golgi apparatus. One mutation identified in the transmembrane domain (TMD) evoked a partial retention in the endoplasmic reticulum (ER), while a second mutation located close to the C-terminus of ST3GalIII completely abolished transport out of the ER. Analysing the expression of the mutant enzymes pointed towards a misfolding of the C-terminal mutant leading to the elimination of the protein by the ER associated degradation system (ERAD). By forced overexpression small amounts of the C-terminal mutant protein could be obtained for *in vitro* activity testing. Compatible with the assumed misfolding of the protein, a drastic reduction of activity was observed. The identification of this mutation in patients impressively demonstrates that brain development is crucially dependant on the integrity of the sialylation pathway.

Chapter 1 - General introduction

1. Sialylation

Glycosylation is a complex modification of biomolecules, which determines numerous important cellular functions. For instance glycosylation influences protein folding and half-life, the catalytic activity of enyzmes, the organisation of the extracellular matrix, the functionality of the immune system, the binding of receptors, and finally determines the host susceptibility for toxins, viruses, bacteria and parasites (reviewed in Varki, 1993). In comparison to possible combinations of the four bases of DNA or the 20 amino acids of proteins, glycans offer an extremely high diversity, adding to the 10 most important building blocks the diversity of glycosidic linkage and of numerous sugar modifications (Krishnamoorthy and Mahal, 2009; Cohen and Varki, 2010).

Sialic acid (Sia), a nona-sugar with a carboxylate function in position one, is of particular importance as it decorates terminal positions of glycans and thus plays a pivotal role in cellular communication processes (Varki and Varki, 2007). 5-N-acetylneuraminic acid (Neu5Ac) and 5-N-glycolylneuraminic acid (Neu5Gc) (see Fig. 1) are the most common Sia species found in mammals (Traving and Schauer, 1998; Varki and Varki, 2007), while 2-keto-3-deoxy-D-glycero-D-galacto-nonulosonic acid (Kdn) is frequently found in fish and a major component in bacteria and lower vertebrates (reviewed in Inoue and Kitajima, 2006).

Sialic acids are typically found in α2,3- or α2,6-linkage attached to a galactosyl or N-acetylgalactosyl residue, while polysialic acid (polySia) consists exclusively of α2,8-linked monomers. The negative charge at the C1 atom is an individual property of sialic acid and mediates its unusual biophysical properties (Traving and Schauer, 1998).

Transfer of sialic acids onto glycoconjugates is mediated by specialised sialyltransferases that reside in the Golgi apparatus. The sialyltransferases use the activated form, CMP-Sia, as a donor substrate. The synthesis of this activated donor sugar is performed by the CMP-sialic acid-synthetase, a nuclear localised enzyme (reviewed in Münster-Kühnel, 2004) and afterwards transported to the Golig by the CMP-Sia transporter (Eckhardt and Gerardy-Schahn 1997; Aoki *et al.*, 2003).
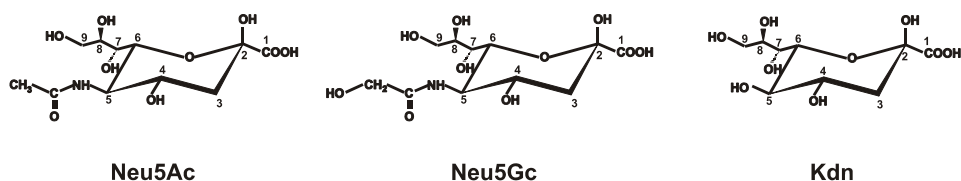
Fig. 1: Chemical structures of the three most abundant sialic acids. Neu5Ac, 5-N-acetylneuraminic acid; Neu5Gc, 5-N-glycolylneuraminic acid; Kdn, 2-keto-3-deoxy-D-glycero-D-galacto-nonulosonic acid.

2. Sialyltransferases

The mammalian sialyltransferase family consists of 20 members (Audry *et al.*, 2010). As mentioned above, all localise to the Golgi apparatus and use the CMP-activated form to transfer Sia onto glycoproteins or glycolipids. The enzymes are classified into 4 families according to the synthesised linkages: β-galactoside α2,6-sialyltransferases (ST6Gal I-II), β-N-acetylgalactoside α2,6-sialyltransferases (ST6GalNAc I-VI), β-galactoside α2,3-sialyltransferases (ST3Gal I-VI) and α2,8-sialyltransferases (ST8Sia I-VI) (Audry *et al.*, 2010; Harduin-Lepers *et al.*, 2001; for an overview see Table 1).

All sialyltransferases belong to the class of type II membrane proteins and thus consist of a short N-terminal cytoplasmic tail followed by a transmembrane domain (TMD), a stem region and a catalytic domain (see Fig. 2). Four motifs are highly conserved among sialyltransferases: the sialylmotif L (large), which was shown to be involved in binding of the sugar donor CMP-Neu5Ac (Datta *et al.*, 1995), sialylmotif S (small), which is involved in both donor and acceptor binding (Datta *et al.*, 1998) and sialylmotif III and VS (very small), which are further required for activity (Geremia *et al.*, 1997; Kitazume-Kawaguchi *et al.*, 2001; Jeanneau *et al.*, 2004). In the sialylmotif L and S, highly conserved cysteine residues were observed to be important for activity and to be involved in the formation of a disulfide bond (Datta *et al.*, 1998; Datta *et al.*, 2001).

Regulation of sialyltransferase activity takes place at a transcriptional level and influences cell surface sialylation and glycosylation patterns (reviewed in Harduin-Lepers *et al.*, 2001).

The high number of sialyltransferases exhibiting distinct but overlapping expression patterns in the organism underlines their role in the fine tuning of sialylation processes and the importance of accurate regulation of sialylation patterns.
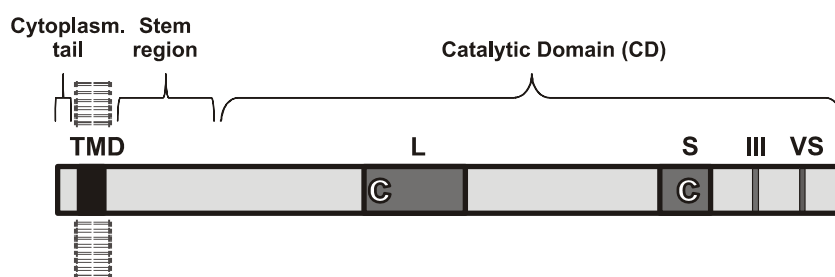
Fig. 2: Schematic representation of a sialyltransferase. TMD: transmembrane domain; L, S, III, VS: sialylmotifs L, S, III and VS, C: cysteine residue.

Sialyltransferase	Accptor	Synthesised structure
ST6GalI	glycoproteins, oligosaccharides	**Neu5Ac**-α2,6-Gal-β1,4-GlcNAc-
ST6GalII	glycoproteins, oligosaccharides	**Neu5Ac**-α2,6-Gal-β1,4-GlcNAc-
ST6GalNAcI	glycoproteins (O-linked)	$(\text{Neu5Ac-}\alpha2,3)_{0-1}$-(Gal-β1,3)$_{0-1}$-GalNAc / **Neu5Ac-α2,6**
ST6GalNAcII	glycoproteins (O-linked)	$(\text{Neu5Ac-}\alpha2,3)_{0-1}$-Gal-β1,3-GalNAc-Ser / **Neu5Ac-α2,6**
ST6GalNAcIII	glycolipids	Neu5Ac-α2,3-Gal-β1,3-GalNAc-R / **Neu5Ac-α2,6**
ST6GalNAcIV	glycoproteins (O-linked)	Neu5Ac-α2,3-Gal-β1,3-GalNAc-R / **Neu5Ac-α2,6**
ST6GalNAcV	glycolipids	G_{D1a}, $G_{T1a\alpha}$, $G_{Q1b\alpha}$
ST6GalNAcVI	glycolipids	$G_{D1\alpha}$, $G_{T1a\alpha}$, $G_{Q1b\alpha}$
ST3GalI	glycoproteins, glycolipids (O-linked)	**Neu5Ac-α2,3**-Gal-β1,3-GalNAc-
ST3GalII	glycoproteins, glycolipids (O-linked)	**Neu5Ac-α2,3**-Gal-β1,3-GalNAc-
ST3GalIII	glycoproteins	**Neu5Ac-α2,3**-Gal-β1,3-GlcNAc- (**Neu5Ac-α2,3**-Gal-β1,4-GlcNAc-)
ST3GalIV	glycoproteins	**Neu5Ac-α2,3**-Gal-β1,4-GlcNAc- (**Neu5Ac-α2,3**-Gal-β1,3-GalNAc-)
ST3GalV	glycolipids	G_{M3}: **Neu5Ac-α2,3**-Gal-β1,4-Glc-Cer
ST3GalVI	glycoproteins, glycolipids	**Neu5Ac-α2,3**-Gal-β1,4-GlcNAc-
ST8SiaI	glycolipids	G_{D3}: **Neu5Ac-α2,8**-Neu5Ac-α2,3-Gal-β1,4-Glc-Cer
ST8SiaII	glycoproteins	**(Neu5Ac-α2,8)$_{poly}$**-Neu5Ac-α2,3-Gal-β1,4-GlcNAc-
ST8SiaIII	glycoproteins, (glycolipids)	**(Neu5Ac-α2,8)$_{oligo}$**-Neu5Ac-α2,3-Gal-β1,4-GlcNAc-
ST8SiaIV	glycoproteins	**(Neu5Ac-α2,8)$_{poly}$**-Neu5Ac-α2,3-Gal-β1-R
ST8SiaV	glycolipids	G_{D1c}, G_{T1a}, G_{Q1b}, G_{T3}
ST8SiaVI	glycoproteins (O-linked), oligosaccharides	**Neu5Ac-α2,8**-Neu5Ac-α2,3(6)-Gal-

Table 1: Overview of to date characterised sialyltransferases with their acceptor structures and synthesised products. (reviewed in Harduin-Lepers *et al.*, 2001 and Takashima *et al.*, 2008)

2.1. ST3GalIII

The β-galactoside α2,3-sialyltransferases ST3GalIII is mainly expressed in uterus and skeletal muscle tissue, but also in brain, adrenal gland, peripheral blood leukocytes, spleen, testis, placenta and heart tissue and a variety of fetal tissues (Kitagawa *et al.*, 1994; Grahn *et al.*, 2002). So far, 26 different mRNAs derived by alternative splicing have been identified, most of which are lacking crucial parts of the catalytic domain including sialylmotifs and thus are supposed to be inactive (Grahn *et al.*, 2002; Grahn *et al.*, 2004). ST3GalIII preferentially acts on Gal-β1,3-GlcNAc-residues (so called type I precursors) present on glycoproteins, while Gal-β1,4-GlcNAc-residues (type II precursors) represent weaker acceptors (Kono *et al.*, 1997). Thus, ST3GalIII is a major enzyme in the synthesis of sialyl Lewis a glycotopes (sLe^a). However, an increase in both sLe^a and sLe^x epitope was reported upon overexpression of ST3GalIII in gastrointestinal carcinoma cells (Carvalho *et al.*, 2010).

sLe^x is involved in recruiting peripheral blood leukocytes to sites of inflammation and infection by interaction with E- and P-selectins (Phillips *et al.*, 1990; Tyrrell *et al.*, 1991; Polley *et al.*, 1991), but E-selectin has also been demonstrated to bind to sLe^a (Tyrrell *et al.*, 1991; Berg *et al.*, 1991). sLe^a and sLe^x are further supposed to play a role in cancer malignancy (Iwai *et al.*, 1993). Transfection of neuroblastoma cells with ST3GalIII resulted in an up-regulation of α2,3 sialylated structures and to the overexpression of polySia (Georgopoulou *et al.*, 1999a). However, since elevated polySia expression was also observed upon transfection of cells with a β-galactoside α2,6-sialyltransferase, this seems to be caused by an increased allocation of terminally α2,3- or α2,6-sialylated glycan structures on NCAM molecules, which both provide acceptors for polysialylation (Georgopoulou *et al.*, 1999b).
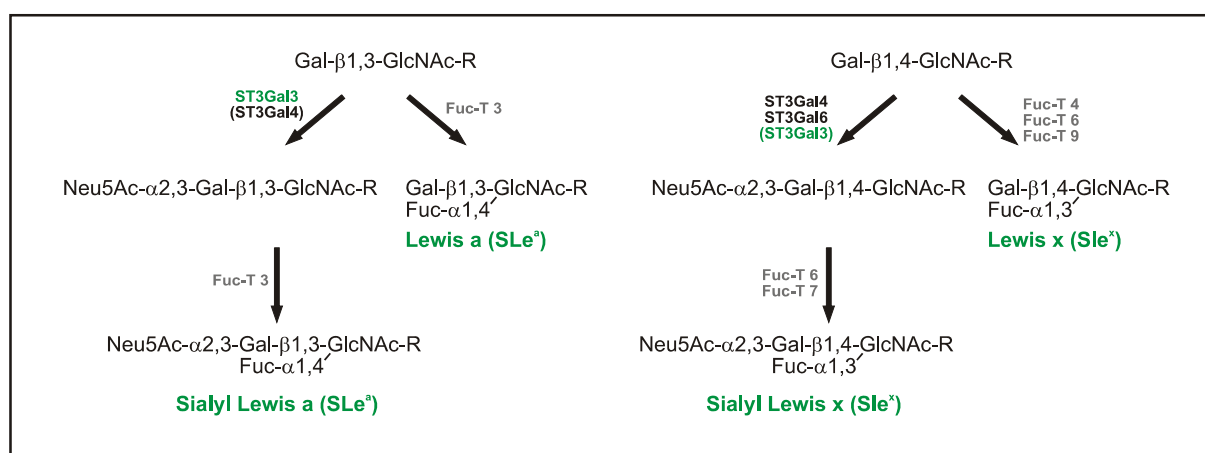
Fig. 3: Biosynthesis of Lewis and Sialyl-Lewis epitopes (modified from Grahn *et al.*, 2002).

2.2. Polysialyltransferases

The polysialyltransferases (polySTs) ST8SiaII and ST8SiaIV mediate the biosynthesis of polySia, a linear homopolymer of $\alpha 2,8$-linked sialic acid, which is specifically attached to a small group of protein acceptors. The main carrier of polySia is the Neural Cell Adhesion Molecule (NCAM), which by this modification is turned from an adhesive into an anti-adhesive molecule. PolySia is a bulky, highly hydrated and negatively charged structure, which increases the hydrodynamic radius of NCAM and thus impairs the molecules intrinsic capability to perform heterophilic and homophilic interactions in *trans* (i.e. between neighbouring cells) (Rutishauser *et al.*, 1988; Yang *et al.*, 1994; Fujimoto *et al.*, 2001; Johnson *et al.*, 2005; reviewed in Mühlenhoff *et al.*, 1998; Rutishauser, 2008).

ST8SiaII and ST8SiaIV exhibit the common structure of sialyltransferases. Apart from the four sialylmotifs conserved in all sialyltransferases, the polySTs comprise two additional specific regions: the polysialyltransferase domain (PSTD) (Nakata *et al.*, 2006) which seems to be involved in polysialyltransferase activity *per se* and the polybasic region (PBR) which seems to play a special role in NCAM polysialylation (Foley *et al.*, 2009).

Furthermore, both polysialyltransferases comprise three cystein residues in sialylmotif L (SM L), one in sialylmotif S (SM S) and one at the C-terminus. Using ST8SiaIV as a model, Angata *et al.* (2001) observed the formation of two disulfide bonds, which were formed between the first cysteine residue in SM L and the cysteine residue in SM S and the second cysteine in SM L and the cysteine residue located at the enzymes' C-terminus, while the third cysteine residue in SM L was not involved in disulfide bond formation, but still showed to be important for activity.

ST8SiaII and ST8SiaIV are decorated by 6 and 5 N-glycosylation sites, respectively, namely Asn^{60}, Asn^{72}, Asn^{89}, Asn^{134}, Asn^{219} and Asn^{234} (murine ST8SiaII) and Asn^{50}, Asn^{74}, Asn^{119}, Asn^{204} and Asn^{219} (hamster ST8SiaIV). Mutation of the highly conserved 3rd N-glycosylation site in ST8SiaII and the corresponding 2nd N-glycosylation site in ST8SiaIV leads to inactivation of the enzymes. In ST8SiaII, the 5th and, though to a lesser extend, the 6th N-glycosylation contribute to the installation of full catalytic activity (Mühlenhoff *et al.*, 2001; Close *et al.*, 2001; Günzel, 2008). Both enzymes can modify themselves in a process called autopolysialylation, shown to involve N-glycosylation site 3, 5, 6 in ST8SiaII and 2, 3, 4 in ST8SiaIV (Close *et al.*, 2000; Mühlenhoff *et al.*, 2001; Günzel, 2008).
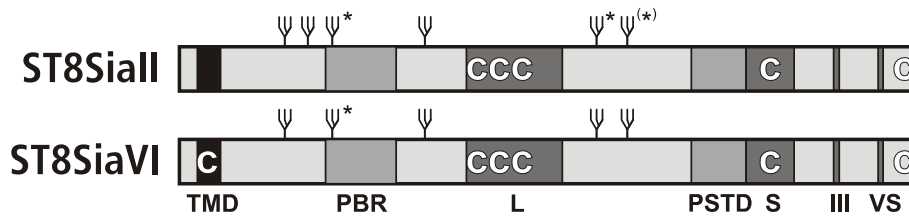
Fig. 4: Schematic representation of the polySTs. TMD: transmembrane domain; L, S, III, VS: sialylmotifs L, S, III and VS; PBR: polybasic region; PSTD: polysialyltransferase domain; Ψ: N-glycosylation site; C: Cysteine residue. N-glycosylation sites that are involved in enzymatic activity are marked by asterisks.

3. PolySia acceptors

As mentioned before, polysialylation is a highly specific reaction occurring only on a restricted number of proteins. Apart from the polysialyltransferases themselves, five polySia acceptors have been identified to date: the Neural Cell Adhesion Molecule (NCAM) (Finne *et al.*, 1983; see Colley, 2010 and Hildebrandt *et al.*, 2010 for a detailed review on NCAM polysialylation), the α-subunit of the voltage-dependant sodium channel (Zuber *et al.*, 1992), a soluble fragment of the scavenger receptor CD 36 found in human milk (Yabe *et al.*, 2003), neuropilin-2 on dendritic cells (Curreli *et al.*, 2007) and the synaptic cell adhesion molecule SynCAM 1 (Galuska *et al.*, 2010). Two of these acceptors, namely SynCAM 1 and NCAM will be described in more detail in the following.

3.1. The Synaptic Cell Adhesion Molecule (SynCAM)

The Synaptic Cell Adhesion Molecule (SynCAM) family consists of 4 members, SynCAM 1-4, which are expressed throughout the brain, suggesting an important function in all brain structures. SynCAM 1 (also named CADM1, nectin-like protein-2 (necl-2), tumor suppressor in lung cancer 1 (TSLC-1), spermatogenic Ig superfamily molecule (SgIGSF) and RA-175) is a potent inducer of synapse formation and is further involved in reducing complexity of migrating growth cones and the number of filopodia in a FAK dependant way, and thus supports axons in maintaining target contacts for synapse formation (Biederer *et al.*, 2002; Stagi *et al.*, 2010). Furthermore, SynCAM 1 was shown to recruit NMDA receptors and possibly AMPA receptors via its intracellular protein 4.1 binding motif (Hoy *et al.*, 2009).

The overall molecule structure is conserved among family members, comprising three N-terminally located Immunglobulin like (Ig) domains, followed by a stem region, a transmembrane domain and a cytoplasmic tail containing a protein 4.1 and a PDZ domain binding site for intracellular signalling (Biederer *et al.*, 2002; Biederer *et al.*, 2006; Fogel *et al.*,

2007; Hoy *et al.*, 2009; Stagi *et al.*, 2010). SynCAM 1 contains 6 N-glycosylation sites, namely Asn^{70}, Asn^{104} and Asn^{116}, located in Ig1, Asn^{168} in Ig2 and Asn^{307} and Asn^{311} in Ig3. Moreover, alternatively spliced exons can be inserted in the stem region bearing potential O-glycosylation sites (Biederer *et al.*, 2006).

SynCAMs 1-3 are capable of homophilic binding, however, heterocomplexes of SynCAM 1 and 2 or 3 and 4, respectively, represent the most stable binding states. Weaker binding is observed between SynCAM 1 and 3 and has also been detected for SynCAM 2 and 4 (Fogel *et al.*, 2007; Thomas *et al.*, 2008). The binding site of SynCAM 1 for homophilic interactions and binding to SynCAM 2 has been mapped to Ig1 and Ig2 (Fogel *et al.*, 2007; Fogel *et al.*, 2010).

The Ig1 domains of SynCAM 1 and 2 are decorated by three or one N-glycosylation site, respectively. While the presence of the N-glycan on Asn ^{60} of SynCAM 2 has been shown to reduce interaction with both SynCAM 1 and 2, glycosylation of Asn^{70} and Asn^{104} of the SynCAM 1 Ig1 domain in contrast enhances both homophilic binding and binding to SynCAM 2, and these effects have been shown to directly translate into functional effects in synapse formation. These findings, together with the notion, that glycosylation of SynCAM 1 is developmentally altered, suggests a regulatory role of N-glycan modification in SynCAM function (Fogel *et al.*, 2010). Interestingly, enzymatic removal of sialic acid from SynCAM 1 resembled the effect of complete deglycosylation on homophilic binding, pointing towards a role for Sia in regulating SynCAM function. In the course of my thesis SynCAM 1 was identified as a novel polySia acceptor and first insights have been obtained into the functional relevance of polysialylated SynCAM 1 (see chapter 4; Galuska *et al.*, 2010).

3.2. The Neural Cell Adhesion Molecule (NCAM)

3.2.1. The biological impact of polySia-NCAM

The biological impact of polySia on NCAM has been impressively demonstrated by a series of mouse models with progressively lowered polySia expression (for review see Hildebrandt *et al.*, 2007). NCAM knockout mice retain ~5% of total polySia in the brain as compared to wild-type mice (Cremer *et al.*, 1994, Galuska *et al.*, 2010) and, surprisingly, despite of the depletion of two major neurodevelopmental markers (polySia and NCAM), exhibit a mild phenotype. A prominent morphological characteristic found in NCAM-knock-out mice was a small olfactory bulb (ob), which resulted from a defective migration of subventricular zone (SVZ) derived neuronal precursors along the rostral migratory stream (RMS) (Tomasiewicz *et al.*, 1993; Cremer *et al.*, 1994; Ono *et al.*, 1994; Hu *et al.*, 1996; Chazal *et al.*, 2000). Additionally, defects in mossy fibre lamination (Tomasiewicz *et al.*, 1993; Cremer *et al.*, 1997; Seki and Rutishauser

1998) and electrophysiological alterations associated with deficits in learning and memory (Cremer *et al.*, 1994; Becker *et al.*, 1996; Muller *et al.*, 1996; Muller *et al.*, 2000; Bukalo *et al.*, 2004; Dityatev *et al.*, 2004) were observed. Similarly, knock-out mice lacking ST8SiaII (Angata *et al.*, 2004) or ST8SiaIV (Eckhardt *et al.*, 2000) were found to exhibit a mild phenotype. Importantly, since both single knock-outs retained significant polySia expression levels, these models demonstrated that the polysialyltransferases are able to substitute for each other to a certain extent.

In marked contrast to the previous models, double knock-out mice lacking both polySTs were found to exhibit a postnatally lethal phenotype. While gross anatomical structures are normal at the day of birth, polySia-depleted mice fail to thrive and > 80% die within 3 weeks after birth. The double-knock-out mice develop a hydrocephalus with high incidence and show defects in important commissural and non-commissural fibre tracts (Hildebrandt *et al.*, 2009). Remarkably, further ablation of NCAM in the polySia-negative background rescues the severe phenotype and *ST8Sia2$^{-/-}$ST8Sia4$^{-/-}$NCAM$^{-/-}$* triple knock-out mice display a phenotype similar to that of NCAM knock-out mice. These results demonstrate the importance of polySia for the regulation of its acceptor molecule NCAM. In fact, recent studies carried out in our laboratory show that polySia is essential to prevent untimed functions of the NCAM-protein (Weinhold *et al.*, 2005; Hildebrandt *et al.*, 2009).

3.2.2. NCAM Structure

The three main isoforms of NCAM are named after their apparent molecular weight NCAM-120, NCAM-140 and NCAM-180 and derive from alternative splicing. NCAM consists of 5 N-terminally located Ig domains followed by two fibronectin III like (FN) domains, a GPI anchor (NCAM-120) or a transmembrane domain followed by a short cytoplasmic tail (NCAM-140 and NCAM-180), respectively (see Fig. 5). Six N-glycosylation sites were identified, which are located in Ig3 (Asn^{204}), Ig4 (Asn^{297} and Asn^{329}) and Ig5 (Asn^{405}, Asn^{431} and Asn^{460}) (numbers are according to murine NCAM) (Cunningham *et al.*, 1987). Polysialylation has been shown to be restricted to the 5th and 6th N-glycosylation site (Nelson *et al.*, 1995; Liedtke *et al.*, 2001; von der Ohe *et al.*, 2002) and to depend on the priming of polySia acceptor glycan structures by the addition of α2,3- or α2,6-linked sialic acid residues (Mühlenhoff *et al.*, 1996a).
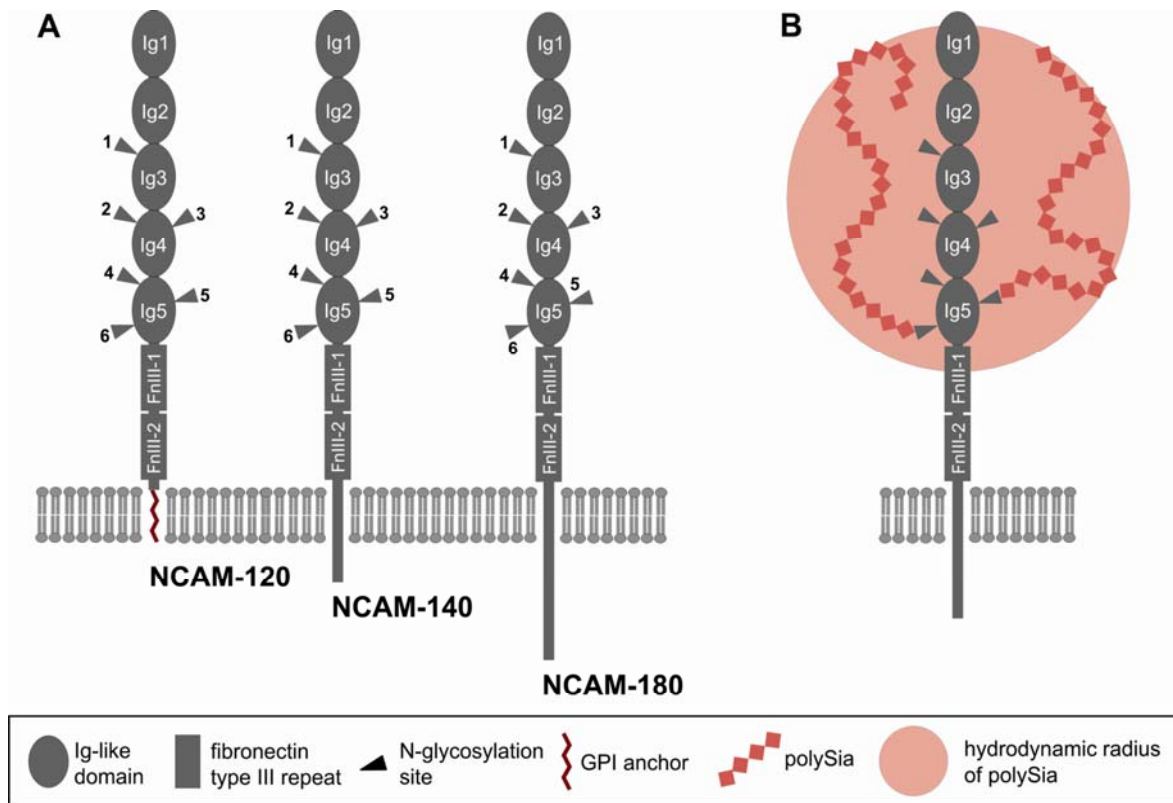
Fig. 5: Schematic representation of the three NCAM isoforms (A) and polysialylated NCAM displaying an enlarged hydrodynamic radius (B).

As mentioned above, polysialylation is a highly specific modification restricted to a small number of proteins. This suggests a specific protein-protein interaction between the polySTs and the acceptor protein. However, to date little is known about structural motifs that determine NCAM as the main carrier for the polySia occurs. Mendiratta *et al.* (2005) described membrane-spacing, i.e. the correct distance of the respective polysialylation sites to the plasma membrane, to be important for interaction. In contrast, Foley *et al.* (2010a) demonstrated that the placement of artificial polysialylation sites within Ig5 allows for flexibility in rotational orientation.

Other studies conducted to elucidate the molecular details underlying the specific interaction of NCAM and the polySTs used truncation and deletion of NCAM domains. Thereby, the minimal polySia acceptor was determined to comprise the NCAM domains Ig5 and FN1 (Mendiratta *et al.*, 2005). However, data from this and an earlier study (Nelson *et al.*, 1995) suggest a supporting role of Ig4 in polysialyltransferase recognition.

By use of bioinformatics Mendiratta *et al.* (2006) identified unique elements in NCAM that may promote the interaction with the polySTs. Studies using site directed mutagenesis confirmed the relevance of these elements which comprise an α-helix between β-strands 4 and 5 and an acidic patch consisting of Asp^{497}, Asp^{511}, Glu^{512} and Glu^{514} in FN1. In a recent follow up study the

group identified the QVQ and PYS sequence as polyST interaction motifs in NCAM. For the identification of these motifs NCAM was compared to a close relative, the Olfactory Cell Adhesion Molecule (OCAM), which is not an acceptor for polySia transfer. Moreover, in subsequent mutational studies the authors demonstrate that the α-helix and the QVQ motif are important for polysialylation of N-glycans in NCAM, while the acidic patch and the PYS motif play a role in the polysialylation of O-glycans (Foley *et al.*, 2010b). Since polySia in NCAM is chiefly bound to N-glycans, the O-linked polySia fraction is very small and may have been overlooked in earlier studies. Interestingly, an artificial fragment consisting only of FN1 and FN2, which is naturally lacking N-linked polySia acceptors, as well as an NCAM-OCAM chimera, where FN1 of NCAM had been replaced by OCAM FN1, were found to be heavily polysialylated on O-linked glycans (Mendiratta *et al.*, 2005; Foley *et al.*, 2010b). It is important in this context to stress the point that NCAM is a complex transcriptional unit of which >100 protein isoforms can be formed. Some of these contain potential O-glycan attachment sites. The finding by Foley *et al.* (2010b) thus points towards the need for improved reagents suited to monitor the dynamics that underlies NCAM and polySia expression during neurodevelopment.

3.2.3. NCAM interactions

NCAM homophilic interactions have been subject to intense investigation, resulting in different binding models, which are, however, still under controversial discussion (Rao *et al.*, 1992; Rao *et al.*, 1993; Rao *et al.*, 1994; Ranheim *et al.*, 1996; Kiselyov *et al.*, 1997; Jensen *et al.*, 1999; Atkins *et al.*, 1999; Atkins *et al.*, 2001; Kasper *et al.*, 2000; Soroka *et al.*, 2003; Johnson *et al.*, 2004; Wieland *et al.*, 2005; Kiselyov *et al.*, 2005). As the study of homophilic NCAM-NCAM interactions is subject of investigation in this doctorial thesis, a detailed summary of the existing data is given in the introduction of chapter 2.

Apart from homophilic binding and its transient but specific contact made to polySTs, NCAM has been shown to be involved in diverse heterophilic interactions. Among those, binding to other cell adhesion molecules such as Tag-1 (Milev *et al.*, 1996), L1 (Kadmon *et al.*, 1990a; Kadmon *et al.*, 1990b; Horstkorte *et al.*, 1993) and cadherins (Fujimoto *et al.*, 2001) were observed. Moreover, NCAM interacts with collagen (Probstmeier *et al.*, 1992) and chondroitin sulphate proteoglycans such as neurocan (Friedlander *et al.*, 1994; Retzler *et al.*, 1996) and phosphacan, which represents the extracellular domain of protein-tyrosine-phosphatase-ζ/β (Grumet *et al.*, 1993; Milev *et al.*, 1994) and with heparan sulphate proteoglycans such as agrin (Cole *et al.*, 1986; Lubec *et al.*, 1986; Storms *et al.*, 1996) as well as to prion protein (Schmitt-Ulms *et al.*, 2001).

NCAM is further known to interact with the fibroblast growth factor receptor-1 (FGFR-1) (Saffell *et al.*, 1997; Ronn *et al.*, 2000; Kiselyov *et al.*, 2003) and the glial derived neurotrophic factor (GDNF) (Paratcha *et al.*, 2003), while the brain derived neurotrophic factor (BDNF) and the platelet-derived growth factor (PDGF) bind to the polySia-portion of NCAM and are thus only indirectly associated with NCAM functions (Vutskits *et al.*, 2001; Zhang *et al.*, 2004).

3.2.4. NCAM signalling

NCAM is involved in a variety of signalling events leading to neurite outgrowth, reorganisation of the cytoskeleton, formation of focal adhesion contacts, cell migration, adhesion and differentiation and neuronal survival (Beggs *et al.*, 1994; Cavallaro *et al.*, 2001; Prag *et al.*, 2002; Ditlevsen *et al.*, 2003; Bazou *et al.*, 2008; Röckle *et al.*, 2008; Francavilla *et al.*, 2009; for a detailed review on NCAM signalling pathways see Hinsby *et al.*, 2004a and Ditlevsen *et al.*, 2008).

The molecule has been shown to promote the formation of focal adhesions, but its role in cell migration and adhesion is still under debate and the signalling pathways involved remain unclear (Cavallaro *et al.*, 2001; Prag *et al.*, 2002; Francavilla *et al.*, 2009). Moreover, also the role of polySia in modulating NCAM signalling in cell migration and adhesion remains largely elusive and is topic of the current study (see Chapter 3 of this thesis).

The best studied example of NCAM signalling is the process of neurite outgrowth. The prevailing model assumes that NCAM acts via homophilic trans-interactions, which in turn lead to binding and activation of FGF receptors (FGFR) in *cis*, i.e. within the plane of the same membrane (Saffell *et al.*, 1997; Ronn *et al.*, 2000; Kiselyov *et al.*, 2003). Complex formation between NCAM and FGFR results in intracellular binding of FGFR substrate 2 (Frs2) and of docking protein Shc, which together recruit the adaptor protein Grb2 and the GTP exchange factor SOS. Bound SOS than activates the small GTP binding protein Ras (Hadari *et al.*, 1998; Rozakis-Adcock *et al.*, 1992; Hinsby *et al.*, 2004b), resulting in activation of the serine/threonine kinase Raf followed by activation of the MAP kinase kinase (MEK) and finally phosphorylation of ERK MAP kinases (Kolkova *et al.*, 2000; Schmid *et al.*, 1999). Via ERK MAP kinases and PKA, NCAM has been shown to activate cAMP-responsive-element-binding protein (CREB), a transcription factor associated with neurite outgrowth as well as learning and memory processes (Schmid *et al.*, 1999; Jessen *et al.*, 2001).

In addition, NCAM-induced FGFR activation may activate PLCγ which leads to the cleavage of PIP_2 into IP_3 and DAG (Saffell *et al.*, 1997). IP_3 activates Ca^{2+} from intracellular stores (Berridge *et al.*, 1993), while DAG mediates an increased Ca^{2+} influx by elevating activity of N-

and L-type Ca^{2+} channels (Doherty *et al.*, 1991; Williams *et al.*, 1994). An increase in intracellular calcium levels seems to be crucial for NCAM-mediated neurite outgrowth, either by directly activating protein kinase C (PKC) and Ca^{2+}/Calmodulin kinase II (CaMKII) or by indirect activation of protein kinase A (PKA) via a Ca^{2+}/Calmodulin sensitive adenylyl cyclase, (Kolkova *et al.*, 2000; Kolkova *et al.*, 2005; Williams *et al.*, 1995; Ditlevsen *et al.*, 2007; Jessen *et al.*, 2001).

Moreover, NCAM mediated neurite outgrowth and neuronal survival has been shown to rely on phosphatidyl inositol-3 kinase (PI3K) (Ditlevsen *et al.*, 2003). PI3K can be activated by FGFR via the docking protein Gab1 (Ong *et al.*, 2001), by phosphorylated focal adhesion kinase (FAK) (Chen *et al.*, 1996), by G-proteins and by Ras, and probably acts via the serine/threonine kinase Akt, which becomes activated by binding to lipid products of PI3K (Ditlevsen *et al.*, 2003).

FGFR independant NCAM signalling relies on lipid raft association of NCAM-120 and NCAM-140 and results in activation of the non-receptor tyrosine kinase Fyn (Beggs *et al.*, 1997; Kramer *et al.*, 1999; Niethammer *et al.*, 2002; Lehembre *et al.*, 2008), which is probably mediated by the receptor protein tyrosine phosphatase RPTPα. Fyn activation was shown to result in FAK recruitment and leads to phosphorylation of ERK MAP kinases and activation of CREB (Beggs *et al.*, 1997, Schmid *et al.*, 1999; Bodrikov *et al.*, 2005). In this, the FGFR and Fyn dependant pathways seem to converge, most probably at the level of Ras, and act together to regulate neurite outgrowth (Kolkova *et al.*, 2000, Niethammer *et al.*, 2002).

To allow for neurite outgrowth to take place, a reorganisation of the cytoskeleton is required. An important link from NCAM to the cytoskeleton has been established by the finding that NCAM, and preferentially the NCAM-180 isoform, binds to the actin binding protein spectrin spectrin (Pollerberg *et al.*, 1986; Pollerberg *et al.*, 1987; Leshyns'ka *et al.*, 2003). The growth-associated protein-43 (GAP-43) seems to act as a switch between NCAM-180 and NCAM-140 signalling; in the presence of GAP-43, NCAM-induced neurite outgrowth depends on the NCAM-180/spectrin/GAP-43 pathway, while in the absence of GAP-43, the NCAM-140/Fyn pathway is pivotal (Korshunova *et al.*, 2007). GAP-43 binds and modifies F-actin and thus influences cytoskeletal reorganisation and growth cone motility (Caroni *et al.*, 2001; Oestreicher *et al.*, 1997). Furthermore, ERK MAP kinases are associated with microtubuli and phosphorylate microtubuli-associated proteins (Gundersen *et al.*, 1999). They further activate myosin light chain (MLC) kinase, resulting in phosphorylation of MLC and thus enhanced actomyosin-mediated contraction, which influences growth cone advancement or retraction (Cheresh *et al.*, 1999; Suter *et al.*, 1998; Suter *et al.*, 2000).

More recently, it has been demonstrated that NCAM in association with the GDNF receptor alpha1 can also act as a signalling receptor for ligands of the GDNF family, resulting in activation of Fyn and FAK and inducing Schwann cell migration and axonal growth in hippocampal and cortical neurons (Paratcha *et al.*, 2003; Nielsen *et al.*, 2009).

Objectives

The modification of biomolecules with sialic acid (Sia) is crucially involved in steering molecular, cellular and physiological processes. The polymeric form of Sia, polysialic acid (polySia), is found on a restricted number of proteins with the major carrier being the neural cell adhesion molecule NCAM. The expression of polySia-NCAM has been shown to play a pivotal role in brain development and to influence cancer malignancy. Thus, an in depth understanding of the polysialylation reaction is a prerequisite to understand and influence this process.

The first goal of this study was therefore to produce soluble recombinant polysialyltransferase and NCAM proteins to enable *in vitro* investigations on structure-function-relationships that underly the polysialylation reaction. A major focus was thereby set on the question, which structural determinants qualify NCAM as the preferred acceptor for polysialyltransferases. Further, NCAM fragments should be produced and used in studies to dissect NCAM-dependant from –independant polySia specific functions and to elucidate the functional impact of individual NCAM domains on cellular signal transduction processes associated with cell migration and focal adhesion formation.

In the course of my studies, the β-galactoside α2,3-sialyltransferase ST3Gal-III was found to be mutated in individuals affected by non-syndromal autosomal recessive intellectual disability (NSARID). A second goal of this thesis was therefore to biochemically characterise how the identified mutations impact the functionality of the sialyltransferase.

Chapter 2 - Studies towards understanding the structural elements promoting NCAM-NCAM homophilic interactions and interactions between NCAM and the polysialyltransferases.

Preface

In this study, a production sytem for recombinant murine ST8SiaII as well as a series of human NCAM fragments was established, using a baculoviral expression system in insect cells. Purified proteins were used to determine the oligomerisation status of NCAM in solution. Using analytical ultracentrifugation and size exclusion chromatography, the soluble ectodomain of NCAM was identified to form a stable dimer. Consequently, NCAM fragments were used to dissect the influence of individual subdomains on dimer formation. Moreover, by use of the same experimental techniques, trials were undertaken to investigate complex formation between ST8SiaII and NCAM. Because recombinant proteins could be expressed in good yields and purified close to homogeneity, crystallisation trials were set up to obtain functional 3D structures of the NCAM ectodomain and NCAM-ST8SiaII complexes.

Chapter 2 - Studies towards understanding the structural elements promoting NCAM-NCAM homophilic interactions and interactions between NCAM and the polysialyltransferases.

Abstract

Polysialic acid (polySia) is a post-translational modification of the Neural Cell Adhesion Molecule NCAM consisting of $\alpha 2,8$-linked 5-N-Acetylneuraminic acid (Neu5Ac). Its expression on NCAM plays a pivotal role in brain development, neural plasticity in the adult brain and nerve repair. Two polysialyltransferases (polySTs) have been identified to add polySia onto NCAM, namely ST8SiaII and ST8SiaIV. To provide a basis for the investigation of the structural features that promote the preferred recognition of NCAM by the polySTs, robust expression systems for NCAM and ST8SiaII were established. Since the functionality of polySTs and of NCAM depends on disulfide bond formation and N-glycosylation, a baculoviral-based insect cell expression system was used for the production of these proteins. In addition a library of NCAM fragments was generated to enable evaluation of the impact of individual domains on NCAM homo-dimer formation. All proteins were generated in quantities and qualities sufficient to pursue detailed protein-protein interaction studies and to initiate first crystallisation trials. Moreover, with the help of analytical ultracentrifugation studies we were able to demonstrate that dimerisation of the NCAM ectodomain in solution is mediated by the immunoglobulin (Ig) like domains Ig1 and Ig2 and to a lesser extend by the fibronectin III like domain FN2.

Introduction

The neural cell adhesion molecule (NCAM) is a type I transmembrane protein, consisting of five N-terminal immunoglobulin like (Ig) domains and two fibronectin III like (FN) domains. These are, depending on the NCAM isoform, followed by a glycosylphosphatidylinositol anchor in NCAM-120 or a transmembrane domain and a cytoplasmic tail in NCAM-140 and NCAM-180. Of the six N-glycosylation sites, the fifth and sixth, both located in Ig5, can be modified by polysialic acid (polySia), a linear homopolymer consisting of $\alpha2,8$-linked N-acetyl neuraminic acid (reviewed in Mühlenhoff *et al.*, 1998). Due to the bulky structure of this hydrated and highly negatively charged polymer, polySia modulates NCAM functions, attenuates cell adhesion mediated by both NCAM dependant and NCAM independant mechanisms, and increases membrane repulsion (Rutishauser *et* al., 1988; Fujimoto *et* al., 2001; Johnson *et al.*, 2005b). These specific features combined with the high expression level of NCAM and polySia in the nervous system make them crucial factors in neural development, which has been impressively demonstrated using a series of mouse models with progressively lowered polySia expression (Cremer *et al.*, 1994; Eckhardt *et al.*, 2000; Angata *et al.*, 2004; Weinhold *et al.*, 2005; Hildebrandt *et al.*, 2009; Schiff *et al.*, 2010) reviewed in Hildebrandt 2007). Existing data further indicate that polySia and NCAM impact cell adhesion and migration, axon branching, fasciculation and pathfinding and are involved in steering synaptic and neuronal plasticity in the adult organism (reviewed in Mühlenhoff *et al.*, 2009 and Rutishauser 2008). Moreover, polySia has been shown to positively impact nerve regeneration. Reconstitution of plasticity by overexpression of polySia has therefore gained considerable attraction as a potential therapeutic approach after nerve lesions (El Maarouf *et al.*, 2006; Jungnickel *et* al., 2009; Haastert-Talini *et al.*, 2010).

The biosynthesis of polySia is mediated by two polysialyltransferase, ST8SiaII and ST8SiaIV.
 Both ST8SiaII and ST8SiaIV can independantly act on NCAM and in principal hold the same function, but differ in details of acceptor specificity, length of synthesised polySia (Kojima *et al.*, 1997; Kitazume-Kawaguchi *et al.*, 2001; Angata *et al.*, 2002; Oltmann-Norden *et al.*, 2008; Galuska *et al.*, 2008), and in temporal and spatial expression patterns (Ong *et al.*, 1998; Hildebrandt *et al.*, 1998). During development, ST8SiaII is highly expressed in all neural tissues, while the expression of ST8SiaIV is lower in the level. After birth, ST8SiaII expression levels decrease more drastically than those of ST8SiaIV, so that the latter becomes the dominant polyST in adult brain. Accordingly, ST8SiaIV is the prominent enzyme espressed in areas of ongoing neuronal and synaptic plasticity in the adult (Ong *et al.*, 1998; Hildebrandt *et al.*, 1998; Oltmann-Norden *et al.*, 2008)

NCAM-mediated effects on cellular processes upon polySia removal was shown to depend on both heterophilic and homophilic interactions (reviewed in Hinsby *et al.*, 2004 and Ditlevsen *et al.*, 2008). Understanding the structural basis of these homophilic interactions has been subject to intense discussion with partially ambiguous or opposing conclusions (reviewed in Kiselyov *et al.*, 2005). Using a mutational approach Rao *et al.* mapped the homophilic binding site to Ig domain 3 and identified a sequence KYSFNYDGSE spanning from Lys^{243} to Glu^{252} to be crucially involved in this interaction (Rao *et al.*, 1992; Rao *et al.*, 1993; Rao *et al.*, 1994). Using bead aggregation assays, Ranheim *et al.* (1996) demonstrated binding of Ig1 to Ig5 and of Ig2 to Ig4 in addition to Ig3-Ig3 reciprocal binding. However, surface plasmon resonance binding studies by Kiselyov *et al.* (1997) did not confirm any of these interactions, but demonstrated an interaction of Ig1 with Ig2 instead. This was confirmed by size-exclusion chromatography, NMR and analytical ultracentrifugation studies and the crystal structure of Ig1-Ig2 (Jensen *et al.*, 1999; Atkins *et al.*, 1999; Atkins *et al.*, 2001; Kasper *et al.*, 2000). Atkins *et al.* (2001) also confirmed the lack of reciprocal binding of the soluble Ig3 domain. The crystal structure of Ig1-Ig2-Ig3 seemed to shed more light on these seemingly contradictory data by revealing three binding states of NCAM: *cis* dimerisation mediated by reciprocal binding of Ig1 to Ig2, and two modes of *trans* interactions leading to the formation of the so called flat zipper (mediated by interaction of Ig2 with Ig3) and dense zipper (mediated by interaction of Ig1 with Ig3 and Ig2 reciprocal binding) or cluster structures upon combination of both zipper models. Interestingly, the Ig3-Ig1 interface involved in the formation of the dense zipper included the sequence Lys^{243}-Glu^{252} identified by Rao *et al.* to be responsible for Ig3 reciprocal binding (Soroka *et al.*, 2003).

Studies using surface force measurements and atomic force microscopy confirmed the existence of two *trans*-binding states, which were interrupted by deletion of Ig1 and 2 or Ig3, respectively (Johnson *et al.*, 2004; Wieland *et al.*, 2005). The authors interpret the data in support of the primarily described models displaying a reciprocal overlap of (1) all five Ig-domains and (2) Ig1 and Ig2, respectively. However, the data obtained by these experiments are not unambiguous and further studies are required to eventually solve the dynamics inhering NCAM homophilic binding.

Similarly, the mechanism of NCAM interaction with the polySTs is barely understood, although, based on the high specificity of the polysialylation reaction, it is supposed to rely on protein-protein interactions. Supporting this, Colley and colleagues have found that ST8SiaIV coprecipitates with NCAM in pull down experiments (Colley, 2010). Mediratta *et al.* (2005) identified an NCAM fragment consisting of the domains Ig5 and FN1 to be the minimally required acceptor structure for recognition by the ST8SiaIV. FN1 seems to be crucially involved

in making the contact to the enzyme, since deletion of this domain abolished polysialylation of N-glycans on Ig5. Bioinformatic evaluations conducted by this group identified structures in FN1 involved in enzyme recognition in more detail. Thereby, an α-helix linking β-strands 4 and 5 of the β-sandwich structure, which is unique to NCAM FN1, and the so called QVQ sequence support polysialylation of Ig5 N-glycans, while the core residues of the so called acidic patch and the PYS sequence play a role in O-glycan polysialylation (Mendiratta *et* al., 2006; Foley 2010b).

The polySTs ST8SiaII and ST8SiaIV are type II membrane proteins containing the sialylmotifs L, S, III and VS, shared as a common feature with all characterised mammalian sialyltransferases (reviewed in Harduin-Lepers *et al.*, 2001). The enzymes further comprise a polybasic region directly upstream of sialylmotif S, conserved only among the polySTs, and thus called Polysialyltransferase Domain (PSTD). Mutation of central amino acids or deletion of the whole domain resulted in drastically reduced activity (Nakata *et al.*, 2006). In ST8SiaIV, this domain has been shown to be important for NCAM- as well as for autopolysialylation, indicating a general role in the polysialylation process. In contrast, mutations in the polybasic region (PBR) located upstream of sialylmotif L, strongly decreased NCAM polysialylation, while only partially impacting autopolysialylation, suggesting a role in interaction with the NCAM molecule (Foley *et al.*, 2009).

ST8SiaIV and ST8SiaII are decorated by 5 and 6 N-glycosylation sites, respectively, and it has been shown that the presence of the highly conserved N-glycosylation site 2 in ST8SiaIV and 3 in ST8SiaII is essential for enzyme activity. In ST8SiaII, N-glycosylation sites 5 and, to a lesser extend, 6 are further required for full catalytic activity (Mühlenhoff *et al.*, 2001; Close *et al.*, 2001). As the aim of this study was to obtain material for an in depth structural and biochemical analysis of the polyST/NCAM interaction, expression constructs were cloned to allow the production of both proteins in insect cell systems. The set of proteins produced enabled a differential evaluation of homophilic NCAM interactions and NCAM-polyST interactions. Moreover, initial steps have been implemented towards determining the crystal structure of NCAM and the polyST ST8SiaII.

Material and Methods

ST8SiaII constructs

The constructs pFastBac-HBM-6xHis-mST8SiaIIΔ56 and pFastBac-HBM-6xHis-mST8SiaIIΔ72 were cloned by Almut Günzel as described in Günzel (2004). ST8SiaII fragments were PCR amplified using the following primer pairs: KS93: GCATCCATGGTTGTAATAAATGGCTCTTCA / KS10r: TGAAGCTTTTACGTAGCCCCATCACA CTG (pFastBac-HBM-6xHis-mST8SiaIIΔ56) and KS94: GCATCCATGGAAAGCCTTAAGCACAA CATC / KS10r : TGAAGCTTTTACGTAGCCCCATCACACTG (pFastBac-HBM-6xHis-mST8SiaIIΔ72).

For the generation of pFastBac-HBM-6xHis-mST8SiaIIΔ56(+3,5) and pFastBac-HBM-6xHis-mST8SiaIIΔ56(+3,5,6) the ST8SiaII portion was PCR amplified from pFastBac-HBM-ST8SiaIIΔ31 (+3,5)-mycHis and pBlueScript-STX Δ1,2,4, respectively, using the primer pair KS93: GCAT<u>CCATGG</u>TTGTAATAAATGGCTCTTCA / KE01: GCTGAAGCTTTTACGTAGCCCCATCACAC, and ligated into pFastBac-HBM-6xHis via *Nco*I and *Hind*III restriction sites.

The primers originally used for mutation of the N-glycosylation sites are described in Mühlenhoff *et al.* (2001).

For the generation of pFastBac-HBM-mST8SiaIIΔ56-HRV3C-myc-6xHis, the ST8SiaII fragment was PCR amplified from pFastBac-HBM-6xHis-mST8SiaIIΔ56 using the primer pair KE07: GCTTGAGCTCGAGAGTTGTAATAAATGGCTCTTCAC / KE08: CGTTTCTAGATTACGTA GCCCCATCACAC and cloned into the myc-6xHis tag containing vector pFastBac-HBM-PST-MH via restriction sites for *Sac*I and *Xba*I, and a subsequent adaptor ligation using the primer pair KE02: CTAGAAGTGGTGGTGGCCTTGAAGTCCTCTTTCAGGGACCCGGTTCAACTAGTGGTGGT GGCGGTTCTAATAACAATCCTCCTACTG / KE03: CTAGCAGTAGGAGGATTGTTATTAGAACCGCCACC ACCACTAGTTGAACCGGGTCCCTGAAAGAGGACTTCAAGGCCACCACCACTT resulted in insertion of the HRV3C protease cleavage site via an *Xba*I restriction site.

For the generation of pFastBac-HBM-protA-6xHis-HRV3C-mST8SiaIIΔ56, the protA-6xHis-HRV3C portion was PCR amplified from pProtA-His-HRV3C using the primer pair KE04: GATCCGAGCTCAGCTGATAACAATTTCAACAAAG / KE05: ATCGTACCATGGCTGGGCCTTGGA ACAGCA. PCR products were ligated into pFastBac-HBM-6xHis by the use of *Sac*I and *Nco*I.

For the generation of pFastBacDual*6xHis-mST8SiaIIΔ56*6xHis-NCAM Ig1-FN2*, the ST8SiaII fragment was subcloned from pFastBac-6xHis-mST8SiaIIΔ56 using the restriction sites for *Bss*HII and *Hind*III. The NCAM fragment was subsequently PCR amplified from pFastBac-6xHis-NCAM Ig1-FN2 using the primer pair KE09: GAAGCTCGAGATGAAATTCTT AGTCAACGTTG / KE10: GCCGGCTAGCTTAGGTCCTGAACACAAAATGA and ligated into the vector using *Xho*I and *Nhe*I restriction sites.

NCAM constructs

The insert for NCAMIg1-FN2 was PCR amplified from the plasmid pAM1 containing the sequence for human NCAM-140. All further constructs were amplified from pFastBac-HBM-6xHis-NCAM Ig1-FN2 using the following primer pairs:

Construct	Primer pair
NCAM Ig1-Fn2	tk07: 5'-GCAGGGATCCCTGCAGGTGGATATTG-3'
	tk05r: 5'-ATCGCGGCCGCCGAGGTCCTGAACAC-3'
NCAM Ig4-Fn1	tk23: 5'-TTTGCGTCGACCAAAATCACTTATGTAGAG-3'
	tk04r: 5'-GTTAAAGCTTTTATGGCTGCGTCTTGAAC-3'
NCAM Ig5-Fn1	tk02: 5'-ACCGGATCCCAGGACTCCCAGTC-3'
	tk04r: 5'-GTTAAAGCTTTTATGGCTGCGTCTTGAAC-3'
NCAM Ig3-Fn2	KE24: 5'-GATCGGCGCCATGAGAACCATCCAGGCCAGGCAG-3'
	tk08: 5'-GTGGGAAGCTTTTAGGTCCTGAACAC-3'
NCAM Ig3-Fn1	KE24: 5'-GATCGGCGCCATGAGAACCATCCAGGCCAGGCAG-3'
	tk04: 5'-GTTAAAGCTTTTATGGCTGCGTCTTGAAC-3'
NCAM Ig1-Ig5	KE13: 5'-TGACCTCGAGTG ATGAAATTCTTAGTCAACGTT-3'
	KE25: 5'-TAGCAAGCTTTTATGCTTGAACAAGGATGAATTCC-3'
NCAM Fn1-Fn2	KE26: 5'-GATCGGCGCCGACACCCCCTCTTCACCAT-3'
	KS7R: 5'-CAACAATTGCATTCATTTTAT-3'

The PCR products were cloned into a modified pFastBac HT A vector (Invitrogen) containing a Honey Bee Mellitin secretion signal and an N-terminal Hexahistidine (6xHis) tag using the following restriction sites: *Not*I/*Bam*HI (NCAM Ig1-Fn2), *Sal*I/*Hind*III (NCAM Ig4-Fn1), *Bam*HI/*Hind*III (NCAM Ig5-Fn1) and *Kas*I/*Hind*III (NCAM Ig3-Fn2, NCAM Ig3-Fn1, NCAM Ig1-Ig5 and NCAM Fn1-Fn2). NCAM Ig1-Fn1sec was generated by two sequential adaptor ligations introducing the sequence of primer pairs KE18/KE19 (*Bsi*WI/*Kpn*I) and KE20/KE21 (*Kas*I/*Hind*III) into the plasmid pFastBac NCAM Ig1-Fn2.

	Primer pair
1st adaptor ligation	KE18: 5'-GTACGCCGTAAGGCTGGCGGCGCTCAATGGCAAAGGGCT GGGTGAGATCAGCGCGGCCTCCGAGTTCAAGACGCAACCGGTCCGT AC-3'
	KE19: 5'-CGGACCGGTTGCGTCTTGAACTCGGAGGCCGCGCTGATCT CACCCAGCCCTTTGCCATTGAGCGCCGCCAGCCTTACGGC-3'
2nd adaptor ligation	KE20: 5'- CCGGTCAAGAACATAGCACAGAATCACTGCTGCAACATG TTCCAAGCTGGACTGCATAATGCACTGATGAAGTAAA-3'
	KE21: 5'- AGCTTTTACTTCATCAGTGCATTATGCAGTCCAGCTTGGA ACATGTTGCAGCAGTGATTCTGTGCTATGTTCTTGA-3'

The constructs code for the following NCAM protein fragments (according to UniProt 13596), none of them comprising the VASE exon:

Construct	protein fragment
NCAM Ig1-Fn2	Ser^{19}-Thr^{702}
NCAM Ig4-Fn1	Lys^{309}-Pro^{607}
NCAM Ig5-Fn1	Gln^{393}-Pro^{607}
NCAM Ig3-Fn2	Thr^{213}-Thr^{702}
NCAM Ig3-Fn1	Thr^{213}-Pro^{607}
NCAM Ig1-Ig5	Ser^{19}-Ala^{507}
NCAM Fn1-Fn2	Ala^{497}-Thr^{702}
NCAM Ig1-Fn1sec	Ser^{19}-Val^{608} followed by the sec-sequence: KNIAQNHCCNMFQAGLHNALMK

Sf9 insect cell culture

*Sf*9 insect cells were grown in suspension culture at a density of 0.5-$5x10^6$ cells/ml in protein free Insect Xpress Medium (BioWhittaker, Cambrex-Lonza) at 70-90 rpm and 27 °C. Cells were counted and diluted to a density of $0.5x10^6$ cells/ml with fresh medium every 2-3 days.

For long-term storage, cells were pelleted by centrifugation at 150xg for 4 min and resuspended in 50 % conditioned medium containing 7.5 % DMSO at a density of $2x10^7$ cells/ml. 1 ml-Aliquots of this suspension were frozen stepwise (4 °C for 30 min, -20 °C for 1h and -80 °C over night) before being transferred to liquid nitrogen.

For recovering frozen cells, samples were incubated in a water bath at 37 °C and cells were transferred into 29 ml of fresh medium immediately after thawing. Cells were counted daily and kept at a density of 0.7-2x10^6 cells/ml during the first 2 weeks after thawing.

Protein expression in Sf9 insect cells

Baculoviruses coding for the respective NCAM fragments were generated using the Bac-to-Bac® Baculovirus Expression System (Invitrogen) according to the manufacturer's instructions. In short, pFastBac derived plasmids were transformed into *E. coli* DH$_{10}$Bac, and the gene of interest was transposed into the contained bacmid. Bacmids were purified by anion exchange chromatography and transfected into *Sf*9 insect cells to generate a low-titer virus stock (P1) which was harvested after 7 days' incubation. To enhance virus concentration, freshly seeded cells were infected with P1 in a dilution of 1:100 and incubated for 3-4 days to generate a medium-titer virus stock (P2). Infection of cells with P2 (1:1000) and incubation for another 4 days yielded a high-titer virus stock (P3).

log-phase *Sf*9 cells at a density of 1.7-2x10^6 cells/ml were infected with different amounts of P3 virus stock with dilutions ranging between 1:100 and 1:1000. Every 24 h cells were counted and examined microscopically to analyse viability and infection status of the cells, and the cell culture supernatants were analysed in SDS-PAGE and western blots directly and after TCA precipitation (3.4.). Thus, optimal viral dilutions for infection and harvesting timepoints were determined.

Protein precipitation by trichloroacetic acid (TCA)

200 µl TCA were added to 800 µl cell culture supernatant and incubated on ice for 10 min. After centrifugation at 13,500 rpm and 4 °C for 10 min, pellets were washed with 500 µl acetone and centrifuged again (13,500 rpm, 4 °C, 10 min). Pellets were resuspended in 40 µl 2 x Laemmli buffer containing 5 % β-mercaptoethanol.

SDS-PAGE

SDS-PAGE was performed according to Laemmli (1970) under reducing conditions. Gels were composed of a 3 % stacking gel (125 mM Tris-HCl pH 6.8, 0.1 % SDS 3 % acrylamide [40 % 4K-Mix, AppliChem]) and an 8 % or 10 % separating gel (375 mM Tris-HCl pH 8.8, 0.1 % SDS, 8 % or 10 % acrylamide [40 % 4K-Mix, AppliChem]). Polymerisation was mediated by addition of 0.1 % TEMED and 1 % ammonium persulfate.

Samples were diluted with 2x Laemmli buffer containing 5 % β-mercaptoethanol and incubated for 5 min at 99 °C or for 10 min at 60 °C if containing heat sensitive polySia.

Electrophoresis was performed in 50 mM Tris buffer containing 350 mM glycine and 0.1 % SDS at 70 V, while samples traversed the stacking gel, and 140 V after entering into the separating gel.

Gels were subjected to western blotting (3.7.) for specific staining or developed with colloidal Coomassie blue staining (Roti-Blue, Roth) or silver staining for unspecific protein staining. For the latter purpose, gels were incubated in fixation solution (1.85 % formaldehyde, 10 % acetic acid, 30 % ethanol) for 20 min, washed three times in 50 % ethanol for 20 min and incubated for 1 min in a solution of 0.2 mg/ml $Na_2S_2O_3$. After washing three times in deionised water for 20 s, gels were incubated in silver staining solution (0.2 % $AgNO_3$, 2.8 % formaldehyde) for 20 min and washed twice in deionised water for 20 s. Gels were incubated in developing solution (6 % Na_2CO_3, 4 µg/ml $Na_2S_2O_3$, 1.85 % formaldehyde) until bands became visible. Staining was stopped by washing with deionised water and incubation with stop solution (10 % acetic acid, 30 % ethanol). Gels were incubated in drying solution (10 % glycerol, 20 % ethanol) and dried in cellophane foil.

Western Blotting

Western blotting was performed at 2 mA/cm^2 in blotting buffer (48 mM Tris buffer, 39 mM glycine) for 45 min. Proteins were transferred onto nitrocellulose membranes (Schleicher & Schüll) using a semidry blotting chamber (Biometra).

Membranes were blocked in blocking buffer (2 % milk powder in PBS containing 0.02 % NaN_3) for 1 h at room temperature or over night at 4 °C and incubated with 1 µgml anti 5xHis antibody (Qiagen) or 5 µg/ml monoclonal antibody 735 or 3.76 µg/ml mouse IgG (Pierce) in blocking buffer. After washing three times with PBS, the membranes were incubated with alkaline phosphatase (AP) conjugated goat anti mouse antibody (Dianova) diluted 1:5,000 in blocking buffer. After washing twice with PBS and once with AP buffer (100 mM Tris-HCl pH 9.5, 100 mM NaCl, 5 mM $MgCl_2$), bands were visualized by incubation with 162.5 µg/ml BCIP and 325 µg/ml NBT in AP buffer.

Protein purification

1-4 l of *Sf*9 insect cell cultures were infected with the optimal amount of P3 baculoviral stock and incubated at the optimal timeframe as determined earlier. Cell culture supernatants were centrifuged at 300xg and 4 °C for 10 min. Supernatants were adjusted to pH 7.5 by adding 5 M

NaOH and centrifuged again at 7,000xg and 4 °C for 25 min. After filtration (0.2 μm, Steritop, Millipore) the supernatants were concentrated using an Ultrasette (Pall, MWCO 10,000) at 4 °C. After concentration to ca. 100 ml, the supernatant was diluted 1:5 with buffer D (50 mM Tris-HCl pH 7.5, 100 mM NaCl) and concentrated to 50-100 ml. After filtration (0.2 μm, Millex, Millipore), 10 % Glycerol was added. Expressed proteins were bound to an appropriate volume of Ni^{2+} chelating matrix (1-4 ml ProBond Resin, Invitrogen) or to 1-2 x 1 ml HisTrap columns (GE Healthcare) over night. The columns were washed and eluted using an Äkta FPLC system (GE Healthcare) at a flow rate of 1 ml/min. Using buffers A (50 mM Tris-HCl pH 7.5, 100 mM NaCl, 10 % Glycerol) and B (50 mM Tris-HCl pH 7.5, 100 mM NaCl, 400 mM Imidazole, 10 % Glycerol), a stepwise imidazole gradient was generated for washing the column and eluting the 6xHis tagged proteins.

Fractions containing ST8SiaII or NCAM, respectively, were pooled and concentrated using an Amicon Ultra (Amicon) or Vivaspin (Vivascience) ultrafiltration device. Size-exlusion chromatography was applied for further purification and for analysis of the oligomerisation status.

Therefore, a Superdex 200 HR 10/300 GL (Amersham Biosciences; used for mST8SiaIIΔ56, NCAM Ig4-Fn1, NCAM Ig5-Fn1, NCAM Ig3-Fn1, NCAM Ig1-Ig5, NCAM Fn1-Fn2) or HiLoad 16/60 Superdex 200 (Amersham Biosciences; used for NCAM Ig1-Fn2, NCAM Ig3-Fn2, NCAM Ig1-Fn1sec) gelfiltration column was equilibrated with 1-2 volumes of buffer G (10 mM Tris-HCl pH 7.5, 100 mM NaCl) with the pH adjusted to the respective temperatures (room temperature using Superdex 200 HR 10/300 GL; 4 °C using HiLoad 16/60 Superdex 200). Samples were loaded onto the column, using a 500 μl-loop for Superdex 200 HR 10/300 GL and a 5 ml-loop for HiLoad 16/60 Superdex 200, and separated at a flow-rate of 0.5 ml/min. Fractions containing ST8SiaII or NCAM, respectively, were pooled and further concentrated to 1 mg/ml total protein as determined by Bio-Rad Protein Assay (BioRad). Samples were shock frozen in liquid nitrogen and stored at -80 °C.

Polysialyltransferase activity assay

37.5 μg/ml mST8SiaIIΔ56 were incubated with 125 μg/ml NCAM produced in CHO 2A10 or insect cells, respectively, and 1 mM CMP-Neu5Ac in 10 mM MES buffer pH 6.5 containing 10 mM MnCl$_2$. 2A10 cells lack polysialyltransferase activity due to a mutation in the ST8SiaIV gene, and thus produce NCAM in an unpolysialylated form (Windfuhr *et al.*, 2000). After three hours incubation, 0.05-0.1 μg/ml endoneuraminidase (EndoN) was added for specific degradation of polySia chains. To avoid competing re-building of the chains, this incubation step

was performed in Laemmli buffer under reducing conditions which inactivates mST8SiaII but not EndoN. Samples were applied to 10 % SDS-PAGE and western blotting with subsequent immunostaining of the membranes.

The radioactive version of this assay has been described in Eggers (2006).

Crystallisation

Purified proteins were concentrated to 5 mg/ml or 10 mg/ml (ST8SiaII), or 10 mg/ml (NCAM), respectively, in 10 mM Tris-HCl buffer pH 7.5 containing 100 mM NaCl and were subjected to crystallisation trials performed as sitting drop vapour diffusion experiments in our laboratory and at the High Throughput Crystallisation facility of the European Molecular Biology Lab (EMBL) in Hamburg (Muller-Dieckmann, 2006).

Prior to shock freezing the obtained crystals in liquid nitrogen, 15% ethylenglycole were successively added to the buffer as a cryoprotectant.

Analytical ultracentrifugation

Analytical ultracentrifugation experiments were performed with an An-50 Ti rotor in a Beckman Optima XL-A or a Beckman Coulter ProteomeLab XL-I analytical ultracentrifuge using the respective Beckman Coulter software for programming and data recording. Concentration profiles were measured at 280 nm using the centrifuge's UV absorption scanning optics.

Sedimentation velocity experiments were performed at 23,000-50,000 rpm in 3 or 12 mm double sector centrepieces filled with 100 µl or 400 µl, respectively, and obtained data were analysed using the SEDFIT program package providing a model for diffusion corrected differential sedimentation coefficient distributions (c(s) distributions) (Schuck *et al.*, 2000). Measured s-values were corrected to $s_{20,W}$ using the partial specific volumes calculated from amino acid composition (Durchschlag *et al.*, 1986)

Sedimentation equilibrium experiments were carried out in standard 3 or 12 mm double sector centrepieces filled with 40 µl or 150 µl sample, respectively, and the samples were centrifuged at 12,000, 14,000, 18,000, 22,000, 25,000 and 28,000 rpm until no change in the concentration gradients could be observed for at least 12 h. Scans from these 12 h were averaged and molar masses were evaluated using BPCFIT software as described in Witte *et al.* (2005).

Results

1. Production of recombinant ST8SiaII

The restricted accessibility of recombinant polySTs is a major problem for their structural characterisation. The aim of this study was therefore to establish a robust protocol for the production of mammalian polySTs. Based on pioneering expression studies carried out by a previous doctorial student in the laboratory (Dr. Almut Günzel), murine ST8SiaII (mST8SiaII) was chosen as a model protein. Trials to express mST8SiaII in a bacterial system were unsuccessful as activity and soluble expression of the enzyme is dependant on correct disulfide bonds and the presence of N-glycosylation sites. In my diploma thesis (Eggers 2006), expression of murine ST8SiaII was tested in different eukaryotic expression systems. Since expression in CHO cells resulted in low protein yields, a production system was established using High Five and *Sf*9 insect cells in combination with a baculoviral system to express the murine enzyme lacking the first 56 amino acids and carrying an N-terminal hexa-histidine tag (6xHis-mST8SiaIIΔ56).

This part of my thesis was aimed at further optimising the described purification procedure to gain active and stable enzyme in reasonable amounts to start crystallisation trials and to provide material for further investigations of the polysialylation reaction.

Determination of an enzymatically active mST8SiaII construct harbouring optimal features for recombinant expression in insect cells.

Sialyltransferases are typical type II membrane proteins with a short cytoplasmic tail located at the N-terminus, a single transmembrane spanning region and a large catalytic domain facing the Golgi lumen (Harduin-Lepers *et al.*, 2001). For production of the recombinant enzyme we intended the expression of the isolated catalytic domain. However, because it is known that the extend of truncation can impact protein expression, N-terminally truncated constructs of variable length were generated. The constructs with 72 and 56 amino acid deletions (mST8SiaIIΔ72 and mST8SiaIIΔ56) (see Fig. 1) were comparatively tested in this study. Furthermore, as protein crystallisation was an important goal in this study, attempts were undertaken to facilitate crystallisation by reducing conformational flexibility. Therefore, the number of N-glycosylation sites in the recombinant mST8SiaII variants were reduced to a minimum, since N-glycans were shown to potentially disturb crystallisation. As described in the introduction (Mühlenhoff *et al.*, 2001; Close *et al.*, 2001) the N-glycan residing on the highly conserved 3rd N-glycosylation site (Asn[89]) is essential for activity and Asn[219] (N-glycosylation site 5) and, to a lesser extend, Asn[234]

(N-glycosylation sites 6) support the functionality of the recombinant protein. Thus, two constructs containing only the above described N-glycosylation sites were generated by mutating the respective Asn residues to Gln (constructs mST8SiaIIΔ56(+3,5) and mST8SiaIIΔ56(+3,5,6); see Fig. 1). All constructs contained an N-terminal 6xHis tag (see Fig. 1).

In preliminary experiments (diploma thesis Eggers 2006), affinity purification using Ni^{2+} chelating chromatography showed that efficiency and specificity in this first binding step was not always optimal. Therefore, a second aim of this study was to improve affinity purification by using alternative epitope tags allowing for usage of antibody based affinity chromatography. As shown in Fig. 1, constructs containing a C-terminal myc epitope or an N-terminal protein A (protA) tag, respectively, were generated (mST8SiaIIΔ56-HRV3C-myc-6xHis and protA-6xHis-HRV3C-mST8SiaIIΔ56), Both epitope tags are removable by usage of the HRV3C protease cleavage site, thus allowing elution of the enzyme by highly specific on-column cleavage. Furthermore, the protA tag was chosen to potentially improve solubility and expression level.
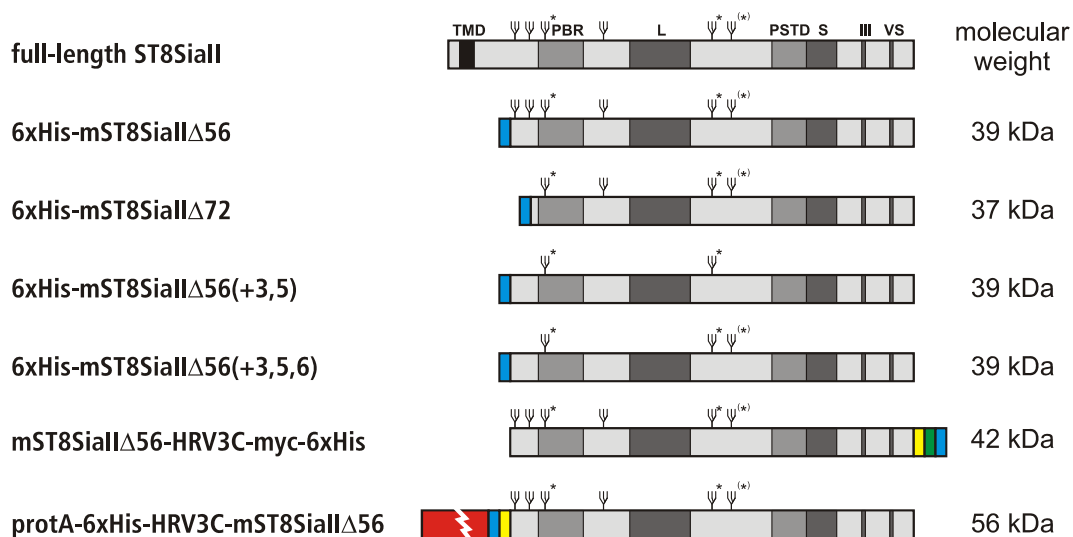
Fig. 1: Schematic of ST8SiaII constructs. ψ: N-glycosylation site, TMD: transmembrane domain, PBR: polybasic region, PSTD: polysialyltransferase domain, L: sialylmotif L, S: sialylmotif S, III: sialylmotif III, VS: sialylmotif VS, blue: 6xHis tag, red: protA tag, yellow: HRV3C protease cleavage site, green: myc tag, N-glycosylation sites crucial for activity are marked by asterisks.

All constructs were cloned into a pFastBac vector containing a honey bee mellitin (HBM) secretion signal and were transformed into *E. coli* DH$_{10}$Bac to obtain a transposition of the gene of interest into the contained bacmid for the generation of baculovirus. The bacmid DNA was purified and transfected into *Sf*9 cells for generation of a low-titer virus stock. The high-titer virus stock was generated by two amplification steps in freshly seeded cells. For optimisation of expression conditions, a test expression was performed using different dilutions of the viral stock and different harvesting time points. To detect recombinant proteins, which were secreted by use of the HBM signal, cell culture supernatants were analysed by Western blotting before and after 20-fold concentration by protein precipitation.

The test expression shown in Fig. 2 clearly demonstrated that depletion of N-glycan attachment sites in mST8SiaII resulted in a considerable reduction of protein expression. While mST8SiaIIΔ56 was readily detectable already after 24h in the supernatant of transfected cells, all variants with reduced N-glycosylation sites were only detectable after 20-fold concentration. Notably, the expression level of the more intensely truncated variant mST8SiaIIΔ72 was low compared to mST8SiaIIΔ56. However, as this construct lacks the first two N-glycosylation sites, reduction of protein expression may also be due to incomplete N-glycosylation.
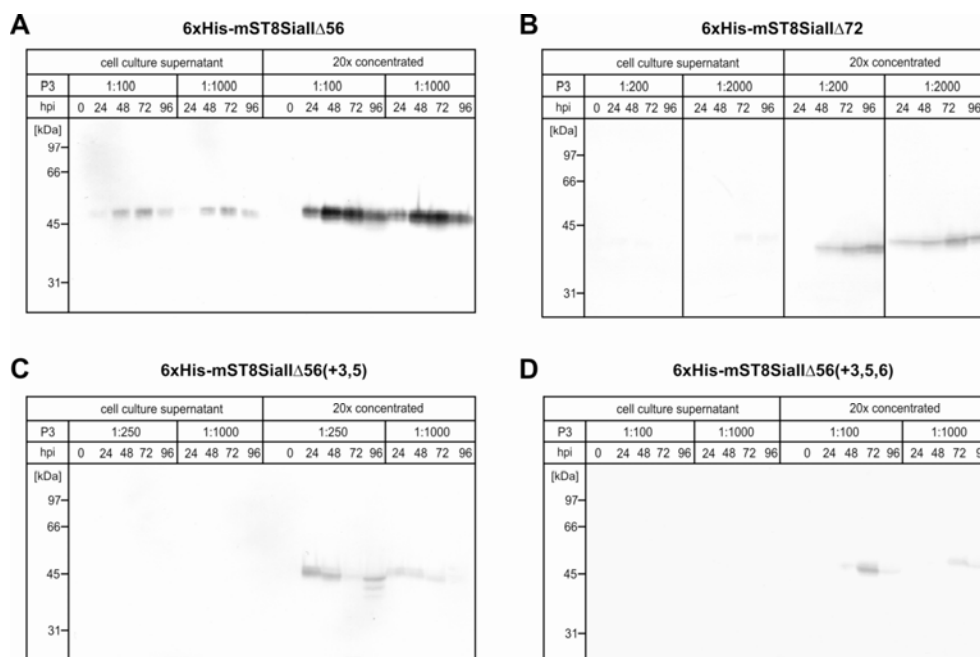
Fig. 2: Test expression of mST8SiaII truncation and glycosylation mutants. *Sf*9 cells were infected with varying dilutions of a P3 baculoviral stock, and cell culture supernatants were harvested at varying time points, as indicated. Samples were analysed before and after 20-fold concentration by TCA precipitation on a 10% SDS-PAGE followed by Western blotting. Blot membranes were immunostained with anti 5xHis antibody. hpi, hours post infection

Typically, migration of glycoproteins in SDS-PAGE is shifted to higher molecular weights by 3 kDa per occupied N-glycosylation site. Accordingly, all protein bands appear at a higher

molecular weight as expected from the amino acid sequence (Fig. 1). This effect increases with the number of N-glycosylation sites present (Fig. 2).

Due to the impressive differences in expression levels, mST8SiaIIΔ56 was used for further optimisation in all following studies.

To evaluate the suitability of alternative tag sequences, the constructs mST8SiaIIΔ56-HRV3C-myc-6xHis and protA-6xHis-HRV3C-mST8SiaIIΔ56 (Fig. 1) were expressed in insect cells as described above and cell culture supernatants were analysed by western blotting. For the myc tagged variant mST8SiaIIΔ56-HRV3C-myc-6xHis, no protein could be detected in two independant experiments starting from the generation of baculovirus (data not shown). In contrast, the construct containing a cleavable protA-6xHis tag (protA-6xHis-HRV3C-mST8SiaIIΔ56) was well expressed and appeared as a double band at ~60 kDa. Since the expression level was comparable to that of the respective non-cleavable 6xHis tagged construct (6xHis-mST8SiaIIΔ56), protA-6xHis-HRV3C-mST8SiaIIΔ56 seemed a suited candidate for the development of an alternative purification procedure.

Fig. 3: Test expression of ProtA-6xHis-HRV3C-mST8SiaIIΔ56. Indicated dilutions of a P3 viral stock were used to infect *Sf*9 cells. Cell culture supernatants were harvested at indicated time points and analysed on a 10% SDS-PAGE followed by western blotting and immunostaining with anti 5xHis antibody. Supernatants were analysed before or after 20x concentration by TCA precipitation. (hpi: hours post infection)
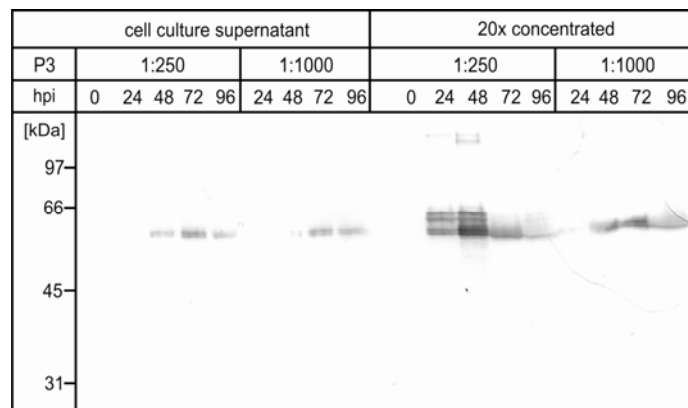
Thus, purification trials for protA-6xHis-HRV3C-mST8SiaIIΔ56 were performed. The enzyme was expressed using the optimised conditions, and extracted with IgG-sepharose beads. Subsequently, release of the enzyme was performed by HRV3C protease cleavage and beads and supernatants were analysed in parallel by SDS-PAGE and coomassie staining or by western blotting, using anti-protA and anti-5xHis antibodies (the latter recognising the 6xHis tagged HRV3C protease and the tag released from protA-6xHis-HRV3C-mST8SiaIIΔ56). Results are shown in Fig. 4 and demonstrate that more than 50% of the protein could be cleaved by this procedure. However, it is remarkable that despite of efficient cleavage, only a minor portion of

the expressed protein was eluted, since again, more than 50% of the cleaved protein adhered unspecifically to the beads.

As the activity of polySTs depends on the presence of divalent cations, we speculated that the EDTA contained in the protease buffer may have a negative influence on the conformation of mST8SiaII and thus promote adherence to the beads. The experiment was therefore repeated in the absence of EDTA. Moreover, sodium chloride concentrations were increased in the washing buffer to overcome non-specific protein interactions. However, considerable improvement of the purification could not be achieved. Since despite of high expression levels only a minor portion of the recombinant protein could be isolated, the construct 6xHis-mST8SiaIIΔ56 was used in subsequent experiments.
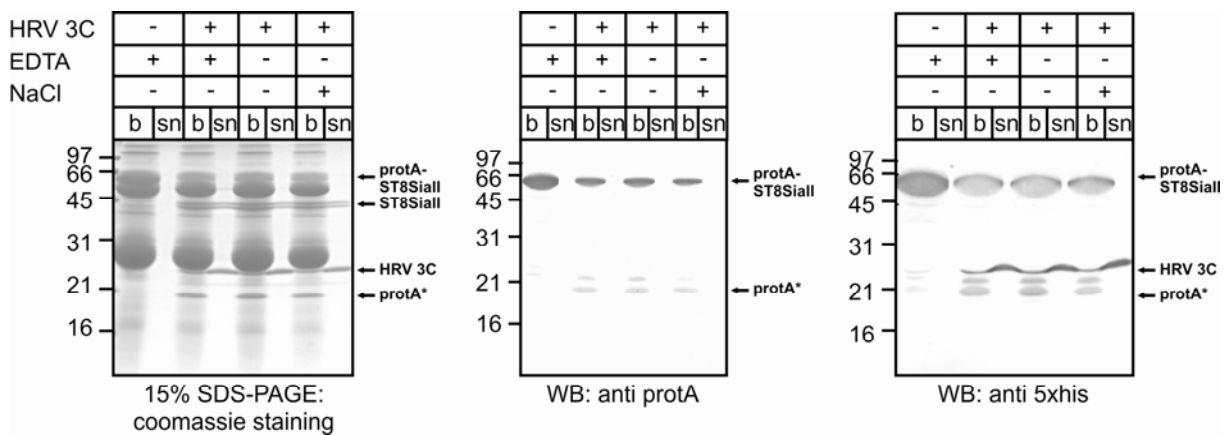
Fig. 4: Purification trials for ProtA-HRV3C-mST8SiaIIΔ56. 300 ml of *Sf*9 cells were infected with a P3 viral stock at a 1:250 dilution. Cell culture supernatants were harvested 72 h post infection, and protA tagged proteins were extracted with IgG sepharose. To release ST8SiaIIΔ56 from the fusion tag, beads were treated with HRV3C and after an incubation time of 13 h, released (sn) and bead-bound (b) protein fractions were analysed by coomassie stained 15% SDS-PAGE and by western blot using mouse IgG (anti protA) and anti 5xHis antibody.

Simultaneous expression of mST8SiaIIΔ56 and NCAM Ig1-FN2

Glycosyltransferases are typically expressed at very low level inside the mammalian cell and although expression of soluble proteins variants may improve protein yields, the large scale expression of glycosyltransferases remains a challenge (Kleene and Berger, 1993; Malissard *et al.*, 1999). Assuming that this restriction might be overcome if the nascent glycosyltransferase could form an enzyme-acceptor complex, an expression system for the co-expression of mST8SiaII with its interaction partner NCAM was established. Therefore, both 6xHis-mST8SiaIIΔ56 and a construct termed NCAM Ig1-FN2, which represents the N-terminally 6xHis tagged ectodomain of NCAM (for more details see page 42) were subcloned into the

vector pFastBacDual, which allows the simultaneous expression of two proteins under the control of two independant late promoters, namely the p10 and the polyhedrin promoter.

Baculovirus particles were produced as described and used for transfection of *Sf*9 cells. The expression of pFastBacDual*6xHis-mST8SiaIIΔ56*6xHis-NCAM Ig1-FN2* resulted in the production of two proteins displaying the expected sizes (Fig. 5). However, if compared to samples expressing the single proteins, expression levels were not increased. Nevertheless, with the availability of this system new possibilities arise for the intended studies on NCAM-polyST interactions.
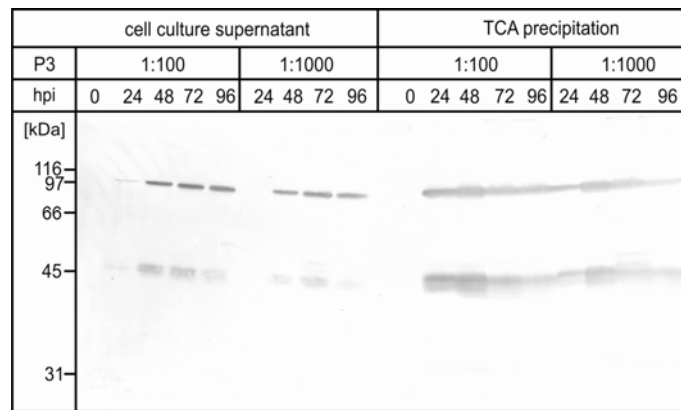
Fig. 5: Test expression of pFastBacDual*6xHis-mST8SiaIIΔ56*6xHis-NCAM Ig1-FN2*. Cell culture supernatants were applied to 10% SDS-PAGE before or after 20-fold concentration by TCA precipitation and analysed by anti 5xHis staining after western blotting.

Large-scale expression and purification of 6xHis-mST8SiaIIΔ56

To obtain material for biochemical and structural investigations, 6xHis-mST8SiaIIΔ56 was expressed in a 4 l culture of *Sf*9 insect cells under optimised conditions as determined in the small-scale test expression. Secreted enzyme was bound to Ni^{2+} sepharose and subsequently eluted with a stepwise gradient of imidazole. Size-exclusion chromatography (SEC) was used for further purification of the protein and to determine the quarternary structure. Upon calibrating the column with protein standards, it could be concluded that the recombinant ST8SiaII elutes exclusively as a monomer (data not shown).

Using this purification strategy, 250-500 mg of pure protein were obtained per litre cell culture, serving as the fundament for further characterisation of the enzyme.
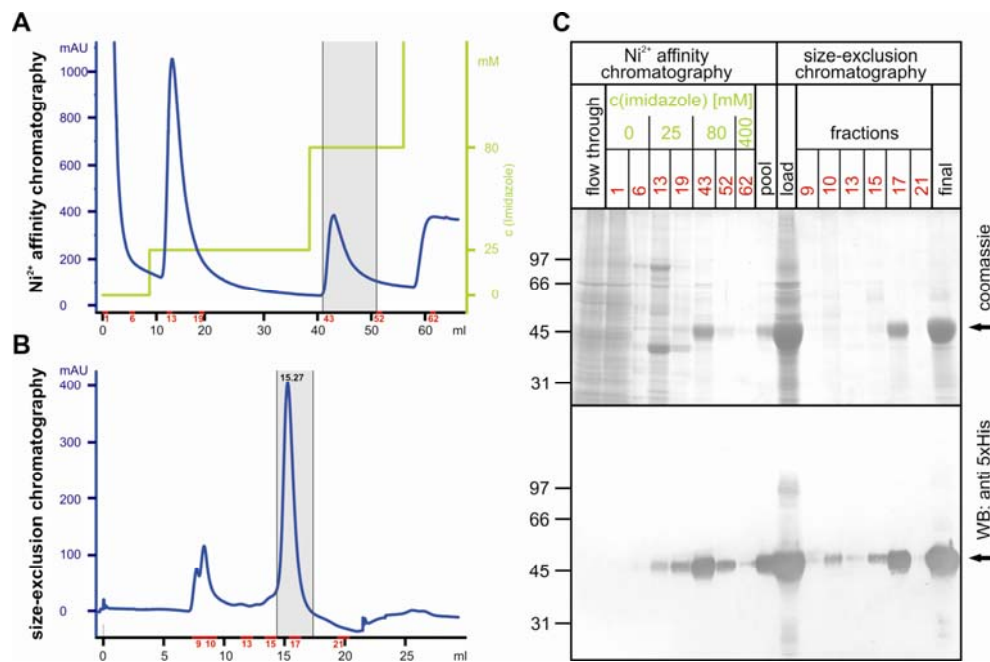
Fig. 6: Purification of 6xHis-mST8SiaIIΔ56. A, Elution profile of Ni^{2+} chelating chromatography. Absorbance at 280 nm representing protein concentration is depicted in blue, while the imidazole concentration is depicted in green. Fractions that were analysed in SDS-PAGE are marked in red, fractions that were combined and used for further purification are shaded in gray. **B**, Elution profile of size-exclusion chromatography. **C**, Analysis of selected fractions on 10% SDS-PAGE followed by coomassie staining (upper panel) or western blotting followed by anti 5xHis staining (lower panel).

Activity testing of 6xHis-mST8SiaIIΔ56

The activity of 6xHis-mST8SiaIIΔ56 in NCAM polysialylation and autopolysialylation has already been demonstrated in Eggers (2006) (Fig. 7A). Therefore, the enzyme was incubated with radiolabelled substrate CMP-[^{14}C]Neu5Ac in the presence or absence of NCAM. Samples were applied to a SDS-PAGE, and radiolabelled products were visualised by autoradiography. The diffuse radioactive smear indicates activity of 6xHis-mST8SiaIIΔ56. Treatment of polysialylated samples with EndoN specifically removes polySia. However, because EndoN is not able to remove the proximal 5 – 7 sialic acid residues, former polySia-carriers can still be visualised by autoradiography. As shown in Fig. 7A, bands corresponding to the molecular weight of NCAM and ST8SiaII appeared in the gel, confirming that the proteins were polysialylated. Remarkably, autopolysialylation of the recombinant 6xHis-mST8SiaIIΔ56 was found to be high in the presence, but not in the absence of NCAM (Fig. 7A).

When autopolysialylation of polySTs was first detected, Mühlenhoff *et al.* (1996b) showed that there are profound mechanistic differences between the process of autopolysialylation and

polysialylation of NCAM. With ST8SiaIV as a model the authors demonstrated that an initiating sialic acid residue at the non-reducing end of the polySia-acceptor glycans in NCAM was required for transfer of polySia. In marked contrast, a terminal galactose residue on polySia-acceptor sites of the enzyme was sufficient to allow for autopolysialylation (Mühlenhoff *et al.*, 1996a). Given that insect cell produced proteins contain mostly paucimannosidic type N-glycans, NCAM derived from *Sf*9 cells was not expected to act as an acceptor for ST8SiaII. However, when performing the activity assay using insect cell derived NCAM Ig1-FN2 (see page 42) small amounts of polySia could be detected by monoclonal antibody 735 after western blotting (Fig. 7B). These results imply that further analytical steps are needed to determine the structures that underlie these polysialylated proteins.
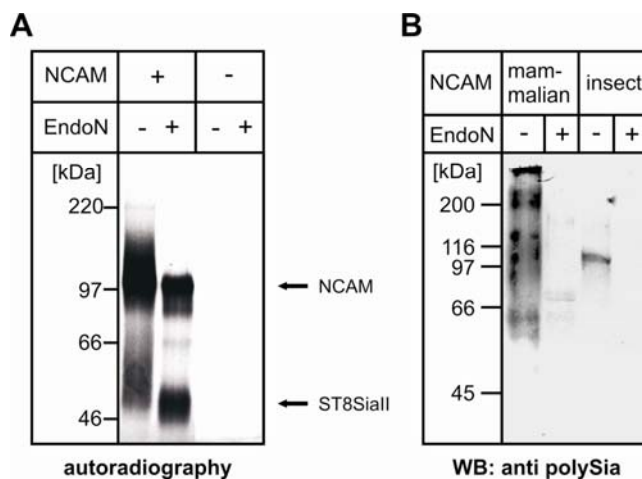
Fig. 7: NCAM polysialylation and autopolysialylation activity of mST8SiaIIΔ56. A, Figure taken from Eggers (2006). mST8SiaIIΔ56 was incubated with radiolabelled substrate in the presence or absence of CHO cell derived NCAM. Synthesised polySia was specifically degraded by EndoN. Samples were analysed by 10% SDS-PAGE and products were visualised by autoradiography. **B**, polysialyltransferase assay performed with cold substrate. PolySia was detected with mAb 735 after western blotting. In addition to the CHO cell derived NCAM (mammalian), NCAM Ig1-FN2 produced in *Sf*9 cells (insect) was used as an acceptor.

The purified enzyme appears to be very stable, since long-term storage at -80°C, even in presence of 80 mM imidazole, repeated thawing and re-freezing or storage at 4°C for three weeks did not notably change activity (data not shown). Moreover, and important in the light of the recent detection of SynCAM 1 as a novel polySia acceptor, the purified ST8SiaII was also able to polysialylate SynCAM 1 (Galuska *et al.*, 2010; see chapter 4).

Crystallisation trials

To gain further insights into the structure of ST8SiaII, crystallisation trials were performed at the High Throughput Crystallisation facility of the European Molecular Biology Lab (EMBL) in Hamburg. Approximately 1,000 buffer conditions were tested for ST8SiaII preparations at a concentration of 5 mg/ml or 10 mg/ml, respectively. Promising hits are depicted in Fig. 8, but conditions have to be further optimised to obtain crystals for X-ray diffraction. Since the structural studies require significantly more time investment, these are planned to be followed up in a future PhD study.

	Buffer conditions
	JCSG F10: 1.1 M sodium malonate pH 7.0 0.1 M HEPES pH 7 0.5% Jeffamine ED-2001 pH 7.0 c (ST8SiaII) = 10 mg/ml
	Jena1-4 C6: 100 mM MES sodium salt pH 6.5 30% (w/v) PEG 4,000 c (ST8SiaII) = 10 mg/ml
	Wizard C12: 0.1 M Tris pH 7.0 0.2 M MgCl2 10% (w/v) PEG 8,000 c (ST8SiaII) = 10 mg/ml

Fig. 8: Crystallisation trials for 6xHis-mST8SiaIIΔ56. Pre-crystals were obtained for 10 mg/ml mST8SiaII solution in 10 mM Tris pH 7.5, 100 mM NaCl by sitting drop crystallisation at the EMBL Hamburg (left panel). The respective buffer conditions are depicted in the right panel.

2. Production of NCAM fragments

To gain a deeper insight into NCAM function and to enable dissection of the roles of individual domains, a series of NCAM fragments as depicted in Fig. 9 were cloned and expressed in *Sf*9 insect cells as described above. All constructs described here comprise N-terminal 6xHis tags. In addition, a C-terminally 6xHis tagged construct of NCAM Ig1-FN2 was generated (NCAM Ig1-FN2-6xHis). The constructs' names indicate the first and last domain of the NCAM fragments; internal domains are in the natural order without deletions. All constructs except NCAM Ig4-FN1 were purified to a satisfying purity in good yields (see Fig. 9B). NCAM Ig1-Ig5 has so far been processed until test expression, so that only the large-scale purification of this fragment remains to complete the series of NCAM fragments.

Fig. 9: Schematic of NCAM fragments (A) and analysis in SDS-PAGE (B). Purified samples were applied to 10% SDS-PAGE and analysed after coomassie staining (upper panel) and western blotting followed by anti 5xHis staining (lower panel). (Ω: Ig domain, black boxes: FNIII like domain, sec: sec sequence).
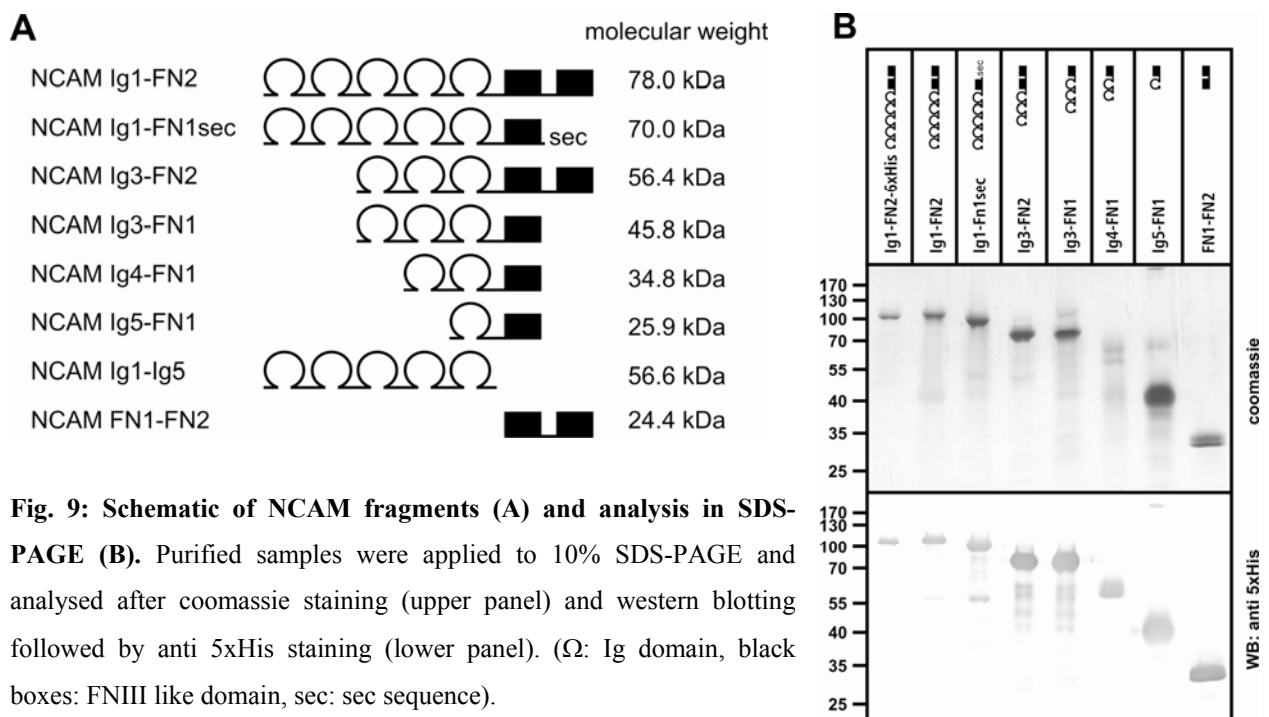
The produced fragments were used in co-crystallisation trials with mST8SiaII (NCAM Ig1-FN2, Ig5-FN1 and Ig4-FN1), crystallisation trials addressing NCAM homophilic binding (N-terminally and C-terminally 6xHis tagged NCAM Ig1-FN2 and NCAM Ig1-FN1sec) and oligomerisation studies using analytical ultracentrifugaion (NCAM Ig1-FN2, NCAM Ig3-FN2, NCAM Ig3-FN1 and NCAM Ig5-FN1), which will be described in detail in the following.

Moreover, a series of these fragments was used in a study addressing polySia and NCAM signalling in the context of tumour biology (see Chapter 3).

Crystallisation trials

Co-crystallisation with the polysialyltransferase ST8SiaII

The fact that polysialylation is restricted to specific acceptor molecules led us to the assumption that protein-protein interactions are crucially involved in the recognition of the protein acceptors. Supporting this, intensive interactions between NCAM and ST8SiaIV have been demonstrated by Colley *et al.* in a pull-down assay (Colley, 2010).

To gain deeper insight into this interaction, the co-crystallisation of ST8SiaII and NCAM was an aim of this study. Therefore, the minimally required acceptor domain of NCAM as proposed by Close *et al.* (2003) was generated (NCAM Ig5-FN1). However, studies by Nelson *et al.* (1995) and Fujimoto *et al.* (2001) suggest that Ig4 is not crucially required for, but might support NCAM recognition by the polySTs. Bearing in mind that binding of the polyST to the "minimal fragment" may be significantly reduced, also NCAM Ig4-FN1 and NCAM Ig1-FN2 were generated for use in co-crystallisation studies.

The purification of NCAM Ig4-FN1 yielded small amounts of this fragment, containing a considerable amount of protein contaminants (see Fig. 9B). Thus, it can be used as a basis for further studies relying on robust and undemanding methods. However, to obtain protein for methods as demanding as crystallisation in terms of purity and material input, further optimisation remains to be performed. The fragments NCAM Ig1-FN2 and NCAM Ig5-FN1 were purified with good yields and purity, allowing us to start the co-crystallisation trials (data not shown).

Crystallisation of the NCAM ectodomain

The nature of NCAM-NCAM homophilic interaction has been subject to intense and converse discussions (reviewed in Kiselyov *et al.*, 2005). The prevailing model is based on the crystal structure of Ig1-Ig2-Ig3. However, it cannot be excluded that *trans* interactions take place that cannot be observed in this structure due to the severe truncation of the Ig1-Ig2-Ig3 fragment. The crystal structure of the entire ectodomain of NCAM would open possibilities towards a deeper understanding of these probably complex interactions.

Purification of NCAM Ig1-FN2-6xHis for crystallisation trials

The preparation of N-terminally 6xHis tagged NCAM Ig1-FN2 contained considerable amounts of degradation products (Fig. 9B), which were recognised by an anti 5xHis antibody, indicating the integrity of the tag and thus arguing for C-terminal degradation. Changing the position of the

6xHis tag from the N-terminus to the C-terminus was supposed to possibly interfere with C-terminal degradation and, furthermore, C-terminally degraded products would be left untagged and thus unable to bind to the Ni^{2+} column. On this basis, the C-terminally tagged NCAM Ig1-FN2-6xHis was generated with the intention to increase stability and purity of the protein. Indeed, after test expression the samples showed less degradation upon harvesting cell culture supernatants 72 h post infection (Fig. 10A). However, large-scale production reproduced the appearance of degradation products (Fig. 10B).
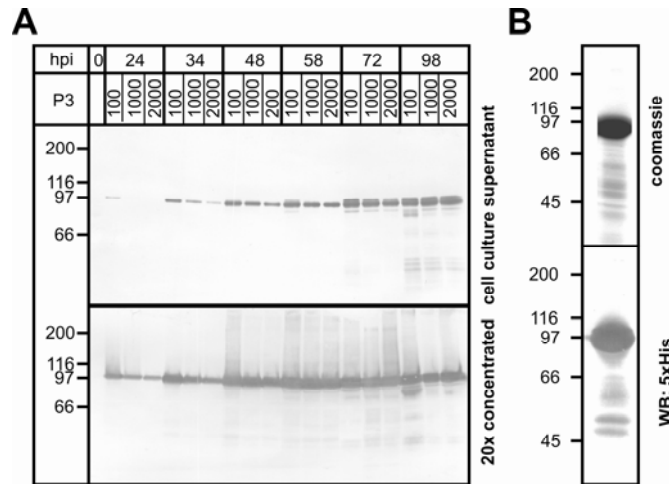
Fig. 10: Testexpression (A) of NCAM Ig1-FN2-6xHis and purified protein sample (B). **A**, Cell culture supernatants were applied to 8% SDS-PAGE before (upper panel) or after 20x concentration by TCA precipitation (lower panel) and analysed by anti 5xHis staining after western blotting. **B**, After large-scale purification the purified sample was analysed by 8% SDS-PAGE followed by coomassie (upper panel) or anti 5xHis staining after western blotting (lower panel).

Crystallisation of NCAM Ig1-FN1sec

Another trial to obtain more stable protein was to express the naturally secreted variant of NCAM, NCAMsec, which consists of all 5 Ig domains followed by FN1 and the so called sec sequence (KNIAQNHCCNMFQAGLHNALMK). This construct was expected to be less prone to degradation due to its naturally occurring sequence. Additionally, structural studies on NCAM suggest another advantage of using NCAMsec in crystallisation studies. Becker *et al.* (1989) observed a bend in NCAM molecules when performing electron microscopy studies and proposed a flexible hinge region located between Ig5 and FN1. Studies by Johnson *et al.* further supported the existence of a hinge region (Johnson *et al.*, 2005a; Johnson *et al.*, 2005b). Based on the crystal structure of FN1-FN2, Carafoli *et al.* (2008) suggested the hinge region to be located between FN1 and FN2. If these data hold true, the construct NCAM Ig1-FN1sec would not only promise a higher homogeneity of the purified sample, but also lack the flexible hinge region, which might have a negative impact on crystallisation. The protein was purified with a

very good yield and a purity comparable to that of NCAM Ig1-FN2 (Fig. 9B). Crystallisation trials were carried out at the High Throughput Crystallisation facility of the EMBL Hamburg, testing ~1000 buffer conditions at a protein concentration of 10 mg/ml applying the sitting drop method. Promising results are shown in Fig. 11.

	Buffer conditions		Buffer conditions
	Index G8 0.1 M HEPES pH 7.0 5% (v/v) tacsimate pH 7.0 10% (w/v) PEG methyl ether 5,000		**MembFac G5** 0.1 M HEPES sodium salt pH 7.5 0.1 M potassium sodium tartrate 0.1 M Li$_2$SO$_4$
	Jena1-4 A12 0.05 mM MgSO$_4$ 0.2 M LiCl 8% (w/v) PEG 8,000		**Natrix B6** 0.05 M Tris-HCl pH 7.5 0.01 MgCl$_2$ 5% (v/v) 2-propanol
	Jena1-4 B1 0.1 M MES sodium salt pH 6.5 15% (w/v) PEG 400		**Natrix H3** 0.05 M sodium cacodylate pH 6.5 0.2 M ammonium acetate 0.01 M CaCl$_2$ 10% (w/v) PEG 4,000

Fig. 11: Crystallisation trials for NCAM Ig1-FN1sec. Depicted are the (pre-)crystals and the respective buffer conditions.

	Buffer conditions		Buffer conditions
	Grid B1 0.1 M citric acid pH 4.0 5% (w/v) PEG 6,000		**Wizard A2** 0.1 M acetate pH 4.5 1 M ammonium hydrogen phosphate
	J5-8 G3 0.1 M Tris-HCl pH 8.5 0.1 MgCl$_2$ 17% (w/v) PEG 20,000		**Wizard B5** 0.1 imidazole pH 8.0 1 M ammonium hydrogen phosphate
	Qia Classic B5 0.1 M HEPES pH 7.5 1 M sodium acetate 0.05 M cadmium sulfate		**Wizard B8** 0.1 M Tris-HCl pH 8.5 1 M ammonium hydrogen phosphate
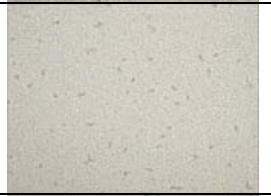
Fig. 12: Crystallisation trials for NCAM Ig1-FN2. Depicted are the (pre-)crystals and the respective buffer conditions.

Crystallisation of NCAM Ig1-FN2

Also for the N-terminally 6xHis tagged NCAM Ig1-FN2 (c = 10 mg/ml), ~1,000 buffer conditions were tested for crystallisation at the EMBL Hamburg. Promising results are depicted in Fig. 12. Two especially promising crystallisation conditions were further optimised in our lab by varying pH and precipitant concentrations (Fig. 13).

	Buffer conditions		Buffer conditions
	Jena1-4 G4 0.1 M Tris-HCl pH 8.5 0.2 lithium sulfate 16% (w/v) PEG 4,000		**Wizard B7** 0.1 M MES pH 6.0 0.2 M lithium sulfate 35% (v/v) MPD
	optimised condition 1 0.1 M Tris-HCl pH 8.7 10% PEG 4,000		**optimised condition 2** 0.07 M MES pH 6.5 0.2 M Li$_2$SO$_4$ 25% MPD
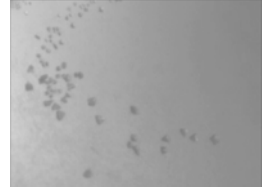
Fig. 13: Optimisation of crystallisation conditions for NCAM Ig1-FN2. Depicted are the (pre-)crystals and the respective buffer conditions.

For the PEG conditions (Fig. 13, left panels), small crystals with a brownish colour were observed. For the MPD conditions (Fig. 13, right panels), bigger crystals of the same brownish colour were obtained with a maximal size of 200 μm, and successfully shock frozen in liquid nitrogen.

A small crystal was dissolved and analysed on an SDS-PAGE (Fig. 14). Silver staining revealed two bands of much too small size (~30 and 35 kDa), demonstrating that the crystals did not consist of NCAM protein, but of a contamination which most probably derived from the insect cell medium. Crystals of this contamination have already been reported in Stummeyer 2004, and the fact that all protein preparations obtained in the course of this study contain small amounts of this easy-to-crystallise protein (see Fig. 6 and 9B), the urge for an efficient method to eliminate this contamination becomes clear. Analysing the 35 kDa band using mass spectrometry did not reveal similarity to any known protein in a first trial.

Fig. 14: Composition of crystals grown in optimised buffer condition 2. A small crystal was dissolved in 2x Laemmli buffer containing 5% β-mercaptoethanol and analysed by 10% SDS-PAGE followed by silver staining.
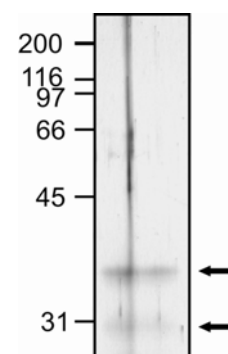
3. Oligomerisation studies

NCAM Ig1-FN2 forms dimers in solution

During purification of NCAM Ig1-FN2, an unexpected running behaviour in size-exclusion chromatography (SEC) was observed. Calculated by the retention time on the calibrated SEC column, NCAM Ig1-FN2 showed an oligomerisation status of 4.0, corresponding to a tetramer. To obtain further insights into NCAM homophilic oligomerisation, analytical ultracentrifugation (AUC) experiments were conducted.

In a first experiment, the composition of the sample was analysed by observing the progressing sedimentation of all molecular species contained in the solution over time (sedimentation velocity experiment), and the concentration of the species was plotted against their sedimentation coefficient after normalising to 20°C and water as a solvent (corrected differential sedimentation coefficient distribution (c(s) distribution); Schuck *et al.*, 2000) (Fig. 15A). The sedimentation coefficient of a particle is influenced by the size, mass and shape of the particle, thus providing information about the oligomerisation state, and is determined by its sedimentation velocity.

First sedimentation velocity experiments for NCAM Ig1-FN2 showed that the protein sample was inhomogeneous, containing a high amount of species with high sedimentation coefficients (20-30% of the total protein mass, data not shown). This might be due to aggregation of degrading protein. The fact that frozen samples appeared clowdy after thawing and white precipitates were obtained after centrifugation is in line with this explanation. But also the formation of higher organised NCAM molecules building large clusters in solution cannot be excluded. Consequently, the samples were analysed at high rotor velocity (45,000 rpm) and the first measurements, obtained during sedimentation of higher organised species, were excluded from analysis in all further studies.

As shown in Fig. 15A, two peaks at 4.2 S and 5.1 S were obtained for NCAM Ig1-FN2. As the sedimentation coefficient is a combined measure for shape and size of a particle and the shape of NCAM molecules has not been unequivocally described, it is not possible to directly assign sedimentation coefficients and oligomer species. However, as the ratio between the two peaks changed with NCAM concentrations (Fig. 15A), it is very likely that this represents a change in the equilibrium between two oligomerisation states.

To obtain further information about the shape and oligomeric state of NCAM molecules, different oligomeric compositions of the sample were assumed and the resulting frictional ratio was determined, providing information on the shape of a particle. For a hydrated spherical

protein, the frictional ratio is 1.1-1.2, whereas increasing deviation from this value argues for an increasingly asymmetric form and/or the presence of unstructured loops.

Assuming that the major peak of NCAM Ig1-FN2 corresponds to a dimer, a frictional ratio of ~2 is observed. This is an unusual high value, arguing for a highly asymmetric shape of NCAM Ig1-FN2. NCAM has been described as an elongated, rod-shaped molecule (Becker *et al.*, 1989; Johnson *et al.*, 2005a; Johnson *et al.*, 2005b) and its consistently reported abnormal running behaviour in SDS-PAGE underlines the assumption that NCAM forms a unique asymmetric structure. Thus, the unusually high frictional ratio agrees perfectly with previous observations.

Moreover, it should be noted that, assuming dimer a slow reaction for dimer formation, the major peak would represent a slower sedimenting reaction boundary instead of a pure dimer sedimentation boundary. In this case, the pure dimer would sediment faster than observed from this peak, leading to an elevated $s_{20,w}$ and a smaller frictional ratio.

On the other hand, it cannot be excluded that the major peak corresponds to a monomer, while the smaller one arises from a ~42 kDa contaminant, which is visible in SDS-PAGE (Fig. 9). However, this would change the frictional ratio to 1.3, pointing to an almost globular shaped protein, which is not consistent with current observations. Furthermore, the changing ratio between the two peeks depending on protein concentration cannot be explained by this model.

To further analyse the oligomeric state of the protein, sedimentation diffusion equilibrium experiments were performed applying different protein concentrations and rotor speeds (Fig. 16A), and data analysis was performed with the help of the programme BPCfit (Witte *et al.*, 2005). A model using a single species was not sufficient to explain the experimental data (data not shown), while assuming two species resulted in good fits and yielded molecular weights of 62 kDa and 152 kDa, respectively. Data analysis using the programme Sedphat assuming a monomer/dimer equilibrium resulted in similarly good fits with a molecular weight of 80.9 kDa for the monomer (data not shown). This matches very well with the predicted weight of 77.65 kDa.

In sum, the data obtained by analytical ultracentrifugation argue strongly for a monomer/dimer equilibrium of NCAM Ig1-FN2 in solution.

As described above, the oligomerisation state obtained by SEC pointed towards the formation of tetramers, which does not correspond to the results obtained from AUC. However, in SEC, the elution time is not dependant on the mass of a protein but on its hydrodynamic radius (r_H) with a

linear relation between elution and the negative logarithm of r_H. Based on the frictional ratio obtained by AUC, r_H should differ in a factor of about 1.6 from an r_H expected for a spherical protein, thus, an apparent oligomerisation status of 8-9 would be expected to be observed by SEC. However, for molecules of this size, SEC is a very inexact method, and the fact that the column was calibrated with spherical proteins depending on molecular weight rather than on the hydrodynamic radius gives rise to further inaccuracies.

Considering this, the results obtained by AUC appear to be compatible with dimer formation of NCAM Ig1-FN2.
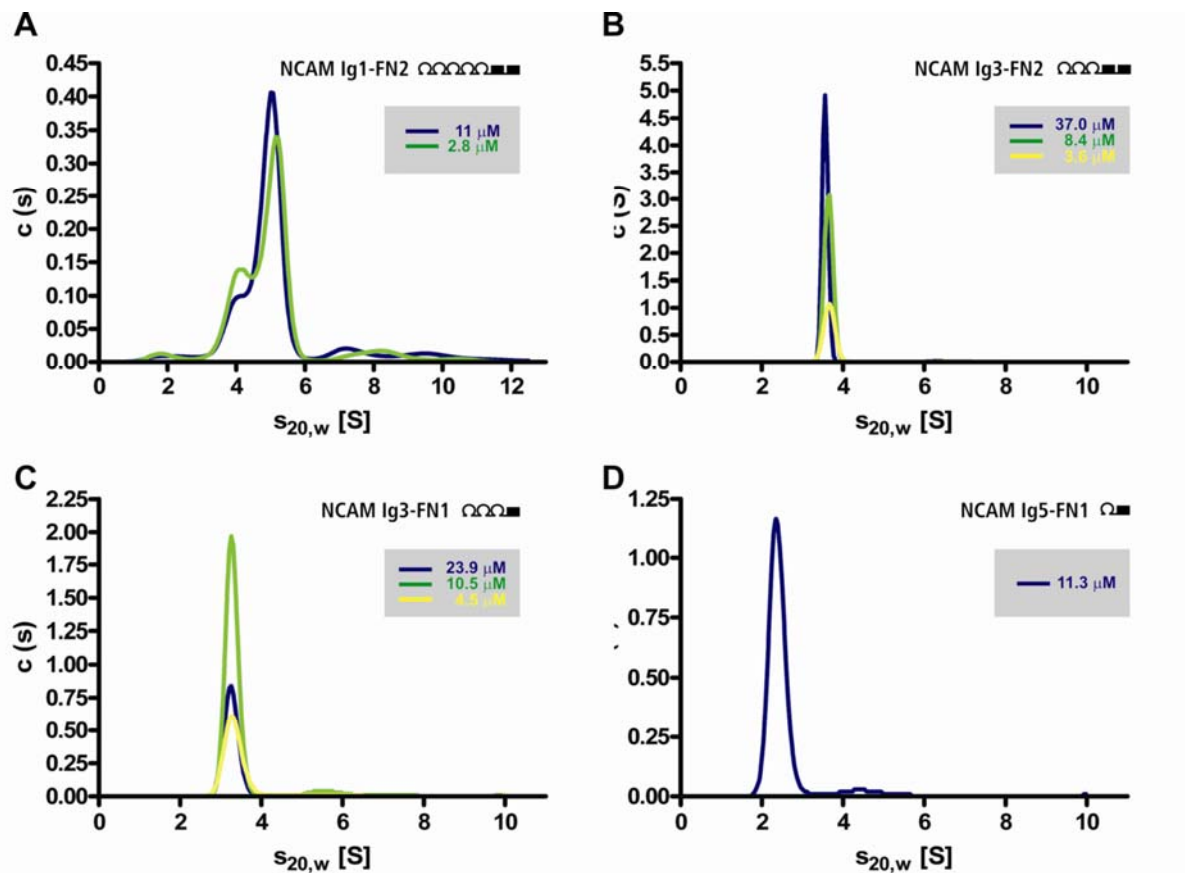
Fig. 15: Analysis of the oligomerisation state by sedimentation velocity experiments (analytical ultracentrifugation). Four different NCAM fragments were analysed at varying concentrations and c(s) distributions were obtained using the programme Sedfit (Schuck *et al.*, 2000).
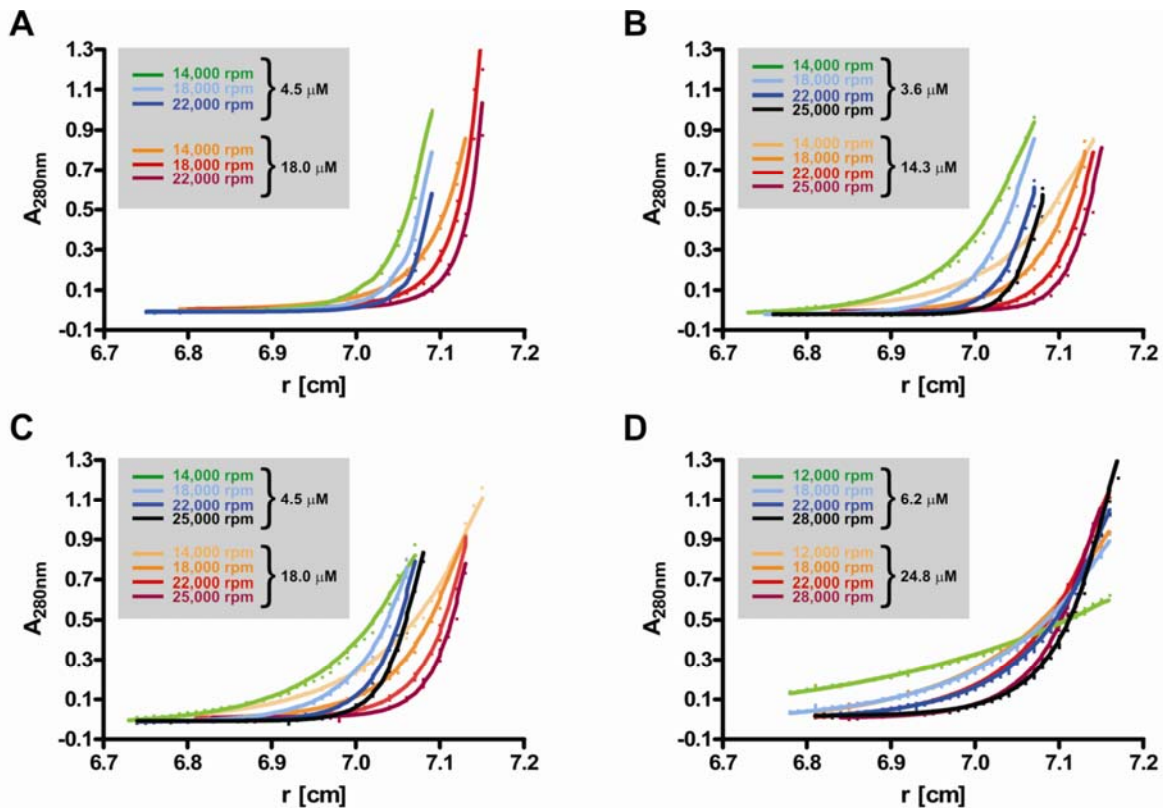
Fig. 16: Analysis of the oligomerisation state by sedimentation diffusion equilibrium experiment (analytical ultracentrifugation). Four different NCAM fragments (**A**, NCAM Ig1-FN2, **B**, NCAM Ig3-FN2, **C**, NCAM Ig3-FN1, **D**, NCAM Ig5-FN1) were analysed at varying concentrations and rotor velocities as indicated. Calculated curves were obtained by use of the programme BPCfit (Witte *et al.*, 2005).

NCAM dimerisation depends on Ig1 and Ig2 and is influenced by the presence of FN2

To analyse the underlying interactions of NCAM dimerisation, three further recombinant NCAM variants were analysed in AUC. Since the crystal structure of the first Ig domains of NCAM (Soroka *et al.*, 2003) suggests the previously described interaction of Ig1 with Ig2 to be responsible for dimerisation (Jensen *et al.*, 1999; Kasper *et al.*, 2000; Atkins *et al.*, 2004), a construct lacking Ig1 and Ig2, was generated (NCAM Ig3-FN2). The crystal structure and SEC experiments of FN1-FN2 (Carafoli *et al.*, 2008) also suggest an influence of FN2 on dimerisation. To test this assumption, an NCAM construct additionally lacking FN2 was analysed (NCAM Ig3-FN1; see Fig. 9). As a control, NCAM Ig5-FN1 (see Fig. 9) was further included in this study.

NCAM Ig3-FN2

In sedimentation velocity experiments, NCAM Ig3-FN2 turned out to be a homogeneous sample, which contained only one species (Fig. 15B) exhibiting an $s_{20,w}$ of 3.7 S. This corresponds to a frictional ratio of 1.47 for a monomer (assumed molecular weight: 56.06 kDa) indicating a less pronounced asymmetric form of the truncated protein when compared to NCAM Ig1-FN2.

Also the analysis of the sedimentation diffusion equilibrium experiment argued for a monomeric state of the protein with a molecular weight of 65-75 kDa (Fig. 16B). The elevated apparent molecular weight might be caused by glycosylation which has not been considered in the above described calculations.

In contrast to the clear presence of only one species in AUC, an equilibrium between monomeric and dimeric state was observed in SEC (Fig. 17), with the major portion being monomeric. Also for NCAM Ig1-FN2, a higher likelihood for oligomerisation has also been observed in SEC, where it elutes as a single peak most probably corresponding to a dimer (data not shown), while an equilibrium between monomers and dimers was observed in AUC.

This is probably due to the significantly higher protein concentrations in the range of mg/ml in these SEC experiments when compared to the AUC studies.

Thus, it can be concluded that deletion of Ig1 and Ig2 abolished dimerisation effeciently in AUC, but residual oligomerisation was observed in SEC, arguing for a contribution of further domains on the process of dimer formation.
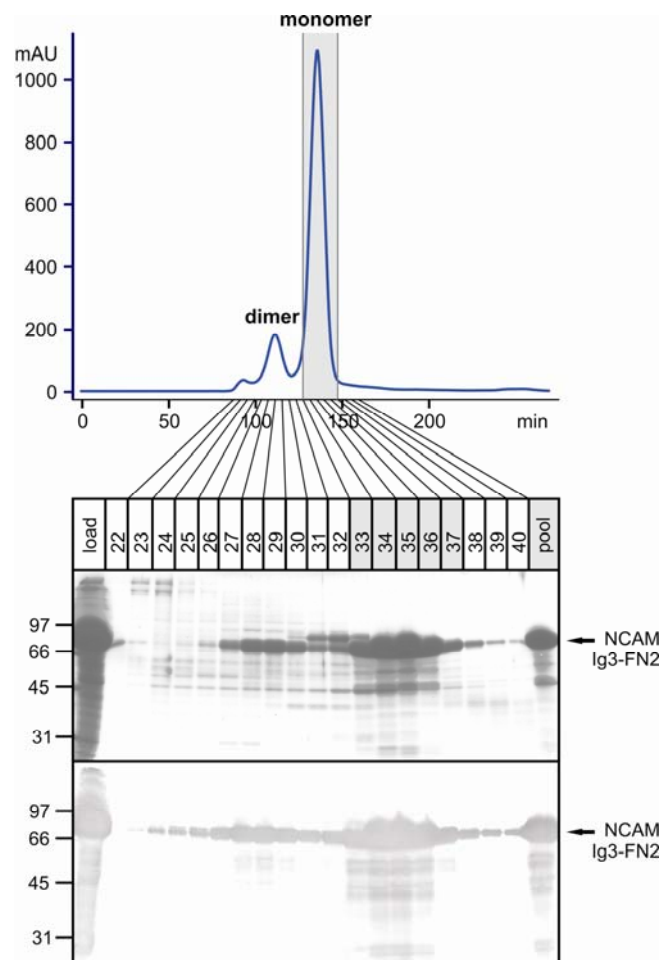
Fig. 17: Analysis of oligomerisation status of NCAM Ig3-FN2 by size-exclusion chromatography. Ni^{2+} affinity purified NCAM Ig3-FN2 was applied to a HiLoad 16/60 Superdex 200 size-exclusion chromatography column. Fractions were analysed on a 10% SDS gel by coomassie staining (upper panel) and anti 5xHis staining following western blotting (lower panel).

NCAM Ig3-FN1

NCAM Ig3-FN1 showed a single peak in the sedimentation experiment at 3.4 S (s20,w), corresponding to a frictional ratio of 1.45 (assumed molecular weight: 45.4 kDa), which is similar to that of NCAM Ig3-FN2 (Fig. 15C). Moreover, also the sedimentation diffusion equilibrium experiment argued for a solution containing only one species with a molecular weight of 55-60 kDa (Fig. 16C). In SEC, this NCAM variant eluted as a single peak, demonstrating that dimerisation was completely abolished by the additional deletion of FN2 (data not shown).

NCAM Ig5-FN1

For NCAM Ig5-FN1, a sedimentation coefficient $s_{20,w}$ of 2.3 S corresponding to a frictional ratio of 1.37 for the monomer was obtained, suggesting a molecular weight of 25.5 kDa (Fig. 15D). In perfect agreement, the sedimentation diffusion equilibrium experiment argued for a monomeric species with a molecular weight of 25.5 kDa (Fig. 16D).

Taken together, these data show that Ig1 and Ig2 are the major mediators of dimerisation, but that also FN2 has an impact on the stability of this interaction.

Interactions between ST8SiaII and NCAM

To gain deeper insight into NCAM-ST8SiaII interaction, complex formation was addressed in analytical ultracentrifugation studies.Therefore, NCAM Ig1-FN2 and mST8SiaIIΔ56 were investigated in sedimentation velocity experiments individually and in combination. The c(s) distribution (Fig. 18) revealed a single species for ST8SiaII, exhibiting an $s_{20,w}$ of 3.1 S (Fig. 18A). This leads to a frictional ratio of 1.3 for a monomer and 2.0 for a dimer, assuming a molecular weight of the enzyme of 39.0 kDa as calculated by the amino acid sequence. Since for ST8SiaII no gross deviations from a globular shape were expected, this confirms the finding from SEC that the enzyme exists in a monomeric state in solution.

The molecular weight obtained by analysis of diffusion broadening of the sedimenting boundary is 40-45 kDa, which is slightly higher than the molecular weight calculated by the amino acid sequence. However, the fact that glycosylation has not been considered in analysis of the AUC data might again be the reason for the deviation of the obtained molecular weight.

The investigation of ST8SiaII or NCAM alone resulted in single peaks. After combining the two protein samples, a shift of the peak exhibiting the higher sedimentation coefficient towards higher s-values would be expected upon complex formation (assuming a slow reaction). The

shifted peak would in this case represent the reaction boundary instead of the sedimentation boundary of the faster sedimenting species.

Since no such shift could be observed and, importantly, the area beyond the peaks for the single proteins did not change considerably, this experiment demonstrated that no effective complex formation occurred, although unphysiologically high protein concentrations in the range of 2-6 μM were used. This demonstrates, that the binding of ST8SiaII to its acceptor NCAM, both derived from insect cells, is a weak interaction, and cannot be detected at these protein concentrations.
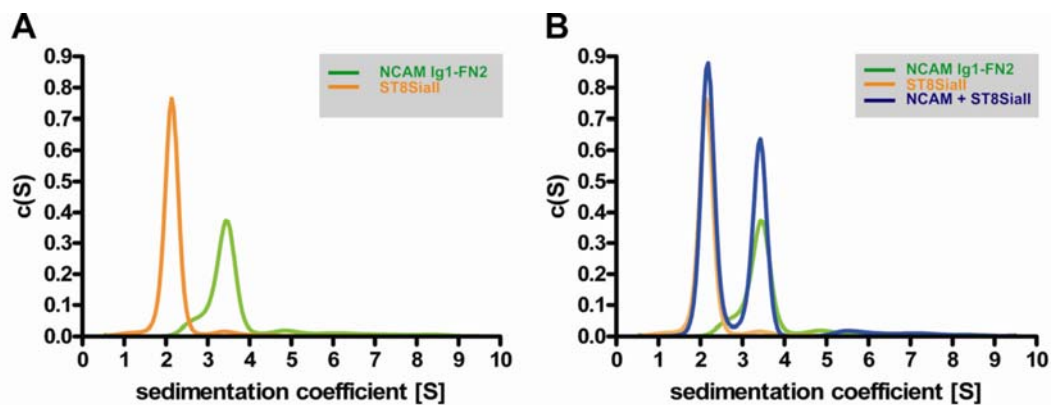
Fig. 18: Sedimentation velocity experiment for the investigation of complex formation between ST8SiaII and NCAM. mST8SiaIIΔ56 and NCAM Ig1-FN2 were analysed individually or in combination in sedimentation velocity experiments at concentrations of 6 μM and 2.8 μM, respectively.

Discussion

Purification of recombinant ST8SiaII and initiation of crystallisation trials

The structural characterisation of the polySTs is mainly hampered by the lack of recombinant protein. The need for correct glycosylation and disulfide bond formation trigger high demands on the expression system. In my diploma thesis (Eggers, 2006), I achieved the baculoviral mediated expression of polySTs in insect cells and implemented the system as a most promising system for a robust production of active ST8SiaII in reasonable yields.

In my doctorial thesis I further optimised this production system. Therefore, several constructs were generated and tested for expression in *Sf*9 insect cells. Constructs differing in length and in the content of N-glycosylation sites were all expressed at low levels when compared to the fully N-glycosylated variant lacking 56 amino acids of the N-terminus used in Eggers (2006). This demonstrated the sensibility of the expression system and confirmed that interfering with N-glycosylation leads to low-level expression.

A protein A (protA) tagged variant of mST8SiaII was efficiently expressed in insect cells and seemed to be a promising candidate for the establishment of an improved purification protocol, allowing for the use of antibody based affinity chromatography und highly specific release of the protein by on-column protease cleavage. However, only a minor portion of the expressed protein could be retrieved by purification due to unspecific adhesion to the matrix.

Thus, the N-terminally 6xHis tagged Δ56 truncation of murine ST8SiaII was chosen to be used in all further studies.

Assuming that acceptor binding of the nascent polyST might stabilise the enzyme and enhance expression levels, simultaneous expression of this construct with a soluble NCAM fragment comprising the complete ectodomain was conducted by use of the vector pFastBacDual. Although the expression level of the polyST was not considerable increased, this system is interesting for the investigation of interactions between the polySTs and NCAM.

To gain material for biochemical and structural studies on the polyST, the purification procedure described in Eggers (2006) was further refined by addition of a size-exclusion chromatography step. The purified ST8SiaII showed to be active in terms of autopolysialylation and was able to transfer polySia onto NCAM and SynCAM 1. Unexpectedly, the protein showed to be very stable and allowed both long-term storage at -80°C and short-term storage at 4°C.

This expression system enabled crystallisation trials for ST8SiaII, which provide information on promising buffer conditions as an ideal basis for future studies.

Polysialylation of insect cell derived glycans

Terminal sialylation in α2,3- or α2,6-linkage showed to be a prerequisite for NCAM polysialylation (Mühlenhoff *et al.*, 1996a). Since the major portion of insect cell derived N-glycans is paucimannosidic (reviewed in Marchal *et al.*, 2001), insect cell produced NCAM was not expected to act as an acceptor for ST8SiaII. However, small amounts of polySia were detected in an *in vitro* assay. The possibility that sialylated complex-type glycan structures occasionally occur in insect cells is an issue of major debate (for review see Marchal *et al.* 2001). With the polysialylated NCAM-fraction obtained in this study, a new starting point has been set for the specific enrichment and detailed glycan analysis of the core structures underlying the polySia chains. Moreover, as it is known that polySTs are capable to synthesise polySia chains on asialo-core glycans in a process called autopolysialylation (Mühlenhoff *et al.*, 1996b), it cannot be excluded that the biosynthesis of polySia chains on the insect cell expressed NCAM occurs in the same way. The detailed analysis of the polysialylated core structures (e.g. bei mass spectrometry) will shed light on these questions.

Production of a library of NCAM fragments

The nature of NCAM homo- and heterophilic interactions influencing cell adhesion and signalling has been subject of intensive discussion (reviewed in Kiselyov *et al.*, 2005; Soroka *et al.*, 2010; Hinsby *et al.*, 2004; Ditlevsen *et al.*, 2008). The NCAM library generated in the course of this project raises new opportunities to elucidate the functions of the individual domains and to gain structural data on NCAM homophilic interactions. Constructs were obtained as soluble proteins in high yields with good purity and can be applied to a variety of experiments (see also chapter 3).

Initiation of NCAM crystallisation trials

The crystallisation trials carried out with the full-length ectodomain of NCAM, NCAM Ig1-FN2, and the fragment representing the natural secreted form of NCAM, NCAM Ig1-FN1sec, provide information on a multiplicity of promising buffer conditions which might lead to the production of diffracting crystals upon further optimisation. For NCAM Ig1-FN2, two buffer conditions were selected and further optimised with respect to pH values and concentration of precipitating agents. In both settings, crystals were obtained exhibiting a brownish colour. Analysing the composition of the larger crystals (around 200 µm) on SDS-PAGE revealed two protein bands at ~30 and ~35 kDa that did not correspond to the NCAM-fragments. Instead, the brownish coloured crystals contained a contamination most probably derived from the insect cell medium.

Similarly, small crystals of identical properties had already been reported by Stummeyer (2004). The repeated crystallisation of this contamination underlines that this is a major problem in growing crystals out of insect cell derived proteins. Given that in every purified sample produced during this project, variably prominent bands of this easy-to-crystallise protein can be observed, it becomes clear, that a major effort should be invested in clearing protein samples for crystallisation of this contamination. As subjecting the ~35 kDa protein to mass spectrometry did not reveal any similarity to known proteins, we were not able to further elucidate the nature of this contaminant.

Studies on the structural domains involved in NCAM dimerisation

Dimerisation of NCAM fragments was studied by analytical ultracentrifugation (AUC) and size-exclusion chromatography (SEC). Thus, it could be demonstrated, that NCAM Ig1-FN2 exhibits an exclusively dimeric state in SEC, while a concentration dependant equilibrium between monomeric and dimeric state was observed in AUC at lower protein concentrations with the main fraction being in the dimeric state. Deletion of Ig1 and Ig2 turned the protein in an exclusively monomeric state in AUC, while at high protein concentrations in SEC an equilibrium was observed with the major fraction in the monomeric state. Further deletion of FN2 finally led to an exclusively monomeric protein. As expected, also the shorter fragment NCAM Ig5-FN1 is only observed as a monomer. These results point towards the importance of the previously described Ig1-Ig2 interaction (Atkins *et al.*, 1999; Jensen *et al.*, 1999; Kasper *et al.*, 2000; Soroka *et al.*, 2003; Atkins *et al.*, 2004) for the dimerisation of this soluble NCAM fragment. However, also interaction mediated by FN2 as described by Carafoli *et al.* (2008) plays a role in dimerisation.

This is in consistence with previously described data. Atkins *et al.* (1999) observed an equilibrium between monomers and dimers for a construct consisting of the two most N-terminal Ig domains (Ig1-Ig2) at a ratio of 12% to 88% in AUC experiments, and this equilibrium was also observed for Ig1-Ig2-Ig3 by Atkins *et al.* (2001). Furthermore, Ig1-Ig2 eluted as a dimer in SEC (Jensen *et al.*, 1999).

Supporting the role of the fibronectin III like domains, Carafoli *et al.* (2008) reported an equilibrium between monomers and dimers for a construct comprising FN1 and FN2 in SEC. In contrast, dimerisation of Ig5-FN1 was reported to occur upon removal, but not in the presence of N-glycosylation site 4. Interestingly, mutation of this N-glycosylation site also showed to impact oligomerisation of the soluble NCAM ectodomain (Foley *et al.*, 2010a)

A reagent interfering with dimerisation could contribute to improved purification, helping to reduce contamination by degradation products, but would also represent an interesting tool to investigate the influence of *cis* dimerisation on *trans* interaction and the role of dimerisation in a physiological context.

Performing AUC sedimentation velocity experiments with NCAM Ig1-FN2 with elevated salt concentrations turned the double peak of the monomer-dimer equilibrium into a single peak exhibiting a sedimentation coefficient exhibiting a value between those of the monomer and the dimer. However, SEC studies did not reveal any difference between low-salt and high-salt conditions (data not shown). Kulahin *et al.* (2005) demonstrated that the heparin binding site located on Ig2 overlaps with the binding site of Ig1 and that application of heparin interferes with binding of Ig1 to Ig2. A small chemical analogue to heparin, sucrose octasulfate (SOS), might thus be an attractive candidate to disrupt homophilic NCAM interactions leading to improved purification protocols.

Moreover, this system should also allow to elucidate how different NCAM mimetic peptides (Berezin and Bock, 2004) impact the dimerisation. The peptides P1-B and P2, for example, are derived from the Ig1 and Ig2 interface and are suggested to disrupt this interaction. Also, a possible influence of plannexin and dennexin, two inhibitors of the respective zipper structures, should be tested.

Interactions between NCAM and ST8SiaII

Until now, only six natural polySia acceptors have been identified. In addition to NCAM, which is by far the most abundant acceptor for polySia, also the polySTs themselves (autopolysialylation) (Mühlenhoff *et al.*, 1996b; Close *et al.*, 2000), the α-subunit of the voltage-dependant sodium channel (Zuber *et al.*, 1992), a soluble fragment of the scavenger receptor CD 36 found in human milk (Yabe *et al.*, 2003), neuropilin-2 on dendritic cells (Curreli *et al.*, 2007) and the synaptic cell adhesion molecule SynCAM 1 (Galuska *et al.*, 2010) have been shown to be targets for polysialylation.

With the aim to elucidate the mechanisms that determine this high selectivity, complex formation of ST8SiaII with NCAM was investigated in analytical ultracentrifugation (AUC). Although stable complex formation of ST8SiaIV in a pull-down assay has been observed by Colley and colleagues (Colley, 2010), no such binding could be detected for ST8SiaII and the soluble ectodomain of NCAM (NCAM Ig1-FN2) by AUC. An experiment carried out by Kojima *et al.* (1997) can potentially help to explain these different findings. By use of transfection experiments in Neuro2A cells the authors showed that ST8SiaII exhibits a high selectivity for

NCAM-180 and NCAM-140, while ST8SiaIV was able to polysialylate a variety of proteins, including all three NCAM isoforms. While this on the one hand might be a hint for a higher specificity of ST8SiaII caused by more frail acceptor binding, it should also be kept in mind that the N-terminal protein domains (cytoplasmic tail, TMD, stem region) missing in the *in vitro* experiment might help selecting the acceptor structure.

Nevertheless, if the differential binding properties of the two polysialyltransferases can be confirmed, this would indicate different physiological roles and might lead to a new insight into the advantage of the existence of two seemingly redundant enzymes.

However, this is so far speculation, since the experiments carried out by Colley and colleagues and in our laboratory are not comparable due to the unequal methods, demanding repetition of the AUC experiments with ST8SiaIV. Importantly, the different expression systems used in these studies might further be a reason for the contradictory results. It is possible that effective polysialyltransferase binding is dependant on complex N-glycosylation, which cannot be performed by insect cells. As already discussed, insect cell produced NCAM was thus not expected to act as an acceptor for the enzyme, and although polyST activity was unexpectedly detected, the amount of polysialylation was extremely low if compared to NCAM isolated from CHO cells. A likely explanation would be that the correct underlying core-structure of N-glycans are needed for polysialylation activity itself, but also a lack of NCAM binding would be an explanation for missing or reduced activity.

Furthermore, it has been reported that the interaction of NCAM with L1 is carbohydrate-dependant (Kadmon *et al.*, 1990), underlining the possible role of glycans in protein binding. Thus, the AUC experiments need to be repeated with mammalian cell derived NCAM to investigate, if N-glycans play a role in the interaction with the polysialyltransferases.

In sum, I was able to obtain material for structural and biochemical characterisation of ST8SiaII and NCAM and to thereby provide a basis for in depth studies on the interaction of these two reaction partners. Interestingly, the NCAM ectodomain was found to dimerise in solution and this interaction was shown to be mediated by the interaction of Ig1-Ig2 and by FN2 binding.

References

Angata, K., Suzuki, M., and Fukuda, M. (2002) ST8Sia II and ST8Sia IV Polysialyltransferases Exhibit Marked Differences in Utilizing Various Acceptors Containing Oligosialic Acid and Short Polysialic Acid - The Basis for Cooperative Polysialylation by Two Enzymes. *Journal of Biological Chemistry* **277**(39):36808-17.

Angata, K., Long, J.M., Bukalo, O., Lee, W., Dityatev, A., Wynshaw-Boris, A., Schachner, M., Fukuda, M., and Marth, J.D. (2004) Sialyltransferase ST8Sia-II Assembles a Subset of Polysialic Acid That Directs Hippocampal Axonal Targeting and Promotes Fear Behavior. *Journal of Biological Chemistry* **279**(31):32603-13.

Atkins, A.R., Osborne, M.J., Lashuel, H.A., Edelman, G.M., Wright, P.E., Cunningham, B.A., and Dyson, H.J. (1999) Association Between the First Two Immunoglobulin-Like Domains of the Neural Cell Adhesion Molecule N-CAM. *FEBS Lett.* **451**(2):162-8.

Atkins, A.R., Chung, J., Deechongkit, S., Little, E.B., Edelman, G.M., Wright, P.E., Cunningham, B.A., and Dyson, H.J. (2001) Solution Structure of the Third Immunoglobulin Domain of the Neural Cell Adhesion Molecule N-CAM: Can Solution Studies Define the Mechanism of Homophilic Binding? *J. Mol. Biol.* **311**(1):161-72.

Atkins, A.R., Gallin, W.J., Owens, G.C., Edelman, G.M., and Cunningham, B.A. (2004) Neural Cell Adhesion Molecule (N-CAM) Homophilic Binding Mediated by the Two N-Terminal Ig Domains Is Influenced by Intramolecular Domain-Domain Interactions. *Journal of Biological Chemistry* **279**(48):49633-43.

Becker, J.W., Erickson, H.P., Hoffman, S., Cunningham, B.A., and Edelman, G.M. (1989) Topology of Cell Adhesion Molecules. *Proc. Natl. Acad. Sci. U. S. A* **86**(3):1088-92.

Berezin, V. and Bock, E. (2003) NCAM Mimetic Peptides - Pharmacological and Therapeutic Potential. *Journal of Molecular Neuroscience* **22**(1-2):33-9.

Carafoli, F., Saffell, J.L., and Hohenester, E. (2008) Structure of the Tandem Fibronectin Type 3 Domains of Neural Cell Adhesion Molecule. *Journal of Molecular Biology* **377**(2):524-34.

Close, B.E., Tao, K., and Colley, K.T. (2000) Polysialyltransferase-1 Autopolysialylation Is Not Requisite for Polysialylation of Neural Cell Adhesion Molecule. *Journal of Biological Chemistry* **275**(6):4484-91.

Close, B.E., Wilkinson, J.M., Bohrer, T.J., Goodwin, C.P., Broom, L.J., and Colley, K.J. (2001) The Polysialyltransferase ST8Sia II/STX: Posttranslational Processing and Role of Autopolysialylation in the Polysialylation of Neural Cell Adhesion Molecule. *Glycobiology* **11**(11):997-1008.

Colley, K.J. (2010): Structural Basis for the Polysialylation of the Neural Cell Adhesion Molecule. *Adv. Exp. Med. Biol.* **663**:111-26.

Cremer, H., Lange, R., Christoph, A., Plomann, M., Vopper, G., Roes, J., Brown, R., Baldwin, S., Kraemer, P., Scheff, S., Barthels, D., Rajewsky, K., and Wille, W. (1994) Inactivation of the N-Cam Gene in Mice Results in Size-Reduction of the Olfactory-Bulb and Deficits in Spatial-Learning. *Nature* **367**(6462):455-9.

Curreli, S., Arany, Z., Gerardy-Schahn, R., Mann, D., and Stamatos, N.M. (2007) Polysialylated Neuropilin-2 Is Expressed on the Surface of Human Dendritic Cells and Modulates Dendritic Cell-T Lymphocyte Interactions. *Journal of Biological Chemistry* **282**(42):30346-56.

Ditlevsen, D.K., Povlsen, G.K., Berezin, V., and Bock, E. (2008) NCAM-Induced Intracellular Signaling Revisited. *Journal of Neuroscience Research* **86**(4):727-43.

Durchschlag, H. (1986) Specific Volumes of Biological Macromolecules and Some Other Molecules of Biological Interest.

Eckhardt, M., Bukalo, O., Chazal, G., Wang, L.H., Goridis, C., Schachner, M., Gerardy-Schahn, R., Cremer, H., and Dityatev, A. (2000) Mice Deficient in the Polysialyltransferase ST8SialV/PST-1 Allow Discrimination of the Roles of Neural Cell Adhesion Molecule Protein and Polysialic Acid in Neural Development and Synaptic Plasticity. *Journal of Neuroscience* **20**(14):5234-44.

Eggers, K. (2006) Studien zur homogenen Darstellung und kinetischen Charakterisierung von Polysialyltransferasen. Diploma thesis. Cellular Chemistry, Hannover Medical School.

El Maarouf, A., Petridis, A.K., and Rutishauser, U. (2006) Use of Polysialic Acid in Repair of the Central Nervous System. *Proceedings of the National Academy of Sciences of the United States of America* **103**(45):16989-94.

Foley, D.A., Swartzentruber, K.G., Lavie, A., and Colley, K.J. (2010a) Structure and Mutagenesis of Neural Cell Adhesion Molecule Domains: Evidence for Flexibility in the Placement of Polysialic Acid Attachment Sites. *J. Biol. Chem.* **285**(35):27360-71.

Foley, D.A., Swartzentruber, K.G., Thompson, M.G., Mendiratta, S.S., and Colley, K.J. (2010b) Sequences From the First Fibronectin Type III Repeat of the Neural Cell Adhesion Molecule Allow O-Glycan Polysialylation of an Adhesion Molecule Chimera. *J. Biol. Chem.* **285**(45):35056-67.

Fujimoto, I., Bruses, J.L., and Rutishauser, U. (2001) Regulation of Cell Adhesion by Polysialic Acid. *Journal of Biological Chemistry* **276**(34):31745-51.

Galuska, S.P., Geyer, R., Gerardy-Schahn, R., Muhlenhoff, M., and Geyer, H. (2008) Enzyme-Dependent Variations in the Polysialylation of the Neural Cell Adhesion Molecule (NCAM) in Vivo. *Journal of Biological Chemistry* **283**(1):17-28.

Galuska, S.P., Rollenhagen, M., Kaup, M., Eggers, K., Oltmann-Norden, I., Schiff, M., Hartmann, M., Weinhold, B., Hildebrandt, H., Geyer, R., Muhlenhoff, M., and Geyer, H. (2010) Synaptic Cell Adhesion Molecule SynCAM 1 Is a Target for Polysialylation in Postnatal Mouse Brain. *Proceedings of the National Academy of Sciences of the United States of America* **107**(22):10250-5.

Günzel, A. (2008) Vertebrate Polysialyltransferases: A study on structure-function relationships. Dissertation. Cellular Chemistry, Hannover Medical School

Haastert-Talini, K., Schaper-Rinkel, J., Schmitte, R., Bastian, R., Muhlenhoff, M., Schwarzer, D., Draeger, G., Su, Y., Scheper, T., Gerardy-Schahn, R., and Grothe, C. (2010) In Vivo

Evaluation of Polysialic Acid As Part of Tissue-Engineered Nerve Transplants. *Tissue Engineering Part A* **16**(10):3085-98.

Harduin-Lepers, A., Vallejo-Ruiz, V., Krzewinski-Recchi, M.A., Samyn-Petit, B., Julien, S., and Delannoy, P. (2001) The Human Sialyltransferase Family. *Biochimie* **83**(8):727-37.

Hildebrandt, H., Becker, C., Murau, M., Gerardy-Schahn, R., and Rahmann, H. (1998) Heterogeneous Expression of the Polysialyltransferases ST8Sia II and ST8Sia IV During Postnatal Rat Brain Development. *Journal of Neurochemistry* **71**(6):2339-48.

Hildebrandt, H., Muhlenhoff, M., Weinhold, B., and Gerardy-Schahn, R. (2007) Dissecting Polysialic Acid and NCAM Functions in Brain Development. *Journal of Neurochemistry* **103**:56-64.

Hildebrandt, H., Muhlenhoff, M., Oltmann-Norden, I., Rockle, I., Burkhardt, H., Weinhold, B., and Gerardy-Schahn, R. (2009) Imbalance of Neural Cell Adhesion Molecule and Polysialyltransferase Alleles Causes Defective Brain Connectivity. *Brain* **132**:2831-8.

Hinsby, A.M., Berezin, V., and Bock, E. (2004) Molecular Mechanisms of NCAM Function. *Frontiers in Bioscience* **9**:2227-44.

Jensen, P.H., Soroka, V., Thomsen, N.K., Ralets, I., Berezin, V., Bock, E., and Poulsen, F.M. (1999) Structure and Interactions of NCAM Modules 1 and 2, Basic Elements in Neural Cell Adhesion. *Nature Structural Biology* **6**(5):486-93.

Johnson, C.P., Fragneto, G., Konovalov, O., Dubosclard, V., Legrand, J.F., and Leckband, D.E. (2005a) Structural Studies of the Neural-Cell-Adhesion Molecule by X-Ray and Neutron Reflectivity. *Biochemistry* **44**(2):546-54.

Johnson, C.P., Fujimoto, I., Rutishauser, U., and Leckband, D.E. (2005b) Direct Evidence That Neural Cell Adhesion Molecule (NCAM) Polysialylation Increases Intermembrane Repulsion and Abrogates Adhesion (Vol 280, Pg 137, 2005). *Journal of Biological Chemistry* **280**(24):23424.

Jungnickel, J., Bramer, C., Bronzlik, P., Lipokatic-Takacs, E., Weinhold, B., Gerardy-Schahn, R., and Grothe, C. (2009) Level and Localization of Polysialic Acid Is Critical for Early Peripheral Nerve Regeneration. *Molecular and Cellular Neuroscience* **40**(3):374-81.

Kadmon, G., Kowitz, A., Altevogt, P., and Schachner, M. (1990) Functional Cooperation Between the Neural Adhesion Molecules L1 and N-Cam Is Carbohydrate Dependent. *Journal of Cell Biology* **110**(1):209-18.

Kasper, C., Rasmussen, H., Kastrup, J.S., Ikemizu, S., Jones, E.Y., Berezin, V., Bock, E., and Larsen, I.K. (2000) Structural Basis of Cell-Cell Adhesion by NCAM. *Nature Structural Biology* **7**(5):389-93.

Kiselyov, V.V., Soroka, V., Berezin, V., and Bock, E. (2005) Structural Biology of NCAM Homophilic Binding and Activation of FGFR. *J. Neurochem.* **94**(5):1169-79.

Kitazume-Kawaguchi, S., Kabata, S., and Arita, M. (2001) Differential Biosynthesis of Polysialic or Disialic Acid Structure by ST8Sia II and ST8Sia IV. *Journal of Biological Chemistry* **276**(19):15696-703.

Kleene, R. and Berger, E.G. (1993): The Molecular and Cell Biology of Glycosyltransferases. *Biochim. Biophys. Acta* **1154**(3-4):283-325.

Kojima, N., Tachida, Y., and Tsuji, S. (1997) Two Polysialic Acid Synthases, Mouse ST8Sia II and IV, Synthesize Different Degrees of Polysialic Acids on Different Substrate Glycoproteins in Mouse Neuroblastoma Neuro2a Cells. *Journal of Biochemistry* **122**(6):1265-73.

Kulahin, N., Rudenko, O., Kiselyov, V., Poulsen, F.M., Berezin, V., and Bock, E. (2005) Modulation of the Homophilic Interaction Between the First and Second Ig Modules of Neural Cell Adhesion Molecule by Heparin. *J. Neurochem.* **95**(1):46-55.

Laemmli, U.K. (1970) Cleavage of Structural Proteins During the Assembly of the Head of Bacteriophage T4. *Nature* **227**(5259):680-5.

Malissard, M., Zeng, S., and Berger, E.G. (1999) The Yeast Expression System for Recombinant Glycosyltransferases. *Glycoconj. J.* **16**(2):125-39.

Marchal, I., Jarvis, D.L., Cacan, R., and Verbert, A. (2001) Glycoproteins From Insect Cells: Sialylated or Not? *Biological Chemistry* **382**(2):151-9.

Mendiratta, S.S., Sekulic, N., Lavie, A., and Colley, K.J. (2005) Specific Amino Acids in the First Fibronectin Type III Repeat of the Neural Cell Adhesion Molecule Play a Role in Its Recognition and Polysialylation by the Polysialyltransferase ST8Sia IV/PST. *Journal of Biological Chemistry* **280**(37):32340-8.

Mendiratta, S.S., Sekulic, N., Hernandez-Guzman, F.G., Close, B.E., Lavie, A., and Colley, K.J. (2006) A Novel Alpha-Helix in the First Fibronectin Type III Repeat of the Neural Cell Adhesion Molecule Is Critical for N-Glycan Polysialylation. *Journal of Biological Chemistry* **281**(47):36052-9.

Muhlenhoff, M., Eckhardt, M., Bethe, A., Frosch, M., and Gerardy-Schahn, R. (1996a) Polysialylation of NCAM by a Single Enzyme. *Curr. Biol.* **6**(9):1188-91.

Muhlenhoff, M., Eckhardt, M., Bethe, A., Frosch, M., and Gerardy-Schahn, R. (1996b) Autocatalytic Polysialylation of Polysialyltransferase-1. *EMBO J.* **15**(24):6943-50.

Muhlenhoff, M., Eckhardt, M., and Gerardy-Schahn, R. (1998) Polysialic Acid: Three-Dimensional Structure, Biosynthesis and Function. *Curr. Opin. Struct. Biol.* **8**(5):558-64.

Muhlenhoff, M., Manegold, A., Windfuhr, M., Gotza, B., and Gerardy-Schahn, R. (2001) The Impact of N-Glycosylation on the Functions of Polysialyltransferases. *J. Biol. Chem.* **276**(36):34066-73.

Muller-Dieckmann, J. (2006) The Open-Access High-Throughput Crystallization Facility at EMBL Hamburg. *Acta Crystallogr. D. Biol. Crystallogr.* **62**:1446-52.

Nakata, D., Zhang, L., and Troy, F.A. (2006) Molecular Basis for Polysialylation: a Novel Polybasic Polysialyltransferase Domain (PSTD) of 32 Amino Acids Unique to the Alpha 2,8-Polysialyltransferases Is Essential for Polysialylation. *Glycoconj. J.* **23**(5-6):423-36.

Nelson, R.W., Bates, P.A., and Rutishauser, U. (1995) Protein Determinants for Specific Polysialylation of the Neural Cell-Adhesion Molecule. *Journal of Biological Chemistry* **270**(29):17171-9.

Oltmann-Norden, I., Galuska, S.P., Hildebrandt, H., Geyer, R., Gerardy-Schahn, R., Geyer, H., and Muhlenhoff, M. (2008) Impact of the Polysialyltransferases ST8SiaII and ST8SiaIV on Polysialic Acid Synthesis During Postnatal Mouse Brain Development. *Journal of Biological Chemistry* **283**(3):1463-71.

Ong, E., Nakayama, J., Angata, K., Reyes, L., Katsuyama, T., Arai, Y., and Fukuda, M. (1998) Developmental Regulation of Polysialic Acid Synthesis in Mouse Directed by Two Polysialyltransferases, PST and STX. *Glycobiology* **8**(4):415-24.

Rutishauser, U., Acheson, A., Hall, A.K., Mann, D.M., and Sunshine, J. (1988) The Neural Cell-Adhesion Molecule (Ncam) As A Regulator of Cell-Cell Interactions. *Science* **240**(4848):53-7.

Rutishauser, U. (2008) Polysialic Acid in the Plasticity of the Developing and Adult Vertebrate Nervous System. *Nature Reviews Neuroscience* **9**(1):26-35.

Schiff, M., Röckle, I., Burkhardt, H., Weinhold, B., Hildebrandt, H. (2010): Thalamocortical pathfinding defects precede degeneration of the reticular thalamic nucleus in polysialic acid-deficient mice. *J. Neurosci., accepted.*

Schuck, P. (2000) Size-Distribution Analysis of Macromolecules by Sedimentation Velocity Ultracentrifugation and Lamm Equation Modeling. *Biophysical Journal* **78**(3):1606-19.

Soroka, V., Kolkova, K., Kastrup, J.S., Diederichs, K., Breed, J., Kiselyov, V.V., Poulsen, F.M., Larsen, I.K., Welte, W., Berezin, V., Bock, E., and Kasper, C. (2003) Structure and Interactions of NCAM Ig1-2-3 Suggest a Novel Zipper Mechanism for Homophilic Adhesion. *Structure.* **11**(10):1291-301.

Stummeyer, K. (2004) Enzymes involved in biosynthesis and degradation of poly-α2,8-sialic acid: structure-function relationships. Dissertation. Cellular Chemistry, Hannover Medical School

Weinhold, B., Seidenfaden, R., Rockle, I., Muhlenhoff, M., Schertzinger, F., Conzelmann, S., Marth, J.D., Gerardy-Schahn, R., and Hildebrandt, H. (2005) Genetic Ablation of Polysialic Acid Causes Severe Neurodevelopmental Defects Rescued by Deletion of the Neural Cell Adhesion Molecule. *J. Biol. Chem.* **280**(52):42971-7.

Windfuhr, M., Manegold, A., Muhlenhoff, M., Eckhardt, M., and Gerardy-Schahn, R. (2000) Molecular Defects That Cause Loss of Polysialic Acid in the Complementation Group 2A10. *Journal of Biological Chemistry* **275**(42):32861-70.

Witte, G., Urbanke, C., and Curth, U. (2005) Single-Stranded DNA-Binding Protein of Deinococcus Radiodurans: a Biophysical Characterization. *Nucleic Acids Research* **33**(5):1662-70.

Yabe, U., Sato, C., Matsuda, T., and Kitajima, K. (2003) Polysialic Acid in Human Milk - CD36 Is a New Member of Mammalian Polysialic Acid-Containing Glycoprotein. *Journal of Biological Chemistry* **278**(16):13875-80.

Zuber, C., Lackie, P.M., Catterall, W.A., and Roth, J. (1992) Polysialic Acid Is Associated With Sodium-Channels and the Neural Cell-Adhesion Molecule N-Cam in Adult-Rat Brain. *Journal of Biological Chemistry* **267**(14):9965-71.

Chapter 3 - Polysialic acid controls NCAM signals at cell-cell contacts to regulate focal adhesion independent from FGF receptor activity

- This manuscript has been submitted for publication to the *Journal of Cell Signalling* on November 30th 2010. -

Katinka Eggers, Andrea Schertzinger, Sebastian Werneburg, Miriam Schiff[a], Matthias Alexander Scharenberg[b], Hannelore Burkhardt, Martina Mühlenhoff, Herbert Hildebrandt *

Institute of Cellular Chemistry, Hannover Medical School, Hannover, Germany

[a] Present address: Department of Neuroscience, Karolinska Institute, Stockholm, Sweden

[b] Present address: Friedrich Miescher Institute for Biomedical Research, Novartis Research Foundation, Basel, Switzerland

* **Author for correspondence**: Herbert Hildebrandt
Institute of Cellular Chemistry, OE 4330, Hannover Medical School, Carl-Neuberg-Str. 1,
30625 Hannover, Germany.
Phone: +49 511 532 9808, Fax:+49 511 532 3956
e-mail: hildebrandt.herbert@mh-hannover.de

Preface

In the course of this study, the influence of polySia-NCAM and in particular the dinstinct impact of these two players on cell migration and stimulation of focal adhesion was investigated. Thereby, NCAM was identified to be the pivotal actor in these events of cell regulation. Furthermore, the pathway leading to stimulation of focal adhesions was shown to depend on a so far unknown heterophilic NCAM receptor and the interaction site was shown to reside in Ig3 and/or Ig4 of NCAM. Further, this pathway showed to be independent from FGF receptor activation and ERK 1/2 phosphorylation. My contribution to this work was to provide a series of NCAM fragments allowing for dissection of the distinct domains' impact, and to perform assays addressing NCAM mediated ERK 1/2 phosphorylation and stimulation of focal adhesions.

Abstract

The polysialic acid (polySia) modification of the neural cell adhesion molecule NCAM is a key regulator of cell migration. Yet its role for NCAM-dependent or NCAM-independent modulation of motility and cell-matrix adhesion is largely unresolved. Here, we demonstrate that loss of polySia attenuates tumour cell migration and augments the number of focal adhesions in a cell-cell contact- and NCAM-dependent manner. In the presence or absence of polySia, NCAM never co-localized with focal adhesions but was enriched at cell-cell contacts. Focal adhesion of polySia- and NCAM-negative cells was enhanced by incubation with soluble NCAM or by removing polySia from heterotypic contacts with polySia-NCAM-positive cells. Focal adhesion was compromised by the src-family kinase inhibitor PP2, while loss of polySia or exposure to NCAM promoted the association of p59^{Fyn} with the focal adhesion scaffolding protein paxillin. Unlike other NCAM responses, NCAM-induced focal adhesion was not prevented by inhibition of FGF receptor activity and could be evoked by NCAM lacking the first two immunoglobulin domains but neither by the NCAM fibronectin domains alone nor by an NCAM-derived peptide known to interact with and activate FGF receptors. Together, these data indicate that polySia regulates cell motility via NCAM-induced but FGF receptor-independent signalling to focal adhesions.

Introduction

The balanced regulation of cell-cell and cell-matrix adhesion is crucial for coordinated cell motility in development, while dysregulated adhesion is a hallmark of tumour progression (Christofori, 2003; Friedl and Wolf, 2010). The neural cell adhesion molecule NCAM, a recognition molecule of the immunoglobulin superfamily plays a pivotal role in cell-cell interactions, as studied mainly in nervous system development (Maness and Schachner, 2007), but also modulates matrix adhesion of tumour cells (Cavallaro et al., 2001). Alternative splicing generates three major NCAM isoforms (NCAM120, NCAM140 and NCAM180) (Cunningham et al., 1987). These differ in their transmembrane and intracellular domains, but have identical extracellular parts composed of five amino-terminal immunoglobulin-like domains (Ig1-Ig5) followed by two fibronectin type 3 modules (FnI, FnII), and therefore can interact with the same extracellular binding partners. Initially, NCAM was characterized to exert homophilic binding (Hoffman and Edelman, 1983), but later numerous heterophilic cis- and trans-interactions have been identified, e.g. with other CAMs of the immunoglobulin superfamily like TAG1 or L1, cellular prion protein, and ligands of the GDNF family and the

GDNF family receptor alpha-1, but also with heparan and chondroitin sulphate proteoglycans of the extracellular matrix through heparin-binding sites localized to the Ig2 domain of NCAM (for review, see Nielsen et al., 2010).

The most studied extracellular interaction partners in terms of NCAM function, however, are members of the FGF receptor family (Maness and Schachner, 2007; Kiselyov, 2010). Activation of FGF receptors is mainly implicated in neurite outgrowth in response to homophilic NCAM trans-interactions (Saffell et al., 1997; Niethammer et al., 2002; Kiselyov et al., 2003), but also contributes to the cell-autonomous modulation of matrix adhesion by an NCAM-dependent signalling complex in pancreatic tumour cells (Cavallaro et al., 2001). More recently, FGF receptor-dependent promotion of cell migration was demonstrated by soluble NCAM applied to NCAM-negative cells (Francavilla et al., 2009). Other functions of NCAM as a signalling receptor are independent from interactions with FGF receptors. Activation of the src-family kinase Fyn and subsequent recruitment of the focal adhesion kinase (FAK) to NCAM140 depends on lipid raft association of NCAM and complements FGF receptor signalling in neuritogenesis induced by homophilic NCAM interactions (Beggs et al., 1997; Niethammer et al., 2002). Similarly, translocation of NCAM from FGF receptor complexes to lipid rafts and activation of Fyn was observed after up-regulation of NCAM in response to a loss of E-cadherin, while knockdown of NCAM caused a loss of focal adhesion and enhanced migration of cells with a mesenchymal phenotype (Lehembre et al., 2008).

Polysialic acid (polySia) is a major determinant of NCAM binding but also a general modulator of cell-cell interactions (Rutishauser, 2008; Hildebrandt et al., 2010). This unusual polymeric sugar can be added to *N*-glycosylation sites within the fifth Ig domain of NCAM by two polysialyltransferases, ST8SiaII (STX) and ST8SiaIV (PST), which exhibit a high specificity for the acceptor protein (Colley, 2010). PolySia, therefore, is confined to a small subset of proteins, with NCAM being by far the most abundant carrier of polySia in most mammalian cells (Colley, 2010; Galuska et al., 2010; Hildebrandt et al., 2010). Although polySia is diminished in the majority of tissues during development, various tumours are known to re-express polySia on NCAM and high polySia levels have been correlated with malignant potential and poor prognosis of small cell lung carcinoma, neuroblastoma, glioblastoma, medulloblastoma, and rhabdomyosarcoma (Scheidegger et al., 1994; Figarella-Branger et al., 1996; Glüer et al., 1998a; Glüer et al., 1998b; Hildebrandt et al., 1998; Tanaka et al., 2000; Daniel et al., 2001; Amoureux et al., 2010). In the developing nervous system, polySia is crucially involved in the migration of

neuronal precursors (Ono et al., 1994; Hu et al., 1996; Chazal et al., 2000; Weinhold et al., 2005; Angata et al., 2007; Burgess et al., 2008) and modulates the responsiveness of oligodendrocyte precursor to chemotactic migration cues (Barral-Moran et al., 2003; Zhang et al., 2004; Glaser et al., 2007). In both settings, polySia seems to affect motility independent from specific functions of its protein carrier NCAM. Instead, polySia may act as a non-specific steric inhibitor of cell–cell apposition or by modulation of chemotactic growth factor sensing. In pancreatic carcinoma cells, enhanced polysialylation of NCAM has been correlated with facilitated migration due to reduced E-cadherin-mediated cell-cell aggregation (Schreiber et al., 2008). So far, however, the impact of polySia on NCAM-induced or NCAM-independent modulation of motility and cell-matrix interactions of tumour cells has not been directly addressed. Here, we demonstrate that loss of polysialic acid reduced migration of tumour cells and increased focal adhesion in a cell-cell contact- and NCAM-dependent manner but independent from FGF receptor activity.

Materials and Methods

Antibodies and reagents

The following commercial reagents were used: FGF receptor inhibitor PD173074, Rho-associated protein kinase inhibitor Y-27632, fluorescein isothiocyanate (FITC) -labelled phalloidin, goat IgG (all from Sigma-Aldrich, St Louis, MO), MFP647 Phalloidin (MoBiTec, Göttingen, Germany), src-family kinase inhibitor PP2 (Merck, Darmstadt, Germany), MEK inhibitor PD98059 (Alexis, San Diego, CA), bovine fibronectin (Biomol, Hamburg, Germany), and heparinases I and III from Flavobacterium heparinum (Sigma-Aldrich).

Mono- and polyclonal primary antibodies (mAb, pAb) were: anti-ERK1/2 rabbit pAb, anti-dually phosphorylated ERK1/2 mouse mAb, clone E10 (New England Biolabs, Ipswich, MA), anti-fibronectin goat pAb, anti-fibronectin mouse mAb, clone FN-15, anti-SynCAM 1 rabbit pAb, (all from Sigma-Aldrich), anti SynCAM 1 chicken mAb 3E1 (MBL, Woburn, MA), anti-FAK rabbit pAb, anti-Fyn rabbit pAb, anti-neuropilin2 rabbit pAb, anti-phospho-tyrosine mouse mAb, clone PY99 (all from Santa Cruz Biotechnology, Santa Cruz, CA), anti-paxillin mouse mAb, clone 394 (BD Biosciences, San Jose, CA), anti-polySia mouse mAb, clone 735 (IgG2a; Frosch et al., 1985), and anti-NCAM mouse mAb, clone 123C3 (IgG1), directed against a membrane-proximal region of NCAM comprising the first fibronectin type III module and reactive with all isoforms of human NCAM (Gerardy-Schahn and Eckhardt, 1994; kindly provided by R. Gerardy-Schahn).

Endo-*N*-acetylneuraminidase F (endoNF) specifically degrading polySia was isolated as described (Stummeyer et al., 2005) and used in cell culture media at a concentration of 200 ng per ml to remove polySia from the cell surface. As a control for endoNF, the inactive double mutant endoNF-R596A/R647A, that binds to polySia but does not degrade it (Stummeyer et al., 2005), was used in some of the experiments. Human IgG$_1$-Fc fragments and secreted, polySia-free NCAM-Fc chimera, consisting of the extracellular domain of human NCAM (amino acids 1–705) fused to the constant (Fc) part of human IgG$_1$, were produced as described (Röckle et al., 2008) and used at a concentration of 1 μg/ml. Soluble NCAM extracellular domain fragments were produced as described below. C3d, a synthetic dendrimeric undeca peptide, which binds to the first Ig-like module of NCAM, its inactive variant C3d2ala (Ronn et al., 1999), and a dimeric form of the FGL peptide derived from the second fibronectin type III module of NCAM, which is capable of binding to and activating FGF receptors (Neiiendam et al., 2004), were kindly provided by E. Bock (Panum Institute, Copenhagen, Denmark).

Production of NCAM protein fragments

NCAM fragments were PCR amplified from human NCAM-140 with the following primer pairs: 5'-GCAGGGATCCCTGCAGGTGGATATTG-3/5'-ATCGCGGCCGCCGAGGTCCTGAACAC-3' (NCAM Ig1-Fn2), 5'-GATCGGCGCCATGAGAACCATCCAGGCCAGGCAG-3'/5'-GTGGGAAGCTTTTAGGTCCTGAACAC-3' (NCAM Ig3-Fn2), 5'-GATCGGCGCCATGAGAACCATCCAGGCCAGGCAG-3'/5'-GTTAAAGCTTTTATGGCTGCGTCTTGAAC-3' (NCAM Ig3-Fn1), 5'-ACCGGATCCCAGGACTCCCAGTC-3'/5'-GTTAAAGCTTTTATGGCTGCGTCTTGAAC-3' (NCAM Ig5-Fn1), 5'-GATCGGCGCCGACACCCCTCTTCACCAT-3'/5'-CAACAATTGCATTCATTTTAT-3' (NCAM Fn1-Fn2). The PCR products were cloned into a modified pFastBac HT A vector (Invitrogen, Paisley, UK) containing a Honey Bee Mellitin secretion signal and an N-terminal His-Tag using the following restriction sites: *Not*I/*Bam*HI (NCAM Ig1-Fn2), *Bam*HI/*Hind*III (NCAM Ig5-Fn1) and *Kas*I/*Hind*III (NCAM Ig3-Fn2, NCAM Ig3-Fn1, NCAM Fn1-Fn2). The constructs code for the following NCAM protein fragments (according to UniProt 13596), none of them comprising the alternatively spliced VASE exon coding for 10 amino acids in the fourth Ig-like domain of NCAM: NCAM Ig1-FnII: Ser^{19}-Thr^{702}; NCAM Ig3-FnII: Thr^{213}-Thr^{702}; NCAM Ig3-FnI: Thr^{213}-Pro^{607}; NCAM Ig5-FnI: Gln^{393}-Pro^{607}; NCAM FnI-FnII: Ala^{497}-Thr^{702}. Baculoviruses coding for the respective NCAM fragments were generated using the Bac-to-Bac® Baculovirus Expression System (Invitrogen) according to the manufacturer's instructions. *Sf*9 insect cells were grown in suspension culture at a density of 0.5-$5x10^6$ cells/ml in protein free Insect Xpress Medium (Lonza, Basel, Switzerland) at 70-90 rpm and 27°C. 1-4 l of *Sf*9 cell cultures were infected at a density of 1.7-2.0 cells/ml with P3 baculoviral stock, cell culture supernatants were harvested 72 h post infection and secreted proteins were purified by Ni^{2+} chromatography using HisTrap columns (GE healthcare, Munich, Germany) followed by size-exclusion chromatography (Superdex 200 HR 10/300 GL or HiLoad 16/60 Superdex 200; Amersham Biosciences, Freiburg, Germany) in 10 mM Tris-HCl buffer pH 7.5, containing 100 mM NaCl.

Tumor cells, culture and transfection

The human neuroblastoma cell lines SH-SY5Y (ATCC-no. CRL-2266), Kelly (ECACC-no. 92110411) and LS (Rudolph et al., 1991) and the rhabdomyosarcoma cell line TE-671 (ATCC-no. CRL-7774) were used. SH-SY5Y$_{EGFP}$, stably transfected to express cytosolic EGFP and LS cell clones stably transfected to express either polySia-negative NCAM-140, (LS$_{AM1}$), polysialylated NCAM-140 (LS$_{AM1PST}$) or polysialylated NCAM-140 plus cytosolic EGFP LS$_{AM1PSTegfp}$ were generated as described previously (Seidenfaden et al., 2003; Seidenfaden et al.,

2006). Cells were cultured at 37°C and 9% CO2 in DMEM-Ham's F12 medium containing 10% (v/v) heat-inactivated fetal bovine serum and 2mM glutamate (all from Biochrom, Berlin, Germany). Media were changed every two days and cells were re-plated before confluency.

Cell migration

Time-lapse videomicroscopy and measurements of single cell motility were performed as described elsewhere (Röckle et al., 2008). For 2D scratch wound migration assays, cells were grown to confluency in 35 mm Petri dishes (uncoated, if not stated otherwise). A plastic pipette tip was used to produce a scratch wound of approximately 10 mm length and 500 μm widths. Medium was replaced to remove dead cells and to apply reagents, as specified for each experiment. After acute cellular reactions at the wound edge had abated (time point t0) and 6 hours later (time point t6) the entire scratch was documented using the MosaiX module of AxioVision software (see "Image acquisistion"). To assess the number of cells that invaded the cell free area a mask outlining the edges of the scratch at t0 was superimposed on the image of the same region at t6 using CorelDraw X3 software and the area newly covered by cells was determined using the thresholding and particle analyses tools of NIH ImageJ software.

Immunoprecipitation and immunoblotting

Immunoprecipitation of neuropilin-2 and SynCAM 1 was performed from cells lysed in 50 mM Tris-HCl, pH 7.4 containing 1% Triton X-100, 0.5% sodium deoxycholate, 150 mM NaCl, 5 mM EDTA, 1 mM phenylmethylsulfonylfluoride (PMSF), 10 pg/ml leupeptin and 10 mg/ml aprotinin. After centrifugation at 20,000 x g (15 minutes, 4°C), supernatants were pre-cleared by incubation with normal IgG for 30 minutes and Protein G-Sepharose beads (GE-Healthcare, Freiburg, Germany) for 30 minutes followed by centrifugation at 9,000 x g. 1 μg of primary antibody was added to extracts containing 1 mg protein in a 1 ml volume. After overnight incubation at 4 °C with gentle inversion, immune complexes were recovered by incubation with 15 μl bed volume of Protein G-Sepharose (4 hours, 4°C). Pellets were collected by centrifugation at 9,000 x g for 1 minute, washed 3 times with lysis buffer and reacted with 1 μg endoNF for 30 minutes on ice, where indicated. Proteins were eluted in reducing SDS sample buffer and separated by 10% SDS polyacrylamide gel electrophoresis.

Immunoprecipitation of Fyn and paxillin was conducted in the same way, but cells were lysed in Brij 96 lysis buffer consisting of 20 mM Tris-HCl, pH 7.4, 1% Brij 96, 150 mM NaCl, 10 mM NaF, 1 mM EDTA, 1 mM EGTA, 1 mM Na3VO4, 1 mM PMSF, 10 pg/ml leupeptin and 10 mg/ml aprotinin. Protein A Sepharose was used with the mouse anti- paxillin mAb.

Immunoblotting and analysis of ERK1/2 mitogen activated protein (MAP) kinase or protein tyrosine phosphorylation was performed as described (Seidenfaden et al., 2003). Except for analyses of Fyn immunoprecipitation and detection of SynCAM 1, which were performed by enhanced chemiluminescence (ECL; Seidenfaden et al., 2003; Galuska et al., 2010), the Odyseey Infrared Imaging system (LI-COR Biosystems, Homburg, Germany) was used for semi-quantitative evaluation. To assess ERK1/2 phosphorylation, cells were washed with ice-cold PBS and harvested with a cell scraper in ice-cold Brij 96 lysis buffer. After 10 minutes of incubation on ice the lysates were centrifuged at 20,000 x g (15 min, 4 °C) and supernatants were mixed with reducing electrophoresis buffer. 20 or 40 µg of protein were separated on 10% SDS polyacrylamide gels. After transfer to PVDF membranes, double-immunostaining was performed by combined incubation with rabbit anti-ERK and mouse anti-phospho ERK primary antibodies followed by IRDye 680- and 800-labelled secondary antibodies diluted in Odyssey Blocking Buffer according to the manufacturer's instructions. Signals were detected and quantified with the Odyssey Infrared Imaging System. If antibodies from different species were available, the presence of two antigens was assessed by double-immunolabelling and simultaneous detection with the Odyssey Infrared Imaging System, as described for the analysis of ERK phosphorylation. For further detection or application of a second primary antibody from the same species, antibodies were washed off with NewBlot Stripping Buffer (LI-COR Biosystems). Prior to re-probing, membranes were scanned to ensure complete antibody removal.

Immunocytochemistry

Immunostaining was performed as described before (Seidenfaden and Hildebrandt, 2001; Schiff et al., 2009). Briefly, cells were fixed with 4% paraformaldehyde (PFA) for 30 min, blocked with 2% bovine serum albumin, and incubated with primary antibodies overnight at 4°C. For detection of intracellular epitopes, cells were permeabilized with 0.1% Triton X-100. Rabbit and mouse IgG-specific and subtype-specific Cy3- (Chemicon, Temecula, CA), Alexa488-, Alexa568-, and Alexa647- (Molecular Probes/Invitrogen) conjugated antibodies and phalloidin conjugates were used as suggested by the suppliers. In double stained immunofluorescence samples, cross-reactivity of secondary antibodies was controlled by omitting either of the two primary antibodies. Cells were coverslipped in Vectashield mounting medium with 4',6'-diamidino-2-phenylindole (DAPI; Vector Laboratories, Burlingame, CA).

Image acquisition, counting, and statistics

Microscopy was performed using a Zeiss Axiovert 200 M equipped with an ApoTome device for near confocal imaging, AxioCam MRm digital camera and AxioVison software (Carl Zeiss Microimaging, Göttingen, Germany). For evaluation of scratch migration, high contrast bright field micrographs covering the entire area of the approximately 1 cm scratch wound were acquired using the MosaiX module. For co-localization studies, optical sections of 0.81 μm thickness were obtained using a 63x Plan-Apochromat oil immersion objective with 1.4 numerical aperture (Zeiss).

For evaluation of peripheral focal adhesions, stained cultures and micrographs were coded and randomized to ensure that the observer was blind to the experimental conditions. Per culture, a minimum of 30 micrographs were acquired at 63x magnification. Positions of frames were selected using only the channel for nuclear stain (DAPI) first, before the frame was adjusted to image the entire cell of interest using the channel for actin staining (FITC- or MFP647-phalloidin). Typical peripheral focal adhesions were identified as sites of FAK immunofluorescence colocalized with actin staining and counted by visual inspection assisted by the interactive event counting tool of AxioVision software.

Statistical analyses were performed using Graphpad Prism software. Differences between two groups were evaluated with Student's t test (two-tailed). For more than two groups to compare, one way ANOVA with Newman-Keuls multiple comparison post hoc test (two-tailed) was applied.

Results

PolySia enforces and NCAM inhibits cell-cell contact-dependent cell migration

The role of polySia in migration of tumour cells was studied in vitro with 2D scratch wound assays. In a first approach, an EGFP transfected clone of the polySia- and NCAM-positive neuroblastoma cell line SH-SY5Y was used (SH-SY5Y$_{EGFP}$) (Seidenfaden et al., 2003). As illustrated in Fig. 1A, the number of cells populating the cell free area within 6 hours was significantly reduced in the presence of endo-*N*-acetylneuraminidase (endosialidase, endo), which reliably removes polySia from the surface of living cells (Seidenfaden et al., 2003; see also supplementary material Fig. S1). Image analyses revealed that significantly less new cell clusters were detected in the scratched area (Fig. 1B), whereas the size of the newly arrived clusters was unaltered (Fig. 1C). In contrast to these results with cells that move in close contact with each other, we found that removal of polySia had no influence on the motility of single cells (Fig. 1D, and supplementary material Movie 1, Movie 2 and Fig. S2).

Figure 1: PolySia removal attenuates migration in scratch wound assays with SH-SY5Y$_{EGFP}$ cells. (A) Representative micrographs of SH-SY5Y$_{EGFP}$ cells migrating into a scratch wound over a period of 6 hours in the absence (ctrl.) or presence of 200 ng/ml endoneuraminidase (endo). Scale bar, 250 μm. (B, C) Number and size of newly appearing cell clusters within the cell-free area of scratch wounds after 6 hours as shown in (A). (D) Velocity of solitary SH-SY5Y cells traced in low density cultures in the absence (ctrl.) or presence of 200 ng/ml endoneuraminidase (endo) for variable periods during which the cell of interest had no contact with other cells. Average observation times (+/- standard error of the mean, SEM) were 363 +/- 56 minutes and 364 +/- 54 minutes for the control or endo-treated group, respectively. Means +/- SEM from n= 4-7 independent experiments (B, C) or n = 16 cells, each (D). *n.s.*, not significant ($P > 0.01$), ***, significant with $P < 0.001$, *t*-test.
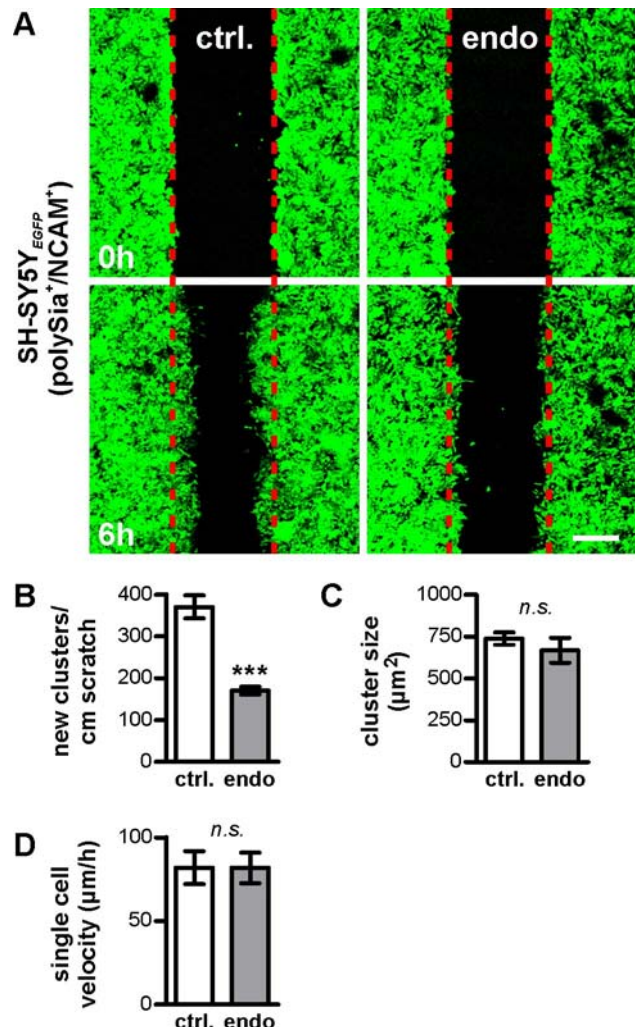
As described before, SH-SY5Y cells express the two transmembrane isoforms of NCAM, NCAM140 and NCAM180, and the entire NCAM pool is polysialylated (Seidenfaden et al., 2000; Seidenfaden and Hildebrandt, 2001). To corroborate that the effect of endo treatment was indeed caused by removal of polySia from NCAM, polysialylation of two recently identified alternative polySia acceptors, neuropilin-2 and SynCAM 1 (Curreli et al., 2007; Galuska et al., 2010) was analysed. Affinity isolation revealed that both proteins were present in SH-SY5Y cells, but neither of them was immunopositive for polySia (supplementary material Fig. S3).

Further scratch wounds assays were performed with non-transfected SH-SY5Y and other cell lines using image analysis of high contrast bright field images (see Materials and Methods for details and supplementary material Movie 3, Movie 4 and Fig. S4 for an example). Consistent with the results described above, a significant reduction of cells repopulating a scratch wounded, cell-free area indicated reduced migration after removing polySia from SH-SY5Y (Fig. 2A) as well as from Kelly (neuroblastoma) and TE671 (rhabdomyosarcoma, Fig. 2B), two other polySia- and NCAM-positive tumour cell lines (Seidenfaden et al., 2000). As with SH-SY5Y$_{EGFP}$ (Fig. 1), analyses were restricted to a 6 hour time window to avoid a major bias due to the slightly reduced cell proliferation in response to polySia removal or NCAM exposure (Seidenfaden et al., 2003).

Asking whether changes in NCAM binding abilities may be responsible for reduced migration in response to endo treatment, we used the NCAM peptide ligand C3d (Ronn et al., 1999) and a non-polysialylated NCAM-Fc chimera to interfere with or to mimic interactions of polySia-free NCAM. C3d is known to bind to NCAM in the absence of polySia and thus prevents the formation of other NCAM contacts (Seidenfaden et al., 2003). In the presence of endo, i.e. after loss of polySia, C3d improved migration of SH-SY5Y cells (Fig. 2A). In contrast, C3d had no effect on migration if added to native, polySia-NCAM-positive SH-SY5Y (Fig. 2A) or LS neuroblastoma cells (Fig. 2C), which are negative for polySia- and NCAM (Seidenfaden et al., 2003). Migration of LS cells, however, was attenuated by the addition of NCAM-Fc indicating that these cells respond to heterophilic NCAM contacts (Fig. 2C, see also supplementary material Movie 3, Movie 4 and Fig. S4). The assumed modulation of migration via polySia-negative NCAM was substantiated by the observation that addition of C3d to two different NCAM140-expressing, polySia-negative LS clones significantly enhanced the repopulation of a scratch wound (Fig. 2D). Finally, reduced migration after endo treatment and its reversal by the C3d peptide was confirmed with LS$_{AMIPST}$ transfected to express polysialylated NCAM140 (Fig.

2E). Previous and current observations indicate that polysialylated NCAM as well as non-polysialylated NCAM after endo treatment is concentrated at sites of cell-cell contact (Seidenfaden et al., 2003; see also Fig. 3D, E). This localization and the results from the scratch wound assays suggest that reduced migration after removal of polySia is due to enhanced NCAM-mediated cell-cell contacts.
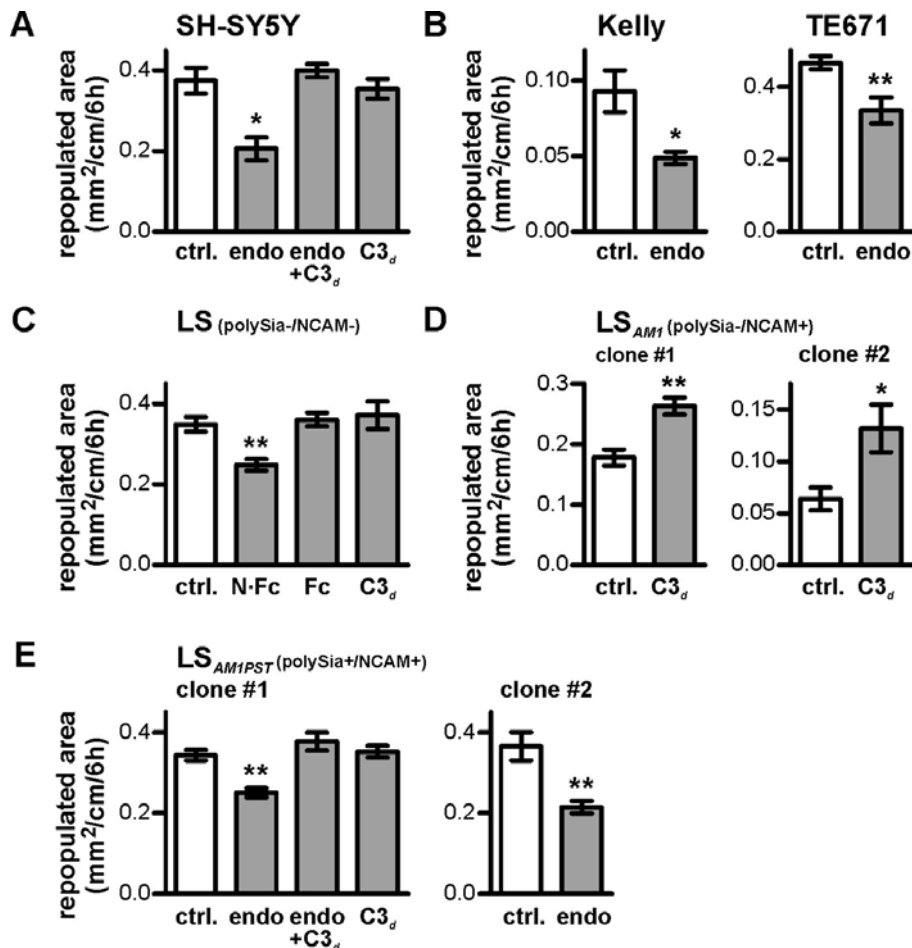
Figure 2: Reduced migration after polySia removal depends on NCAM.

Scratch wound assays were performed with polySia-NCAM-positive SH-SY5Y or Kelly neuroblastoma or TE671 rhabdomyosarcoma cells (A, B), polySia- and NCAM-negative LS neuroblastoma cells (C), LS cell transfectants expressing polySia-negative NCAM-140 (LS$_{AM1}$, D), or polysialylated NCAM-140 (LS$_{AM1PST}$, D). Repopulation of the cell-free area was analysed after 6 hours of incubation with either cell culture medium alone (ctrl.) or with medium containing 200 ng/ml endoneuraminidase (endo), 1 μM of the NCAM binding peptide C3d, or 1 μg/ml soluble NCAM-Fc (N·Fc) or Fc fragment, as indicated. Means +/- SEM from at least 6 (A, B, E) or 3 independent scratch wound assays (C, D). In A, C, and E (clone #1), one-way ANOVA indicated significant differences ($P<0.001$) and Newman-Keuls post test was applied. *t*-tests were performed in B, D, and E (clone #2). *, $P < 0.05$; **, $P < 0.01$ versus all other groups.

PolySia and NCAM modulate peripheral focal adhesions

Cell migration requires the continuous formation and disassembly of adhesions to transmit motion generated by the actin cytoskeleton to the extracellular environment (Webb et al., 2002; Geiger et al., 2009; Parsons et al., 2010). We therefore analysed changes of actin-associated focal adhesions as a measure for altered cell-substrate adhesiveness and a potential cause of altered cell motility after endo treatment or exposure to soluble NCAM-Fc. The polySia-NCAM-positive clone LS$_{AM1PST}$ and parental, polySia- and NCAM-negative LS cells appeared particularly suited for such analyses. These cells display a clearly discernible pattern of peripheral focal adhesions characterized as focal adhesion kinase (FAK) and paxillin immunoreactive spots located at the tip of actin fibres (see Fig. 3A,G for FAK and Supplementary Material, Fig. S5, for paxillin).

Consistent with the data obtained by migration assays, LS$_{AM1PST}$ cells responded to endo treatment with a significant increase in the number of peripheral focal adhesions per cell (Fig. 3A-C). Application of a mutant, enzymatically inactive variant of endo had no effect. Notably, the endo-induced increase was observed only in cells that were in contact with each other and not in isolated cells (Fig. 3C). Independent from the presence or absence of polySia, NCAM was enriched at cell-cell contacts and never co-localized with focal adhesions (Fig. 3D,E). Application of the C3d peptide, which interferes with NCAM binding, completely blocked the cellular response to the enzymatic removal of polySia by endo (Fig. 3F). The observation that NCAM-induced modulation of cell motility is tightly linked to altered focal adhesion was further substantiated by experiments with NCAM-negative LS cells. Both, isolated LS cells and LS cells in contact with each other, showed an increased focal adhesion upon exposure to soluble NCAM-Fc (Fig. 3G-I). Finally, mixed co-cultures of EGFP-transfected, polySia-NCAM-positive LS$_{AM1PST}$ cells (LS$_{AM1PSTegfp}$) and NCAM-negative LS cells were treated with endo followed by an evaluation of focal adhesions of EGFP-negative LS cells in contact with EGFP-positive LS$_{AM1PSTegfp}$, and vice versa (Fig. 3J-L). Under these conditions, focal adhesion was increased exclusively in NCAM-negative cells. This outcome provides direct evidence that unmasking NCAM by enzymatic removal of polySia instructs neighbouring cells to form more focal adhesions. Since these neighbouring cells do not need to express NCAM themselves to respond to the NCAM signal, focal adhesion must be induced by heterophilic NCAM binding.
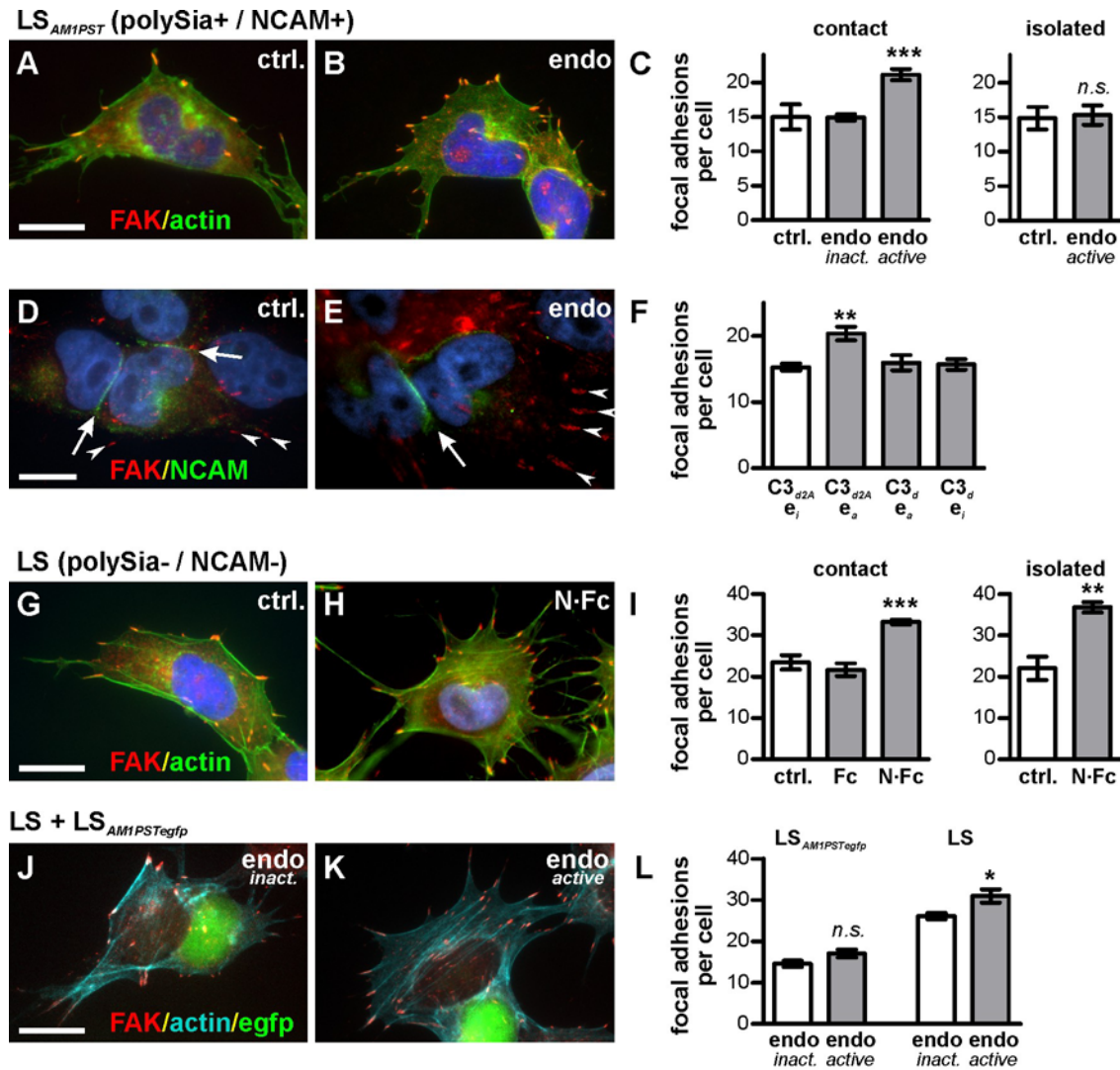
Figure 3: Removal of polySia and trans-interacting NCAM enhance focal adhesion.

(A, B) Detection of peripheral focal adhesions with FAK-specific antibody (red), actin staining with FITC-phalloidin (green) and nuclear counterstain with DAPI (blue) in LS cell transfectants expressing polysialylated NCAM-140 (LS$_{AM1PST}$). In (B), cells were incubated for 30 minutes with 200 ng/ml endoneuramindase (endo). (C) Evaluation of peripheral focal adhesions per cell in cultures incubated for 30 minutes with only cell culture medium (ctrl.) or medium containing 200 ng/ml of either active or mutated, inactive endo, as indicated. Cells in contact with other cells and isolated cells were evaluated separately. Per condition, a minimum of 30 cells were evaluated in each culture. Data represent means +/- SEM from 4-8 independent experiments for each condition. One-way ANOVA indicated significant differences ($P<0.001$) for cells in contact. ***, $P < 0.001$ versus all other groups (Newman-Keuls post test); *n.s.*, not significant ($P > 0.01$), *t*-test.

(D, E) LS$_{AM1PST}$ cells immunolabelled for FAK (red), NCAM (green) and counterstained with DAPI (blue) under control conditions (D) and after treatment with 200 ng/ml endo for 30 minutes (E). Note enrichment of NCAM at cell-cell contact sites (arrows) and lack of co-localization with FAK-positive peripheral focal adhesions (arrowheads) under both conditions.

(F) Number of peripheral focal adhesions in LS$_{AMIPST}$ cells treated with 200 ng/ml inactive or active endo (e$_i$, e$_a$) in the presence of 1 μM of control peptide C3d2ala (C3$_{d2A}$) or NCAM-binding peptide C3d (C3$_d$). Means +/- SEM from 4 independent experiments, each. One-way ANOVA ($P<0.01$) with Newman-Keuls post test. **, $P < 0.01$ versus all other groups.

(G, H) Staining of focal adhesions (see A, B) in polySia- and NCAM-negative LS cells incubated for 30 minutes in the presence or absence of soluble NCAM-Fc (N·Fc). (I) Evaluation of peripheral focal adhesions in LS cells in contact and in isolated cells treated with 1 μg/ml soluble NCAM-Fc (N·Fc) or Fc fragment, as indicated. Means +/- SEM from 3-4 independent experiments, each. One-way ANOVA ($P<0.01$) with Newman-Keuls post test ('contact') or t-test ('isolated') was applied. ***, $P < 0.001$ versus all other groups (post test); **, $P < 0.01$ (*t*-test).

(J, K) LS cells in contact with co-cultured polySia-NCAM-140- and EGFP-positive LS$_{AMIPSTegfp}$ (green) after 30 minutes of incubation with 200 ng/ml inactive (J) or active endo (K). Immunolabelling of FAK (red) and actin staining with MFP647 Phalloidin (cyan). (L) Evaluation of peripheral focal adhesions in LS$_{AMIPSTegfp}$ contacting only LS cells and in LS cells with contact to at least one LS$_{AMIPSTegfp}$ after incubation with inactive or active endo (see J. K). Means +/- SEM from 4 independent experiments, each. *n.s.*, not significant ($P > 0.01$); *, $P < 0.05$ (*t*-test).

Scale bars: 20 μm (A-B, F-G, J-K), 10 μm (D-E).

The data presented so far strongly argue that NCAM interactions at cell-cell contacts induce reduced cell motility by increased focal cell-substrate adhesion. This raises the question of which matrix components may be involved. When scratch wound migration assays were performed on standard cell culture plastic, LS cells efficiently organized a fibronectin-containing extracellular matrix (Fig. 4), which assembled independent from the presence or absence of additional fibronectin coating of the plastic surface (compare Fig. 4B and C). Cell-associated fibronectin did not co-localize with peripheral focal adhesions visualized by FAK immunoreactivity, but frequently aligned with FAK-positive streaks indicative of fibrillar adhesions (for review, see Parsons et al., 2010) (Fig. 4D-F). Consistent with the observation that substrate coating of plastic surfaces had no significant effects on the assembly of cell-associated fibronectin, only minor alterations in cell migration were seen in scratch wound assays that were performed on fibronectin-coated plates and further attenuation of migration could be achieved by the addition of NCAM-Fc in the case of NCAM-negative LS cells and by enzymatic polySia removal in the case of polySia-NCAM-positive LS$_{AMIPST}$ cells (Fig. 4G,H). Thus, exposure of polySia-free NCAM attenuates cell migration on fibronectin, but the segregation of fibronectin-containing adhesions and peripheral focal adhesions suggests a modulation of fibronectin-independent cell-substrate interactions.

NCAM interactions with heparin-like molecules are involved in neuronal cell-cell and cell

substrate adhesion (Cole et al., 1986; Cole and Glaser, 1986) and NCAM-induced inhibition of glioma cell motility is modulated by interference with heparin or heparan sulphate proteoglycan (HSPG) binding (Prag et al., 2002). Moreover, polySia promotes NCAM binding to HSPGs and these interactions are sensitive to digestion of heparan sulfates by combined heparinase I and III treatment (Storms and Rutishauser, 1998). Indeed, migration of the polySia-NCAM-positive LS$_{AMIPST}$ cells was significantly enhanced by application of heparinase I and III, but the same effect was observed with parental, polySia- and NCAM-negative LS cells (Fig. 4I,J). In addition, heparinase treatment prevented neither the inhibition of migration (Fig. 4I,J) nor the increase of focal adhesion after treatment with polySia-negative NCAM-Fc or in response to enzymatic removal of polySia, respectively (Fig. 4K,L). The migration promoting effects of heparinase, therefore, were not related to the altered migration and focal adhesion induced by NCAM application or polySia removal.

Figure 4: Peripheral focal adhesions are not co-localized with fibronectin and neither fibronectin coating nor heparinase application prevents effects of polySia-NCAM-related treatments.

(A-C) Phase contrast image (A) and fibronectin staining (FN; B, C) of LS cells at the edge of a scratch wound. Cells were grown on uncoated (A, B) or fibronectin-coated plastic (2 µg/cm^2; C). (D-E) LS cells double labelled for FN (red, D) and FAK (green, E); merged image (F). Note the co-localization at fibrillar adhesions (arrows in D) but not at peripheral focal adhesions (arrowheads in F). Scale bars, 20 µm.
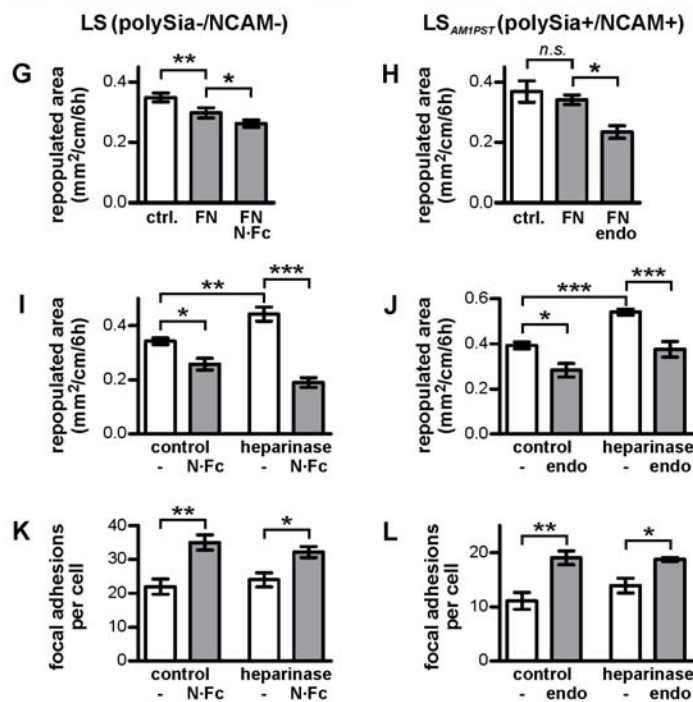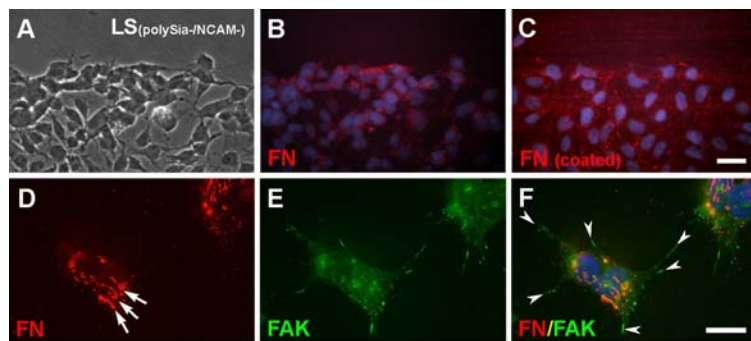
(G-J) Evaluation of scratch wound migration assays performed with LS (G, I) or LS$_{AMIPST}$ cells (H, J) on uncoated (ctrl.) or fibronectin-coated plastic (FN; 2 µg/cm^2; G, H) or in

the presence or absence of freshly dissolved heparinase I and III (0.5 U/ml, each; I, J) combined with soluble NCAM-Fc (N'Fc; 1 µg/ml) or active endo (200 ng/ml), as indicated. Means +/- SEM from at least 3 independent assays, each (n = 3 in G, H; n = 3 for N'Fc or n = 6 for all other groups in I; n = 6 in J).

(K, L) Number of peripheral focal adhesions in LS (K) or LS$_{AMIPST}$ cells (L) pre-treated for 2h with cell culture medium (control) or with medium containing freshly dissolved heparinase I and III (0.5 U/ml, each) before N'Fc (1 µg/ml; K) or active endo (200 ng/ml; L) was added for 30 minutes, as indicated. Means +/- SEM from 4 (K) or 5 (L) independent experiments, respectively.

In (G-L) one-way ANOVA ($P < 0.01$ in G, H, K; $P < 0.001$ in I, J, L) with Newman-Keuls post test was applied. ***, $P < 0.001$; **, $P < 0.01$; *, $P < 0.05$; *n.s.*, not significant for pair-wise comparisons, as indicated.

PolySia-free NCAM promotes focal adhesion independent of FGF receptor activity

The absence of NCAM from the sites of focal adhesion together with the promotion of focal adhesion by soluble NCAM implies that these effects are not caused by direct adhesive interactions of NCAM but are mediated by a cellular signalling cascade. Together with the dynamic modulation of the actin cytoskeleton, the src-family kinase Fyn and the focal adhesion scaffolding protein paxillin are well established determinants of focal adhesion turnover (Webb et al., 2002; Mitra et al., 2005; Schaller, 2010). To demonstrate that focal adhesions of LS cells depend on both components we used PP2 for pharmacological inhibition of Fyn and the Rho-dependent protein kinase (ROCK) inhibitor Y27632 to disrupt actin fibre assembly. As expected, both treatments effectively reduced the number of focal adhesions in LS cells (Fig. 5A-D). Furthermore, co-immunoprecipitation experiments indicated the recruitment of Fyn to the focal adhesion scaffolding protein paxillin after treating LS cells with NCAM-Fc or LS$_{AMIPST}$ with endo (Fig. 5E,F).

Engagement of ERK1/2 is on the one hand a hallmark of NCAM-induced signalling initiated by the loss of polySia (Seidenfaden et al., 2003; Seidenfaden et al., 2006) and triggered at least in part by activation of FGF receptors (Kolkova et al., 2000; Cavallaro et al., 2001; Niethammer et al., 2002; Francavilla et al., 2009). On the other hand, the ERK1/2 pathway is in intimate cross-talk with the regulation of focal adhesion in a stimulus- and cell-type specific manner (for review, see Schwartz and Ginsberg, 2002; Huang et al., 2004; Mitra et al., 2005). We therefore wondered if the NCAM-induced increase of focal adhesion in LS cells depends on ERK1/2 and FGF receptor activity. Confirming previous findings, exposure of LS cells to soluble NCAM-Fc enhanced and pre-incubation with the MEK inhibitor PD98059 completely abolished the fraction

of dually phosphorylated, active ERK1/2 (Fig. 5G). Consistent with the observed tyrosine phosphorylation of Fyn associated with paxillin (Fig. 5E, lower panel) NCAM-Fc also induced an increase in tyrosine phosphorylation of Fyn immunoprecipitated from LS cell lysates (Fig. 5H). Surprisingly, however, inhibition with PD98059 was not able to prevent this increase indicating that activation of ERK1/2 occurs either downstream or independent of Fyn phosphorylation (Fig. 5H).

Figure 5: PolySia-free NCAM recruits Fyn to paxillin.

(A) PP2 inhibits Fyn. Fyn was immunoprecipitated from lysates of LS cells incubated for 1 hour with medium containing 10 μM PP2 or solvent (DMSO) and analysed by Western blot (WB) with phospho-tyrosine- (upper) or Fyn-specific antibodies (lower panel). (B) PP2 treated LS cells round up and loose focal adhesions. Immunofluorescent staining with FAK-specific antibody (red), actin staining with FITC-phalloidin (green) and nuclear counterstain with DAPI (blue). (C, D) Evaluation of peripheral focal adhesions in LS cells treated with medium containing PP2 (10 μM for 1 hour, C), ROCK inhibitor Y27632 (30 μM for 30 minutes, D) or solvent (s, DMSO for C, PBS for D). Means +/- SEM from 9 (C) or 3 (D) independent assays, each. ***, $P < 0.001$; **, $P < 0.01$ (t-test).

(E, F) Immunoprecipitation (IP) of paxillin (pax) from lysates of LS or LS$_{AM1PST}$ incubated for 30 minutes with cell culture medium (ctrl.) or medium containing 1 μg/ml of either NCAM-Fc (N·Fc) or Fc (E), or 200 ng/ml of either active or mutated, inactive endo (F), as indicated. IP fractions were analysed by Western blot (WB) for Fyn, paxillin, and phospho-tyrosine (pY in E). Note the phospho-tyrosine band at the position of Fyn (E, arrow) migrating below the strong signal indicating tyrosine phosphorylated paxillin. This band is particularly prominent in the NCAM-Fc treated sample. Such a separate phospho-tyrosine band could not be observed in the IP
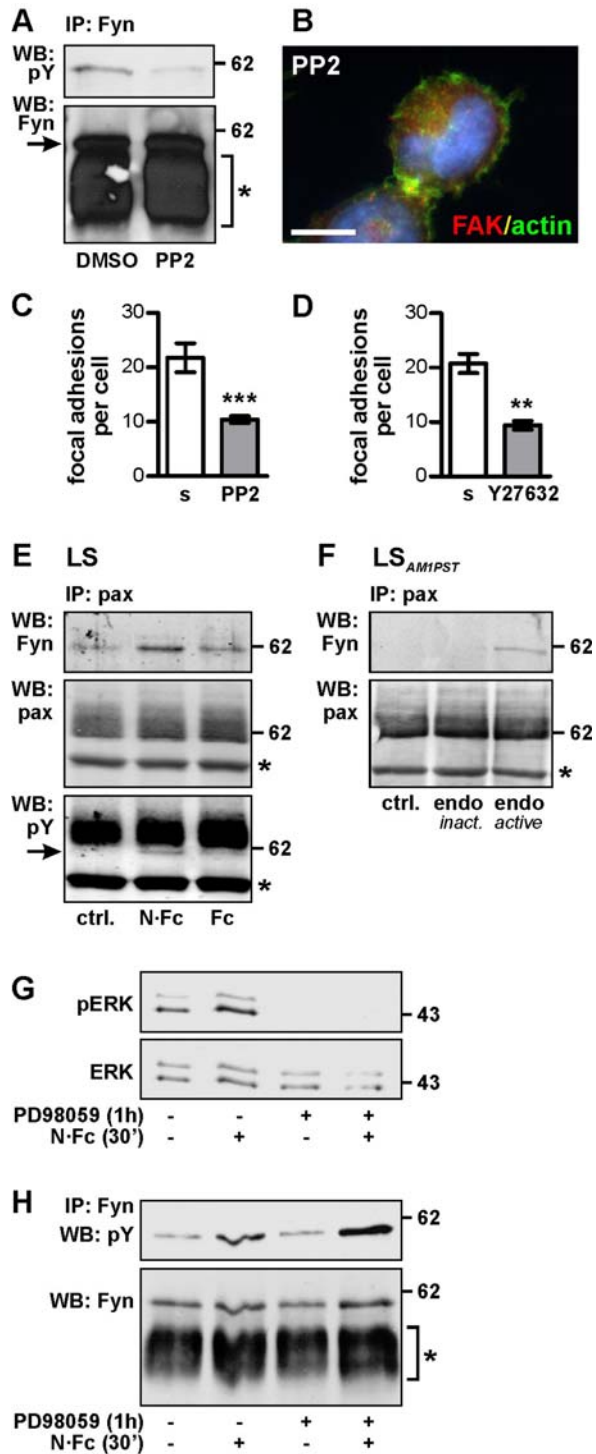
fractions from LS$_{AM1PST}$, most likely because the weak signal is overshadowed by the strong signal for tyrosine phosphorylated paxillin.

(G, H) Western blot analysis of dually phosphorylated ERK (pERK) and total ERK protein in LS cell lysates (G) and tyrosine phosphorylation of Fyn immunoprecipitated from LS cells (H) pre-incubated for 1 hour with 50 μM PD98059 (+) or solvent (DMSO, -) followed by incubation with or without 1 μg/ml soluble NCAM-Fc for 30 minutes, as indicated.

Arrows in (A) and (E) indicate the position of Fyn, * denotes secondary antibody binding to the IP antibody.

To address a possible involvement of FGF receptor activity in the up-regulation of focal adhesion after NCAM exposure or polySia removal we used PD173074, which specifically inhibits signalling of the FGF receptor, leaving other tyrosine kinases unaffected (Skaper et al., 2000). Consistent with recent data by Francavilla et al. (2009) pre-incubation with PD173074 inhibited the NCAM-Fc induced stimulation of ERK1/2 (Fig. 6A). In contrast, the same protocol of PD173074 pre-treatment was not able to prevent the increase of focal adhesion induced by NCAM-Fc (Fig. 6B). Along the same line, the previously described activation of ERK1/2 after polySia removal with endo (Seidenfaden et al., 2003), but not the increase of focal adhesion, was prevented by pre-incubation of LS$_{AM1PST}$ with PD173074 (Fig. 6C,D).

Figure 6: NCAM exposure or polySia removal promotes focal adhesion independent from FGF receptor and ERK1/2 activation.

(A, C) Western blot analyses of dually phosphorylated ERK (pERK) and total ERK protein in lysates of LS (A) or LS$_{AM1PST}$ cells (B) pre-incubated for 1 hour with 5 μM PD173074 (+) or solvent (DMSO, -) followed by incubation with or without 1 μg/ml soluble NCAM-Fc for 10 minutes (A), or 200 ng/ml endo for 30 min (C), as indicated.
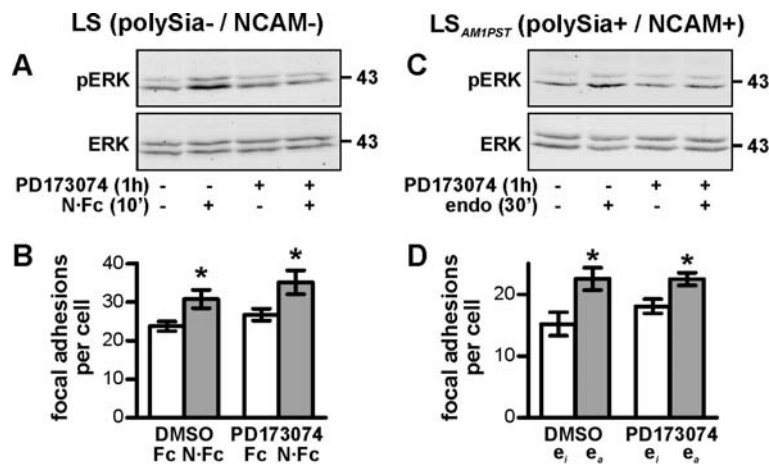
(B, D) Evaluation of peripheral focal adhesions in LS cells pre-incubated for 1 hour with 5 μM PD173074 or solvent (DMSO) and 1 μg/ml Fc or NCAM-Fc for 10 min (B) or 200 ng/ml inactive or active endo (e$_i$, e$_a$) for 30 min (D), as indicated. Means +/- SEM from 5 independent assays, each. *, $P < 0.05$ (t-test).

These results indicate that FGF receptor activity is involved in ERK1/2 activation but not in the modulation of focal adhesion in response to polySia removal or NCAM-induced signals.

According to the prevailing model, homophilic NCAM binding (in trans) involves the first two immunoglobulin domains (Ig1, Ig2) (Kiselyov, 2010) and activates FGF receptors by cis-interactions involving the two fibronectin (Fn) modules of NCAM (Kiselyov et al., 2003; Christensen et al., 2006). Interestingly, peptides corresponding to sites in either FnI or FnII are able to bind to the FGF receptor and activate ERK1/2 (Kiselyov et al., 2003; Neiiendam et al., 2004; Anderson et al., 2005; Jacobsen et al., 2008; Palser et al., 2009), whereas NCAM-Fc lacking the second Fn module failed to elicit various FGF receptor-dependent responses induced by NCAM-Fc containing the entire NCAM extracellular domain (Francavilla et al., 2007; Francavilla et al., 2009). To elucidate which of these NCAM modules are necessary for specifically stimulating focal adhesion in addition to ERK1/2, a number of different NCAM fragments were created (summarized in Fig. 7A). In addition to the entire NCAM extracellular domain (ecd) comprising the five Ig domains (Ig1-Ig5) and the two Fn modules (FnI and FnII), deletion constructs consisting of Ig3 through FnII (3-II), Ig3 through FnI (3-I), Ig5 and FnI (5-I) or FnI and FnII (I-II) were expressed in insect cells. Purified recombinant proteins were adjusted to approximately equimolar concentrations as evidenced by immunodetection with the NCAM specific antibody mAb 123C3, which maps to a region comprising FnI and therefore is able to bind to all fragments (Fig. 7A). In a first step, activity of NCAM$_{ecd}$ was confirmed by dose dependent activation of ERK1/2 (Fig. 7B) before the other constructs were tested at concentrations of approximately 0.1 μM (corresponding to 10μg NCAM$_{ecd}$ per ml; Fig. 7C). As summarized in Fig. 7D all NCAM fragments were equally able to activate ERK1/2. In stark contrast, only the fragments containing Ig3 through FnI but not those consisting of only FnI-FnII or Ig5-FnI induced an increase of focal adhesion (Fig. 7E). Thus, Ig1, Ig2 and FnII were dispensable for NCAM-induced activation of ERK1/2 and focal adhesion in NCAM-negative LS cells, while the Ig3-Ig4 region of NCAM is needed to trigger enhanced focal adhesion. On the one hand, this suggests that interactions with chondroitin or heparan sulphate containing proteoglycans via the heparin-binding domain in Ig2 were not involved, which is consistent with the inability of heparinase treatment to interfere with the effects of NCAM exposure or polySia removal (see Fig. 4I-L). On the other hand, the observation that FnI-FnII stimulated ERK1/2 but not focal adhesion is in perfect agreement with the assumption that enhanced focal adhesion in response to NCAM is not mediated by activation of FGF receptor and ERK1/2 signalling.
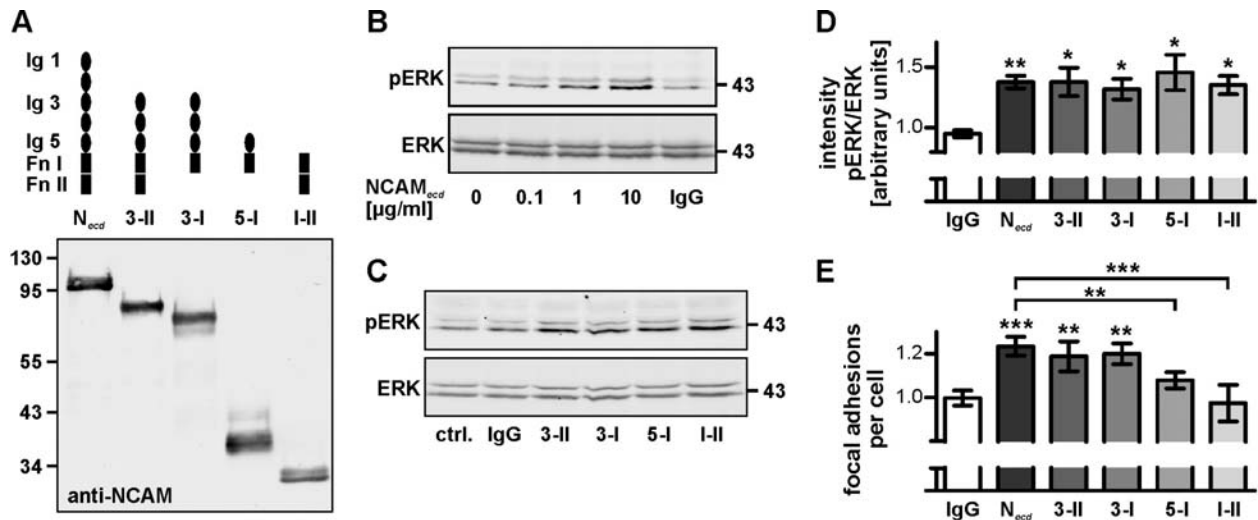
Figure 7: Some NCAM fragments activate ERK1/2 but fail to promote focal adhesion.

(A) Imunoblot analysis of NCAM$_{ecd}$ and other soluble NCAM fragments consisting of different Ig- and Fn-modules as indicated. Detection with mAb 123C3 mapping to a region comprising FnI. For each NCAM fragment, concentrations were adjusted to approximately 0.1 μM.

(B) LS cells were incubated for 10 minutes with 10 μg/ml goat IgG or different concentrations of NCAM$_{ecd}$ as indicated, lysed and analysed by immunoblotting with combined detection of phospho-ERK 1/2 (pERK) and total ERK 1/2 (ERK) using the LI-COR Odyssey imaging system.

(C) LS cells were incubated for 10 minutes with 10 μg/ml goat IgG or 0.1 μM of the different NCAM fragments, as indicated. Immunodetection of pERK and ERK, as in (B).

(D) Densitometric evaluation of pERK relative to ERK protein bands for the experiment described in (C). Since ERK1 and ERK2 were not always separated unambiguously, the respective bands were evaluated together. For each experiment, values were normalized to untreated controls. Values are means (+/- SEM) from 5-9 independent incubations for each of the NCAM fragments or IgG controls. ANOVA ($P<0.01$) with Newman-Keuls post test. **, $P < 0.01$, *, $P < 0.05$ versus IgG treated controls.

(E) Evaluation of peripheral focal adhesions in LS cells incubated as described in (C). For each experiment, values were normalized to untreated controls. Values are means (+/- SEM) from 6-15 independent incubations for each of the NCAM fragments or IgG controls. ANOVA ($P < 0.0001$) with Newman-Keuls post test. ***, $P < 0.001$, **, $P < 0.01$, *, $P < 0.05$ versus IgG treated controls or between experimental groups as indicated.

NCAM-induced activation of FGF receptor and ERK1/2 signalling can be mimicked by a peptide comprising the FG loop region of the NCAM FnII module involved in FGF receptor binding (FGL; Kiselyov et al., 2003; Neiiendam et al., 2004; Francavilla et al., 2009). We therefore used this peptide to further dissect the effects of NCAM on focal adhesion and FGF

receptor signalling. A dose-dependent, saturating activation of ERK1/2 was achieved by FGL application (Fig. 8A,B) and in line with previous data (Neiiendam et al., 2004; Francavilla et al., 2009) the FGL-induced ERK1/2 activation was efficiently prevented by pre-incubation with PD173074 (Fig. 8C). The capacity of FGL to promote focal adhesion of LS and LS$_{AM1PST}$ cells was tested in direct comparison with application of NCAM$_{ecd}$. Unlike NCAM$_{ecd}$, which promoted focal adhesion in both cell types, the application of FGL had no such effect (Fig. 8D,E). In the absence of polySia-free NCAM, the NCAM-binding C3d peptide also had no effect on focal adhesion. These distinct activities indicate that FGL recapitulates FGFR-dependent functions of NCAM, but is unable to mimic NCAM-induced focal adhesion.

Figure 8: ERK1/2 activation by the FGL peptide depends on FGF receptor activity but FGL fails to promote focal adhesion.

(A, C) Western blot analyses of dually phosphorylated ERK (pERK) and total ERK protein in lysates of LS cells incubated with FGL peptide at the indicated concentrations (A) or pre-incubated for 1 hour with 5 μM PD173074 (+) or solvent (DMSO, -) followed by incubation with or without 1 μg/ml FGL for 30 minutes, as indicated (C). (B) Densitometric evaluation of pERK relative to ERK protein bands for the experiment shown in (A). Means
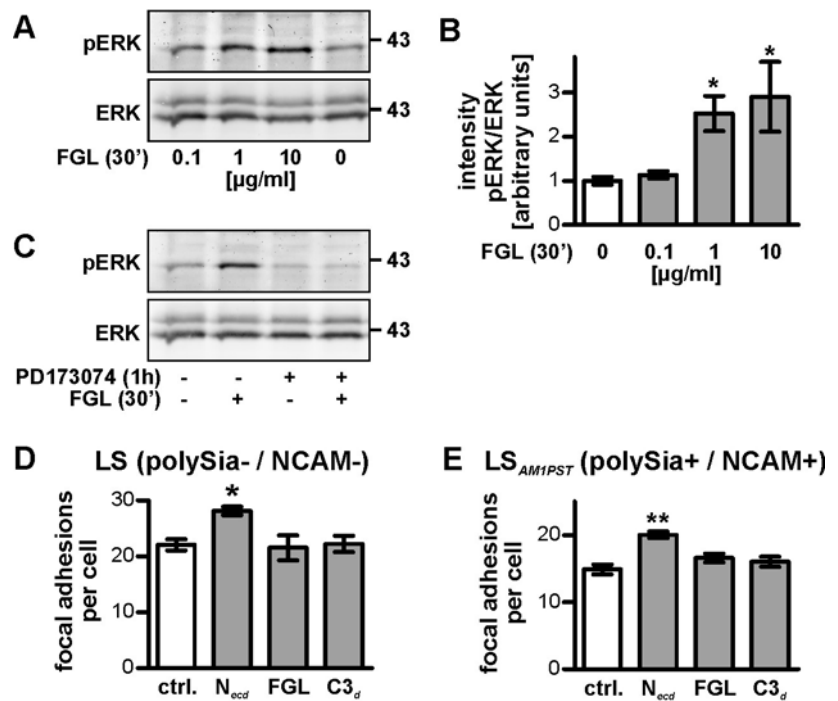
(+/- SEM) from 3-4 independent incubations, each, normalized to untreated controls. ANOVA ($P < 0.01$) with Newman-Keuls post test. *, $P < 0.05$ versus controls.

(D, E) Evaluation of peripheral focal adhesions in LS (D) or LS$_{AM1PST}$ cells (E) incubated with medium (ctrl.), 0.1 μM NCAM$_{ecd}$ (N$_{ecd}$), 1 μg/ml (0.3 μM) FGL or 0.3 μM C3d peptide for 30 minutes, as indicated. Means +/- SEM from 4 independent assays, each. ANOVA ($P < 0.05$ in D; $P < 0.001$ in E) with Newman-Keuls post test. **, $P < 0.01$, *, $P < 0.05$ versus all other groups.

Discussion

Numerous studies describe a close correlation of polySia-NCAM expression with increased tumour invasion and metastatic potential (Scheidegger et al., 1994; Figarella-Branger et al., 1996; Figarella-Branger et al., 1996; Tanaka et al., 2000; Daniel et al., 2000; Daniel et al., 2001; Trouillas et al., 2003; Suzuki et al., 2005; Amoureux et al., 2010). In all these studies, a role of polySia in promoting tumour cell motility has been inferred from its long-known role in modulating adhesiveness and migration in the nervous system (Sadoul et al., 1983; Hoffman and Edelman, 1983; Ono et al., 1994; Wang et al., 1994; Hu et al., 1996; Chazal et al., 2000) but the NCAM-dependent or NCAM-independent modulation of tumour cell migration by polySia has been elusive. In the current study we demonstrate that migration of neuroblastoma and rhabdomyosarcoma cells in a 2D scratch assay is promoted by the presence of polySia. This outcome is not unexpected, since it has been shown before in similar scratch assays that migration of oligodendrocyte precursors is attenuated after removal of polySia (Barral-Moran et al., 2003) and that over-expression of polySia after transfection with ST8SiaII (STX) promotes migration of Schwann cells and embryonic stem cell-derived glial precursors (Lavdas et al., 2006; Glaser et al., 2007). Surprising, however, are the findings that loss of polySia promotes focal adhesion in an NCAM-dependent manner although NCAM is enriched at cell-cell contacts and not localized to focal adhesions. The resulting implication is that removal of polySia promotes focal adhesion by initiating NCAM-induced cellular signalling. This is supported by the observed recruitment of phosphorylated Fyn to the focal adhesion scaffolding protein paxillin in response to polySia removal or application of polySia-negative NCAM. Together, these results suggest a novel role of polySia-regulated NCAM signalling in the crosstalk between cell-cell and cell-matrix adhesion to control cell migration.

Removing polySia from NCAM caused reduced migration and promoted focal adhesion only if cells were in contact with each other. Both effects were prevented by the NCAM-binding peptide C3d, a potent inhibitor of NCAM interactions (Ronn et al., 1999; Ronn et al., 2000; Kiryushko et al., 2003; Kiselyov et al., 2009), and could be recapitulated by exposing NCAM-negative cells to NCAM. Moreover, the loss of polySia from NCAM-positive cells enhanced focal adhesion of adjacent NCAM-negative cells. These data provide strong evidence that removal of polySia initiates interactions of NCAM as a heterophilic ligand at cell-cell contacts. This mechanism is on the one hand consistent with earlier studies showing that polySia controls instructive NCAM signals and that heterophilic NCAM interactions can direct the differentiation of NCAM-negative neuroblastoma cells and of neural progenitors derived from NCAM-deficient mice

(Amoureux et al., 2000; Seidenfaden et al., 2003; Röckle et al., 2008). Along the same lines some of the phenotypic traits of mice with complete or partial ablation of polySia are not caused by the reduced amounts of polySia itself but depend strictly on the untimely appearance of polySia-negative NCAM (Weinhold et al., 2005; Hildebrandt et al., 2009).

On the other hand, this mode of polySia-regulated cell motility differs clearly from the role of polySia as a permissive factor in neuronal migration. Streaming of interneuron precursors from the subventricular zone towards the olfactory bulb is disturbed by either ablation of polySia alone or by a loss of polySia due to NCAM deficiency (Ono et al., 1994; Hu et al., 1996; Chazal et al., 2000; Weinhold et al., 2005) and therefore has been attributed to the general anti-adhesive properties of polySia caused by steric inhibition of membrane-membrane apposition independent of NCAM-mediated interactions (Fujimoto et al., 2001; Rutishauser, 2008). In the context of tumour cell motility, the suggested mechanism that a loss of polySia causes NCAM to act as a ligand in trans also excludes, at least for the experimental setting of the current study where NCAM negative cells are effected, that polySia modulates the function of NCAM as a signalling receptor (Beggs et al., 1997; Kolkova et al., 2000; Niethammer et al., 2002; Hinsby et al., 2004; Bodrikov et al., 2005; Cassens et al., 2010; Kleene et al., 2010a; Kleene et al., 2010b). Moreover, the current data are neither compatible with a role of polySia in the assembly of an NCAM-dependent signalling complex or other cell-autonomous functions of NCAM (Cavallaro et al., 2001; Prag et al., 2002; Lehembre et al., 2008) nor with the assumption that polySia on either NCAM or neuropilin-2 modulates a cell's sensitivity towards chemotactic migration cues (Zhang et al., 2004; Glaser et al., 2007; Rey-Gallardo et al., 2010). Notably, constitutive shedding of soluble NCAM extracellular domain fragments was held responsible for enhanced migration of rat B35 neuroblastoma cells transfected with NCAM-140, whereas the inhibition of shedding reduced migration and increased attachment to fibronectin (Diestel et al., 2005). This raises the possibility that polySia removal affects migration and adhesion by modulating NCAM shedding. In this scenario, the concurrent effects of soluble NCAM and cell contact-dependent interactions after polySia removal would predict that loss of polySia increases cell surface NCAM by inhibition of shedding. There is, however, no reason to assume that NCAM shedding is facilitated by the presence of polySia and all data so far indicate that shed NCAM fragments are not polysialylated (Diestel et al., 2005; Hübschmann et al., 2005; Hinkle et al., 2006; Kalus et al., 2006).

Unlike activation of the ERK MAP-kinase pathway, the stimulation of focal adhesion by

removal of polySia or exposure to polySia-negative NCAM was independent from FGF receptor activity and could not be achieved by the NCAM modules containing the sites that were identified to mediate FGF receptor interaction. This again was unexpected, because most of the previously described NCAM signalling functions depend on FGF receptor activation, either directly or via FGF receptor co-signalling (Kolkova et al., 2000; Cavallaro et al., 2001; Niethammer et al., 2002; Hinsby et al., 2004; Francavilla et al., 2009). Furthermore, a study on the role of NCAM in regulating the motility of glioma cells indicates a crucial function of the intracellular NCAM domain as well as the involvement of heterophilic interactions of the first two Ig modules with membrane associated heparansulfate proteoglycans (Prag et al., 2002). Heterophilic binding of NCAM to heparan sulphate proteoglycans is well-known (Cole and Akeson, 1989), but this binding is promoted by the presence of polySia (Storms and Rutishauser, 1998), i.e., in contrast to the results of the current study, removal of polySia and NCAM exposure should have contrary effects. In fact, our results argue that the polySia-dependent effects observed in the current study are not caused by interactions of polySia or NCAM with glycosaminoglycans. First, the second Ig domain containing the heparin or chondroitin sulfate binding site of NCAM was dispensable for NCAM-induced focal adhesion. Second, heparinase treatment promotes migration per se, but interferes neither with the inhibition of migration nor with enhanced focal adhesion induced by NCAM-treatment or polySia-removal.

In summary, polySia promotes tumour cell motility by acting as a negative regulator of NCAM-induced but FGF receptor-independent signalling from cell-cell contacts to focal adhesions. The heterophilic NCAM interactions responsible for activating the cellular response initiated by a loss of polySia remain to be defined. Nevertheless, the proposed mechanism allows for several important predictions concerning future development and assessment of polySia- or NCAM-directed tools aiming at a reduction of motility of the highly metastatic polySia-NCAM-positive tumours. First, attempts to reduce polySia levels should target the glycan itself without interfering with the expression of NCAM or with trans-interactions of polySia-free NCAM. Second, NCAM mimetic peptides targeted at FGF receptor interaction and activation are not likely to directly enhance cell-matrix adhesiveness but, as shown by others (Kiselyov et al., 2003; Neiiendam et al., 2004; Francavilla et al., 2009) and confirmed in the current study, exert potent effects via activation of ERK MAP kinase signalling and possibly other pathways. Third, motifs contained within the Ig3 and Ig4 modules of the NCAM extracellular domain, but not the regions comprising Ig1 and Ig2 or Ig5 through FnII, appear to be crucially involved in the heterophilic trans-interactions that cause enhanced focal adhesion. Fourth, strategies to mimic

these heterophilic NCAM contacts seem to be as promising as approaches to prevent or abolish polysialylation. It remains a major challenge for future studies to define these interactions and to address the question on the role of polySia in regulating NCAM binding to FGF receptors. An anti-apoptotic effect of ERK activation in response to heterophilic NCAM interactions after polySia removal has been demonstrated before (Seidenfaden et al., 2003). Assuming that the underlying NCAM contacts correspond to those responsible for the FGF-receptor-mediated activation of ERK by applying NCAM-Fc or FGL peptide to NCAM-negative neuroblastoma (this study) or Hela cells (Francavilla et al., 2009) even raises the possibility to develop different NCAM mimetic peptides in order to dissect the survival promoting function of NCAM from its inhibitory effect on tumour cell motility due to the stimulation of focal adhesion.

References

Amoureux, M. C., Cunningham, B. A., Edelman, G. M. and Crossin, K. L. (2000). N-CAM binding inhibits the proliferation of hippocampal progenitor cells and promotes their differentiation to a neuronal phenotype. *J. Neurosci.* **20**, 3631-3640.

Amoureux, M. C., Coulibaly, B., Chinot, O., Loundou, A., Metellus, P., Rougon, G. and Figarella-Branger, D. (2010). Polysialic acid neural cell adhesion molecule (PSA-NCAM) is an adverse prognosis factor in glioblastoma, and regulates olig2 expression in glioma cell lines. *BMC Cancer* **10**, 91.

Anderson, A. A., Kendal, C. E., Garcia-Maya, M., Kenny, A. V., Morris-Triggs, S. A., Wu, T., Reynolds, R., Hohenester, E. and Saffell, J. L. (2005). A peptide from the first fibronectin domain of NCAM acts as an inverse agonist and stimulates FGF receptor activation, neurite outgrowth and survival. *J. Neurochem.* **95**, 570-583.

Angata, K., Huckaby, V., Ranscht, B., Terskikh, A., Marth, J. D. and Fukuda, M. (2007). Polysialic acid-directed migration and differentiation of neural precursors is essential for mouse brain development. *Mol. Cell Biol.* **27**, 6659-6668.

Barral-Moran, M. J., Calaora, V., Vutskits, L., Wang, C., Zhang, H., Durbec, P., Rougon, G. and Kiss, J. Z. (2003). Oligodendrocyte progenitor migration in response to injury of glial monolayers requires the polysialic neural cell-adhesion molecule. *J. Neurosci. Res.* **72**, 679-690.

Beggs, H. E., Baragona, S. C., Hemperly, J. J. and Maness, P. F. (1997). NCAM140 interacts with the focal adhesion kinase p125(fak) and the SRC- related tyrosine kinase p59(fyn). *J. Biol. Chem.* **272**, 8310-8319.

Bodrikov, V., Leshchyns'ka, I., Sytnyk, V., Overvoorde, J., Den Hertog, J. and Schachner, M. (2005). RPTPalpha is essential for NCAM-mediated p59fyn activation and neurite elongation. *J. Cell Biol.* **168**, 127-139.

Burgess, A., Wainwright, S. R., Shihabuddin, L. S., Rutishauser, U., Seki, T. and Aubert, I. (2008). Polysialic acid regulates the clustering, migration, and neuronal differentiation of progenitor cells in the adult hippocampus. *Dev. Neurobiol.* **68**, 1580-1590.

Cassens, C., Kleene, R., Xiao, M. F., Friedrich, C., Dityateva, G., Schafer-Nielsen, C. and Schachner, M. (2010). Binding of the receptor tyrosine kinase TrkB to the neural cell adhesion molecule (NCAM) regulates phosphorylation of NCAM and NCAM-dependent neurite outgrowth. *J. Biol. Chem.* **285**, 28959-28967.

Cavallaro, U., Niedermeyer, J., Fuxa, M. and Christofori, G. (2001). N-CAM modulates tumour-cell adhesion to matrix by inducing FGF-receptor signalling. *Nat. Cell Biol.* **3**, 650-657.

Chazal, G., Durbec, P., Jankovski, A., Rougon, G. and Cremer, H. (2000). Consequences of neural cell adhesion molecule deficiency on cell migration in the rostral migratory stream of the mouse. *J. Neurosci.* **20**, 1446-1457.

Christensen, C., Lauridsen, J. B., Berezin, V., Bock, E. and Kiselyov, V. V. (2006). The neural cell adhesion molecule binds to fibroblast growth factor receptor 2. *FEBS Lett.* **580**, 3386-3390.

Christofori, G. (2003). Changing neighbours, changing behaviour: cell adhesion molecule-mediated signalling during tumour progression. *EMBO J.* **22**, 2318-2323.

Cole, G. J. and Akeson, R. (1989). Identification of a heparin binding domain of the neural cell adhesion molecule N-CAM using synthetic peptides. *Neuron* **2**, 1157-1165.

Cole, G. J. and Glaser, L. (1986). A heparin-binding domain from N-CAM is involved in neural cell-substratum adhesion. *J. Cell Biol.* **102**, 403-412.

Cole, G. J., Loewy, A. and Glaser, L. (1986). Neuronal cell-cell adhesion depends on interactions of N-CAM with heparin-like molecules. *Nature* **320**, 445-447.

Colley, K. J. (2010). Structural basis for the polysialylation of the neural cell adhesion molecule. *Adv. Exp. Med. Biol.* **663**, 111-126.

Cunningham, B. A., Hemperly, J. J., Murray, B. A., Prediger, E. A., Brackenbury, R. and Edelman, G. M. (1987). Neural cell adhesion molecule: structure, immunoglobulin-like domains, cell surface modulation, and alternative RNA splicing. *Science* **236**, 799-806.

Curreli, S., Arany, Z., Gerardy-Schahn, R., Mann, D. and Stamatos, N. M. (2007). Polysialylated neuropilin-2 is expressed on the surface of human dendritic cells and modulates dendritic cell-T lymphocyte interactions. *J. Biol. Chem.* **282**, 30346-30356.

Daniel, L., Trouillas, J., Renaud, W., Chevallier, P., Gouvernet, J., Rougon, G. and Figarella-Branger, D. (2000). Polysialylated-neural cell adhesion molecule expression in rat pituitary transplantable tumors (spontaneous mammotropic transplantable tumor in Wistar-Furth rats) is related to growth rate and malignancy. *Cancer Res.* **60**, 80-85.

Daniel, L., Durbec, P., Gautherot, E., Rouvier, E., Rougon, G. and Figarella-Branger, D. (2001). A nude mice model of human rhabdomyosarcoma lung metastases for evaluating the role of polysialic acids in the metastatic process. *Oncogene* **20**, 997-1004.

Diestel, S., Hinkle, C. L., Schmitz, B. and Maness, P. F. (2005). NCAM140 stimulates integrin-dependent cell migration by ectodomain shedding. *J. Neurochem.* **95**, 1777-1784.

Figarella-Branger, D., Dubois, C., Chauvin, P., Devictor, B., Gentet, J. C. and Rougon, G. (1996). Correlation between polysialic-neural cell adhesion molecule levels in CSF and medulloblastoma outcomes. *J. Clin. Oncol.* **14**, 2066-2072.

Francavilla, C., Loeffler, S., Piccini, D., Kren, A., Christofori, G. and Cavallaro, U. (2007). Neural cell adhesion molecule regulates the cellular response to fibroblast growth factor. *J. Cell Sci.* **120**, 4388-4394.

Francavilla, C., Cattaneo, P., Berezin, V., Bock, E., Ami, D., de Marco, A., Christofori, G. and Cavallaro, U. (2009). The binding of NCAM to FGFR1 induces a specific cellular response mediated by receptor trafficking. *J. Cell Biol.* **187**, 1101-1116.

Friedl, P. and Wolf, K. (2010). Plasticity of cell migration: a multiscale tuning model. *J. Cell Biol.* **188**, 11-19.

Frosch, M., Gorgen, I., Boulnois, G. J., Timmis, K. N. and Bitter-Suermann, D. (1985). NZB mouse system for production of monoclonal antibodies to weak bacterial antigens: isolation of an IgG antibody to the polysaccharide capsules of Escherichia coli K1 and group B meningococci. *Proc. Natl. Acad. Sci. USA* **82**, 1194-1198.

Fujimoto, I., Bruses, J. L. and Rutishauser, U. (2001). Regulation of cell adhesion by polysialic acid: Effects on cadherin, IgCAM and integrin function and independence from NCAM binding or signaling activity. *J. Biol. Chem.* **276**, 31745-31751.

Galuska, S. P., Rollenhagen, M., Kaup, M., Eggers, K., Oltmann-Norden, I., Schiff, M., Hartmann, M., Weinhold, B., Hildebrandt, H., Geyer, R., Mühlenhoff, M. and Geyer, H. (2010). Synaptic cell adhesion molecule SynCAM 1 is a target for polysialylation in postnatal mouse brain. *Proc. Natl. Acad. Sci. USA* **107**, 10250-10255.

Geiger, B., Spatz, J. P. and Bershadsky, A. D. (2009). Environmental sensing through focal adhesions. *Nat. Rev. Mol. Cell Biol.* **10**, 21-33.

Gerardy-Schahn, R. and Eckhardt, M. (1994). Hot spots of antigenicity in the neural cell adhesion molecule NCAM. *Int. J. Cancer Suppl.* **8**, 38-42.

Glaser, T., Brose, C., Franceschini, I., Hamann, K., Smorodchenko, A., Zipp, F., Dubois-Dalcq, M. and Brustle, O. (2007). Neural cell adhesion molecule polysialylation enhances the sensitivity of embryonic stem cell-derived neural precursors to migration guidance cues. *Stem Cells* **25**, 3016-3025.

Glüer, S., Schelp, C., Madry, N., Von Schweinitz, D., Eckhardt, M. and Gerardy-Schahn, R. (1998a). Serum polysialylated neural cell adhesion molecule in childhood neuroblastoma. *Br. J. Cancer* **78**, 106-110.

Glüer, S., Schelp, C., Von Schweinitz, D. and Gerardy-Schahn, R. (1998b). Polysialylated neural cell adhesion molecule in childhood rhabdomyosarcoma. *Pediat. Res.* **43**, 145-147.

Hildebrandt, H., Becker, C., Glüer, S., Rösner, H., Gerardy-Schahn, R. and Rahmann, H. (1998). Polysialic acid on the neural cell adhesion molecule correlates with expression of polysialyltransferases and promotes neuroblastoma cell growth. *Cancer Res.* **58**, 779-784.

Hildebrandt, H., Mühlenhoff, M., Oltmann-Norden, I., Röckle, I., Burkhardt, H., Weinhold, B. and Gerardy-Schahn, R. (2009). Imbalance of neural cell adhesion molecule and polysialyltransferase alleles causes defective brain connectivity. *Brain* **132**, 2831-2838.

Hildebrandt, H., Mühlenhoff, M. and Gerardy-Schahn, R. (2010). Polysialylation of NCAM. *Adv. Exp. Med. Biol.* **663**, 95-109.

Hinkle, C. L., Diestel, S., Lieberman, J. and Maness, P. F. (2006). Metalloprotease-induced ectodomain shedding of neural cell adhesion molecule (NCAM). *J. Neurobiol.* **66**, 1378-1395.

Hinsby, A. M., Lundfald, L., Ditlevsen, D. K., Korshunova, I., Juhl, L., Meakin, S. O., Berezin, V. and Bock, E. (2004). ShcA regulates neurite outgrowth stimulated by neural cell adhesion molecule but not by fibroblast growth factor 2: evidence for a distinct fibroblast growth factor receptor response to neural cell adhesion molecule activation. *J. Neurochem.* **91**, 694-703.

Hoffman, S. and Edelman, G. M. (1983). Kinetics of homophilic binding by embryonic and adult forms of neural cell adhesion molecule. *Proc. Natl. Acad. Sci. USA* **80**, 5762-5766.

Hu, H., Tomasiewicz, H., Magnuson, T. and Rutishauser, U. (1996). The role of polysialic acid in migration of olfactory bulb interneuron precursors in the subventricular zone. *Neuron* **16**, 735-743.

Huang, C., Jacobson, K. and Schaller, M. D. (2004). MAP kinases and cell migration. *J. Cell Sci.* **117**, 4619-4628.

Hübschmann, M. V., Skladchikova, G., Bock, E. and Berezin, V. (2005). Neural cell adhesion molecule function is regulated by metalloproteinase-mediated ectodomain release. *J. Neurosci. Res.* **80**, 826-837.

Jacobsen, J., Kiselyov, V., Bock, E. and Berezin, V. (2008). A peptide motif from the second fibronectin module of the neural cell adhesion molecule, NCAM, NLIKQDDGGSPIRHY, is a binding site for the FGF receptor. *Neurochem. Res.* **33**, 2532-2539.

Kalus, I., Bormann, U., Mzoughi, M., Schachner, M. and Kleene, R. (2006). Proteolytic cleavage of the neural cell adhesion molecule by ADAM17/TACE is involved in neurite outgrowth. *J. Neurochem.* **98**, 78-88.

Kiryushko, D., Kofoed, T., Skladchikova, G., Holm, A., Berezin, V. and Bock, E. (2003). A synthetic peptide ligand of neural cell adhesion molecule (NCAM), C3d, promotes neuritogenesis and synaptogenesis and modulates presynaptic function in primary cultures of rat hippocampal neurons. *J. Biol. Chem.* **278**, 12325-12334.

Kiselyov, V. V. (2010). NCAM and the FGF-receptor. *Adv. Exp. Med. Biol.* **663**, 67-79.

Kiselyov, V. V., Skladchikova, G., Hinsby, A. M., Jensen, P. H., Kulahin, N., Soroka, V., Pedersen, N., Tsetlin, V., Poulsen, F. M., Berezin, V. and Bock, E. (2003). Structural basis for a direct interaction between FGFR1 and NCAM and evidence for a regulatory role of ATP. *Structure* **11**, 691-701.

Kiselyov, V. V., Li, S., Berezin, V. and Bock, E. (2009). Insight into the structural mechanism of the bi-modal action of an NCAM mimetic, the C3 peptide. *Neurosci. Lett.* **452**, 224-227.

Kleene, R., Cassens, C., Bahring, R., Theis, T., Xiao, M. F., Dityatev, A., Schafer-Nielsen, C., Doring, F., Wischmeyer, E. and Schachner, M. (2010a). Functional consequences of the interactions among the neural cell adhesion molecule NCAM, the receptor tyrosine kinase TrkB, and the inwardly rectifying K+ channel KIR3.3. *J. Biol. Chem.* **285**, 28968-28979.

Kleene, R., Mzoughi, M., Joshi, G., Kalus, I., Bormann, U., Schulze, C., Xiao, M. F., Dityatev, A. and Schachner, M. (2010b). NCAM-induced neurite outgrowth depends on binding of calmodulin to NCAM and on nuclear import of NCAM and fak fragments. *J. Neurosci.* **30**, 10784-10798.

Kolkova, K., Novitskaya, V., Pedersen, N., Berezin, V. and Bock, E. (2000). Neural cell adhesion molecule-stimulated neurite outgrowth depends on activation of protein kinase C and the ras-mitogen-activated protein kinase pathway. *J. Neurosci.* **20**, 2238-2246.

Lavdas, A. A., Franceschini, I., Dubois-Dalcq, M. and Matsas, R. (2006). Schwann cells genetically engineered to express PSA show enhanced migratory potential without impairment of their myelinating ability in vitro. *Glia* **53**, 868-878.

Lehembre, F., Yilmaz, M., Wicki, A., Schomber, T., Strittmatter, K., Ziegler, D., Kren, A., Went, P., Derksen, P. W., Berns, A., Jonkers, J. and Christofori, G. (2008). NCAM-induced focal adhesion assembly: a functional switch upon loss of E-cadherin. *EMBO J.* **27**, 2603-2615.

Maness, P. F. and Schachner, M. (2007). Neural recognition molecules of the immunoglobulin superfamily: signaling transducers of axon guidance and neuronal migration. *Nat. Neurosci.* **10**, 19-26.

Mitra, S. K., Hanson, D. A. and Schlaepfer, D. D. (2005). Focal adhesion kinase: in command and control of cell motility. *Nat. Rev. Mol. Cell Biol.* **6**, 56-68.

Neiiendam, J. L., Kohler, L. B., Christensen, C., Li, S., Pedersen, M. V., Ditlevsen, D. K., Kornum, M. K., Kiselyov, V. V., Berezin, V. and Bock, E. (2004). An NCAM-derived FGF-receptor agonist, the FGL-peptide, induces neurite outgrowth and neuronal survival in primary rat neurons. *J. Neurochem.* **91**, 920-935.

Nielsen, J., Kulahin, N. and Walmod, P. S. (2010). Extracellular protein interactions mediated by the neural cell adhesion molecule, NCAM: heterophilic interactions between NCAM and cell adhesion molecules, extracellular matrix proteins, and viruses. *Adv. Exp. Med. Biol.* **663**, 23-53.

Niethammer, P., Delling, M., Sytnyk, V., Dityatev, A., Fukami, K. and Schachner, M. (2002). Cosignaling of NCAM via lipid rafts and the FGF receptor is required for neuritogenesis. *J. Cell Biol.* **157**, 521-532.

Ono, K., Tomasiewicz, H., Magnuson, T. and Rutishauser, U. (1994). N-CAM mutation inhibits tangential neuronal migration and is phenocopied by enzymatic removal of polysialic acid. *Neuron* **13**, 595-609.

Palser, A. L., Norman, A. L., Saffell, J. L. and Reynolds, R. (2009). Neural cell adhesion molecule stimulates survival of premyelinating oligodendrocytes via the fibroblast growth factor receptor. *J. Neurosci. Res.* **87**, 3356-3368.

Parsons, J. T., Horwitz, A. R. and Schwartz, M. A. (2010). Cell adhesion: integrating cytoskeletal dynamics and cellular tension. *Nat. Rev. Mol. Cell Biol.* **11**, 633-643.

Prag, S., Lepekhin, E. A., Kolkova, K., Hartmann-Petersen, R., Kawa, A., Walmod, P. S., Belman, V., Gallagher, H. C., Berezin, V., Bock, E. and Pedersen, N. (2002). NCAM regulates cell motility. *J. Cell Sci.* **115**, 283-292.

Rey-Gallardo, A., Escribano, C., Delgado-Martin, C., Rodriguez-Fernandez, J. L., Gerardy-Schahn, R., Rutishauser, U., Corbi, A. L. and Vega, M. A. (2010). Polysialylated neuropilin-2 enhances human dendritic cell migration through the basic C-terminal region of CCL21. *Glycobiology* **20**, 1139-1146.

Röckle, I., Seidenfaden, R., Weinhold, B., Mühlenhoff, M., Gerardy-Schahn, R. and Hildebrandt, H. (2008). Polysialic acid controls NCAM-induced differentiation of neuronal precursors into calretinin-positive olfactory bulb interneurons. *Dev. Neurobiol.* **68**, 1170-1184.

Ronn, L. C., Olsen, M., Ostergaard, S., Kiselyov, V., Berezin, V., Mortensen, M. T., Lerche, M. H., Jensen, P. H., Soroka, V., Saffells, J. L., Doherty, P., Poulsen, F. M., Bock, E. and Holm, A. (1999). Identification of a neuritogenic ligand of the neural cell adhesion molecule using a combinatorial library of synthetic peptides. *Nat. Biotechnol.* **17**, 1000-1005.

Ronn, L. C., Doherty, P., Holm, A., Berezin, V. and Bock, E. (2000). Neurite outgrowth induced by a synthetic peptide ligand of neural cell adhesion molecule requires fibroblast growth factor receptor activation. *J. Neurochem.* **75**, 665-671.

Rudolph, G., Schilbach-Stuckle, K., Handgretinger, R., Kaiser, P. and Hameister, H. (1991). Cytogenetic and molecular characterization of a newly established neuroblastoma cell line LS. *Hum. Genet.* **86**, 562-566.

Rutishauser, U. (2008). Polysialic acid in the plasticity of the developing and adult vertebrate nervous system. *Nat. Rev. Neurosci.* **9**, 26-35.

Sadoul, R., Hirn, M., Deagostini-Bazin, H., Rougon, G. and Goridis, C. (1983). Adult and embryonic mouse neural cell adhesion molecules have different binding properties. *Nature* **304**, 347-349.

Saffell, J. L., Williams, E. J., Mason, I. J., Walsh, F. S. and Doherty, P. (1997). Expression of a dominant negative FGF receptor inhibits axonal growth and FGF receptor phosphorylation stimulated by CAMs. *Neuron* **18**, 231-242.

Schaller, M. D. (2010). Cellular functions of FAK kinases: insight into molecular mechanisms and novel functions. *J. Cell Sci.* **123**, 1007-1013.

Scheidegger, E. P., Lackie, P. M., Papay, J. and Roth, J. (1994). In vitro and in vivo growth of clonal sublines of human small cell lung carcinoma is modulated by polysialic acid of the neural cell adhesion molecule. *Lab. Invest.* **70**, 95-106.

Schiff, M., Weinhold, B., Grothe, C. and Hildebrandt, H. (2009). NCAM and polysialyltransferase profiles match dopaminergic marker gene expression but polysialic acid is dispensable for development of the midbrain dopamine system. *J. Neurochem.* **110**, 1661-1673.

Schreiber, S. C., Giehl, K., Kastilan, C., Hasel, C., Mühlenhoff, M., Adler, G., Wedlich, D. and Menke, A. (2008). Polysialylated NCAM represses E-cadherin-mediated cell-cell adhesion in pancreatic tumor cells. *Gastroenterology* **134**, 1555-1566.

Schwartz, M. A. and Ginsberg, M. H. (2002). Networks and crosstalk: integrin signalling spreads. *Nat. Cell Biol.* **4**, E65-E68.

Seidenfaden, R. and Hildebrandt, H. (2001). Retinoic acid-induced changes in NCAM polysialylation and polysialyltransferase mRNA expression of human neuroblastoma cells. *J. Neurobiol.* **46**, 11-28.

Seidenfaden, R., Gerardy-Schahn, R. and Hildebrandt, H. (2000). Control of NCAM polysialylation by the differential expression of polysialytransferases ST8SiaII and ST8SiaIV. *Eur. J. Cell Biol.* **79**, 680-688.

Seidenfaden, R., Krauter, A., Schertzinger, F., Gerardy-Schahn, R. and Hildebrandt, H. (2003). Polysialic acid directs tumor cell growth by controlling heterophilic neural cell adhesion molecule interactions. *Mol. Cell Biol.* **23**, 5908-5918.

Seidenfaden, R., Krauter, A. and Hildebrandt, H. (2006). The neural cell adhesion molecule NCAM regulates neuritogenesis by multiple mechanisms of interaction. *Neurochem. Int.* **49**, 1-11.

Skaper, S. D., Kee, W. J., Facci, L., Macdonald, G., Doherty, P. and Walsh, F. S. (2000). The FGFR1 inhibitor PD 173074 selectively and potently antagonizes FGF-2 neurotrophic and neurotropic effects. *J. Neurochem.* **75**, 1520-1527.

Storms, S. D. and Rutishauser, U. (1998). A role for polysialic acid in neural cell adhesion molecule heterophilic binding to proteoglycans. *J. Biol. Chem.* **273**, 27124-27129.

Stummeyer, K., Dickmanns, A., Mühlenhoff, M., Gerardy-Schahn, R. and Ficner, R. (2005). Crystal structure of the polysialic acid-degrading endosialidase of bacteriophage K1F. *Nat. Struct. Mol. Biol.* **12**, 90-96.

Suzuki, M., Suzuki, M., Nakayama, J., Suzuki, A., Angata, K., Chen, S., Sakai, K., Hagihara, K., Yamaguchi, Y. and Fukuda, M. (2005). Polysialic acid facilitates tumor invasion by glioma cells. *Glycobiology* **15**, 887-894.

Tanaka, F., Otake, Y., Nakagawa, T., Kawano, Y., Miyahara, R., Li, M., Yanagihara, K., Nakayama, J., Fujimoto, I., Ikenaka, K. and Wada, H. (2000). Expression of polysialic acid and STX, a human polysialyltransferase, is correlated with tumor progression in non-small cell lung cancer. *Cancer Res.* **60**, 3072-3080.

Trouillas, J., Daniel, L., Guigard, M. P., Tong, S., Gouvernet, J., Jouanneau, E., Jan, M., Perrin, G., Fischer, G., Tabarin, A., Rougon, G. and Figarella-Branger, D. (2003). Polysialylated neural cell adhesion molecules expressed in human pituitary tumors and related to extrasellar invasion. *J. Neurosurg.* **98**, 1084-1093.

Wang, C., Rougon, G. and Kiss, J. Z. (1994). Requirement of polysialic acid for the migration of the O-2A glial progenitor cell from neurohypophyseal explants. *J. Neurosci.* **14**, 4446-4457.

Webb, D. J., Parsons, J. T. and Horwitz, A. F. (2002). Adhesion assembly, disassembly and turnover in migrating cells - over and over and over again. *Nat. Cell Biol.* **4**, E97-E100.

Weinhold, B., Seidenfaden, R., Röckle, I., Mühlenhoff, M., Schertzinger, F., Conzelmann, S., Marth, J. D., Gerardy-Schahn, R. and Hildebrandt, H. (2005). Genetic ablation of polysialic acid causes severe neurodevelopmental defects rescued by deletion of the neural cell adhesion molecule. *J. Biol. Chem.* **280**, 42971-42977.

Zhang, H., Vutskits, L., Calaora, V., Durbec, P. and Kiss, J. Z. (2004). A role for the polysialic acid-neural cell adhesion molecule in PDGF-induced chemotaxis of oligodendrocyte precursor cells. *J. Cell Sci.* **117**, 93-103.

Supplementary Material

Supplementary Figure S1:

Endoneuraminidase efficiently removes polySia.

PolySia produced by LS$_{AM1PST}$ cells is associated with NCAM-140 and can be efficiently removed by active but not mutant endoneuraminidase (endo$_{active}$, endo$_{inact.}$) applied to live cells for 30 minutes or 6 hours as indicated. Per lane, 60 μg of cell lysate were applied and Western blots were simultaneously reacted with polySia-specific mAb 735 (mouse IgG2a) and NCAM-specific mAb

123C3 (mouse IgG1), followed by detection with sub-type specific secondary antibodies and Odyseey Infrared Imaging. Polysialylated NCAM is displayed as a diffuse high molecular weight smear hardly detectable with mAb123C3, whereas sharp bands at 140 kDa indicate non-polysialylated NCAM-140 (arrow). Efficient removal of polySia by active endo is indicated by the absence of polySia-specific bands. The lack of sharp bands at 140 kDa in controls and after treatment with inactive endo demonstrates that the entire pool of NCAM-140 is polysialylated in LS$_{AM1PST}$ cells.
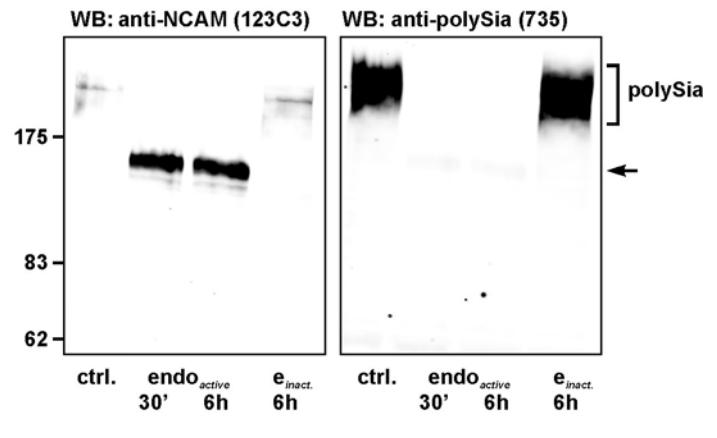
Supplementary Figure S2:

Migration of single SH-SY5Y cells is not affected by polySia removal.

(A, B) Selected frames from time lapse-recordings (available as supplementary Movie 1 and 2) of control (left column) and endo-treated SH-SY5Y cells (right column) seeded at low density to observe single cell migration. Images at 0, 2, 4, and 6 hours recording time and tracks of cell movements over 6 h are shown (C, D). After fixation, cultures were stained with polySia-specific mAb 735. Combined bright field and immunofluorescence images of representative cells are shown. Scale bars: 100 μm (A,B), 20 μm (C, D).
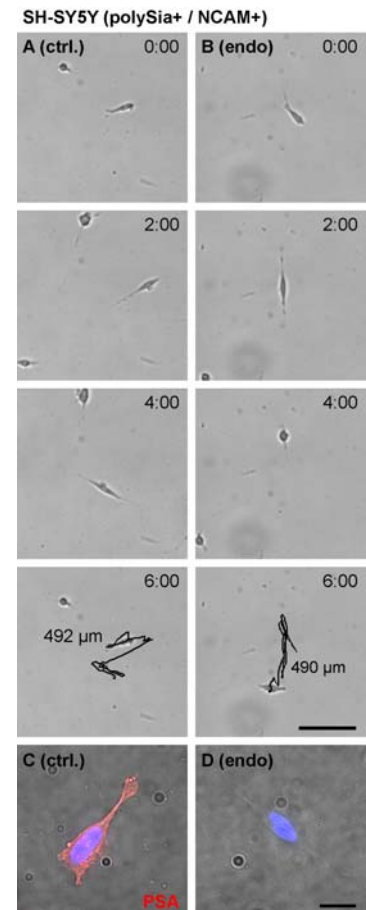
Supplementary Figure S3:

SH-SY5Y cells express non-polysialylated neuropilin-2 and SynCAM 1.

Immunoprecipitation (IP) of neuropilin-2 (A) or SynCAM 1 (B) from SH-SY5Y cell lysates and Western blot (WB) analyses of polySia and neuropilin-2 or SynCAM 1 immunoreactive bands.

(A) IP and immunodetection of neuropilin-2 (NRP-2) by Western blot with Odyssey Infrared Imaging. Cell lysate was split and treated with endoneuraminidase (endo) to remove polySia, where indicated. Lysate prior to IP (Pre-IP, 20 μg) and IP fractions were subjected to Western blot analysis. Detection with neuropilin-2 specific rabbit pAb yielded a doublet band lacking the characteristic shift after endo treatment, which would be indicative for the presence of polySia (Curreli et al., 2007). This is consistent with the absence of immunoreactive signals with polySia-specific mAb 735 at the position of the NRP-2 bands (right panel, arrows). Endo treatment abolished the immunoreactive band corresponding to the expected size of polysialylated NCAM in the cell lysates confirming removal of polySia. *, unspecific signal resulting from antibody used for IP.

(B) Immunodetection of SynCAM 1 by Western blot and ECL using chicken anti-SynCAM 1 mAb 3E1. Cell lysates (60 μg) before, but not after IP (Pre- and Post-IP, respectively), as well as the IP fraction obtained with SynCAM-specific rabbit pAb yielded an immunoreactive band centered at approximately 110 kDa (left panel). After stripping and re-probing with polySia-specific mAb 735, an immunoreactive band corresponding to the expected size of polysialylated NCAM was obtained with cell lysates. No polySia signals were detected in the IP fraction (right panel). Arrow, position of SynCAM 1 imunoreactive band. *, unspecific signal resulting from antibody used for IP.
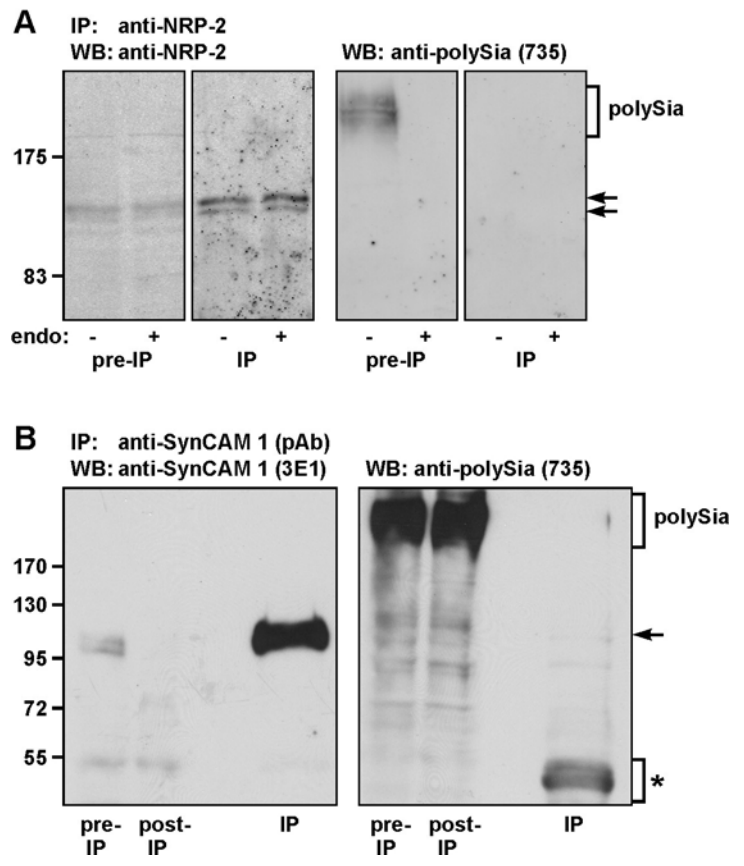
Supplementary Figure S4:

NCAM-Fc attenuates migration of LS neuroblastoma cells into a scratch wound.

(A, B) Selected frames from time lapse-recordings (available as supplementary Movie 3 and 4) of control (upper row) and NCAM-Fc treated LS cells (lower row) migrating into a scratch wound. Images at 0, 3, and 6 hours recording time are shown. Scale bar: 250 μm. Please note that time-lapse

LS (polySia- / NCAM-)
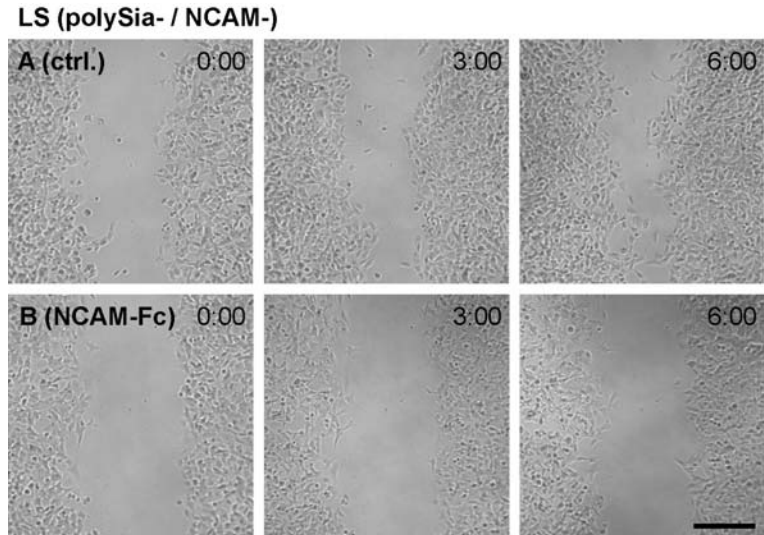
videomicroscopy was performed with cells maintained in a microscope stage incubation chamber (controlled for temperature and CO_2). In contrast, all results summarized in Figs 1 and 2 were obtained with cells incubated under standard conditions during the 6 hours of treatment.

LS_{AM1PST} (polySia+ / NCAM+)
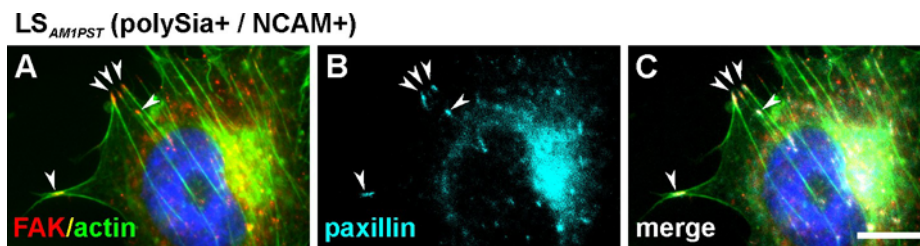
Supplementary Figure S5: Focal adhesions of LS neuroblastoma cells. LS cells stained for FAK (red), paxillin (cyan), actin (green) and nuclear counterstain with DAPI (blue). FAK and paxillin co-localize at peripheral focal adhesions located at the tip of actin fibers. Scale bar: 10 μm.

Chapter 4 – Synaptic cell adhesion molecule SynCAM 1 is a target for polysialylation in postnatal mouse brain.

- This manuscript has originally been published in the journal *Proceedings of the National Academy of Sciences (PNAS).* -

Sebastian P. Galuska[a], Manuela Rollenhagen[b], Moritz Kaup[a], **Katinka Eggers**[b], Imke Oltmann-Norden[b], Miriam Schiff[b], Maike Hartmann[b], Birgit Weinhold[b], Herbert Hildebrandt[b], Rudolf Geyer[a], Martina Mühlenhoff[b,1] and Hildegard Geyer[a,1]

[a] Institute of Biochemistry, Faculty of Medicine, University of Giessen, D-35392 Giessen, Germany

[b] Institute of Cellular Chemistry, Hannover Medical School, D-30625 Hannover, Germany

[1] To whom correspondence should be addressed. E-mail: hildegard.geyer@biochemie.med. uni-giessen.de or muehlenhoff.martina@mh-hannover.de.

Preface

In the course of this study, SynCAM 1 was identified as a novel carrier for polysialic acid. PolySia on SynCAM 1 was shown to reside on Asn[116] and to be restricted to SynCAM 1 on NG-2 glial cells. SynCAM 1 was polysialylated by ST8SiaII and ST8SiaIV *in vitro* and polysialylation abolished homophilic binding. My contribution to this study was to provide recombinant ST8SiaII produced in insect cells and to contribute to ST8SiaIV production.

Synaptic cell adhesion molecule SynCAM 1 is a target for polysialylation in postnatal mouse brain

Sebastian P. Galuska[a,1], Manuela Rollenhagen[b,1], Moritz Kaup[a], Katinka Eggers[b], Imke Oltmann-Norden[b,2], Miriam Schiff[b], Maike Hartmann[b], Birgit Weinhold[b], Herbert Hildebrandt[b], Rudolf Geyer[a], Martina Mühlenhoff[b,3,4], and Hildegard Geyer[a,3,4]

[a]Institute of Biochemistry, Faculty of Medicine, University of Giessen, D-35392 Giessen, Germany; and [b]Institute of Cellular Chemistry, Hannover Medical School, D-30625 Hannover, Germany

Among the large set of cell surface glycan structures, the carbohydrate polymer polysialic acid (polySia) plays an important role in vertebrate brain development and synaptic plasticity. The main carrier of polySia in the nervous system is the neural cell adhesion molecule NCAM. As polySia with chain lengths of more than 40 sialic acid residues was still observed in brain of newborn $Ncam^{-/-}$ mice, we performed a glycoproteomics approach to identify the underlying protein scaffolds. Affinity purification of polysialylated molecules from $Ncam^{-/-}$ brain followed by peptide mass fingerprinting led to the identification of the synaptic cell adhesion molecule Syn-CAM 1 as a so far unknown polySia carrier. SynCAM 1 belongs to the Ig superfamily and is a powerful inducer of synapse formation. Importantly, the appearance of polysialylated SynCAM 1 was not restricted to the $Ncam^{-/-}$ background but was found to the same extent in perinatal brain of WT mice. PolySia was located on N-glycans of the first Ig domain, which is known to be involved in homo- and heterophilic SynCAM 1 interactions. Both polysialyltransferases, ST8SiaII and ST8SiaIV, were able to polysialylate SynCAM 1 in vitro, and polysialylation of SynCAM 1 completely abolished homophilic binding. Analysis of serial sections of perinatal $Ncam^{-/-}$ brain revealed that polySia-SynCAM 1 is expressed exclusively by NG2 cells, a multifunctional glia population that can receive glutamatergic input via unique neuron-NG2 cell synapses. Our findings suggest that polySia may act as a dynamic modulator of SynCAM 1 functions during integration of NG2 cells into neural networks.

polysialic acid | NG2 cells | glycosylation | polysialyltransferases | glycoproteomics

Glycosylation represents the most complex posttranslational modification, with an overwhelming diversity of oligosaccharide structures. Moreover, a single protein can be variably glycosylated giving rise to multiple glycoforms with distinct biological functions. Unraveling the impact of glycosylation on the structure and function of proteins is therefore often an arduous task. A striking example for the capability of an individual glycan structure to induce dramatic functional changes on the underlying protein is polysialic acid (polySia). In vertebrates, this linear α2,8-linked homopolymer of 5-N-acetylneuraminic acid (Neu5Ac) was first described as a developmentally regulated modification of the neural cell adhesion molecule (NCAM) (1–3). Polysialylation disrupts the adhesive properties of NCAM and appearance of the bulky polyanionic glycan on the cell surface generally increases the intercellular space (4, 5). Thus, polySia is a modulator of cell interactions involved in dynamic processes such as neural cell migration, neurite outgrowth, neural path finding, and synaptic plasticity (6–9). Although it is abundantly expressed during embryonic and early postnatal brain development, polySia is restricted to areas with ongoing neurogenesis and synaptic plasticity in adult brain (10–12).

In mammals, polysialylation is catalyzed by the Golgi-resident polysialyltransferases (polySTs) ST8SiaII and ST8SiaIV, and simultaneous ablation of both enzymes leads to a complete loss of polySia (13, 14). In contrast to $Ncam^{-/-}$ mice, which still contain residual amounts of polySia and manifest only a mild phenotype (15), $St8sia2^{-/-}St8sia4^{-/-}$ double KO mice are characterized by postnatal lethality and severe malformations of major axon tracts (14, 16, 17). Lethality and brain wiring defects could be attributed to erroneous exposure of polySia-free NCAM (14, 18), highlighting the crucial role of polySia in masking the underlying protein and thereby preventing improper interactions.

Although NCAM is by far the most abundant polySia carrier in mammals, context-dependent polysialylation of a restricted set of other glycoproteins has been described. These are CD36 in human milk, the α-subunit of a voltage-gated sodium channel in adult rat brain, and neuropilin-2 in mature human dendritic cells (19–21). Based on the observation that $Ncam^{-/-}$ brains still contain low but clearly detectable amounts of polySia (ref. 15 and the present study), we performed a glycoproteomic approach to screen for respective polySia carriers. This led to the identification of the synaptic cell adhesion molecule SynCAM 1 as a target for polysialylation. SynCAM 1 is a member of the Ig superfamily composed of three Ig modules comprising six potential N-glycosylation sites, a variable stem region with several putative O-glycosylation sites, a single transmembrane domain, and a short carboxyl-terminal intracellular tail (22). Because of its identification in different tissues, SynCAM 1 (official gene name $Cadm1$) has various names: nectin-like protein 2 (Necl-2) (23), tumor suppressor in lung cancer 1 (TSLC-1) (24), spermatogenic Ig superfamily molecule (SgIGSF) (25), Ig superfamily 4 (IgSF4) (26), and RA175 (27). SynCAM 1 contributes to a variety of intercellular junctions by mediating Ca^{2+}-independent cell adhesion through homo- and heterophilic interactions (22, 23, 28–30). In the brain, SynCAM 1 localizes to synapses, bridges the synaptic cleft by homo- and heterophilic transinteraction with SynCAM 2, and acts as a potent inducer of synapse formation (22, 31). Here we demonstrate that, in vivo, a subfraction of SynCAM 1 is selectively polysialylated at the third N-glycosylation site and expressed by a subset of NG2 cells. In vitro polysialylation by either ST8SiaII or ST8SiaIV completely abolished homophilic SynCAM 1 binding, implying that polysialylation affects SynCAM 1 functions and may serve as a crucial modulator of SynCAM 1 interactions during integration of NG2 glia into neural networks.

Results

Characterization of PolySia in Perinatal Brain of *Ncam*$^{-/-}$ Mice. By immunostaining with an anti-polySia antibody, Cremer et al. identified residual amounts of polySia in brain of *Ncam*$^{-/-}$ mice (15). To analyze residual polySia, i.e., polymer length and total amounts in more detail, we applied the 1,2-diamino-4,5-methylenedioxybenzene (DMB)–HPLC method (13, 32, 33) to whole brain lysates of newborn *Ncam*$^{-/-}$ animals. Released polySia chains were fluorescently labeled and separated according to the degree of polymerization by anion exchange chromatography. Although the amount of all polymer species was drastically reduced compared with WT samples, polySia with more than 40 residues was still detectable in NCAM-deficient brain (Fig. 1 *A* and *B*). Quantification revealed that brain of *Ncam*$^{-/-}$ mice contained only 3.5% of the WT polySia level (Fig. 1*C*). Taking into account that visualization of long polySia chains strongly depends on the amount of material applied (34), one might assume that polySia synthesized in *Ncam*$^{-/-}$ and WT brain reaches similar chain lengths.

Identification of SynCAM 1 as PolySia Carrier in Developing Mouse Brain. Polysialylated protein(s) in whole brain lysates of newborn *Ncam*$^{-/-}$ mice were characterized by Western blotting applying the tenfold amount of lysate compared with WT samples to compensate for the low polySia level. In WT samples, immunostaining with the polySia-specific mAb 735 revealed the typical broad polySia-NCAM signal at approximately 250 kDa, which was completely abolished after treatment with polySia-specific endosialidase N (endoN; Fig. 2*A*). Reprobing with anti-NCAM mAb H28 displayed a similar high molecular weight band which, after endoN treatment, gave rise to two focused bands representing the NCAM isoforms NCAM-140 and -180. In contrast, the main endoN sensitive signal observed with mAb 735 in lysate of *Ncam*$^{-/-}$ brain centered at approximately 110 kDa and no signal was obtained with mAb H28. To identify the underlying protein scaffold, polysialylated molecules were isolated from *Ncam*$^{-/-}$ brain extracts by affinity chromatography using mAb 735. After separation by SDS/PAGE, a gel slice spanning the molecular mass range of 100 to 150 kDa was used for tryptic in-gel digest. Analysis of the resulting peptides by peptide mass fingerprinting and mass spectrometric fragmentation analysis resulted in the identification of SynCAM 1 with significant probability scores of 78 and 186 (*P* < 0.05), respectively (Fig. S1). To verify this result, polysialylated proteins were affinity-isolated from *Ncam*$^{-/-}$ brain extracts and characterized by Western blotting with an anti-SynCAM 1 antibody. As shown in Fig. 2*B*, a broad band with an apparent molecular mass of 100 to 120 kDa was observed. After endoN digest, the signal broadened and bands with apparent molecular masses ranging from 85 kDa to 110 kDa could be distinguished. The fact that no discrete bands were formed is most likely because of the
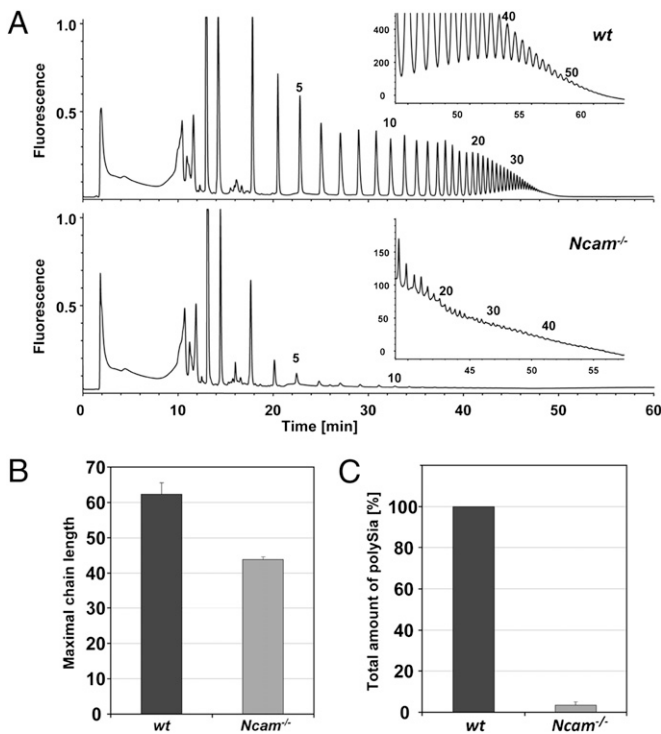
Fig. 1. Chromatographic profiles of polySia from WT and NCAM KO mouse brains. (*A*) Delipidated brain homogenates obtained from WT and NCAM KO (*Ncam*$^{-/-}$) mice (postnatal day 1) were directly derivatized with the fluorescence dye DMB and separated on an anion exchange column according to the number of sialic acid residues. In each case, 9% of the total brain homogenate (equivalent to 7 mg of original brain tissue) was injected. To determine the maximally detectable chain length, respective profiles were also generated with 86% aliquots (equivalent to 69 mg of brain tissue; *Insets*). The number of sialic acid residues is given for selected peaks on top of the profiles. (*B*) The average maximal chain length was determined from four independent experiments and amounted to approximately 62 and approximately 44 for WT and *Ncam*$^{-/-}$ mice, respectively. (*C*) Peak areas corresponding to polySia chains with more than eight sialic acid residues were calculated and summarized to obtain the total amount of polySia in brains of WT and *Ncam*$^{-/-}$ mice. Values are means of four independent experiments and were set to 100% for WT. The amount of polySia in *Ncam*$^{-/-}$ brains comprised only approximately 3.5% of the WT value.
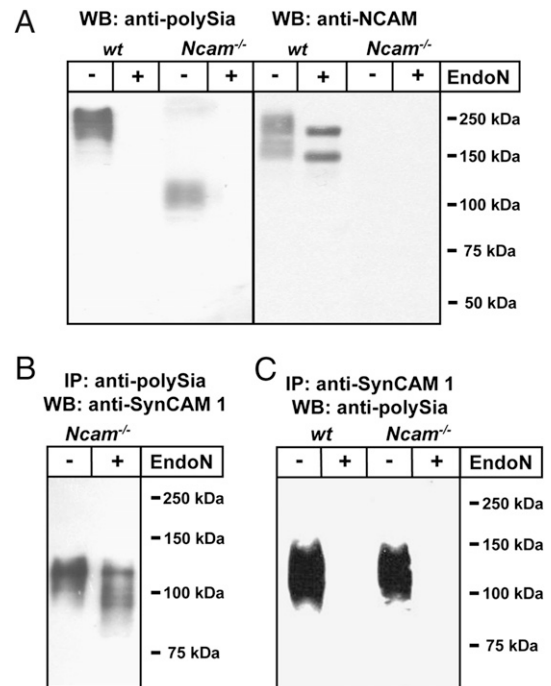
Fig. 2. Characterization of polysialylated proteins from WT and *Ncam*$^{-/-}$ mouse brains by SDS/PAGE and Western blotting (WB). Apparent molecular masses of standard proteins are indicated in kDa. (*A*) Brain homogenates of WT and *Ncam*$^{-/-}$ mice were separated by 10% SDS/PAGE using 4 μg (WT) or 40 μg (*Ncam*$^{-/-}$) protein per lane with or without prior endoN pretreatment and immunostained using anti-polySia mAb 735 or anti-NCAM mAb H28. (*B*) PolySia proteins of *Ncam*$^{-/-}$ mice were immunoaffinity purified (IP) using mAb 735, separated by SDS/PAGE, blotted, and stained with rabbit polyclonal anti-SynCAM 1 antibody before and after endoN treatment. (*C*) Equal amounts of brain lysates (60 mg wet weight each) of newborn WT and *Ncam*$^{-/-}$ mice were used for immunoprecipitation with polyclonal anti-SynCAM 1 antibody. Immunoprecipitates were analyzed before and after endoN treatment by Western blot analysis with anti-polySia mAb 735.

described heterogeneous glycosylation of SynCAM 1 by N- and O-glycans and/or the presence of different isoforms (35, 36). In a second experiment, SynCAM 1 immunoprecipitated with an anti-SynCAM 1 antibody was analyzed by immunoblotting with mAb 735 (Fig. 2C). Again, a polySia-signal in the molecular mass range of 100 to 150 kDa was observed, which was not detected after endoN pretreatment. The amount of total SynCAM 1 in perinatal $Ncam^{-/-}$ brain decreased only slightly after complete removal of the polySia-SynCAM 1 fraction by immunoprecipitation with mAb 735 (Fig. S2A). Thus, only a subfraction of SynCAM 1 is modified by polySia. Further analysis of the polySia-SynCAM 1 levels at postnatal d 2, d 21, and adult stage demonstrated a drastic decrease of polySia-SynCAM 1 during postnatal development, whereas no obvious change in the level of total SynCAM 1 was detected (Fig. S3).

Although our results clearly identified SynCAM 1 as a target for polysialylation in $Ncam^{-/-}$ mice, the question remained whether this is a compensatory response to the lack of NCAM. Consequently, polysialylation of SynCAM 1 was studied in perinatal brain of WT mice using 10 times the amount of brain extracts compared with Fig. 1A (Fig. S2B). Under these conditions, the polySia signal covered not only the dominating high molecular mass band of polySia-NCAM but also the mass range around 110 kDa, where polySia-SynCAM 1 migrates. To prove the presence of polysialylated SynCAM 1 in WT brain, immunoprecipitates obtained with an anti-SynCAM 1 antibody were stained with mAb 735 (Fig. 2C). In both WT and $Ncam^{-/-}$ brain, comparable amounts of polySia-SynCAM 1 were detected. Together these data demonstrate that SynCAM 1 is an NCAM-independent polySia carrier.

Polysialic Acid Chains Are Located on N-Glycans of the First Ig Domain. To determine whether polysialylation of SynCAM 1 occurs on N- or O-glycans, polysialylated SynCAM 1 immunoprecipitated from perinatal $Ncam^{-/-}$ brain was treated with N-glycosidase F (PNGaseF). As shown in Fig. 3A, PNGaseF digestion almost completely abolished mAb 735 staining, indicating that polySia chains were linked to N-glycans. The faint residual band in the range of approximately 90 kDa is presumably a result of incomplete PNGase F digestion. Parallel staining with anti-SynCAM 1 antibody (Fig. 3B) revealed that removal of N-glycans from polySia-SynCAM 1 resulted in two prominent bands. The molecular masses of approximately 48 and 65 kDa match with the masses described for unglycosylated and O-glycosylated SynCAM 1 variants, respectively (22, 35, 36).

For allocation of the polySia chains to distinct N-glycosylation sites, the total fraction of polysialylated glycopeptides was immunoaffinity-isolated from whole brain homogenates and analyzed by MALDI-TOF MS. After de-N-glycosylation by PNGaseF, only one additional signal at m/z 1377.7 was detected (Fig. 3C), corresponding to the deglycosylated tryptic SynCAM 1 peptide comprising the third N-glycosylation site (Asn_{116}) in which the glycosylated Asn has been converted to Asp as a result of PNGaseF action. Tandem MALDI-TOF MS analysis verified the sequence of this peptide as $V_{112}SLT\underline{D}VSISDEGR_{124}$ (Fig. 3D), demonstrating that SynCAM 1 is polysialylated on N-glycans at Asn_{116}. Thus, within the limit of detection, the presence of other proteins carrying polySia on N-glycans can be ruled out.

SynCAM 1 Is Polysialylated by ST8SiaII and ST8SiaIV in Vitro. To investigate whether SynCAM 1 is a target for the two polysialyltransferases ST8SiaII and ST8SiaIV, an in vitro assay was performed using soluble SynCAM 1 as Protein A fusion protein or C-terminally tagged with a Myc-epitope. SynCAM 1 adsorbed to Sepharose beads was incubated with CMP-[^{14}C]sialic acid in the presence of ST8SiaII or ST8SiaIV. A corresponding Protein A–NCAM chimera was used as positive control, and reaction products were analyzed before and after treatment with endoN. As shown in Fig. 4A, both ST8SiaII and ST8SiaIV were able to pol-
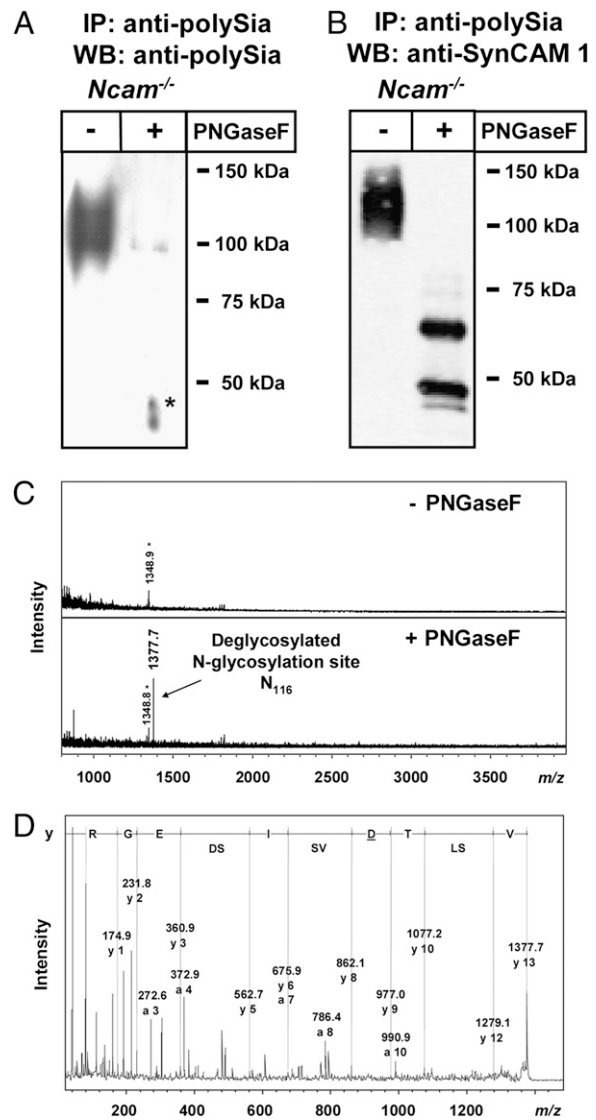
Fig. 3. Identification of the polysialylated glycosylation site in polySia-SynCAM 1 of $Ncam^{-/-}$ mice. (A and B) Western blot analyses of immunoaffinity purified (mAb 735) polySia–SynCAM 1 using anti-polySia mAb 735 (A) or polyclonal anti-SynCAM 1 antibody (B) with or without prior PNGaseF treatment. Apparent molecular masses of standard proteins are indicated in kDa. The asterisk indicates artifact. (C) MALDI-TOF MS spectra of immunopurified polysialylated glycopeptides before (–) or after (+) PNGaseF treatment. Monoisotopic masses of the pseudomolecular ions [M+H]$^+$ are given. The asterisk indicates unknown contaminant. (D) Sequencing of the deglycosylated peptide by MALDI-TOF MS/MS. Sequence-specific ions are labeled according to previous studies (48) and the deduced amino acid sequence is shown. The Asp residue detected instead of Asn as a result of the known conversion of N-glycosylated Asn during PNGaseF release of N-glycans is underlined. After replacing Asp by Asn, the identified peptide sequence was used for database search (Mascot) verifying again SynCAM 1 with a significant score.

ysialylate SynCAM 1 as demonstrated by the appearance of radiolabeled protein that migrated significantly more slowly than the same protein after endoN treatment. To prove that polySia was added to SynCAM 1, reaction products obtained after polysialylation with nonradiolabeled substrate were analyzed by Western blotting with anti–SynCAM 1 antibody (Fig. 4B). Before polysialylation, soluble SynCAM 1 migrated with an apparent molecular mass of approximately 55 kDa (Fig. 4B Left), whereas after incubation with either ST8SiaII or ST8SiaIV, a broad smear

ranging from 55 to 250 kDa appeared. This smear was sensitive to endoN, confirming that polySia was added to SynCAM 1. Notably, SynCAM 1 expressed in CHO-6B2 cells was not used as an acceptor molecule (Fig. 4B Right). Because of a lack of a functional CMP-sialic acid transporter, CHO-6B2 cells express exclusively asialo-glycoconjugates (37). Thus, the presence of terminally monosialylated glycans is a prerequisite for both ST8SiaII and ST8SiaIV to polysialylate SynCAM 1.

Homophilic SynCAM 1 Binding Is Abrogated by Polysialylation. To study the impact of polysialylation on SynCAM 1–mediated interactions, we monitored the effect of this modification on homophilic SynCAM 1 binding. An Fc-chimera of the extracellular part of SynCAM 1 fused to the Fc region of human IgG was expressed in CHO-2A10 cells and isolated by affinity chromatography on protein G–Sepharose. Fluorophore-labeled beads were coated with purified SynCAM 1-Fc and bead aggregation was monitored before and after in vitro polysialylation (Fig. 4C). Extensive aggregation, leading to large bead clusters, was observed for the nonpolysialylated form of SynCAM 1. However, after in vitro polysialylation of SynCAM 1 by either ST8SiaII or ST8SiaIV, aggregation was abrogated and only monodisperse beads were visible. Subsequent removal of polySia by endoN restored SynCAM 1 binding, and reaggregation of the beads to large clusters was observed. Thus, polysialylation of SynCAM 1 inhibits homophilic binding in vitro, strongly indicating a functional role in modulating SynCAM 1 interactions in vivo (Fig. 4D).

PolySia-SynCAM 1 Is Expressed on NG2 Cells. Analysis of serial brain sections obtained from newborn Ncam$^{-/-}$ mice revealed that polySia-positive cells were scattered throughout the gray matter but scarcely found in the white matter such as corpus callosum. PolySia staining was particularly abundant in the pontomedullary hindbrain and completely absent in brain sections of Ncam$^{-/-}$ St8sia2$^{-/-}$St8sia4$^{-/-}$ triple KO mice (Fig. 5A). PolySia colocalized with SynCAM 1 and was restricted to a subpopulation of cells that are positive for the proteoglycan NG2 (Fig. 5 B and C

and Fig. S4), a marker protein characteristic for a distinct type of glia cells. As NG2-negative cells that are wrapped by NG2-positive processes can be mistaken for NG2-positive cells, we confirmed our results by analyzing single cells in primary cultures from basal hindbrain of newborn Ncam$^{-/-}$ mice. Again, polySia was found colocalized with SynCAM 1 and associated with cells positive for NG2 and Olig2, a transcription factor frequently used as a second marker for NG2 cells (38) (Fig. S5). Consistent with described characteristics of NG2 cells (39), polySia-SynCAM 1–positive cells were negative for glial fibrillary acidic protein, β-III-tubulin, and microtubule-associated protein 2 (Figs. S4 and S5).

Discussion

In the present study, we show that the synaptic cell adhesion molecule SynCAM 1 is a target for polysialylation in developing mouse brain. In vivo, polySia is selectively added to N-glycans at the third N-glycosylation site located within the first Ig domain, which is involved in homo- and heterophilic SynCAM 1 interactions (36). Addition of the bulky polyanionic carbohydrate polymer completely blocked homophilic binding in vitro. Although we cannot exclude differences in the extend of polysialylation under in vitro and in vivo conditions, this finding implicates that polySia serves as a potent regulator of SynCAM 1 interactions in vivo as it is known for NCAM (6). Compared with NCAM, which is composed of five Ig and two fibronectin type III modules, SynCAM 1 contains only three Ig-like domains. Both molecules comprise six N-glycosylation sites but only particular sites are used for polysialylation in vivo. Intriguingly, the polySia acceptor sites of both NCAM and SynCAM 1 are located in an Ig domain that is two domains apart from the membrane (Fig. S7). As polySTs are also transmembrane proteins, proper spacing might determine accessibility and in vivo selectivity for particular N-glycosylation sites as indicated by loss of site specificity in N-glycosylation mutants if both enzyme and acceptor molecule lack their transmembrane domain (Fig. S7).

In the perinatal brain, polySia-SynCAM 1 was found exclusively on a subset of NG2 cells. These glia cells (also known as
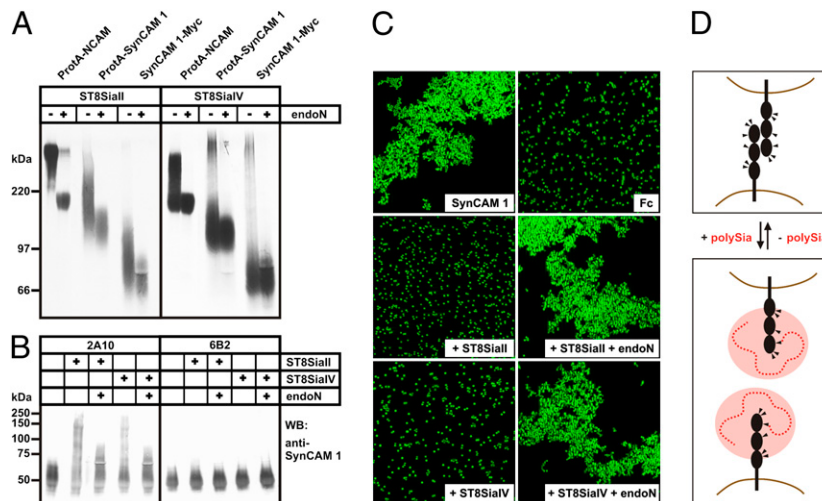
Fig. 4. In vitro polysialylation of SynCAM 1 by ST8SiaII and ST8SiaIV. (A) Soluble Protein A (ProtA) fusion proteins of NCAM and SynCAM 1 as well as soluble SynCAM 1 with a C-terminal Myc-epitope were adsorbed to Sepharose beads and incubated with ST8SiaII (Left) or ST8SiaIV (Right) in the presence of CMP-[^{14}C]sialic acid. Reaction products were separated by 7% SDS/PAGE before and after treatment with endoN and analyzed by autoradiography. (B) Soluble SynCAM 1-Myc was expressed in sialylation-competent CHO-2A10 (Left) and sialylation-deficient CHO-6B2 cells (Right). After adsorption to Sepharose beads, SynCAM 1 was incubated with CMP-sialic acid in the presence or absence of ST8SiaII or ST8SiaIV. Reaction products were separated by 8% SDS/PAGE before and after endoN treatment and analyzed by Western blotting (WB) with anti-SynCAM 1 mAb 3E1. (C) Homophilic SynCAM 1 binding is abrogated by polysialylation. Fluorescent Protein A beads were loaded with purified SynCAM 1-Fc chimera or with isolated Fc-fragments as control. Extensive clustering of SynCAM 1 coated beads was completely abolished by ST8SiaII and ST8SiaIV catalyzed polysialylation and was fully restored after removal of polySia by endoN treatment. (D) Proposed model for abrogation of homophilic SynCAM 1 binding by polysialylation. Ig-like domains are represented as black spheres, N-glycans are indicated by triangles, and polySia is shown as dashed red line with the hydrodynamic radius indicated by a red disk.
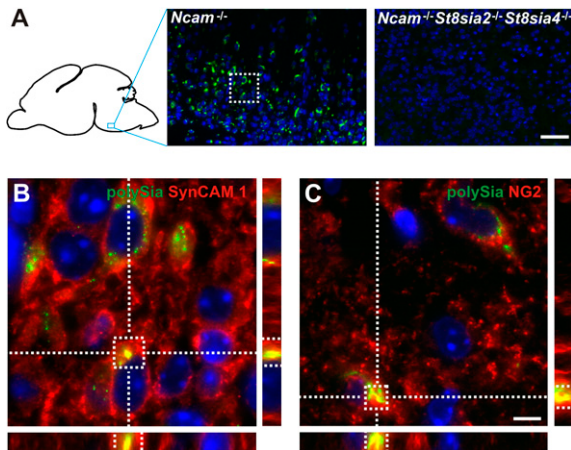
Fig. 5. PolySia-SynCAM 1 is expressed on NG2 cells. (*A*) Representative immunofluorescence image showing abundant polySia expression (labeled by anti-polySia mAb 735; green) in the pontomedullary hindbrain of newborn *Ncam*$^{-/-}$ brain. Specificity of the staining was controlled on equivalent brain sections of *Ncam*$^{-/-}$*St8sia2*$^{-/-}$*St8sia4*$^{-/-}$ mice, where no polySia signal was detected. (*B*) Magnification of the boxed area in *A*. A 3D reconstruction of ApoTome z-stack images shows colocalization of polySia (labeled by mAb 735; green) and SynCAM 1 (labeled by mAb 3E1; red). Specificity of mAb 3E1 for SynCAM 1 was controlled by transfection experiments (Fig. S6). (*C*) Colocalization of polySia (green) and NG2 (labeled by NG2 antibodies). Nuclei are stained blue (DAPI stain). (Scale bars: 50 μm in *A*, 5 μm in *B* and *C*.)

polydendrocytes or synantocytes) are distinct from mature oligodendrocytes, astrocytes, and microglia, and make up 5% to 10% of all glia in the developing and mature CNS (39–41). They are scattered throughout the developing and adult brain and are considered as multipotential progenitor pool that can give rise to oligodendrocytes, astrocytes, and neurons. Remarkably, a subset of NG2 cells can promote presynaptic specialization in neurons, leading to unique synaptic association between NG2 cells and neurons (39, 41).

SynCAM 1 is known as a powerful inducer of synaptic differentiation. When coexpressed with glutamate receptors in nonneuronal cells, SynCAM 1 is sufficient to induce artificial synapses with cocultured neurons (22). To date, little is known what drives the assembly of neuron-NG2 cell synapses. To our knowledge, this is the first report of SynCAM 1 expression on NG2 cells, suggesting that this cell adhesion molecule could play a role in inducing this specialized neuron-glia synapse. By attenuating SynCAM 1–mediated functions, polysialylation of SynCAM 1 may have an important regulatory role in the formation of neuron-NG2 cell interactions. Moreover, polySia-SynCAM 1 has the potential to regulate the communication between NG2 cells and neurons, as it is known that polySia directly increases the probability of the open state of AMPA-type glutamate receptors (42), the receptor type through which NG2 cells receive synaptic inputs (43, 44).

Remarkably, only a subfraction of SynCAM 1 is polysialylated in perinatal brain. In contrast, at this developmental stage when both polySTs reach peak level and almost ubiquitous expression, NCAM is quantitatively converted to its polysialylated form (13, 45). As SynCAM 1 is broadly expressed in all brain regions perinatally, polysialylation might be restricted to particular glyco- and/or isoforms of SynCAM 1. Alternative splicing of three variable exons can theoretically give rise to eight transmembrane isoforms that differ only in the region between Ig3 and the transmembrane domain. The variably spliced peptides contain two to 17 putative O-glycosylation sites, leading to multiple glycoforms (35). In vitro, both polySTs were able to polysialylate soluble SynCAM 1 lacking the variable stem region, demonstrating that Ig1-3 modules are sufficient to mediate interaction with polySTs. However, it is still possible that, in vivo, only particular isoforms allow proper spacing and accessibility of the N-glycan acceptor site.

In summary, we characterized SynCAM 1 as a polySia acceptor in the developing brain and demonstrated that polySia-SynCAM 1 is restricted to a subpopulation of NG2 cells. NG2 cells form functional synapses in the postnatal brain and serve as the primary source of myelinating oligodendrocytes during development and myelin repair. Future experiments will be needed to determine the exact role of polySia-SynCAM 1 for NG2 cell functions.

Materials and Methods

Please refer to the *SI Materials and Methods* for details on mice, antibodies, and further methods.

Identification of SynCAM 1 as Polysialylated Glycoprotein and Intramolecular Localization of PolySia. Isolation of polysialylated proteins, isolation and deglycosylation of polySia-glycopeptides, immunoblot, and DMB-HPLC analysis were carried out as previously described (13, 33, 45). PolySia-SynCAM 1 was identified by in-gel tryptic digest, peptide mass fingerprint analysis using MALDI-TOF MS, MS fragmentation analysis, and database search. Isolated polySia-glycopeptides were chemically desialylated, treated with PNGase F and analyzed by tandem MALDI-TOF MS.

In Vitro Polysialylation and Bead Aggregation Assay. SynCAM 1 lacking transmembrane domain and variably spliced stem region was produced in CHO cells either as a Protein A–SynCAM 1 chimera or C-terminally tagged with a Myc-epitope. After immunoadsorption to either IgG- or Protein G–Sepharose coupled with anti-Myc mAb 9E10, in vitro polysialylation was performed as described previously (46) with purified soluble ST8SiaII and ST8SiaIV. Homophilic SynCAM 1 binding was analyzed in a bead aggregation assay with purified SynCAM 1 fused to the Fc-part of human IgG1 (36).

Immunohistochemistry. Dissection of brains from transcardially perfused mice, preparation of paraffin sections, immunofluorescence staining and microscopy were performed as described (13, 47).

1. Finne J, Finne U, Deagostini-Bazin H, Goridis C (1983) Occurrence of alpha 2-8 linked polysialosyl units in a neural cell adhesion molecule. *Biochem Biophys Res Commun* 112:482–487.
2. Rothbard JB, Brackenbury R, Cunningham BA, Edelman GM (1982) Differences in the carbohydrate structures of neural cell-adhesion molecules from adult and embryonic chicken brains. *J Biol Chem* 257:11064–11069.
3. Edelman GM, Chuong CM (1982) Embryonic to adult conversion of neural cell adhesion molecules in normal and staggerer mice. *Proc Natl Acad Sci USA* 79:7036–7040.
4. Johnson CP, Fujimoto I, Rutishauser U, Leckband DE (2005) Direct evidence that neural cell adhesion molecule (NCAM) polysialylation increases intermembrane repulsion and abrogates adhesion. *J Biol Chem* 280:137–145.
5. Fujimoto I, Bruses JL, Rutishauser U (2001) Regulation of cell adhesion by polysialic acid. Effects on cadherin, immunoglobulin cell adhesion molecule, and integrin function and independence from neural cell adhesion molecule binding or signaling activity. *J Biol Chem* 276:31745–31751.

6. Rutishauser U (2008) Polysialic acid in the plasticity of the developing and adult vertebrate nervous system. *Nat Rev Neurosci* 9:26–35.
7. Kleene R, Schachner M (2004) Glycans and neural cell interactions. *Nat Rev Neurosci* 5:195–208.
8. Hildebrandt H, Mühlenhoff M, Weinhold B, Gerardy-Schahn R (2007) Dissecting polysialic acid and NCAM functions in brain development. *J Neurochem* 103 (suppl 1):56–64.
9. Gascon E, Vutskits L, Kiss JZ (2007) Polysialic acid-neural cell adhesion molecule in brain plasticity: From synapses to integration of new neurons. *Brain Res Rev* 56:101–118.
10. Seki T, Arai Y (1993) Distribution and possible roles of the highly polysialylated neural cell adhesion molecule (NCAM-H) in the developing and adult central nervous system. *Neurosci Res* 17:265–290.
11. Angata K, et al. (1997) Human STX polysialyltransferase forms the embryonic form of the neural cell adhesion molecule. Tissue-specific expression, neurite outgrowth, and chromosomal localization in comparison with another polysialyltransferase, PST. *J Biol Chem* 272:7182–7190.

12. Ong E, et al. (1998) Developmental regulation of polysialic acid synthesis in mouse directed by two polysialyltransferases, PST and STX. *Glycobiology* 8:415–424.

13. Galuska SP, et al. (2006) Polysialic acid profiles of mice expressing variant allelic combinations of the polysialyltransferases ST8SiaII and ST8SiaIV. *J Biol Chem* 281: 31605–31615.

14. Weinhold B, et al. (2005) Genetic ablation of polysialic acid causes severe neuro-developmental defects rescued by deletion of the neural cell adhesion molecule. *J Biol Chem* 280:42971–42977.

15. Cremer H, et al. (1994) Inactivation of the N-CAM gene in mice results in size reduction of the olfactory bulb and deficits in spatial learning. *Nature* 367:455–459.

16. Hildebrandt H, Mühlenhoff M, Gerardy-Schahn R (2010) Polysialylation of NCAM. *Adv Exp Med Biol* 663:95–109.

17. Angata K, et al. (2007) Polysialic acid-directed migration and differentiation of neural precursors are essential for mouse brain development. *Mol Cell Biol* 27:6659–6668.

18. Hildebrandt H, et al. (2009) Imbalance of neural cell adhesion molecule and polysialyltransferase alleles causes defective brain connectivity. *Brain* 132:2831–2838.

19. Yabe U, Sato C, Matsuda T, Kitajima K (2003) Polysialic acid in human milk. CD36 is a new member of mammalian polysialic acid-containing glycoprotein. *J Biol Chem* 278:13875–13880.

20. Zuber C, Lackie PM, Catterall WA, Roth J (1992) Polysialic acid is associated with sodium channels and the neural cell adhesion molecule N-CAM in adult rat brain. *J Biol Chem* 267:9965–9971.

21. Curreli S, Arany Z, Gerardy-Schahn R, Mann D, Stamatos NM (2007) Polysialylated neuropilin-2 is expressed on the surface of human dendritic cells and modulates dendritic cell-T lymphocyte interactions. *J Biol Chem* 282:30346–30356.

22. Biederer T, et al. (2002) SynCAM, a synaptic adhesion molecule that drives synapse assembly. *Science* 297:1525–1531.

23. Shingai T, et al. (2003) Implications of nectin-like molecule-2/IGSF4/RA175/SgIGSF/TSLC1/SynCAM1 in cell-cell adhesion and transmembrane protein localization in epithelial cells. *J Biol Chem* 278:35421–35427.

24. Kuramochi M, et al. (2001) TSLC1 is a tumor-suppressor gene in human non-small-cell lung cancer. *Nat Genet* 27:427–430.

25. Wakayama T, Ohashi K, Mizuno K, Iseki S (2001) Cloning and characterization of a novel mouse immunoglobulin superfamily gene expressed in early spermatogenic cells. *Mol Reprod Dev* 60:158–164.

26. Gomyo H, et al. (1999) A 2-Mb sequence-ready contig map and a novel immuno-globulin superfamily gene IGSF4 in the LOH region of chromosome 11q23.2. *Genomics* 62:139–146.

27. Urase K, Soyama A, Fujita E, Momoi T (2001) Expression of RA175 mRNA, a new member of the immunoglobulin superfamily, in developing mouse brain. *Neuroreport* 12:3217–3221.

28. Wakayama T, et al. (2007) Heterophilic binding of the adhesion molecules poliovirus receptor and immunoglobulin superfamily 4A in the interaction between mouse spermatogenic and Sertoli cells. *Biol Reprod* 76:1081–1090.

29. Masuda M, et al. (2002) The tumor suppressor protein TSLC1 is involved in cell-cell adhesion. *J Biol Chem* 277:31014–31019.

30. Furuno T, et al. (2005) The spermatogenic Ig superfamily/synaptic cell adhesion molecule mast-cell adhesion molecule promotes interaction with nerves. *J Immunol* 174:6934–6942.

31. Sara Y, et al. (2005) Selective capability of SynCAM and neuroligin for functional synapse assembly. *J Neurosci* 25:260–270.

32. Inoue S, Inoue Y (2001) A challenge to the ultrasensitive chemical method for the analysis of oligo- and polysialic acids at a nanogram level of colominic acid and a milligram level of brain tissues. *Biochimie* 83:605–613.

33. Galuska SP, Geyer R, Gerardy-Schahn R, Mühlenhoff M, Geyer H (2008) Enzyme-dependent variations in the polysialylation of the neural cell adhesion molecule (NCAM) in vivo. *J Biol Chem* 283:17–28.

34. Galuska SP, Geyer R, Mühlenhoff M, Geyer H (2007) Characterization of oligo- and polysialic acids by MALDI-TOF-MS. *Anal Chem* 79:7161–7169.

35. Biederer T (2006) Bioinformatic characterization of the SynCAM family of immunoglobulin-like domain-containing adhesion molecules. *Genomics* 87:139–150.

36. Fogel AI, et al. (2007) SynCAMs organize synapses through heterophilic adhesion. *J Neurosci* 27:12516–12530.

37. Eckhardt M, Mühlenhoff M, Bethe A, Gerardy-Schahn R (1996) Expression cloning of the Golgi CMP-sialic acid transporter. *Proc Natl Acad Sci USA* 93:7572–7576.

38. Ligon KL, et al. (2006) Development of NG2 neural progenitor cells requires Olig gene function. *Proc Natl Acad Sci USA* 103:7853–7858.

39. Nishiyama A, Komitova M, Suzuki R, Zhu X (2009) Polydendrocytes (NG2 cells): multifunctional cells with lineage plasticity. *Nat Rev Neurosci* 10:9–22.

40. Butt AM, Hamilton N, Hubbard P, Pugh M, Ibrahim M (2005) Synantocytes: The fifth element. *J Anat* 207:695–706.

41. Trotter J, Karram K, Nishiyama A (2010) NG2 cells: Properties, progeny and origin. *Brain Res Rev* 63:72–82.

42. Vaithianathan T, et al. (2004) Neural cell adhesion molecule-associated polysialic acid potentiates alpha-amino-3-hydroxy-5-methylisoxazole-4-propionic acid receptor currents. *J Biol Chem* 279:47975–47984.

43. Bergles DE, Roberts JD, Somogyi P, Jahr CE (2000) Glutamatergic synapses on oligodendrocyte precursor cells in the hippocampus. *Nature* 405:187–191.

44. Ziskin JL, Nishiyama A, Rubio M, Fukaya M, Bergles DE (2007) Vesicular release of glutamate from unmyelinated axons in white matter. *Nat Neurosci* 10:321–330.

45. Oltmann-Norden I, et al. (2008) Impact of the polysialyltransferases ST8SiaII and ST8SiaIV on polysialic acid synthesis during postnatal mouse brain development. *J Biol Chem* 283:1463–1471.

46. Mühlenhoff M, Eckhardt M, Bethe A, Frosch M, Gerardy-Schahn R (1996) Auto-catalytic polysialylation of polysialyltransferase-1. *EMBO J* 15:6943–6950.

47. Schiff M, Weinhold B, Grothe C, Hildebrandt H (2009) NCAM and polysialyltransferase profiles match dopaminergic marker gene expression but polysialic acid is dispensable for development of the midbrain dopamine system. *J Neurochem* 110:1661–1673.

48. Medzihradszky KF (2005) Peptide sequence analysis. *Methods Enzymol* 402:209–244.

110

Supporting Information

Galuska et al. 10.1073/pnas.0912103107

SI Materials and Methods

Antibodies, Enzymes, and Chemicals. Anti-NCAM mAb H28 (1) and mouse anti-polySia mAb 735 [IgG$_{2a}$ (2)] as well as endoN were purified as previously described (3). For affinity chromatography, mAb 735 was coupled to Protein A–conjugated magnetic beads (Invitrogen). Rabbit polyclonal anti-SynCAM 1 antibody (pAb), mouse anti–β-III-tubulin mAb (IgG$_{2b}$,), rabbit anti-GFAP pAb, and mouse anti-MAP2 mAb were purchased from Sigma-Aldrich. Chicken anti-SynCAM 1 mAb 3E1 (IgY) was obtained from MBL, rabbit anti-NG2 pAb from Millipore, and rabbit anti-Olig2 pAb, rabbit anti-SynCAM 2 pAb, and rabbit anti-SynCAM 3 pAb were purchased from Abcam. Horseradish peroxidase conjugated secondary antibodies were from Dako. Rabbit and mouse IgG-specific and IgY-specific Alexa 568– or Alexa 488–conjugated antibodies were obtained from Molecular Probes. CMP-[^{14}C]Neu5Ac (10.5 GBq/mmol) was purchased from GE Healthcare and CMP-Neu5Ac from Sigma. DMB was obtained from Dojindo and PNGaseF from Roche.

Animals. $Ncam1^{-/-}$ mice were provided by H. Cremer (Developmental Biology Institute of Marseille Luminy, Campus de Luminy, Marseille, France) (4). $Ncam1^{-/-}$ and $Ncam1^{-/-}St8sia2^{-/-}$ $St8sia4^{-/-}$ triple KO mice (5) were back-crossed to the C57BL/6J genetic background for 10 generations. Genotyping was performed as described (5). All protocols for animal use were in compliance with the German law for protection of animals and approved by the local authorities.

Isolation of Polysialylated Proteins from Mouse Brain Extracts. Postnatal d 1 brains of NCAM KO mice were homogenized in 20 mM Tris/HCl buffer, pH 8.0, containing 5 mM EDTA, 150 mM NaCl, 1% (vol/vol) Triton X-100, 200 U/mL aprotinin, 1 mM phenylmethylsulfonylfluoride, and 20 μg/mL leupeptin (1 mL per brain) (3). The lysate was shaken overnight at 4 °C and, after centrifugation, supernatants were mixed with mAb 735–conjugated protein A magnetic beads (500 μL beads/14 mL lysate). The beads were washed 10 times each with 10 mL of washing buffer 1a [20 mM Tris/HCl, pH 8.0, 200 mM NaCl, 0.5% (vol/vol) Triton X-100] and washing buffer 2a (20 mM Tris/HCl, pH 8.0, 150 mM NaCl). Polysialylated proteins were eluted using 100 mM triethylamine buffer, pH 11.5, and lyophilized. Immunopurification using polyclonal anti-SynCAM 1 antibody was performed in an analogous manner.

SDS/PAGE and Western Blotting. Brain lysates as well as purified proteins were resolved by 10% SDS/PAGE under reducing conditions (6). For digestion of polySia chains proteins were treated with endoN (2 ng/μL overnight at 8 °C). Release of N-glycans by PNGaseF was performed as previously described for polysialylated proteins (7). Proteins were transferred to polyvinylidene difluoride membrane (GE Healthcare), probed with 5 μg/mL anti-polySia mAb 735, anti-NCAM mAb H28, anti-SynCAM 1 mAb 3E1, or anti-SynCAM 1 pAb and detected by enhanced chemiluminescence (Pierce).

In-Gel Digest for Peptide Mass Fingerprint Analysis. For the in-gel digest, commercially available gels were used (10%; BioRad). The tryptic digest was performed as described previously (8) with adaptation for membrane proteins and the size of the gel section. Briefly, respective gel slices were transferred with 100 μL H$_2$O into a LoBind tube (Eppendorf) and washed for 15 min under shaking with 100 μL 50 mM ammonium bicarbonate, pH 8.5,

containing 50% (vol/vol) acetonitrile. After removal of the solvent, the gel was dried and 100 μL acetonitrile were added. The washing procedure was repeated twice with 100 μL 50 mM ammonium bicarbonate, pH 8.5, respectively, and the gel piece was dried in a vacuum centrifuge. After reduction and carbamidomethylation trypsin (sequencing grade; Promega), diluted in protease max enhancer (Promega) to a final concentration of 10 ng/μL, was added and incubated for 1 h at 37 °C. Peptides were extracted by sonication with 100 μL 0.1% trifluoroacetic acid for 15 min and desalted using C-18 OMIX-Tips (Varian).

Isolation and Deglycosylation of PolySia-Glycopeptides. Four mouse brains were suspended in 2 mL lysis buffer (20 mM ammonium bicarbonate, pH 8.5, 6 M urea) and carbamidomethylated with iodacetamide. The lysate was diluted to 12 mL with 20 mM ammonium bicarbonate and digested with 100 μg trypsin (sequencing grade; Promega) overnight at 37 °C. Trypsin was inactivated with 10 mM phenylmethylsulfonylfluoride. Resulting peptides were desalted on a P4-Biogel column (1 × 100 cm; BioRad). Desalted (glyco-)peptides were added to 50 μL mAb 735 magnetic beads as described earlier and the beads were washed with washing buffer 1b [20 mM ammonium bicarbonate, pH 8.5, 200 mM NaCl, 0.5% (vol/vol) Triton X-100] and 2b (20 mM ammonium bicarbonate, pH 8.5). PolySia peptides were eluted using 100 mM triethylamine buffer, pH 11.5, and lyophilized. PolySia-glycopeptides were desialylated by mild acid hydrolysis in 200 μL 1 M acetic acid at 80 °C for 30 min before deglycosylation using PNGaseF as described earlier. Deglycosylated glycopeptides were desalted using C-18 OMIX-Tip (Varian).

DMB-HPLC Analysis. To analyze the chain length and the amount of polySia, brains of 1-d-old mice were homogenized and delipidated as described previously (9, 10). The dried tissue was dissolved in 300 μL DMB reaction buffer and incubated for 24 h at 4 °C with shaking. The reaction was stopped by adding 70 μL of 1 M NaOH and insoluble material was removed by centrifugation. For separation of polySia chains, an LKB HPLC system was used, equipped with a DNAPac PA-100 column and a fluorescent detector set at 372 nm for excitation and 456 nm for emission. MilliQ water and 4 M ammonium acetate (E2) were used as eluents as described by Nakata et al. (11). Elution was performed by the following gradient: T_{0min} = 0% (vol/vol) E2; T_{15min} = 8% (vol/vol) E2; T_{40min} = 12% (vol/vol) E2; and T_{160min} = 23% (vol/vol) E2. The column was washed with 100% (vol/vol) E2 for 10 min. Aliquots corresponding to 9% or 86% of the supernatants were injected for quantification of the peak or for determination of the maximal detectable chain length, respectively.

MALDI-TOF MS/MS Analysis. MALDI-TOF MS analyses were performed on an Ultraflex TOF mass spectrometer (Bruker-Daltonik) equipped with a nitrogen laser and a LIFT-MS/MS facility and controlled by FlexControl 3.0 software as described previously (3, 12). The instrument was operated in positive-ion reflector mode. Desalted peptides (1 μL) of the in-gel digest were transferred onto prespotted anchorchip (PAC; Bruker-Daltonik) targets. After drying, the spot was washed with 10 μL 20 mM ammonium phosphate buffer containing 0.1% trifluoroacetic acid. Isolated polysialylated glycopeptides were loaded onto a stainless steel target in 1 μL water and mixed with 1 μL matrix (10 mg/mL 2,5-dihydroxybenzoic acid in 50% acetonitrile, 1% *o*-phosphoric acid) before and after deglycosylation with PNGaseF (13). In general, 500 to 5,000 shots were accumulated in positive ion MS and MS/MS

111

modes, respectively. External calibration of mass spectra was carried out using peptide calibration standard for MS (Bruker-Daltonik). Masses were annotated and processed with FlexAnalysis 3.0. Annotation of fragment ions in the MS/MS mode was performed according to Medzihradszky (14).

Database Search. For peptide mass fingerprinting scoring, the MALDI MS data were searched against the Mascot data search database using the Mascot program (http://www.matrixscience.com) with the following parameters: restriction to *Mus musculus*, peptide mass tolerance, 25 ppm; allow up to one missed cleavage; variable modifications considered were cysteine carbamidomethylation and methionine oxidation. For identification of the polysialylated N-glycosylation site, the peptide mass tolerance was constricted to 15 ppm and potential deamination of asparagine and glutamine was allowed as modification.

Plasmid Construction. To generate a SynCAM 1-Fc chimera, the region encoding the extracellular domains of SynCAM 1 (aa 1–346) was amplified by PCR with the primers MR74s (5′-GACTGC-TAGCATGGCGAGTGTAGTGCTG-3′) and MR75as (5′-GA-CTAGATCTACTTACCTGTATGATCCACTGCCCTGATC-3′) and full-length human SynCAM 1 cDNA (OriGene) lacking the variable spliced exons (accession no. NM_001098517) as template. The resulting PCR product was digested with NheI and BglII and ligated into the NheI/BamHI sites of pcDNA3.1-Ig upstream of the DNA sequence encoding the Fc part of human IgG1 (15). The plasmid used for expression of soluble SynCAM 1 (aa 1–346) with a C-terminal Myc-epitope was generated by PCR with the primers MR72s (5′-GATCGGTACCGAATGGCGAGTGTAGTGCTG-3′) and MR73as (5′-GACTCTCGAGATGATCCACTGCCCTG-ATC-3′). After digestion with KpnI and XhoI, the obtained PCR product was ligated in the corresponding sites of pcDNA3.1-*myc*/His (Invitrogen). The plasmid used for expression of a soluble Protein A–SynCAM 1 fusion protein comprising aa 39 to 346 of SynCAM 1 C-terminally fused to Protein A was generated by PCR using the primers MR58s (5′-GCATGAATTCGATCCCCACAGGTG-ATGGG–3′) and MR59as (5′-GCATGGTACCTTAATGATCC-ACTGCCCTGATCG-3′). The amplified PCR product was digested with EcoRI and KpnI and ligated into the corresponding sites of the vector pPROTA (16). The plasmid encoding the Protein A–NCAM chimera was generated as described previously (17). Full-length cDNAs of murine SynCAM 1, SynCAM 2, and SynCAM 3 were transcribed from 1 µg of total RNA of perinatal mouse brain using the SuperScript First-Strand Synthesis System (Invitrogen). SynCAM 1 cDNA was amplified by PCR with the primer pair MR68s (5′-GATCGGTACCATGGCGAGTGCTGTG-CTG-3′) and MR69as (5′-GCCATGCGGCCGCCTAGATGAA-GTACTCTTTCTTTTCTTCG-3). After digestion with KpnI and NotI, the obtained PCR product was ligated in the corresponding sites of pcDNA3.1-Zeo (Invitrogen). SynCAM 2 cDNA was amplified with the primer pair MR80s (5′-GATCGGATCCGCCAC-CATGATTTGGAAACGCAGCGC-3′) and MR81as (5′-GATC-GCGGCCGCTTAAATGAAATACTCTTTTTTCTC-3′). The obtained PCR product was digested with BamHI and NotI and ligated in the corresponding sites of pcDNA3.1-Zeo (Invitrogen). SynCAM 3 cDNA was amplified with the primer pair MR83s (5′-GATC GATATCGCCACCATGGGGGGCCCCTTCCGC-3′) and MR84as (5′-GATCGCGGCCGC CTAGATGAAATATTCCTT-CTTG-3′) and the resulting PCR product was digested with EcoRV and NotI and ligated into the corresponding sites of pcDNA3.1-Zeo. The identity of all constructs was confirmed by sequencing.

Cell Lines, Transfection, and Culture Conditions. CHO cells were maintained in DMEM/Ham F12 1:1 (Seromed) supplemented with 5% FCS and 1 mM sodium pyruvate in a 37 °C, 5% CO$_2$ incubator. CHO-2A10 cells represent a genetic complementation group characterized by a deficient *St8Sia4* gene rendering

these cells polySia-negative (18, 19). CHO-6B2 cells lack a functional CMP-sialic acid transporter and express exclusively asialo-glycoconjugates (20). The murine fibroblast cell line LMTK$^-$ was maintained in DMEM (Seromed) supplemented with 10% FCS in a 37 °C, 5% CO$_2$ incubator. Transient transfections were performed with Lipofectamine (Invitrogen) as described previously (21). *Spodoptera frugiperda* (Sf9) cells (Gibco) were grown at 27 °C in shaking culture at 75 rpm in protein-free Insect-Xpress medium (BioWhittaker/Lonza) and maintained at a density of 0.5×10^6 to 6×10^6 viable cells per mL. Transient expression of soluble polysialyltransferases was performed upon infection with recombinant baculovirus generated by the Bac-to-Bac System (Invitrogen).

In Vitro Polysialylation Assay. Soluble mouse ST8SiaII (residues 57–375) and hamster ST8SiaIV (residues 26–359) with an N-terminal hexa-histidine tag were secreted by Sf9 cells and purified by affinity chromatography on Ni^{2+}-chelating columns (GE Healthcare). Soluble acceptor proteins were produced in CHO cells. Three days after transfection, cell culture supernatant of one 100-mm dish was harvested and concentrated 10-fold by ultrafiltration (Amicon Ultra-15, 10 kDa cut-off; Millipore). After preclearing with IgG- or Protein G–Sepharose (GE Healthcare), Protein A fusion proteins and SynCAM 1-Myc were isolated by immunoprecipitation with IgG-Sepharose and anti-Myc mAb 9E10 (Roche) covalently coupled to Protein G–Sepharose, respectively. Immunoprecipitates were washed twice with 1 mL of PBS solution (10 mM sodium phosphate, pH 7.4, 100 mM NaCl) and twice with reaction buffer (10 mM Mes, pH 6.7, 10 mM MnCl$_2$). In vitro polysialylation was performed in a final volume of 50 µL containing 2 µg of purified polysialyltransferase. For radioactive incorporation assays, 0.76 mM CMP-[^{14}C]Neu5Ac (0.18 GBq/mmol) and 0.012 mM CMP-[^{14}C]Neu5Ac (10.8 GBq/mmol) were used for assays with ST8SiaII and ST8SiaIV, respectively. For nonradioactive assays, 1 mM CMP-Neu5Ac (Nacalai Tesque) was used. After incubation for 15 h at room temperature in a thermomixer at 1,350 rpm (Eppendorf), reactions were stopped by washing twice with PBS solution. After dividing samples into two aliquots, beads were resuspended in 20 µL Laemmli buffer. For specific degradation of polySia, one aliquot was treated with 1 µg of SDS-resistant endoN for 30 min at 37 °C. Reaction products were separated by SDS/PAGE and analyzed by either autoradiography or Western blotting using anti-SynCAM 1 mAb 3E1.

Production and Purification of SynCAM 1-Fc Protein. Twenty-four hours after transfection of CHO-2A10 cells with the plasmid encoding SynCAM 1-Fc and a Zeocin resistance gene, the medium was supplemented with 0.75 mg/mL of Zeocin (Invitrogen). After 10 d of selection, cells were grown in protein-free CHO-A medium (Invitrogen). Conditioned medium was collected every 2 to 3 d and stored at −20 °C. For isolation of SynCAM 1-Fc, 500 mL of conditioned medium was concentrated 10-fold by tangential flow ultrafiltration (Vivaflow 50, 10 kDa cut-off; Sartorius) and passed over a Protein G Sepharose column (GE Healthcare). After washing with 10 column volumes of 20 mM sodium phosphate (pH 7.0), SynCAM 1-Fc was eluted with glycine buffer (0.1 M glycine, pH 2.7) and fractions were neutralized by addition of 1 M Tris-HCl, pH 9.0.

Bead Aggregation Assay. Homophilic SynCAM 1 binding was analyzed in a bead aggregation assay (22) using purified SynCAM 1-Fc bound to Protein A beads. Protein A (Sigma) was covalently coupled to green fluorescent FluoSpheres (1 µm diameter; Invitrogen) using 1-ethyl-1-3-(3-dimethylaminopropyl)-carbodiimide (Invitrogen) and beads (10 µL of a 2% suspension) were coated with 5 µg of purified SynCAM 1-Fc or human IgG Fc fragment (Jackson Immunoresearch). After washing three times with 1 mL of 0.5% BSA in PBS solution and twice with Mes buffer (10 mM Mes, pH 6.7, 10 mM MnCl$_2$), beads were

incubated with 1 mM CMP-Neu5Ac (Nacalai Tesque) and 2 µg of recombinant soluble ST8SiaII or ST8SiaIV for 15 h at room temperature in a thermomixer (Eppendorf) at 1,350 rpm. For specific degradation of polySia, beads were washed twice with 0.5% BSA in PBS solution and incubated with 2.5 µg endoN for 30 min at 37 °C. After washing three times with 0.5% BSA in PBS solution, beads were monodispersed by applying a 1-s ultrasound pulse in an ultrasonic bath (Sonorex Super; Bandelin) and loaded to chamber slides (µ-Slides; Ibidi). After incubation for 1.5 h at room temperature, beads were imaged under a fluorescence microscope (Axiovert 200 M; Zeiss).

Primary Cell Culture. Basal hindbrain of newborn $Ncam^{-/-}$ mice was dissected, transferred to 1× Hanks Balanced Salt Solution (Gibco), minced, and incubated with 10 mg/mL Trypsin type IX (Sigma) and 0.5 mg/mL DNase I (Roche) at 37 °C for 10 min. During the second half of the incubation period, 0.5 mg/mL DNase I and 12 mM $MgCl_2$ were added. After gentle trituration, cells were collected by centrifugation ($280 \times g$ for 10 min at 4 °C) and resuspended in DMEM (high glucose) containing 2 mM Glutamax, 1% (vol/vol) N2 supplement, 2% (vol/vol) B27 (all from Gibco), 10 µg/mL Insulin (Sigma), 10% (vol/vol) horse serum (Biochrom), and 5 µg/mL gentamycin (Gibco). Single cell suspensions were seeded at densities of 100,000 cells/cm^2 in 24-well plates containing glass coverslips coated with 100 µg/mL poly-D lysine (Sigma). After incubation for 48 h in a 37 °C, 7.5% CO_2 incubator, cells were fixed for immunocytochemistry.

Immunocytochemistry. Cells were fixed with 4% paraformaldehyde for 30 min, permeabilized with 0.1% Triton X-100, blocked with 2% BSA for 1 h at room temperature, and incubated with primary antibodies for 2 h at room temperature. The following antibodies were used: polySia-specific mouse mAb 735 (10 µg/mL), anti-SynCAM 1 IgY mAb 3E1 (5 µg/mL,), NG2 Proteoglycan-specific rabbit pAb (5 µg/mL), Olig2-specific rabbit pAb (1 µg/mL), β-III-tubulin–specific mouse mAb (5 µg/mL), SynCAM 2–specific rabbit pAb (5 µg/mL), and SynCAM 3–specific rabbit pAb (5 µg/m). Rabbit and mouse IgG-specific and IgY-specific Alexa 568– or Alexa 488–conjugated antibodies were used according to

the manufacturer's recommendations. As first-layer control, cells were incubated in blocking solution lacking primary antibody. For double immunofluorescence staining, cross-reactivity of secondary antibodies was controlled by omitting either of the two primary antibodies. For negative controls, cells were pretreated with endosialidase (3 µg/mL in 0.1 M sodium phosphate, pH 7.4) for 1 h at 37 °C before staining with mAb 735. Coverslips were mounted in Vectashield mounting medium containing DAPI (Vector Laboratories).

Immunohistochemistry. Whole brains of newborn $Ncam^{-/-}$ and $Ncam^{-/-}St8sia2^{-/-}St8sia4^{-/-}$ triple KO mice were dissected from animals transcardially perfused with 4% paraformaldehyde in 0.1 M phosphate buffer, pH 7.4, under anesthesia by hypothermia. After overnight postfixation, brains were embedded in a single paraffin block and cut into 3- to 4-µm serial sagittal sections. For immunofluorescence staining, sections were deparaffinzed, rehydrated, blocked for 1 h in PBS solution containing 10% BSA, 0.1% Triton X-100, and incubated with primary antibodies overnight at 4 °C. The following antibodies were used: polySia-specific mouse mAb 735 (10 µg/mL), anti-SynCAM 1 mAb 3E1 (2.5 µg/mL), NG2 Proteoglycan–specific rabbit pAb (5 µg/mL), GFAP-specific rabbit pAb (1:100), and MAP2-specific mouse mAb (2 µg/mL). Rabbit and mouse IgG-specific and IgY-specific Alexa 568– or Alexa 488–conjugated antibodies were used according to the manufacturer's recommendations. Antibody controls were performed as described for immunocytochemistry. Slides were mounted in Vectashield mounting medium containing DAPI (Vector Laboratories).

Microscopy. Microscopy was performed with a Zeiss Axiovert 200 M equipped with ApoTome module, AxioCam MRm digital camera, and AxioVison software (Zeiss). Low-magnification images were acquired using a ×20 Plan-Apochromat (0.8 NA). Near-confocal optical sections of 0.81 µm thickness were obtained by ApoTome technology using a ×63 Plan-Apochromat oil immersion objective with 1.4 numerical aperture (Zeiss). Z stacks (3.5 µm) comprising sequential x-y sections were taken at 0.25-µm z intervals.

1. Hirn M, Pierres M, Deagostini-Bazin H, Hirsch M, Goridis C (1981) Monoclonal antibody against cell surface glycoprotein of neurons. *Brain Res* 214:433–439.
2. Frosch M, Görgen I, Boulnois GJ, Timmis KN, Bitter-Suermann D (1985) NZB mouse system for production of monoclonal antibodies to weak bacterial antigens: Isolation of an IgG antibody to the polysaccharide capsules of Escherichia coli K1 and group B meningococci. *Proc Natl Acad Sci USA* 82:1194–1198.
3. Galuska SP, Geyer R, Gerardy-Schahn R, Mühlenhoff M, Geyer H (2008) Enzyme-dependent variations in the polysialylation of the neural cell adhesion molecule (NCAM) in vivo. *J Biol Chem* 283:17–28.
4. Cremer H, et al. (1994) Inactivation of the N-CAM gene in mice results in size reduction of the olfactory bulb and deficits in spatial learning. *Nature* 367:455–459.
5. Weinhold B, et al. (2005) Genetic ablation of polysialic acid causes severe neurodevelopmental defects rescued by deletion of the neural cell adhesion molecule. *J Biol Chem* 280:42971–42977.
6. Laemmli UK (1970) Cleavage of structural proteins during the assembly of the head of bacteriophage T4. *Nature* 227:680–685.
7. Curreli S, Arany Z, Gerardy-Schahn R, Mann D, Stamatos NM (2007) Polysialylated neuropilin-2 is expressed on the surface of human dendritic cells and modulates dendritic cell-T lymphocyte interactions. *J Biol Chem* 282:30346–30356.
8. Grabitzki J, Ahrend M, Schachter H, Geyer R, Lochnit G (2008) The PCome of Caenorhabditis elegans as a prototypic model system for parasitic nematodes: Identification of phosphorylcholine-substituted proteins. *Mol Biochem Parasitol* 161: 101–111.
9. Inoue S, Inoue Y (2003) Ultrasensitive analysis of sialic acids and oligo/polysialic acids by fluorometric high-performance liquid chromatography. *Methods Enzymol* 362: 543–560.
10. Galuska SP, et al. (2006) Polysialic acid profiles of mice expressing variant allelic combinations of the polysialyltransferases ST8SiaII and ST8SiaIV. *J Biol Chem* 281: 31605–31615.
11. Nakata D, Troy FA, 2nd (2005) Degree of polymerization (DP) of polysialic acid (polySia) on neural cell adhesion molecules (N-CAMS): Development and application

of a new strategy to accurately determine the DP of polySia chains on N-CAMS. *J Biol Chem* 280:38305–38316.
12. Geyer H, Wuhrer M, Resemann A, Geyer R (2005) Identification and characterization of keyhole limpet hemocyanin N-glycans mediating cross-reactivity with Schistosoma mansoni. *J Biol Chem* 280:40731–40748.
13. Stensballe A, Jensen ON (2004) Phosphoric acid enhances the performance of Fe(III) affinity chromatography and matrix-assisted laser desorption/ionization tandem mass spectrometry for recovery, detection and sequencing of phosphopeptides. *Rapid Commun Mass Spectrom* 18:1721–1730.
14. Medzihradszky KF (2005) Peptide sequence analysis. *Methods Enzymol* 402:209–244.
15. Röckle I, et al. (2008) Polysialic acid controls NCAM-induced differentiation of neuronal precursors into calretinin-positive olfactory bulb interneurons. *Dev Neurobiol* 68: 1170–1184.
16. Sanchez-Lopez R, Nicholson R, Gesnel MC, Matrisian LM, Breathnach R (1988) Structure-function relationships in the collagenase family member transin. *J Biol Chem* 263:11892–11899.
17. Mühlenhoff M, Eckhardt M, Bethe A, Frosch M, Gerardy-Schahn R (1996) Autocatalytic polysialylation of polysialyltransferase-1. *EMBO J* 15:6943–6950.
18. Eckhardt M, et al. (1995) Molecular characterization of eukaryotic polysialyltransferase-1. *Nature* 373:715–718.
19. Windfuhr M, Manegold A, Mühlenhoff M, Eckhardt M, Gerardy-Schahn R (2000) Molecular defects that cause loss of polysialic acid in the complementation group 2A10. *J Biol Chem* 275:32861–32870.
20. Eckhardt M, Mühlenhoff M, Bethe A, Gerardy-Schahn R (1996) Expression cloning of the Golgi CMP-sialic acid transporter. *Proc Natl Acad Sci USA* 93: 7572–7576.
21. Mühlenhoff M, Manegold A, Windfuhr M, Gotza B, Gerardy-Schahn R (2001) The impact of N-glycosylation on the functions of polysialyltransferases. *J Biol Chem* 276: 34066–34073.
22. Fogel AI, et al. (2007) SynCAMs organize synapses through heterophilic adhesion. *J Neurosci* 27:12516–12530.
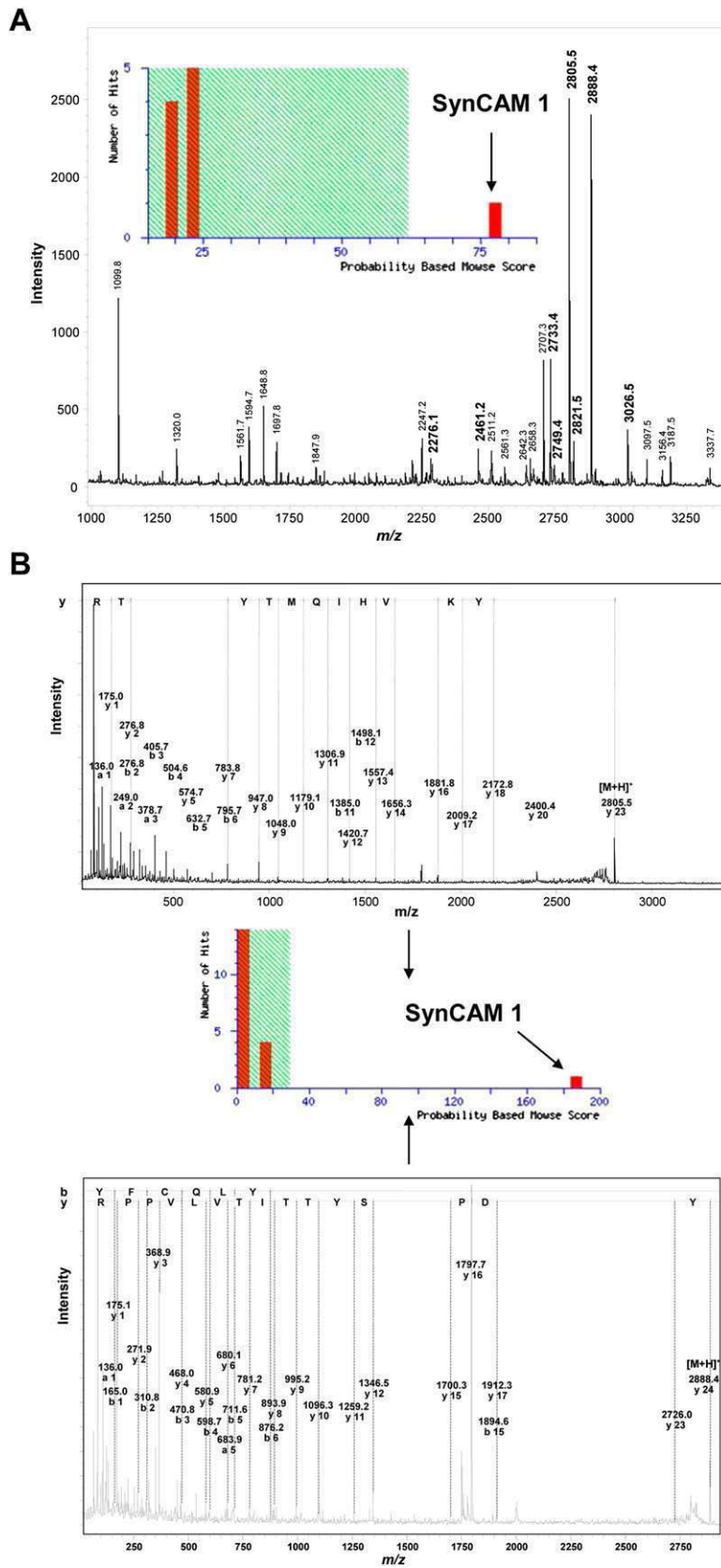
Fig. S1. Identification of the polysialylated protein obtained from postnatal *Ncam*$^{-/-}$ mice. (*A*) The immunoaffinity purified (mAb 735) polysialylated protein was separated by 10% SDS/PAGE and a gel slice covering the mass range of 100 to 150 kDa was excised. After reduction, carbamidomethylation, and treatment with trypsin, resulting peptides were extracted and analyzed by MALDI-TOF MS. Database search (Mascot) revealed SynCAM 1 with a significant score (*Inset*).

Tryptic peptides matching SynCAM 1 are printed in bold. Remaining signals could not be assigned and, therefore, might indicate the presence of additional polysialylated components. (*B*) Peptide signals at *m/z* 2805.5 and 2888.4 were used for fragmentation analysis by tandem MALDI-TOF MS and database search again verified SynCAM 1 as polySia protein. Sequence-specific ions are labeled as described earlier (1) and the deduced amino acid sequences are shown. Monoisotopic masses of the pseudomolecular ions [M+H]$^+$ are given.

1. Medzihradszky KF (2005) Peptide sequence analysis. *Methods Enzymol* 402:209–244.
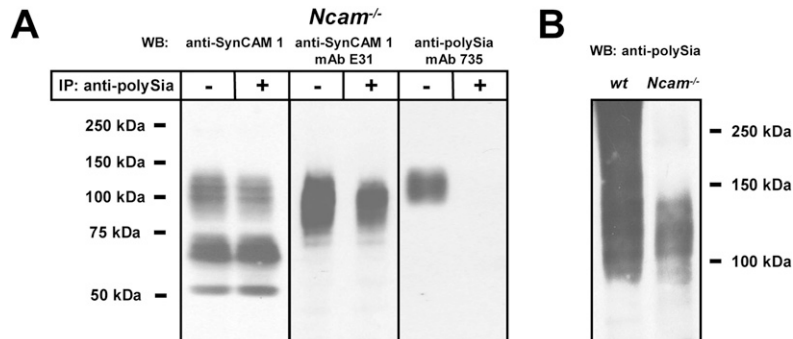
Fig. S2. Characterization of polysialylated SynCAM 1 by SDS/PAGE and Western blotting. (*A*) Determination of the proportion of polysialylated SynCAM 1 in *Ncam*$^{-/-}$ mice. Brain lysates of newborn *Ncam*$^{-/-}$ mice (40 μg protein per lane) were analyzed before or after removal of polysialylated protein by immunoprecipitation using anti-polySia mAb 735. Resulting supernatants were subjected to SDS/PAGE and Western blotting and stained with polyclonal anti-SynCAM 1 antibody, anti-SynCAM 1 mAb 3E1, or anti-polySia mAb 735. Polysialylated protein is completely removed by preceding immunoprecipitation (*Right*), whereas the majority of SynCAM 1 in the mass range of approximately 100 kDa as well as cross-reacting SynCAM 2 and SynCAM 3 (50–75 kDa) are still retained (*Left* and *Middle*; see also Fig. S6). (*B*) Characterization of polysialylated proteins in WT mouse brains by SDS/PAGE and Western blotting. Brain homogenates of WT and *Ncam*$^{-/-}$ mice were separated by 10% SDS/PAGE using 40 μg protein per lane and immunostained with anti-polySia mAb 735. Applying this high protein concentration, the polySia-positive signal of WT brain lysates was further dispersed, covering not only the high molecular mass region of polySia-NCAM at approximately 250 kDa but also the migration range of polySia-SynCAM 1 at approximately 110 kDa. Apparent molecular masses of standard proteins are indicated in kDa.
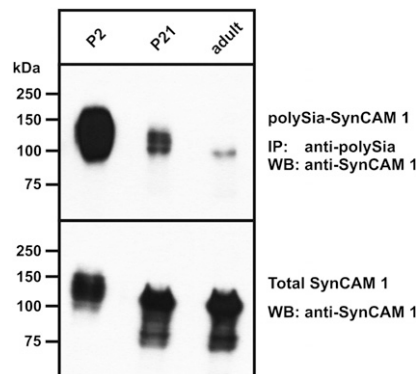
Fig. S3. Developmental changes in the polysialylation status of SynCAM 1. Whole brains of *Ncam*$^{-/-}$ mice were obtained at postnatal d 2, d 21, and from adult stage. PolySia-SynCAM 1 expression was analyzed in brain lysates by immunoprecipitation with anti-polySia mAb 735 followed by Western blot detection with anti-SynCAM 1 mAb 3E1 (*Upper*). Total SynCAM 1 expression was analyzed by separating equal amounts of whole brain lysate by 10% SDS/PAGE followed by Western blotting with anti-SynCAM 1 mAb 3E1 (*Lower*).
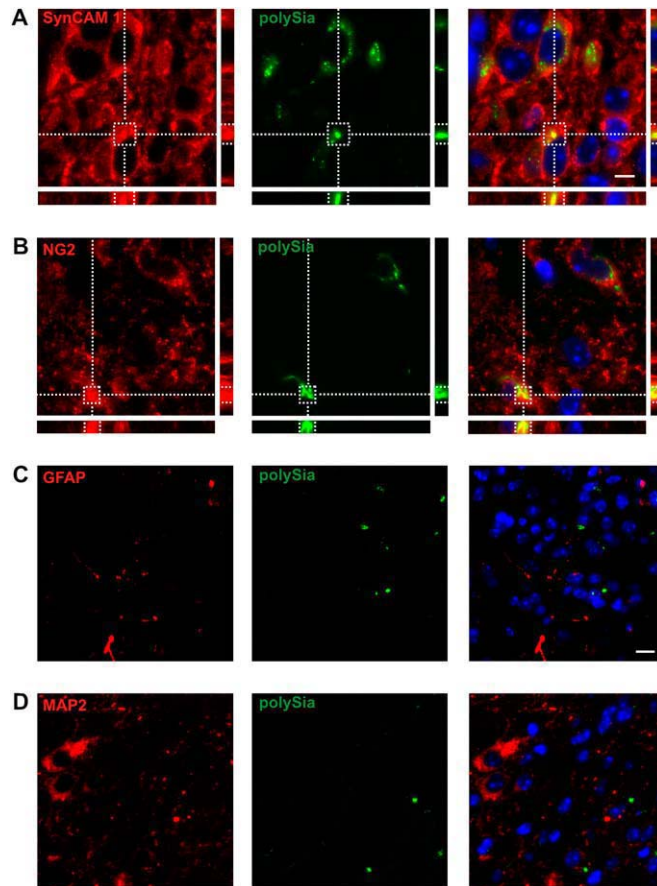
Fig. S4. Immunofluorescence localization of polySia in mouse brain sections of the pontomedullary hindbrain of newborn *Ncam*$^{-/-}$ mice. (*A*) A 3D reconstruction of ApoTome z-stack images of brain sections stained with anti-SynCAM 1 mAb 3E1 (red) and anti-polySia mAb 735 (green). Merged images show colocalization of SynCAM 1 and polySia. (*B*) Staining with anti-NG2 antibodies (red) and anti-polySia mAb 735 (green). Merged images show colocalization of NG2 and polySia. (*C*) Staining with anti-GFAP (glial fibrillary acidic protein) antibodies (red) and anti-polySia mAb 735 (green). Merged images show no overlap. (*D*) Staining with anti-MAP2 (microtubule-associated protein 2) antibodies (red) and anti-polySia mAb 735 (green). Merged images show no overlap. In merged images, nuclei are stained blue (DAPI stain). (Scale bars: 5 μm in *A* and *B*; 10 μm in *C* and *D*.)
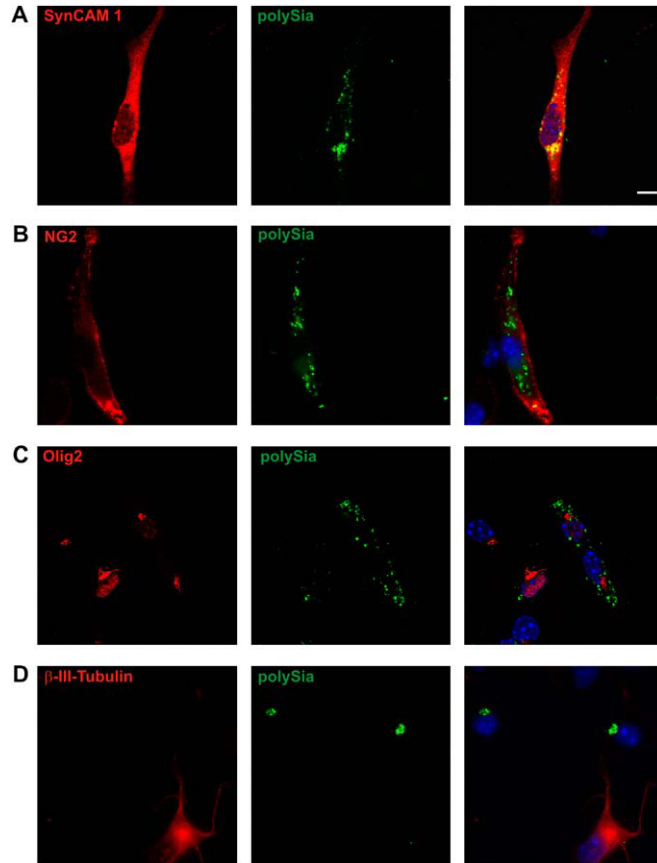
Fig. S5. Immunofluorescence localization of polySia in primary cell cultures obtained from basal hindbrain of newborn *Ncam*$^{-/-}$ mice. (*A*) Representative ApoTome image of fixed primary cells stained with anti-SynCAM 1 mAb 3E1 (red) and anti-polySia mAb 735 (green). Merged images show colocalization of SynCAM 1 and polySia. (*B*) Staining with anti-NG2 antibodies (red) and anti-polySia mAb 735 (green). Merged images show that polySia is expressed by NG2-positive cells. (*C*) Staining with anti-Olig2 antibodies (red) and anti-polySia mAb 735 (green). Merged images show that polySia is expressed by Olig2-positive cells. (*D*) Staining with anti–β-III-tubulin antibodies (red) and anti-polySia mAb 735 (green). Merged images show no overlap. In merged images, nuclei are stained blue (DAPI stain). (Scale bar: 10 μm.)
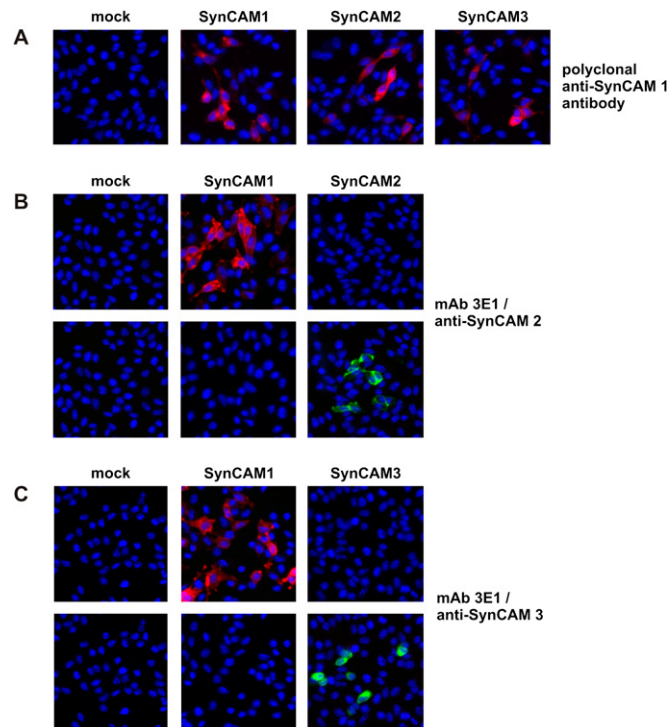
Fig. S6. Specificity of anti-SynCAM antibodies. The mouse fibroblast cell line LMTK⁻ was transiently transfected with full length cDNA of SynCAM 1, SynCAM 2, SynCAM 3, or empty vector (mock). (*A*) Fixed cells were stained with a polyclonal antibody directed against the C terminus of SynCAM 1. As this part shows high sequence similarity with the corresponding part in SynCAM 2 and 3, cross-reactivity with both proteins was observed. (*B* and *C*) Double immunofluorescence staining with anti-SynCAM 1 mAb 3E1 (red) directed against the extracellular part of SynCAM 1 and anti-SynCAM 2 antibody (*B*, green) or anti-SynCAM 3 antibody (*C*, green). No cross-reactivity of mAb 3E1 with SynCAM 2 or SynCAM 3 was observed.
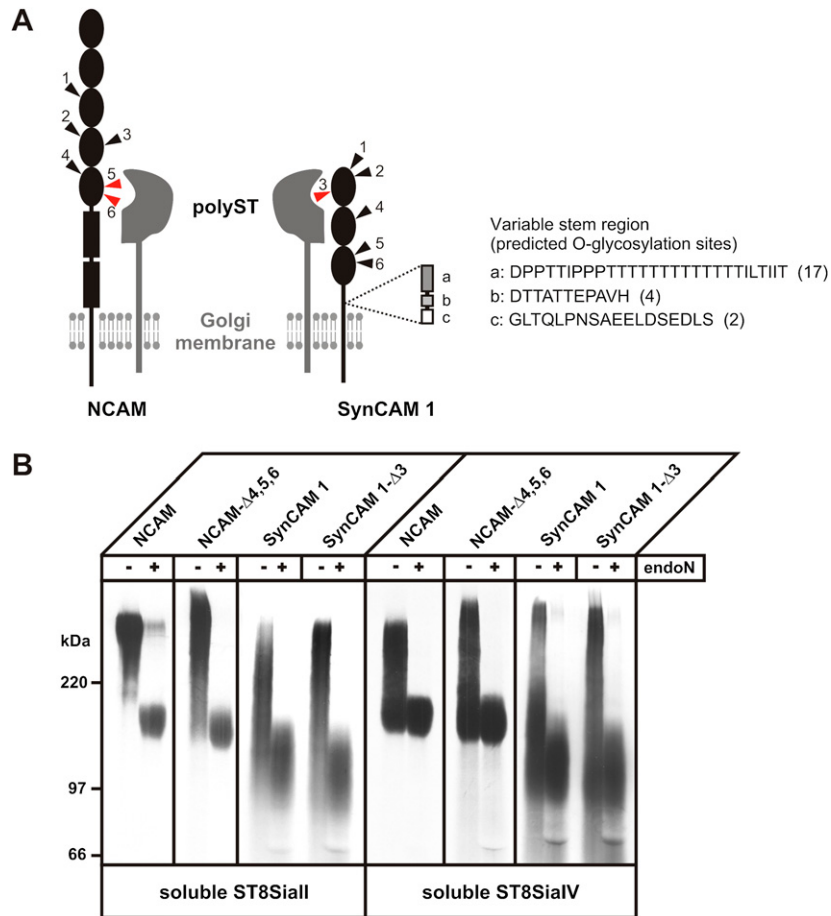
Fig. S7. (*A*) Model for site-specific polysialylation of NCAM and SynCAM 1 in vivo. Schematic representation of the polySia-acceptor proteins NCAM and SynCAM 1 in complex with a Golgi-resident polysialyltransferase (polyST). Ig-like and fibronectin type III domains are represented as black spheres and rectangles, respectively. N-glycans are indicated by triangles with those used as polySia acceptor sites highlighted in red. As a result of alternative splicing, the extracellular part of SynCAM 1 can contain a stem region. Sequences of the respective peptides are given on top with the number of predicted O-glycosylation sites (1) in parentheses. (*B*) In vitro polysialylation of WT and mutant forms of NCAM and SynCAM 1. The fourth, fifth, and sixth N-glycosylation sites of NCAM and the third N-glycosylation site of SynCAM 1 were abolished by introducing Asn-to-Gln exchanges in the respective Asn-X-Ser/Thr sequons. Soluble Protein A fusion proteins containing the extracellular part of WT or mutated forms of NCAM and SynCAM 1 were expressed in CHO-2A10 cells. After adsorption to IgG-Sepharose, acceptor proteins were incubated with soluble ST8SiaII (*Left*) or ST8SiaIV (*Right*) in the presence of CMP-[^{14}C]sialic acid. Reaction products were separated by 7% SDS/PAGE before and after treatment with endoN and analyzed by autoradiography.

1. Biederer T (2006) Bioinformatic characterization of the SynCAM family of immunoglobulin-like domain-containing adhesion molecules. *Genomics* 87:139–150.

Chapter 5 - Defects in the ST3GAL3 gene cause a loss of function in the gene product, which leads to cognitive impairment in homozygous mutation carriers.

Preface

The following study identified mutations in the ST3GalIII gene in two Iranian families affected by intellectual disability. My contribution to this study was the biochemical characterisation of the mutant enzymes. Using cell transfection experiments and enzymatic testing of recombinant proteins, I was able to show that a mutation in the transmembrane domain of ST3GalIII (A13D) interfered with proper Golgi transport of the sialyltransferase and with catalytic activity. The second mutation identified in the C-terminally localised catalytic domain of ST3GalIII (D370Y) abolished Golgi transport, leading to complete retention of the enzyme in the ER. As demonstrated by *in vitro* activity assays, this mutation drastically reduced enzymatic activity.

Chapter 5 - Defects in the ST3GAL3 gene cause a loss of function in the gene product, which leads to cognitive impairment in homozygous mutation carriers.

Abstract

Intellectual disability (ID) severely impacts affected individuals and their families and, with lifetime costs of 1-2 million US Dollar, is the most costly disease in Europe and the United States. Here, we describe for the first time the involvement of ST3GalIII in disease establishment and present a first biochemical characterization of two mutations, which were identified in patients affected by non-syndromic autosomal recessive ID (NSARID) by linkage analysis and homozygosity mapping. The mutations, which are localized in the transmembrane domain and the catalytic domain of the enzyme, respectively, caused protein instability and alterations in cellular localization. Based on the biochemical data it can be concluded that the identified genetic defects translate into reduced functionality at systemic level.

Introduction

Nature's enormous potential for the shaping of structures - most impressively documented in the plant kingdom - is made possible by the use of sugars. This group of molecular building blocks is unique in terms of permutation capacity (Varki *et al.*, 2009). While, for instance, no more than six variant tripeptides or trinucleotides can be built from the respective monomers (amino acids and nucleotides, respectively), the theoretical number of trisaccharides that can be build from three hexoses reaches beyond 9,000. Considering, in addition, that the sugar alphabet in mammals consists of 10 "characters" (Krishnamoorthy and Mahal, 2009), that oligosaccharide additions to proteins and lipids comprise as a rule more than four monosaccharides and that the informational content of glycans is impacted by the scaffold structure and environmental components, it becomes obvious that this system is inexhaustible in terms of information storage and transfer (for a recent review see Cohen and Varki, 2010). Not surprising thus, that the outermost surface, i.e. the communication front of all animal cells consists of a dense array of glycans classically named the glycocalyx (Ito, 1969; Varki, 1993). Sialic acid, a negatively charged nine-carbon sugar, plays an extraordinary role in this scenario (Angata and Varki, 2002).

Exclusively added to terminal (non-reducing end) positions in glycan chains, this sugar primes the negative charge of animal cells and can *per se* or as a component act as a binding partner or carrier of information in a vast number of contextual situations. Vital processes ranging from the steering of cellular interactions to cellular migration and subtle processes like the modulation of synaptic plasticity essentially depend on the presence of sialoglycoconjugates (Schauer, 2009).

Key enzymes in the biosynthesis of sialoglycoconjugates are the sialyltransferases (STs), a family of twenty members that, in accordance with their function in finishing surface exposed and secreted sialo-glycoconjugates, locate in late Golgi compartments. All STs are type II membrane proteins with short cytoplasmic tails and large luminal catalytic domains. All use CMP-activated sialic acid (CMP-Sia) as a donor sugar, but the enzymes differ significantly with respect to their products (sialoglycoconjugates) formed. Decisive in this latter function are the nature of the sugar acceptor (galactose, N-acetyl-galactoseamine, or sialic acid) and the type of the glycosidic linkage that is formed (α2,3; α2,6, α2,8) (for a review see Harduin-Lepers *et al.*, 2001; Breton *et al.*, 2006). Based on these functional characteristics STs have been classified into four subgroups (ST6Gal, ST3Gal, ST6GalNAc, and ST8Sia), each consisting of several members that diverse the chemical nature of the glycan-acceptor carrier (lipid or protein) (Datta *et al.*, 2009).

ST3Gal III, the enzyme of relevance in this study, belongs to the subfamily ST3Gal encompassing a total of six members (ST3Gal I – VI). Together with its closest relatives (ST3Gal V > ST3Gal IV > ST3Gal VI) the enzyme is involved in the biosynthesis of sialyl-Lewis[a] and sialyl-Lewis[x] epitopes, that, expressed on the surface of activated leukocytes mediate the first step in leukocyte extravasation (i.e. leukocyte rolling) into inflamed tissue. Cognate receptors for these glycotopes are E- and P-selectin expressed by the activated endothelial cells (Phillips *et al.*, 1990; Tyrrell *et al.*, 1991; Polley *et al.*, 1991). However, human ST3Gal III exhibits a strong preference for type I core structures, thus essentially catalysing the synthesis of the sialyl-Lewis[a] epitope (Kono *et al.*, 1997).

The human *ST3Gal3* gene is a complex transcriptional unit comprising fifteen exons stretched over 223 Kb. 26 alternatively spliced transcripts were identified to be generated in tissue specific patterns, of which only seven represent active enzymes. Highest isotranscript numbers with patterns different from all other tissues were observed in the neural and muscular tissues (Grahn *et al.*, 2002; Grahn *et al.*, 2004). The biological significance underlying this transcriptional complexity and the functional specialisation of human ST3Gal III, respectively, has not yet been identified.

Here we describe for the first time a role for ST3GalIII in intellectual disability. Linkage analysis and homozygosity mapping in two families with non-syndromic autosomal-recessive intellectual disability (NSARID) carried out by Prof. Dr. Andreas Kuss in the Max-Planck-Institut for Molecular Genetics, Berlin, revealed mutations in the *ST3GAL3* gene at highly conserved positions in Exon 2 (c.215C>A) and Exon 13 (c.1492G>T), respectively.

The goal of this study was to provide a biochemical characterization of these mutations to elucidate their influence on ST3GalIII function.

Materials and Mehods

Recombinant expression of ST3GalIII variants

ST3GalIII variants were expressed in CHO cells (cultured at 37°C and 5% CO2 in DMEM/Ham's F 12 (1:1) medium (Biochrom) containing 5% FCS and 1 mM sodium pyruvate) by transfection with Lipofectamin (Invitrogen) in OptiMEM (Gibco BRL). Cell culture supernatants from 9.5 cm tissue plates were coupled to IgG Fast Flow 6 Sepharose (GE Healthcare). Beads were washed with PBS and incubated at 100°C for 5 min in 25 µl Lämmli buffer containing 5% β-mercaptoethanol prior to applying the samples to 10% SDS-PAGE. Proteins were blotted onto a nitrocellulose membrane (Protran, Whatman) with 2 mA/cm^2 in 50 mM Tris buffer containing 40 mM glycin. Membranes were blocked with 2% milk powder in PBS, containing 0.02% NaN_3 at 4°C over night, incubated in 3.76 µg/ml mouse IgG (Pierce) for 1h at room temperature, washed three times with PBS and incubated with anti-mouse-AP (Dianova, 1:5,000) for 1 h at room temperature. Bands were obtained by BCIP/NBT reaction (162.5 µg/ml BCIP, 325 µg/ml NBT in 100 mM Tris HCl pH 9.5, containing 100 mM NaCl and 5 mM $MgCl_2$).

Protein A quantification assay (ELISA)

96-well round bottom titer plates were coated for 1 h at room temperature with 30 µl of 2 µg/ml mouse IgG (Pierce) per well and, after washing three times with PBS, blocked with 200 µl 1% BSA (Sigma) in PBS, again for 1 h at room temperature or over night at 4°C. After washing three times with PBS, 25 µl of successive dilutions of cell culture supernatants with 1% BSA in PBS were applied (1 h at room temperature) followed by another washing step (three times with PBS) and detection of protein A tagged proteins with 25 µl of biotinylated Fab fragments of anti protein A antibody (SPA-27, Sigma, 1:50,000) in 1% BSA in PBS (1 h at room temperature).

Plates were washed three times with PBS and incubated with 25 μl Streptavidin-horseradish peroxidase (1:20,000, Roche) in 1% BSA in PBS (1 h at room temperature) and, after another washing step, with 50 μl of 0.1 mg/ml TMB in 90 mM sodium acetate, 90 mM citric acid pH 4.9, containing 0.003% H_2O_2 and 10% DMSO, for 20 min. The TMB colour reaction was stopped by adding 25 μl of 2 N H_2SO_4. Absorption was measured at 450 nm using a PowerWave 340 ELISA reader (BioTek).

ST3GalIII activity assay

Protein A tagged N-terminal truncations of ST3GalIII representing the wild-type enzyme and the C-terminal mutant lacking the first 40 amino acids were expressed in CHO cells. The concentration of protein A tagged proteins was determined by ELISA and equal amounts of wild-type and C-terminal mutant were adsorbed to IgG Fast Flow 6 Sepharose (GE Healthcare) for 1 h at 4°C. The beads were washed twice with reaction buffer (50 mM MES pH 6.5, 10 mM $MnCl_2$) and incubated with 1 mM Gal-β1,3-GlcNac-β-para-nitrophenol (Carbosynth) and 50 μM CMP-[^{14}C]Neu5Ac (0,9 kBq) in reaction buffer for 1 h at 37°C and 400 rpm. The reaction mix was loaded onto C_{18} columns (SepPak Plus C_{18}, Waters) which were activated with 3 ml MeOH and washed with 3 ml water in advance. After loading, columns were washed three times with 3 ml water and eluted with 4.5 ml MeOH. Elutes were air-dried, resolved in 3 ml Filtersafe scintillation cocktail (Zinsser Analytic) and measured in an LS 6500 Multi-Purpose Scintillation Counter (Beckman Coulter).

Prior to starting the reaction, 1/6 of the beads were taken as separate aliquots, incubated at 100°C for 5 min in 40 μl 2x Laemmli buffer containing 5% β-mercaptoethanol and applied to 10% SDS-PAGE followed by western blot (2 mA/cm^2 in 50 mM Tris buffer containing 40 mM glycin). Membranes were blocked in Odyssey Blocking Buffer mixed 1:1 with PBS for 1 h at room temperature or over night at 4°C, incubated with 3.76 μg/ml mouse IgG (Pierce) in Odyssey Blocking Buffer/PBS (1:1), washed 5x for 5 min with PBST (0.1% Tween-20 in PBS), incubated with anti mouse-IRDye 680 (LICOR, 1:20,000 in Odyssey Blocking Buffer/PBS (1:1)) for 1 h at room temperature and washed 5x for 5 min with PBST and once with PBS.

Fluorescent bands were detected using an Odyssey Imaging System (LICOR) and quantified using the Odyssey 2.1 software.

Immunofluorescence

LMTK- mouse fibroblasts were cultured in DMEM/Ham's F-12 (1:1) medium (Biochrom) at 37°C and 5% CO_2. Cells were seeded the day before transfection at a density of 3.5×10^5 cells per well in a 6-well plate. Transfection was performed at 60-80% confluency with 1 µg of plasmid DNA and 6 µl Lipofectamine (Invitrogen) in 200 µl OptiMEM (Gibco BRL) and after 6 h of incubation transferred to normal medium containing 10% FCS. Cells were splitted 1:3 the day after transfection and seeded onto glass coverslips in medium containing 10% FCS. 48-72 h after transfection the cells were washed three times with PBS, fixated with 4% PFA (AppliChem) in PBS and stored at 4°C in PBS. For permeabilisation, the coverslips were incubated 30 min in 0.2% Triton-100 in PBS. After washing three times with PBS, cells were incubated with rabbit anti α-mannosidase II antiserum (1:8,570) as a Golgi marker, rabbit anti IRE1 polyclonal antibody (Abcam, 1:40) as an ER marker, 5 µg/ml anti myc antibody 9E10 or (2 µg/ml) anti ST3GalIII antibody, respectively, for 1 h at room temperature, washed again three times with PBS, and incubated with Cy3 conjugated sheep anti mouse IgG (whole molecule) F(ab)$_2$ fragments (Sigma, 1:2,000) and 1 µg/ml Alexa Fluor 488 donkey anti rabbit IgG (H+L) (Invitrogen Molecular Probes) or Cy3 conjugated sheep anti rabbit IgG (whole molecule) F(ab)$_2$ fragments (Sigma, 1:1,000) for 1 h at room temperature in the dark. After washing three times with PBS and once with water, coverslips were dried at 37°C, mounted in Vectashield mounting medium for fluorescence with DAPI (Vector laboratories) and analysed using an Axiovert 200M microscope (Zeiss).

Results and Discussion

The beta-galactoside alpha-2,3-sialyltransferase III (ST3GalIII) is a member of a large family of Golgi resident sialyltransferases (ST). As typical type II membrane proteins, STs consist of a short N-terminally located cytoplasmic tail, a single transmembrane domain (TMD), a stem region and a large catalytic domain (CD) facing the Golgi lumen (see Fig. 1; for review see Harduin-Lepers *et al.*, 2001). Hallmarks for the identification of vertebrate STs are four highly conserved sialylmotifs (L, large; S, small; III, motif III; VS, very small; see Fig. 1), that form parts of the active site (Datta *et al.*, 1995; Datta *et al.*, 1998; Geremia et al.1997; Kitazume-Kawaguchi *et al.*, 2001; Jeanneau et al. 2004). As displayed in Fig. 1, mutations identified in the patients leave intact the sialylmotifs but introduce sequence changes in the TMD (c.215C>A; Ala>Asp, A13D) and the C-terminal part of the CD (c.1492G>T; Asp>Tyr, D370Y).
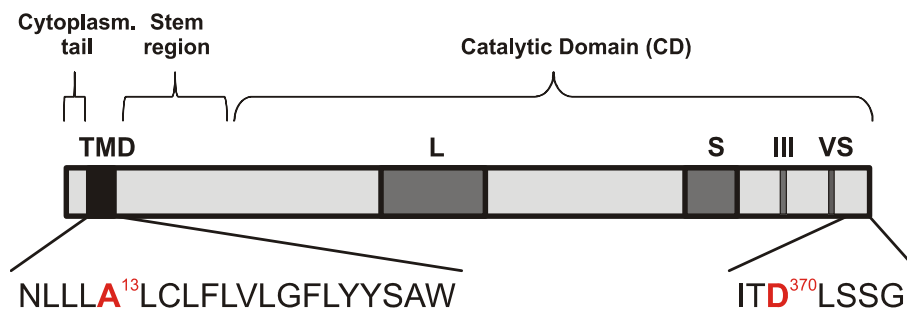
Fig. 1: Schematic representation of ST3GalIII and localization of the mutations found in NSARID patients. Sequences of the putative transmembrane domain (TMD; Kono *et al.*, 1997) and of the C-terminus are depicted in detail and mutated amino acids are coloured in red. L, S, III, VS: sialylmotifs L, S, III, VS.

To address localization of the enzymes, we used the mouse fibroblast cell line LMTK⁻, a well established cellular vessel for the reconstruction of glycosylation pathways. In a pilot experiment the cells were transfected with either ST3GalIII^{wildtype} or the mutants ST3GalIII^{A13D} and ST3GalIII^{D370Y}, and a ST3GalIII specific antibody was used to control expression and subcellular localization of recombinant proteins (Fig. 2A). The expected faint[1] Golgi-type signal could be detected in cells transfected with ST3GalIII^{wildtype}. Conversely, the signal generated by the mutant enzymes was bright and highly reminiscent to ER staining. To further explore these findings, transfection experiments were repeated with the three ST3GalIII variants carrying a myc-tag at their C-termini[2], a measure that (i) improved signal intensities also for the wildtype and (ii) enabled the parallel display of ER and Golgi markers.

---

[1] Glycosyltransferases are generally expressed at very low levels (Kleene and Berger, 1993)

[2] At the N-termini glycosyltransferases carry non-cleavable signal peptides. To not interfere with the integrity of these sequences and in order to not interfere with the instructive nature that the N-terminal parts of the proteins have for subcellular targeting, epitope tags are as a rule added to the C-terminus.
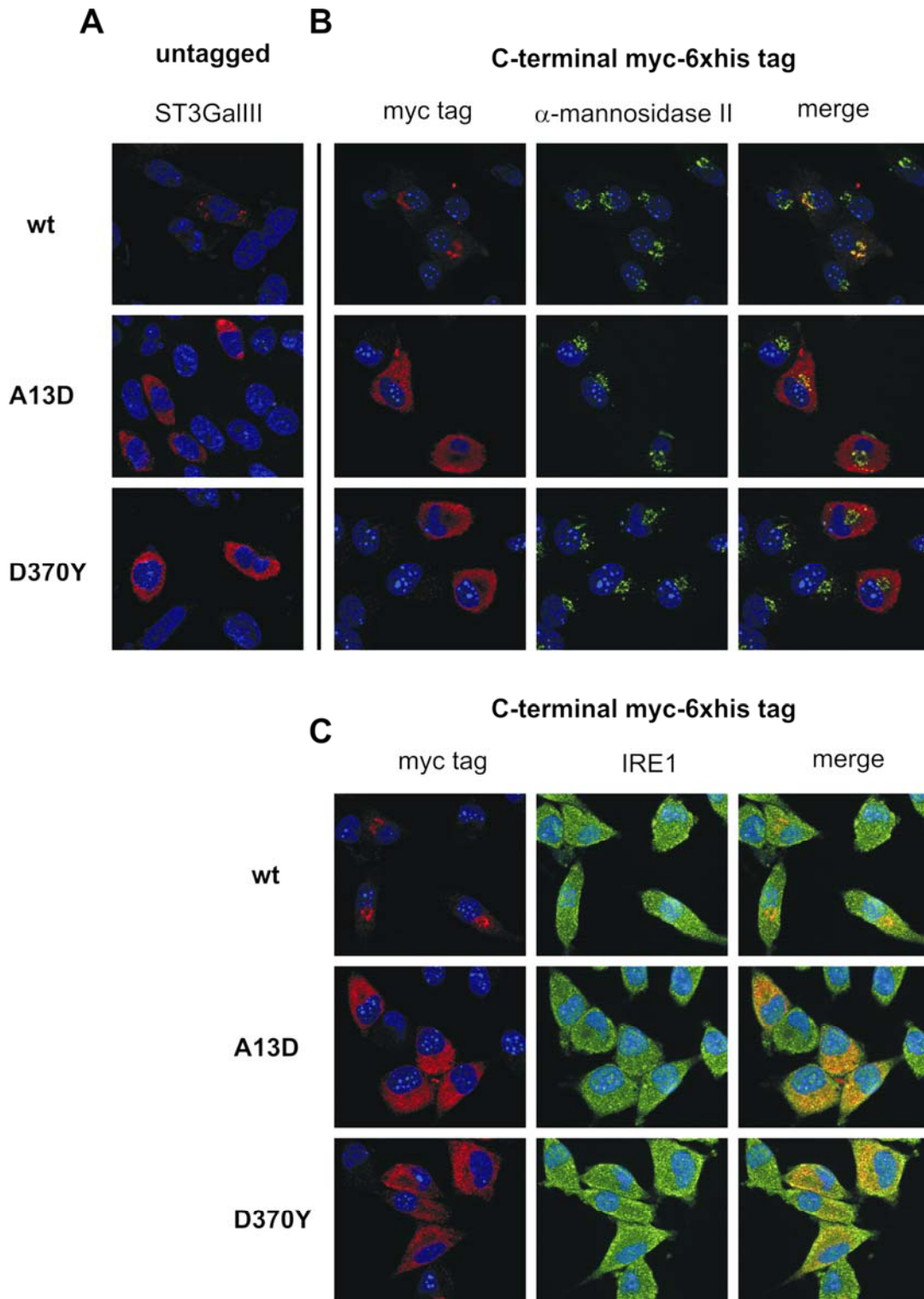
Fig. 2: Mislocalization of ST3GalIII mutants. Transiently transfected LMTK⁻ (myc-tagged constructs) or CHO cells (untagged constructs) were fixated with paraformaldehyde, permeabilised with 0.2% Triton-100 and stained with combinations of antibodies against ST3GalIII, myc tag (9E10), α-mannosidase II as a Golgi marker and IRE1 as an ER marker, as indicated. As secondary antibodies, anti mouse-Cy3 (ST3GalIII, myc-tag) and anti rabbit-Alexa 488 (α-mannosidase II, IRE1) were applied. Wildtype (wt) ST3GalIII displays a punctuate staining co-localizing with Golgi marker α-mannosidase II. A13D mutants display partial retention in the ER, while D370Y mutants exclusively localize to the ER.

Results are shown in Figs. 2A and B and confirm that both mutants are erroneously retained in the ER. Unexpectedly, the segregation from the Golgi marker α-mannosidase II was complete with the CD-mutant ST3GalIII^{D370Y}, indicating that this enzyme never reaches the Golgi apparatus. An intermediate phenotype was found for the TMD-mutant ST3GalIII^{A13D} in repeated experiments.

Because the biosynthesis of glycotopes is a consecutive process and strictly dependant on the vectorial organization of enzymes in ER and Golgi, the obtained data implies a lack of functional ST3GalIII in the patients. However, as cellular systems suited to test this assumption by assaying activity *in cellulo* were not available, an *in vitro* test system was used to compare the activity of wildtype and mutant enzymes.

Therefore, recombinant soluble enzymes were constructed by replacing 40 amino acids of the enzyme's N-terminus (including the TMD) by *Staphylococcus aureus* protein A as a solubility mediating protein (Strati *et al.*, 1983). Fusion constructs generated from wild-type and mutant enzymes were expressed in Chinese Hamster Ovary (CHO) cells, and the kinetic of appearance in the supernatant was monitored by Western blotting of IgG sepharose extracted proteins. The fusion protein produced from the wild-type enzyme (Fig. 3A, left panel) was efficiently secreted, and a maximal protein concentration was found 72 h after transfection. In contrast, the fusion protein containing the CD mutation D370Y appeared at very low level (Fig. 3A, right panel). Asking if the low secretion is due to ER-retention of the mutant protein, total cell lysates were prepared at the respective time points and additionally analysed by western blotting (Fig. 3B). No sign was obtained for an accumulation of mutant protein in the ER. Instead the slightly reduced intracellular expression seen for protA-Δ40^{D370Y} in comparison to the wild-type fusion protein argues for similar translation rates that are followed by a rapid clearance of the putatively misfolded protA-Δ40^{D370Y} protein (Ellgaard and Helenius, 2003; Hoseki *et al.*, 2010). Despite of the low expression level, the production of fusion proteins enabled the *in vitro* testing of activity. Precipitates of the fusion proteins were therefore divided to be in parallel (i) applied in the activity assay (Fig. 4A) and (ii) analysed on a western blot as a loading control (Fig. 4B). Starting with similar protein concentrations, the highly sensitive and reliable radioactive test system indicated a dramatically reduced activity for the CD-mutant enzyme protA-Δ40^{D370Y} (Fig. 4).
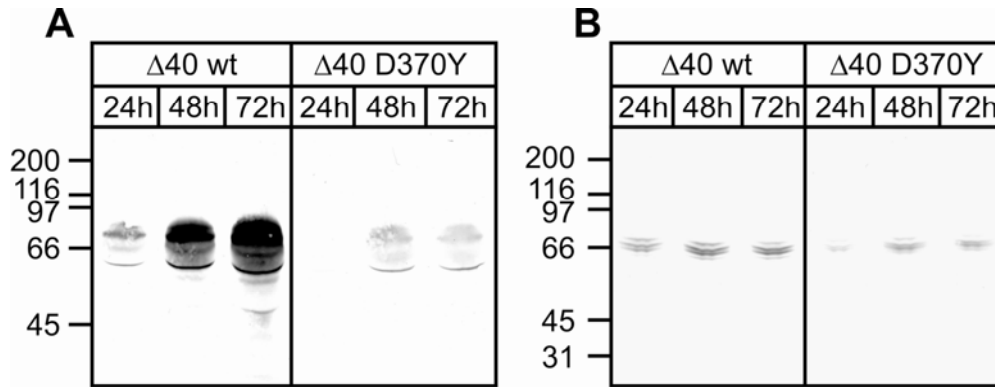
Fig. 3: Expression analysis of N-terminal Δ40 truncations of wild-type (wt) and D370Y mutant ST3GalIII. Transiently transfected CHO cells were harvested at indicated time points post transfection, and cell culture supernatants after immunoprecipitation (**A**) and cell lysates (**B**) were analysed by 10% SDS-PAGE followed by western blotting. Protein A-tagged ST3GalIII truncations were detected by mouse IgG and alkaline phosphatase conjugated anti mouse secondary antibody, followed by BCIP/NBT staining. The D370Y mutant exhibits considerably decreased expression levels as compared to the wild-type enzyme.

Fig. 4: Activity assay with soluble Δ40 truncations of wild-type and D370Y mutant ST3GalIII. **A**, Protein A-tagged ST3GalIII truncations were coupled to IgG sepharose from cell culture supernatants of transiently transfected CHO cells 72h post infection. Beads were washed with reaction buffer and incubated with radiolabelled substrate CMP-[^{14}C]Neu5Ac and acceptor Gal-β1,3-GlcNac-β-para-nitrophenol in 50 mM MES pH 6.5 and 10 mM MnCl$_2$. The acceptor structure was purified on C$_{18}$ columns and subjected to szintillation counting. Uncoupled IgG sepharose was used as a negative control (ctrl.). **B**, Aliquots of ST3GalIII coupled beads were analyzed by 10% SDS-PAGE followed by western blotting as a loading control. ST3GalIII was detected by mouse IgG and alkaline phosphatase conjugated anti mouse secondary antibody, followed by BCIP/NBT staining. At comparable amounts of employed enzyme, the D370Y mutant exhibits remarkably decreased activity.
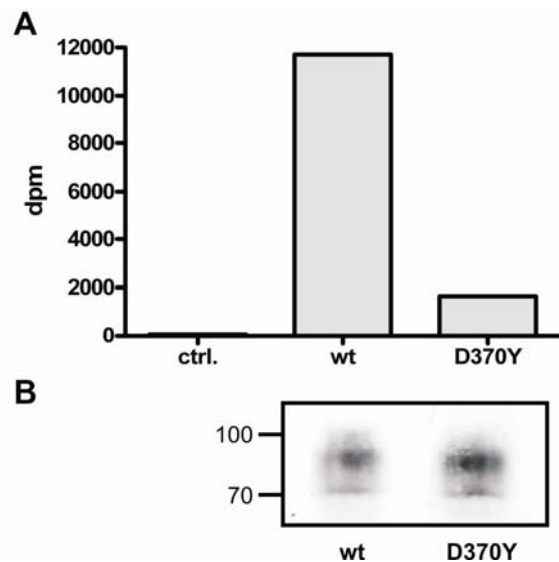
As the N-terminal mutation (A13D), affecting the transmembrane domain, escaped analysis in the above system, the activity assay was repeated with the full-length enzymes, allowing for comparative testing of both mutants after cell lysis and immunoprecipitation. In perfect agreement with the earlier data (see Fig. 4), the activity measured for mutant ST3GalIII[D370Y] is only slightly above background, whereas the mutant ST3GalIII[A13D] preserves significant activity in this *in vitro* assay system (Fig. 5A). Importantly, the amount of recombinant mutant enzymes used was comparable in repeated experiments and always significantly above the level of recombinant wildtype ST3GalIII (Fig. 5B).

The reduced activity of the TMD mutant might be caused be immature glycosylation due to ER retention. Correct N-glycosylation has earlier been shown to be crucially involved in polysialyltransferase activity (Mühlenhoff *et al.*, 2001), and since glycosylation takes place while newly synthesized proteins pass through the secretory pathway, the glycans of the partially mislocalized mutant might escape complete maturation.

The drastically reduced activity of the CD mutant further supports the idea of protein misfolding evoked by this mutation.

Fig. 5: Activity assay with full-length wild-type, A13D and D370Y ST3GalIII mutants. **A**, C-terminally myc-tagged full-length constructs of ST3GalIII wild-type and mutant enzyme were bound to 9E10 anti myc coupled IgG sepharose from cell lysates of transiently transfected CHO cells 72h post infection. Beads were washed with reaction buffer and incubated with radiolabelled substrate CMP-[^{14}C]Neu5Ac and acceptor Gal-β1,3-GlcNac-β-para-nitrophenol in 50 mM MES pH 6.5 and 10 mM MnCl$_2$. The acceptor structure was purified on C$_{18}$ columns and subjected to szintillation counting. Cell lysates from mock transfected cells was used as a negative control (mock). **B**, Aliquots of ST3GalIII coupled beads were analyzed by 10% SDS-PGE followed by western blotting as a loading control. ST3GalIII was detected by mouse IgG and alkaline phosphatase conjugated anti mouse secondary antibody, followed by BCIP/NBT staining. Although the loading control showed elevated enzyme levels for the mutants, decreased activity was observed for both A13D and D370Y.
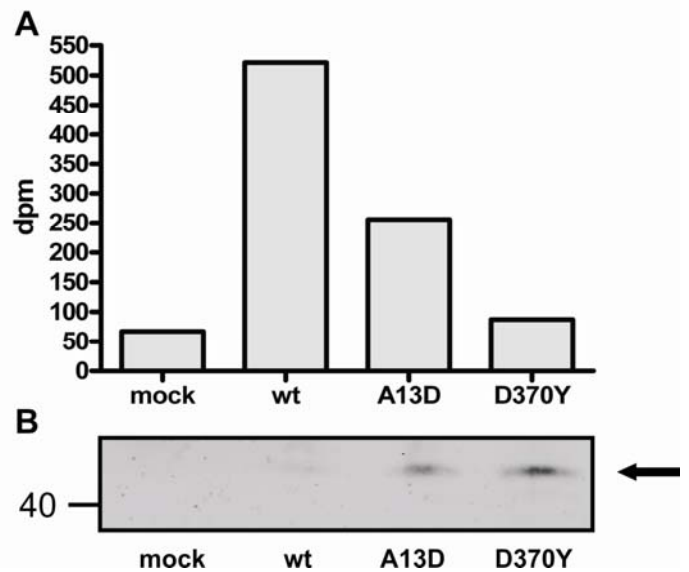
In sum, we here present for the first time a role for ST3GalIII in Intellectual Disability. The mutations identified by linkage analysis and homozygosity mapping in two families affected by NSARID were demonstrated to impact enzyme function by influencing protein stability and/or cellular localization and thus result in a loss of activity.

References

Angata, T. and Varki, A. (2002): Chemical Diversity in the Sialic Acids and Related Alpha-Keto Acids: an Evolutionary Perspective. *Chem. Rev.* **102**(2):439-69.

Breton, C., Snajdrova, L., Jeanneau, C., Koca, J., and Imberty, A. (2006b): Structures and Mechanisms of Glycosyltransferases. *Glycobiology* **16**(2):29R-37R.

Breton, C., Snajdrova, L., Jeanneau, C., Koca, J., and Imberty, A. (2006a): Structures and Mechanisms of Glycosyltransferases. *Glycobiology* **16**(2):29R-37R.

Cohen, M. and Varki, A. (2010): The Sialome--Far More Than the Sum of Its Parts. *OMICS.* **14**(4):455-64.

Datta, A.K. (2009): Comparative Sequence Analysis in the Sialyltransferase Protein Family: Analysis of Motifs. *Current Drug Targets* **10**(6):483-98.

Datta, A.K. and Paulson, J.C. (1995): The Sialyltransferase Sialylmotif Participates in Binding the Donor Substrate Cmp-Neuac. *Journal of Biological Chemistry* **270**(4):1497-500.

Datta, A.K., Sinha, A., and Paulson, J.C. (1998): Mutation of the Sialyltransferase S-Sialylmotif Alters the Kinetics of the Donor and Acceptor Substrates. *Journal of Biological Chemistry* **273**(16):9608-14.

Ellgaard, L. and Helenius, A. (2003): Quality Control in the Endoplasmic Reticulum. *Nature Reviews Molecular Cell Biology* **4**(3):181-91.

Geremia, R.A., Harduin-Lepers, A., and Delannoy, P. (1997): Identification of Two Novel Conserved Amino Acid Residues in Eukaryotic Sialyltransferases: Implications for Their Mechanism of Action. *Glycobiology* **7**(2):v-vii.

Grahn, A., Barkhordar, G.S., and Larson, G. (2002): Cloning and Sequencing of Nineteen Transcript Isoforms of the Human Alpha2,3-Sialyltransferase Gene, ST3Gal III; Its Genomic Organisation and Expression in Human Tissues. *Glycoconj. J.* **19**(3):197-210.

Grahn, A., Barkhordar, G.S., and Larson, G. (2004): Identification of Seven New Alpha2,3-Sialyltransferase III, ST3Gal III, Transcripts From Human Foetal Brain. *Glycoconj. J.* **20**(7-8):493-500.

Harduin-Lepers, A., Vallejo-Ruiz, V., Krzewinski-Recchi, M.A., Samyn-Petit, B., Julien, S., and Delannoy, P. (2001): The Human Sialyltransferase Family. *Biochimie* **83**(8):727-37.

Hoseki, J., Ushioda, R., and Nagata, K. (2010): Mechanism and Components of Endoplasmic Reticulum-Associated Degradation. *J. Biochem.* **147**(1):19-25.

Ito, S. (1969): Structure and Function of the Glycocalyx. *Fed. Proc.* **28**(1):12-25.

Jeanneau, C., Chazalet, V., Auge, C., Soumpasis, D.M., Harduin-Lepers, A., Delannoy, P., Imberty, A., and Breton, C. (2004): Structure-Function Analysis of the Human Sialyltransferase ST3Gal I - Role of N-Glycosylation and a Novel Conserved Sialylmotif. *Journal of Biological Chemistry* **279**(14):13461-8.

Kitazume-Kawaguchi, S., Kabata, S., and Arita, M. (2001): Differential Biosynthesis of Polysialic or Disialic Acid Structure by ST8Sia II and ST8Sia IV. *Journal of Biological Chemistry* **276**(19):15696-703.

Kleene, R. and Berger, E.G. (1993): The Molecular and Cell Biology of Glycosyltransferases. *Biochim. Biophys. Acta* **1154**(3-4):283-325.

Kono, M., Ohyama, Y., Lee, Y.C., Hamamoto, T., Kojima, N., and Tsuji, S. (1997): Mouse Beta-Galactoside Alpha 2,3-Sialyltransferases: Comparison of in Vitro Substrate Specificities and Tissue Specific Expression. *Glycobiology* **7**(4):469-79.

Krishnamoorthy, L. and Mahal, L.K. (2009): Glycomic Analysis: an Array of Technologies. *ACS Chem. Biol.* **4**(9):715-32.

Muhlenhoff, M., Manegold, A., Windfuhr, M., Gotza, B., and Gerardy-Schahn, R. (2001): The Impact of N-Glycosylation on the Functions of Polysialyltransferases. *J. Biol. Chem.* **276**(36):34066-73.

Phillips, M.L., Nudelman, E., Gaeta, F.C.A., Perez, M., Singhal, A.K., Hakomori, S.I., and Paulson, J.C. (1990): Elam-1 Mediates Cell-Adhesion by Recognition of A Carbohydrate Ligand, Sialyl-Lex. *Science* **250**(4984):1130-2.

Polley, M.J., Phillips, M.L., Wayner, E., Nudelman, E., Singhal, A.K., Hakomori, S., and Paulson, J.C. (1991): CD62 and Endothelial Cell-Leukocyte Adhesion Molecule 1 (ELAM-1) Recognize the Same Carbohydrate Ligand, Sialyl-Lewis x. *Proc. Natl. Acad. Sci. U. S. A* **88**(14):6224-8.

Schauer, R. (2009): Sialic Acids As Regulators of Molecular and Cellular Interactions. *Curr. Opin. Struct. Biol.* **19**(5):507-14.

Strati, I., Negut, M., and Codita, I. (1983): [Staphylococcal Protein A in Microbiology Laboratory Practice (I)]. *Rev. Ig Bacteriol. Virusol. Parazitol. Epidemiol. Pneumoftiziol. Bacteriol. Virusol. Parazitol. Epidemiol.* **28**(4):289-310.

Tyrrell, D., James, P., Rao, N., Foxall, C., Abbas, S., Dasgupta, F., Nashed, M., Hasegawa, A., Kiso, M., Asa, D., Kidd, J., and Brandley, B.K. (1991): Structural Requirements for the Carbohydrate Ligand of E-Selectin. *Proceedings of the National Academy of Sciences of the United States of America* **88**(22):10372-6.

Varki, A. (1993): Biological Roles of Oligosaccharides: All of the Theories Are Correct. *Glycobiology* **3**(2):97-130.

Varki, A., Freeze, H.H., and Manzi, A.E. (2009): Overview of Glycoconjugate Analysis. *Curr. Protoc. Protein Sci.* **Chapter 12**:Unit-8.

Chapter 6 - General Discussion

Glycosylation and in particular sialylation crucially impact cell biology, e.g. by influencing protein characteristics, cell communication, virus-host interactions and the function of the immune system (Varki, 1993; Varki and Varki, 2007). Sialylation is essential for the synthesis of gangliosides and thus plays a central role in brain development and function (Rahmann, 1995). More recently, the indispensable function of a polymeric form of sialic acid, polysialic acid (polySia) for brain development and neuronal plasticity has been demonstrated (Rutishauser, 2008; Mühlenhoff *et al.*, 2009). Important in this context is that the dietary supplementation of sialic acid in infancy improves learning and memory (Wang *et al.*, 2007).

Apart from its role in brain function, polySia was shown to be involved in cancer malignancy, being associated with a high metastatic potential and a poor prognosis (Scheidegger *et al.*, 1994; Figarella-Branger *et al.*, 1996; Tanaka *et al.*, 2000; Daniel *et al.*, 2000; Daniel *et al.*, 2001; Trouillas *et al.*, 2003; Suzuki *et al.*, 2005). This study aimed at further investigating the biochemical basis for physiological and pathological roles of sialic acid, polySia and its carriers NCAM and SynCAM 1, especially in cancer biology and brain development and function.

Production of ST8SiaII and a library of NCAM fragments for structural studies on the polysialylation reaction and NCAM homophilic binding

Polysialic acid (polySia) is a post-translational modification of the Neural Cell Adhesion Molecule (NCAM) consisting of α2,8-linked sialic acid residues with a chain length of up to 60 residues in eukaryotes and 200 in prokaryotes (Inoue *et al.*, 2000; Galuska *et al.*, 2006; Barry and Goebel, 1957; McGuire and Binkley, 1964). The bulky structure of this hydrated and negatively charged homopolymer disrupts NCAM-dependant and -independant interactions of cell surface molecules by enlarging the intercellular space (Yang *et al.*, 1994; Fujimoto *et* al., 2001; Johnson *et al.*, 2005).

Thus, NCAM-polySia plays an important role in brain development and cancer malignancy by influencing cell adhesion and migration as well as neuronal differentiation, neurite outgrowth and axon branching, fasciculation and pathfinding (reviewed in Mühlenhoff *et al.*, 1998; Gascon *et al.*, 2007; Rutishauser, 2008; Mühlenhoff *et al.*, 2009).

Studies using mouse models with defects in the biosynthesis of polySia revealed that the molecule acts in two ways namely by (i) evoking effects by itself and (ii) by masking its carrier protein NCAM and thus steering NCAM functions in a time and space specific manner (Weinhold *et al.*, 2005; Hildebrandt *et al.*, 2007; Hildebrandt *et al.*, 2009). An interesting new

field is thus to dissect polySia and NCAM function and to further characterise the complex process of NCAM signalling.

PolySia is synthesised by two polysialyltransferases, ST8SiaII and ST8SiaIV. Both enzymes have been characterised in detailed *in vivo* studies (Eckhardt *et al.*, 2000; Angata *et al.*, 2004; Weinhold *et al.*, 2005; Oltmann-Norden *et al.*, 2008; Galuska *et al.*, 2008; Galuska *et al.*, 2010) however, biochemical and particularly structural investigations have been hampered by the lack of recombinant enzyme. Since the enzymes depend on disulfide bond formation and correct N-glycosylation (Angata *et al.*, 2001; Mühlenhoff *et al.*, 2001), different eukaryotic expression systems were compared for the production of ST8SiaII in my diploma thesis (Eggers, 2006). This study established a baculovirus based insect cell expression system to be the most promising candidate for a robust and efficient production of the polysialytransferase. The aim of the current study was to further optimise and refine ST8SiaII production to gain material for structural studies. Further, a series of NCAM fragments were produced using the same expression system to provide material for structural studies and investigations to dissect the impact of distinct domains on NCAM function.

The test expression of different constructs of the murine ST8SiaII highlighted the general sensibility of the system and in particular the importance of correct N-glycosylation for the enzymes' expression. An N-terminal truncation lacking 56 amino acids but retaining all N-glycosylation sites proved to be the most promising candidate for the establishment of a robust expression system. The purification procedure introduced in Eggers 2006 was further optimised and this resulted in production of pure protein with yields high enough to start crystallisation trials. Conditions that allow the formation of precrystals and tiny crystals have been identified and provide an optimal basis for further structural studies.

The recombinant enzyme isolated from insect cell cultures was active for both autopolysialylation (polysialylation of the enzymes themselves; first described by Mühlenhoff *et al.*, 1996b) and the polysialylation of acceptor proteins like NCAM and SynCAM 1. Surprisingly, mST8SiaII also proved to act on insect cell derived NCAM. This was unexpected because insect cells do not generate sialylated complex N-glycan core structures, which were found to be required for polySia transfer onto NCAM in an earlier study (Mühlenhoff *et al.*, 1996a). In contrast to this, autopolysialylation can be performed on asialoglycans, but is dependant on terminal galactosylation (Mühlenhoff *et al.*, 1996b). However, both glycan structures are expected to be absent or only present in small amounts on insect cell produced proteins. Although unexpected acitivity was observed, only a small portion of the insect cell derived NCAM was found to be polysialylated when compared to the

mammalian cell derived NCAM. This small polysialylated NCAM fraction therefore provides an ideal starting material for further detailed analysis of requirements for glycan core structures to act as acceptors for polysialylation.

The fact that only very few proteins can act as polySia carriers leads to the assumption that the polysialylation reaction relies on specific recognition of target molecules by the polySTs. In fact, co-immunoprecipitation of NCAM with ST8SiaIV has been described by Colley and colleagues (Colley, 2010). Trials undertaken in the current study to observe this protein interaction for ST8SiaII and NCAM by analytical ultracentrifugation (AUC) were not successful. To exclude an impact of the altered glycosylation in insect cells, the experiment should be repeated with mammalian cell derived proteins. Further, the experiment needs to be repeated with ST8SiaIV, as this was the polyST detected in complex with NCAM by Colley and colleagues (Colley, 2010). Finally it has to be considered, that the soluble constructs used in the AUC experiment miss the N-terminal domains of the polyST (cytoplasmic tail, TMD, and parts of the stem region) and C-terminal domains in NCAM (cytoplasmic domain and TMD), respectively. These protein domains may me important in mediating and stabilising protein-protein contacts.

To allow for further characterisation of distinct parts of the NCAM molecule, a series of human NCAM fragments was generated using the same expression and purification system as for ST8SiaII. The purified proteins were used for the above mentioned experiments addressing complex formation with ST8SiaII, for diverse crystallisation trials, for studies concerning NCAM oligomerisation and to further clarify NCAM signalling events. A crystal obtained from the NCAM Ig1-FNII preparation emerged to consist of a contamination derived from the insect cell medium instead of NCAM protein. The fact that crystals of this 35 kDa protein were obtained earlier and that this easy-to-crystallise contamination is ubiquitously found in insect cell derived protein preparations highlights the urge for an efficient method to eliminate this contamination.

The abnormal migration behaviour of NCAM Ig1-FN2 in size-exclusion chromatography (SEC) triggered detailed investigations on NCAM oligomerisation. Using AUC, the NCAM ectodomain was shown to dimerise in solution. Truncating the protein by Ig1 and Ig2 strongly diminished the interaction, while further deletion of FN2 completely abolished dimerisation.

In sum, we successfully established a robust expression system for active ST8SiaII and a library of NCAM fragments, allowing for further characterisation of the impact of distinct domains on NCAM function.

The Influence of polySia-NCAM on regulation of focal adhesions and cell migration

PolySia is well-known to promote cancer malignancy by increasing tumour invasion and metastatic potential (Scheidegger *et al.*, 1994; Figarella-Branger *et al.*, 1996; Tanaka *et al.*, 2000; Daniel *et al.*, 2000; Daniel *et al.*, 2001; Trouillas *et al.*, 2003; Suzuki *et al.*, 2005). Although polysialylated NCAM has earlier been shown to impact cell attachment and migration processes (Sadoul *et al.*, 1983; Hoffman and Edelman, 1983; Ono *et al.*, 1994; Wang *et al.*, 1994; Hu *et al.*, 1996; Chazal *et al.*, 2000), the distinct contributions of NCAM and polySia as single affectors remain elusive.

In this study, we were able to demonstrate that polySia removal from NCAM resulted in reduced cell migration and in stimulation of focal adhesions. These effects were inhibited by the NCAM binding peptide C3d, a potent inhibitor of NCAM interactions (Ronn *et al.*, 1999; Ronn *et al.*, 2000; Kiryushko *et al.*, 2003; Kiselyov *et al.*, 2009), and were reproduced by application of soluble NCAM to NCAM negative cells. This indicates that these effects were evoked by exogenous NCAM, which in this case acted as a ligand.

The hitherto described pathways activated upon NCAM-induced signalling depend on FGF receptor stimulation or NCAM homophilic binding, which mediates signal transfer via RPTPα or the intracellular domain of NCAM-180 (reviewed in Hinsby *et al.*, 2004a and Ditlevsen *et al.*, 2008).

The stimulation of focal adhesions was shown to result in increased phosphorylation of the src-family kinase Fyn and recruitment of phosphorylated Fyn to the adaptor protein paxillin. Further, this process involved actin fibre reassembly, but was independant of FGF receptor activation, as investigated by use of the FGF receptor specific inhibitor PD173074, and of NCAM homophilic interactions in *trans*, as determined by the use of NCAM negative LS neuroblastoma cells. Furthermore, changing amounts of extracellular fibronectin did not impact cell migration and heparin-induced changes in cell migration were independant of the NCAM-mediated effect.

This suggests that a so far unknown heterophilic receptor must exist for transmittance of the signal evoked by exogenous NCAM acting as a ligand, leading to stimulation of focal adhesions.

This notion is supported by the fact that anti-proliferative and pro-differentiating effects of NCAM occur in cells of both wild-type and NCAM negative knock-out mice and thus must rely on heterophilic interactions (Amoureux *et al.*, 2000; Seidenfaden *et al.*, 2003; Röckle *et al.*, 2008). However, this is the first time for a heterophilic NCAM signalling event to be

observed, which is obviously independant from FGF receptor signalling and points towards a so far uncharacterised signalling pathway of ligand NCAM.

Using the NCAM fragments produced in chapter 1, the sites responsible for activation of the pathway influencing focal adhesions could be shown to reside in Ig3 and/or Ig4, while FGF receptor dependant phosphorylation of ERK 1/2 was stimulated by all fragments used, with the minimal fragment consisting of Ig5 and FN1. Also, the NCAM mimicking peptide FGL induced ERK 1/2 phosphorylation as described earlier, but did not impact the number of focal adhesions, further underlining the presence of distinct pathways leading to ERK 1/2 phosphorylation or stimulation of focal adhesions.

These results might be of major importance for drug design targeting cancer malignancy, since it appears to be fundamental to target polySia independantly of its carrier molecule NCAM which increases adhesiveness and reduces migration. Further, it will be important to dissect this effect from the survival promoting action of NCAM mediated by FGF receptor dependant ERK 1/2 phosphorylation, which can be made possible due to the involvement of dinstinct NCAM regions.

Identification of SynCAM 1 as a novel polySia carrier

The crucial role of polySia residing on NCAM in brain development has impressively been demonstrated by the use of various mouse models (Weinhold *et al.*, 2005; Hildebrandt *et al.*, 2007; Hildebrandt *et al.*, 2009; also see General Introduction of this thesis). However, NCAM knock-out mice display a remainder of ~5% of polySia in brain lysates as compared to wild-type (Galuska *et al.*, 2010). Applying peptide mass fingerprinting and mass spectrometric fragmentation analysis, SynCAM 1 was identified as a novel polySia carrier in NCAM positive as well as NCAM negative mice. The addition of polySia was shown to occur on the third N-glycosylation site Asn[116], which is located in the first Ig domain of SynCAM 1 and efficiently interrupts homophilic binding in bead aggregation assays (Galuska *et al.*, 2010). This finding is in accordance with the change in NCAM properties observed upon polysialylation (Yang *et al.*, 1994; Fujimoto *et* al., 2001; Johnson *et al.*, 2005).

SynCAM 1 homophilic binding and binding to SynCAM 2 is responsible for the promotion of synapse assembly of SynCAM 1 (Biederer *et al.*, 2002; Fogel *et al.*, 2007). Deletion of N-glycans on Ig1 of SynCAM 1 results in decreased homophilic binding and this effect was found to be directly translated into reduced synapse formation (Fogel *et al.*, 2010). Based on these observations we hypothesized that polySia on SynCAM 1, similar to polySia on NCAM is involved in regulating SynCAM 1 function by stereo-chemical means.

Recombinant ST8SiaII and ST8SiaIV produced in insect cells were able to polysialylate SynCAM 1 and depended on terminal sialylation, underlining similar acceptor requirements as observed for NCAM (Mühlenhoff *et al.*, 1996a). The similarities in NCAM and SynCAM 1 structure open up new possibilities for investigating the details of the polysialyltransferases' acceptor specificity, e.g. by structural comparison of their Ig domains. Interestingly, requirement for correct membrane spacing of NCAM acceptor has been demonstrated by Close *et al.* (2003) and SynCAM 1 and NCAM polysialylation sites show comparable distances to the plasma membrane.

Immunostaining of brain sections and primary culture cells revealed that polySia on SynCAM 1 localises exclusively to NG-2 glial cells. These cells represent multipotent progenitors that can give rise to oligodendrocytes, astrocytes and neurons. Interestingly, a subset of NG-2 cells form unique neuron-glia synapses, which led to the speculation that polySia might be involved in regulating the timed appearance of the synapse promoting SynCAM 1 molecule. Thus, polySia-SynCAM 1 provides another interesting example for the influence of specific sialylation on brain function.

ST3GALIII and Intellectual Disability

Intellectual disability (ID) severely impacts affected individuals and their families and, with a lifetime cost of 1-2 million US dollar, is the most costly disease in Europe and the United states. However, little public attention is focused on this disease, probably because it is often regarded in a social and educational rather than a medical view (Ropers, 2010). ID is a genetically heterogenous disorder affecting ~0.5% of the population in developed countries (de Brouwer *et al.*, 2007). The majority of patients are non-syndromic (NS), and autosomal recessive (ARID) forms are supposed to be common, yet only few genes have been identified to be involved in NSARID so far (Najmabadi *et al.*, 2007).

By linkage analysis and homozygosity mapping, the sialyltransferase ST3GalIII was identified as a novel gene affected by mutation in two Iranian families affected by NSARID. Sequence analysis revealed two non-related mutation, c.215C>A, leading to mutation of Ala[13] to Asp (A13D) in the transmembrane domain (TMD), and c.1492G>T, leading to a mutation of Asp[370] to Tyr (D370Y) close to the C-terminus of ST3GalIII. The N-terminal region of glycosyltransferases, and especially the transmembrane domain have earlier been shown to be crucial for correct enzyme localisation in the Golgi (Munro *et al.*, 1991; Nilsson *et al.*, 1991; Tang *et al.*, 1992; Wong *et al.*, 1992; Teasdale *et al.*, 1992; Graham *et al.*, 1995; Becker *et al.*,

2000; Sousa *et al.*, 2003). Thus, localisation studies were performed for wild-type and mutant enzymes using immunofluorescent labelling.

The TMD mutant A13D was indeed retained in the ER, although considerable amounts of the enzyme still reached the Golgi. In contrast and to our surprise, a complete retention of the C-terminal D370Y mutant in the ER was observed. This finding and the drastically reduced expression of the D370Y mutant as compared to the wild-type enzyme, when expressed in CHO cells as soluble proteins, supported the idea that this mutant is severely misfolded and thus not transported to the Golgi but rather degraded by the ER associated degradation (ERAD) system. This hypothesis needs to be investigated by further studies addressing ER stress and the unfolded protein response (UPR).

The mislocalisation of the A13D mutant is probably caused by changing transmembrane characteristics through the introduction of a charged residue into this otherwise hydrophobic region.

Interestingly, the length of a transmembrane domain has been correlated to its cellular localisation by the bilayer thickness theory proposed by Bretscher and Munro (1993). This theory is based on the observation that a gradient of cholesterol and sphingolipid concentrations in the membrane can be observed increasing from the ER through the Golgi apparatus to the plasma membrane, probably generating a gradient of increasing membrane thickness by influencing the degree of lipid organisation (Levine *et al.*, 1971; Orci *et al.*, 1981; van Meer, 1989; Bretscher and Munro 1993).

Supporting this, the TMD of glycosyltransferases (GT) localising to the cell surface is in general approximately 5 amino acids longer than that of Golgi localised GTs (Bretscher and Munro, 1993; Tu *et al.*, 2010) and Golgi localisation of a chimera containing the 17 amino acid spanning TMD of ST6Gal I was maintained after substitution of the TMD by 17 leucin residues. In contrast, elongation of this artificial TMD to 23 leucin residues, corresponding to the TMD of the surface localised protein DDIV, shifted the chimera to the plasma membrane (Munro, 1995b). Furthermore, TMDs of Golgi resident GTs are enriched in amino acids with aromatic side chains, especially phenylalanine, when compared to surface localised GTs (Munro, 1995a; Tu *et al.*, 2010) and the accommodation of these residues and of short TMDs is energetically disfavoured in cholesterol enriched membranes (Mouritsen and Bloom, 1993; Lundbaek *et al.*, 2003). The mutation of Ala[13] in ST3GalIII to Asp shortens the hydrophobic transmembrane domain by 4 amino acids. This might lead to a favoured localisation in the thinner and cholesterol poor ER membrane. Since this theory has so far only been applied for

the translocation of proteins from the Golgi apparatus to the plasma membrane, this would be a highly interesting first example accounting for the early part of the secretory pathway.

However, Golgi localisation has been shown to depend on the interplay of a plethora of mechanisms, e.g. on so called oligomerisation/kin interaction and retrograde transport (reviewed in Tu *et al.*, 2010) and further investigations are needed to eventually determine the cause of A13D ST3GalIII mislocalisation.

Activity assays showed that the D370Y mutant exhibited a drastically reduced sialyltransferase activity *in vitro* as a soluble protein A fusion construct as well as in a full-length variant. This effect can be explained by the severe misfolding suggested by the localisation experiments and supported by the drastically decreased expression of the soluble variant of the D370Y mutant. The A13D mutant again displayed an intermediate phenotype with reduced activity when compared to the wild-type, which yet exceeded the drastically decreased activity of the D370Y mutant.

The reduced activity of the A13D mutant might be due to incorrect glycosylation evoked by the altered localisation of the enzyme. Proteins are post-translationally glycosylated as they pass through the ER and the Golgi apparatus and glycosyltransferases display specific localisation to distinct areas of the secretory pathway according to their order of action. Thus, glycans of the mislocalised ST3GalIII A13D mutant might escape maturation.

Correct glycosylation has previously been demonstrated to be crucial for activity of the polysialyltransferases ST8SiaII and ST8SiaIV (Mühlenhoff *et al.*, 2001; Close *et al.*, 2001) and might also be pivotal for ST3GalIII function.

It remains to be elucidated, which products are formed by ST3GalIII and by which means they are required for brain function. The notion that ST3GalIII is only weakly active on glycolipids (Kono *et al.*, 1997) argues against a crucial role for gangliosides in the consequences of ST3GalIII mutation.

Sialic acid was shown by Wang *et al.* (2007) to support learning and memory when fed to newborn piglets, and the crucial role for sialylated gangliosides (Rahmann, 1995) and polySia (Mühlenhoff *et al.*, 2009; Rutishauser, 2008) regulation in brain development further supports the importance of this unusual sugar. Interestingly, also SynCAM 1 function has been shown to depend on correctly regulated sialylation (Fogel *et al.*, 2010). If ST3GalIII takes part in SynCAM 1 sialylation and thus influences its function, needs to be elucidated.

Together, these data strongly highlight the fundamental role of sialic acid in brain function and underline the urge to gain a deeper understanding of the underlying mechanism translating molecular events into a physiological context.

In sum, during the course of this study, a robust expression system for the polysialyltransferase ST8SiaII has been established, which provided material for structural and biochemical studies and was used for the characterisation of SynCAM 1 as a novel polySia carrier. Furthermore, a library of NCAM fragments was generated, enabling crystallisation trials, studies on the nature of NCAM oligomerisation and the dissection of NCAM and polySia functions in cancer biology. Using these constructs, the interaction site of NCAM leading to stimulation of focal adhesion by heterophilic signalling could be mapped to Ig3 and Ig4. Importantly, the identification of mutations in the gene coding for ST3GalIII as a cause for the establishment of intellectual disability demonstrated a pivotal role in brain development and function for this sialyltransferase.

References

Amoureux, M.C., Cunningham, B.A., Edelman, G.M., and Crossin, K.L. (2000): N-CAM Binding Inhibits the Proliferation of Hippocampal Progenitor Cells and Promotes Their Differentiation to a Neuronal Phenotype. *J. Neurosci.* **20**(10):3631-40.

Angata, K., Yen, T.Y., El Battari, A., Macher, B.A., and Fukuda, M. (2001): Unique Disulfide Bond Structures Found in ST8Sia IV Polysialyltransferase Are Required for Its Activity. *Journal of Biological Chemistry* **276**(18):15369-77.

Angata, K., Long, J.M., Bukalo, O., Lee, W., Dityatev, A., Wynshaw-Boris, A., Schachner, M., Fukuda, M., and Marth, J.D. (2004): Sialyltransferase ST8Sia-II Assembles a Subset of Polysialic Acid That Directs Hippocampal Axonal Targeting and Promotes Fear Behavior. *Journal of Biological Chemistry* **279**(31):32603-13.

Aoki, K., Ishida, N., and Kawakita, M. (2003): Substrate Recognition by Nucleotide Sugar Transporters - Further Characterization of Substrate Recognition Regions by Analyses of UDP-Galactose/CMP-Sialic Acid Transporter Chimeras and Biochemical Analysis of the Substrate Specificity of Parental and Chimeric Transporters. *Journal of Biological Chemistry* **278**(25):22887-93.

Atkins, A.R., Osborne, M.J., Lashuel, H.A., Edelman, G.M., Wright, P.E., Cunningham, B.A., and Dyson, H.J. (1999): Association Between the First Two Immunoglobulin-Like Domains of the Neural Cell Adhesion Molecule N-CAM. *FEBS Lett.* **451**(2):162-8.

Atkins, A.R., Chung, J., Deechongkit, S., Little, E.B., Edelman, G.M., Wright, P.E., Cunningham, B.A., and Dyson, H.J. (2001): Solution Structure of the Third Immunoglobulin Domain of the Neural Cell Adhesion Molecule N-CAM: Can Solution Studies Define the Mechanism of Homophilic Binding? *J. Mol. Biol.* **311**(1):161-72.

Audry, M., Jeanneau, C., Imberty, A., Harduin-Lepers, A., Delannoy, P., and Breton, C. (2010): Current Trends in the Structure-Activity Relationships of Sialyltransferases. *Glycobiology*

Barry, G.T. and Goebel, W.F. (1957): Colominic Acid, a Substance of Bacterial Origin Related to Sialic Acid. *Nature* **179**(4552):206.

Bazou, D., Blain, E.J., and Coakley, W.T. (2008): NCAM and PSA-NCAM Dependent Membrane Spreading and F-Actin Reorganization in Suspended Adhering Neural Cells. *Mol. Membr. Biol.* **25**(2):102-14.

Becker, C.G., Artola, A., GerardySchahn, R., Decker, T., Welzl, H., and Schachner, M. (1996): The Polysialic Acid Modification of the Neural Cell Adhesion Molecule Is Involved in Spatial Learning and Hippocampal Long-Term Potentiation. *Journal of Neuroscience Research* **45**(2):143-52.

Becker, B., Haggarty, A., Romero, P.A., Poon, T., and Herscovics, A. (2000): The Transmembrane Domain of Murine Alpha-Mannosidase IB Is a Major Determinant of Golgi Localization. *Eur. J. Cell Biol.* **79**(12):986-92.

Beggs, H.E., Soriano, P., and Maness, P.F. (1994): Ncam-Dependent Neurite Outgrowth Is Inhibited in Neurons From Fyn-Minus Mice. *Journal of Cell Biology* **127**(3):825-33.

Beggs, H.E., Baragona, S.C., Hemperly, J.J., and Maness, P.F. (1997): NCAM140 Interacts With the Focal Adhesion Kinase P125(Fak) and the SRC-Related Tyrosine Kinase P59(Fyn). *Journal of Biological Chemistry* **272**(13):8310-9.

Berg, E.L., Robinson, M.K., Mansson, O., Butcher, E.C., and Magnani, J.L. (1991): A Carbohydrate Domain Common to Both Sialyl Le(a) and Sialyl Le(X) Is Recognized by the Endothelial Cell Leukocyte Adhesion Molecule ELAM-1. *J. Biol. Chem.* **266**(23):14869-72.

Berridge, M.J. (1993): Inositol Trisphosphate and Calcium Signaling. *Nature* **361**(6410):315-25.

Biederer, T., Sara, Y., Mozhayeva, M., Atasoy, D., Liu, X.R., Kavalali, E.T., and Sudhof, T.C. (2002): SynCAM, a Synaptic Adhesion Molecule That Drives Synapse Assembly. *Science* **297**(5586):1525-31.

Biederer, T. (2006): Bioinformatic Characterization of the SynCAM Family of Immunoglobulin-Like Domain-Containing Adhesion Molecules. *Genomics* **87**(1):139-50.

Bodrikov, V., Leshchyns'ka, I., Sytnyk, V., Overvoorde, J., den Hertog, J., and Schachner, M. (2005): RPTP Alpha Is Essential for NCAM-Mediated P59(Fyn) Activation and Neurite Elongation. *Journal of Cell Biology* **168**(1):127-39.

Bretscher, M.S. and Munro, S. (1993): Cholesterol and the Golgi-Apparatus. *Science* **261**(5126):1280-1.

Bukalo, O., Fentrop, N., Lee, A.Y.W., Salmen, B., Law, J.W.S., Wotjak, C.T., Schweizer, M., Dityatev, A., and Schachner, M. (2004): Conditional Ablation of the Neural Cell Adhesion Molecule Reduces Precision of Spatial Learning, Long-Term Potentiation, and Depression in the CA1 Subfield of Mouse Hippocampus. *Journal of Neuroscience* **24**(7):1565-77.

Caroni, P. (2001): Actin Cytoskeleton Regulation Through Modulation of PI(4,5)P-2 Rafts. *Embo Journal* **20**(16):4332-6.

Carvalho, A.S., Harduin-Lepers, A., Magalhaes, A., Machado, E., Mendes, N., Costa, L.T., Matthiesen, R., Almeida, R., Costa, J., and Reis, C.A. (2010): Differential Expression of Alpha-2,3-Sialyltransferases and Alpha-1,3/4-Fucosyltransferases Regulates the Levels of Sialyl Lewis a and Sialyl Lewis x in Gastrointestinal Carcinoma Cells. *International Journal of Biochemistry & Cell Biology* **42**(1):80-9.

Cavallaro, U., Niedermeyer, J., Fuxa, M., and Christofori, G. (2001): N-CAM Modulates Tumour-Cell Adhesion to Matrix by Inducing FGF-Receptor Signalling. *Nature Cell Biology* **3**(7):650-7.

Chazal, G., Durbec, P., Jankovski, A., Rougon, G., and Cremer, H. (2000): Consequences of Neural Cell Adhesion Molecule Deficiency on Cell Migration in the Rostral Migratory Stream of the Mouse. *Journal of Neuroscience* **20**(4):1446-57.

Cheresh, D.A., Leng, J., and Klemke, R.L. (1999): Regulation of Cell Contraction and Membrane Ruffling by Distinct Signals in Migratory Cells. *Journal of Cell Biology* **146**(5):1107-16.

Close, B.E., Tao, K., and Colley, K.T. (2000): Polysialyltransferase-1 Autopolysialylation Is Not Requisite for Polysialylation of Neural Cell Adhesion Molecule. *Journal of Biological Chemistry* **275**(6):4484-91.

Close, B.E., Wilkinson, J.M., Bohrer, T.J., Goodwin, C.P., Broom, L.J., and Colley, K.J. (2001): The Polysialyltransferase ST8Sia II/STX: Posttranslational Processing and Role of Autopolysialylation in the Polysialylation of Neural Cell Adhesion Molecule. *Glycobiology* **11**(11):997-1008.

Close, B.E., Mendiratta, S.S., Geiger, K.M., Broom, L.J., Ho, L.L., and Colley, K.J. (2003): The Minimal Structural Domains Required for Neural Cell Adhesion Molecule Polysialylation by PST/ST8Sia IV and STX/ST8Sia II. *Journal of Biological Chemistry* **278**(33):30796-805.

Cohen, M. and Varki, A. (2010): The Sialome--Far More Than the Sum of Its Parts. *OMICS.* **14**(4):455-64.

Cole, G.J., Loewy, A., and Glaser, L. (1986): Neuronal Cell-Cell Adhesion Depends on Interactions of N-CAM With Heparin-Like Molecules. *Nature* **320**(6061):445-7.

Colley, K.J. (2010): Structural Basis for the Polysialylation of the Neural Cell Adhesion Molecule. *Adv. Exp. Med. Biol.* **663**:111-26.

Cremer, H., Lange, R., Christoph, A., Plomann, M., Vopper, G., Roes, J., Brown, R., Baldwin, S., Kraemer, P., Scheff, S., Barthels, D., Rajewsky, K., and Wille, W. (1994): Inactivation of the N-Cam Gene in Mice Results in Size-Reduction of the Olfactory-Bulb and Deficits in Spatial-Learning. *Nature* **367**(6462):455-9.

Cremer, H., Chazal, G., Goridis, C., and Represa, A. (1997): NCAM Is Essential for Axonal Growth and Fasciculation in the Hippocampus. *Molecular and Cellular Neuroscience* **8**(5):323-35.

Cunningham, B.A., Hemperly, J.J., Murray, B.A., Prediger, E.A., Brackenbury, R., and Edelman, G.M. (1987): Neural Cell Adhesion Molecule: Structure, Immunoglobulin-Like Domains, Cell Surface Modulation, and Alternative RNA Splicing. *Science* **236**(4803):799-806.

Curreli, S., Arany, Z., Gerardy-Schahn, R., Mann, D., and Stamatos, N.M. (2007): Polysialylated Neuropilin-2 Is Expressed on the Surface of Human Dendritic Cells and Modulates Dendritic Cell-T Lymphocyte Interactions. *Journal of Biological Chemistry* **282**(42):30346-56.

Daniel, L., Trouillas, J., Renaud, W., Chevallier, P., Gouvernet, J., Rougon, G., and Figarella-Branger, D. (2000): Polysialylated-Neural Cell Adhesion Molecule Expression in Rat Pituitary Transplantable Tumors (Spontaneous Mammotropic Transplantable Tumor in Wistar-Furth Rats) Is Related to Growth Rate and Malignancy. *Cancer Research* **60**(1):80-5.

Daniel, L., Durbec, P., Gautherot, E., Rouvier, E., Rougon, G., and Figarella-Branger, D. (2001): A Nude Mice Model of Human Rhabdomyosarcoma Lung Metastases for Evaluating the Role of Polysialic Acids in the Metastatic Process. *Oncogene* **20**(8):997-1004.

Datta, A.K. and Paulson, J.C. (1995): The Sialyltransferase Sialylmotif Participates in Binding the Donor Substrate Cmp-Neuac. *Journal of Biological Chemistry* **270**(4):1497-500.

Datta, A.K., Sinha, A., and Paulson, J.C. (1998): Mutation of the Sialyltransferase S-Sialylmotif Alters the Kinetics of the Donor and Acceptor Substrates. *Journal of Biological Chemistry* **273**(16):9608-14.

Datta, A.K., Chammas, R., and Paulson, J.C. (2001): Conserved Cysteines in the Sialyltransferase Sialylmotifs Form an Essential Disulfide Bond. *Journal of Biological Chemistry* **276**(18):15200-7.

de Brouwer, A.P., Yntema, H.G., Kleefstra, T., Lugtenberg, D., Oudakker, A.R., de Vries, B.B., van Bokhoven, H., Van Esch, H., Frints, S.G., Froyen, G., Fryns, J.P., Raynaud, M., Moizard, M.P., Ronce, N., Bensalem, A., Moraine, C., Poirier, K., Castelnau, L., Saillour, Y., Bienvenu, T., Beldjord, C., des, P., V, Chelly, J., Turner, G., Fullston, T., Gecz, J., Kuss, A.W., Tzschach, A., Jensen, L.R., Lenzner, S., Kalscheuer, V.M., Ropers, H.H., and Hamel, B.C. (2007): Mutation Frequencies of X-Linked Mental Retardation Genes in Families From the EuroMRX Consortium. *Hum. Mutat.* **28**(2):207-8.

Ditlevsen, D.K., Kohler, L.B., Pedersen, M.V., Risell, M., Kolkova, K., Meyer, M., Berezin, V., and Bock, E. (2003): The Role of Phosphatidylinositol 3-Kinase in Neural Cell Adhesion Molecule-Mediated Neuronal Differentiation and Survival. *Journal of Neurochemistry* **84**(3):546-56.

Ditlevsen, D.K., Kohler, L.B., Berezin, V., and Bock, E. (2007): Cyclic Guanosine Monophosphate Signalling Pathway Plays a Role in Neural Cell Adhesion Molecule-Mediated Neurite Outgrowth and Survival. *Journal of Neuroscience Research* **85**(4):703-11.

Ditlevsen, D.K., Povlsen, G.K., Berezin, V., and Bock, E. (2008): NCAM-Induced Intracellular Signaling Revisited. *Journal of Neuroscience Research* **86**(4):727-43.

Dityatev, A., Dityateva, G., Sytnyk, V., Delling, M., Toni, N., Nikonenko, I., Muller, D., and Schachner, M. (2004): Polysialylated Neural Cell Adhesion Molecule Promotes Remodeling and Formation of Hippocampal Synapses. *Journal of Neuroscience* **24**(42):9372-82.

Doherty, P., Ashton, S.V., Moore, S.E., and Walsh, F.S. (1991): Morphoregulatory Activities of Ncam and N-Cadherin Can Be Accounted for by G Protein-Dependent Activation of L-Type and N-Type Neuronal Ca2+ Channels. *Cell* **67**(1):21-33.

Eckhardt, M. and Gerardy-Schahn, R. (1997): Molecular Cloning of the Hamster CMP-Sialic Acid Transporter. *Eur. J. Biochem.* **248**(1):187-92.

Eckhardt, M., Bukalo, O., Chazal, G., Wang, L.H., Goridis, C., Schachner, M., Gerardy-Schahn, R., Cremer, H., and Dityatev, A. (2000): Mice Deficient in the Polysialyltransferase ST8SiaIV/PST-1 Allow Discrimination of the Roles of Neural Cell

Adhesion Molecule Protein and Polysialic Acid in Neural Development and Synaptic Plasticity. *Journal of Neuroscience* **20**(14):5234-44.

Eggers, K. (2006) Studien zur homogenen Darstellung und kinetischen Charakterisierung von Polysialyltransferasen. Diploma thesis. Cellular Chemistry, Hannover Medical School.

Figarella-Branger, D., Dubois, C., Chauvin, P., De Victor, B., Gentet, J.C., and Rougon, G. (1996): Correlation Between Polysialic-Neural Cell Adhesion Molecule Levels in CSF and Medulloblastoma Outcomes. *J. Clin. Oncol.* **14**(7):2066-72.

Finne, J., Finne, U., Deagostini-Bazin, H., and Goridis, C. (1983): Occurrence of Alpha 2-8 Linked Polysialosyl Units in a Neural Cell Adhesion Molecule. *Biochem. Biophys. Res. Commun.* **112**(2):482-7.

Fogel, A.I., Akins, M.R., Krupp, A.J., Stagi, M., Stein, V., and Biederer, T. (2007): SynCAMs Organize Synapses Through Heterophilic Adhesion. *Journal of Neuroscience* **27**(46):12516-30.

Fogel, A.I., Li, Y., Giza, J., Wang, Q., Lam, T.T., Modis, Y., and Biederer, T. (2010): N-Glycosylation at the SynCAM (Synaptic Cell Adhesion Molecule) Immunoglobulin Interface Modulates Synaptic Adhesion. *J. Biol. Chem.* **285**(45):34864-74.

Foley, D.A., Swartzentruber, K.G., and Colley, K.J. (2009): Identification of Sequences in the Polysialyltransferases ST8Sia II and ST8Sia IV That Are Required for the Protein-Specific Polysialylation of the Neural Cell Adhesion Molecule, NCAM. *Journal of Biological Chemistry* **284**(23):15505-16.

Foley, D.A., Swartzentruber, K.G., Lavie, A., and Colley, K.J. (2010a): Structure and Mutagenesis of Neural Cell Adhesion Molecule Domains: Evidence for Flexibility in the Placement of Polysialic Acid Attachment Sites. *J. Biol. Chem.* **285**(35):27360-71.

Foley, D.A., Swartzentruber, K.G., Thompson, M.G., Mendiratta, S.S., and Colley, K.J. (2010b): Sequences From the First Fibronectin Type III Repeat of the Neural Cell Adhesion Molecule Allow O-Glycan Polysialylation of an Adhesion Molecule Chimera. *J. Biol. Chem.* **285**(45):35056-67.

Francavilla, C., Cattaneo, P., Berezin, V., Bock, E., Ami, D., de Marco, A., Christofori, G., and Cavallaro, U. (2009): The Binding of NCAM to FGFR1 Induces a Specific Cellular Response Mediated by Receptor Trafficking. *J. Cell Biol.* **187**(7):1101-16.

Friedlander, D.R., Milev, P., Karthikeyan, L., Margolis, R.K., Margolis, R.U., and Grumet, M. (1994): The Neuronal Chondroitin Sulfate Proteoglycan Neurocan Binds to the Neural Cell Adhesion Molecules Ng-CAM/L1/NILE and N-CAM, and Inhibits Neuronal Adhesion and Neurite Outgrowth. *J. Cell Biol.* **125**(3):669-80.

Fujimoto, I., Bruses, J.L., and Rutishauser, U. (2001): Regulation of Cell Adhesion by Polysialic Acid. *Journal of Biological Chemistry* **276**(34):31745-51.

Galuska, S.P., Rollenhagen, M., Kaup, M., Eggers, K., Oltmann-Norden, I., Schiff, M., Hartmann, M., Weinhold, B., Hildebrandt, H., Geyer, R., Muhlenhoff, M., and Geyer, H. (2010): Synaptic Cell Adhesion Molecule SynCAM 1 Is a Target for Polysialylation in Postnatal Mouse Brain. *Proceedings of the National Academy of Sciences of the United States of America* **107**(22):10250-5.

Gascon, E., Vutskits, L., and Kiss, J.Z. (2007): Roles of Polysialic Acid-Neural Cell Adhesion Molecule (PSA-NCAM) in Synaptic Plasticity. *Current Organic Chemistry* **11**(7):627-35.

Georgopoulou, N. and Breen, K.C. (1999a): Overexpression of Alpha2,3 Sialyltransferase in Neuroblastoma Cells Results in an Upset in the Glycosylation Process. *Glycoconj. J.* **16**(10):649-57.

Georgopoulou, N. and Breen, K.C. (1999b): Overexpression of the Alpha 2,6 (N) Sialyltransferase Enzyme in Human and Rat Neural Cell Lines Is Associated With Increased Expression of the Polysialic Acid Epitope. *Journal of Neuroscience Research* **58**(5):641-51.

Geremia, R.A., Harduin-Lepers, A., and Delannoy, P. (1997): Identification of Two Novel Conserved Amino Acid Residues in Eukaryotic Sialyltransferases: Implications for Their Mechanism of Action. *Glycobiology* **7**(2):v-vii.

Graham, T.R. and Krasnov, V.A. (1995): Sorting of Yeast Alpha-1,3 Mannosyltransferase Is Mediated by A Lumenal Domain Interaction, and A Transmembrane Domain Signal That Can Confer Clathrin-Dependent Golgi Localization to A Secreted Protein. *Molecular Biology of the Cell* **6**(7):809-24.

Grahn, A., Barkhordar, G.S., and Larson, G. (2002): Cloning and Sequencing of Nineteen Transcript Isoforms of the Human Alpha2,3-Sialyltransferase Gene, ST3Gal III; Its Genomic Organisation and Expression in Human Tissues. *Glycoconj. J.* **19**(3):197-210.

Grahn, A., Barkhordar, G.S., and Larson, G. (2004): Identification of Seven New Alpha2,3-Sialyltransferase III, ST3Gal III, Transcripts From Human Foetal Brain. *Glycoconj. J.* **20**(7-8):493-500.

Grumet, M., Flaccus, A., and Margolis, R.U. (1993): Functional Characterization of Chondroitin Sulfate Proteoglycans of Brain: Interactions With Neurons and Neural Cell Adhesion Molecules. *J. Cell Biol.* **120**(3):815-24.

Gundersen, G.G. and Cook, T.A. (1999): Microtubules and Signal Transduction. *Current Opinion in Cell Biology* **11**(1):81-94.

Günzel, A. (2008) Vertebrate Polysialyltransferases: A study on structure-function relationships. Dissertation. Cellular Chemistry, Hannover Medical School

Hadari, Y.R., Kouhara, H., Lax, I., and Schlessinger, J. (1998): Binding of Shp2 Tyrosine Phosphatase to FRS2 Is Essential for Fibroblast Growth Factor-Induced PC12 Cell Differentiation. *Molecular and Cellular Biology* **18**(7):3966-73.

Harduin-Lepers, A., Vallejo-Ruiz, V., Krzewinski-Recchi, M.A., Samyn-Petit, B., Julien, S., and Delannoy, P. (2001): The Human Sialyltransferase Family. *Biochimie* **83**(8):727-37.

Hildebrandt, H., Muhlenhoff, M., Weinhold, B., and Gerardy-Schahn, R. (2007): Dissecting Polysialic Acid and NCAM Functions in Brain Development. *Journal of Neurochemistry* **103**:56-64.

Hildebrandt, H., Muhlenhoff, M., Oltmann-Norden, I., Rockle, I., Burkhardt, H., Weinhold, B., and Gerardy-Schahn, R. (2009): Imbalance of Neural Cell Adhesion Molecule and Polysialyltransferase Alleles Causes Defective Brain Connectivity. *Brain* **132**:2831-8.

Hildebrandt, H., Muhlenhoff, M., and Gerardy-Schahn, R. (2010): Polysialylation of NCAM. *Adv. Exp. Med. Biol.* **663**:95-109.

Hinsby, A.M., Berezin, V., and Bock, E. (2004a): Molecular Mechanisms of NCAM Function. *Frontiers in Bioscience* **9**:2227-44.

Hinsby, A.M., Lundfald, L., Ditlevsen, D.K., Korshunova, I., Juhl, L., Meakin, S.O., Berezin, V., and Bock, E. (2004b): ShcA Regulates Neurite Outgrowth Stimulated by Neural Cell Adhesion Molecule but Not by Fibroblast Growth Factor 2: Evidence for a Distinct Fibroblast Growth Factor Receptor Response to Neural Cell Adhesion Molecule Activation. *Journal of Neurochemistry* **91**(3):694-703.

Hoffman, S. and Edelman, G.M. (1983): Kinetics of Homophilic Binding by Embryonic and Adult Forms of the Neural Cell Adhesion Molecule. *Proc. Natl. Acad. Sci. U. S. A* **80**(18):5762-6.

Horstkorte, R., Schachner, M., Magyar, J.P., Vorherr, T., and Schmitz, B. (1993): The 4Th Immunoglobulin-Like Domain of Ncam Contains A Carbohydrate-Recognition Domain for Oligomannosidic Glycans Implicated in Association With L1 and Neurite Outgrowth. *Journal of Cell Biology* **121**(6):1409-21.

Hoy, J.L., Constable, J.R., Vicini, S., Fu, Z.Y., and Washbourne, P. (2009): SynCAM1 Recruits NMDA Receptors Via Protein 4.1B. *Molecular and Cellular Neuroscience* **42**(4):466-83.

Hu, H.Y., Tomasiewicz, H., Magnuson, T., and Rutishauser, U. (1996): The Role of Polysialic Acid in Migration of Olfactory Bulb Interneuron Precursors in the Subventricular Zone. *Neuron* **16**(4):735-43.

Inoue, S. and Kitajima, K. (2006): KDN (Deaminated Neuraminic Acid): Dreamful Past and Exciting Future of the Newest Member of the Sialic Acid Family. *Glycoconjugate Journal* **23**(5-6):277-90.

Iwai, K., Ishikura, H., Kaji, M., Sugiura, H., Ishizu, A., Takahashi, C., Kato, H., Tanabe, T., and Yoshiki, T. (1993): Importance of E-Selectin (ELAM-1) and Sialyl Lewis(a) in the Adhesion of Pancreatic Carcinoma Cells to Activated Endothelium. *Int. J. Cancer* **54**(6):972-7.

Jeanneau, C., Chazalet, V., Auge, C., Soumpasis, D.M., Harduin-Lepers, A., Delannoy, P., Imberty, A., and Breton, C. (2004): Structure-Function Analysis of the Human Sialyltransferase ST3Gal I - Role of N-Glycosylation and a Novel Conserved Sialylmotif. *Journal of Biological Chemistry* **279**(14):13461-8.

Jessen, U., Novitskaya, V., Pedersen, N., Serup, P., Berezin, V., and Bock, E. (2001): The Transcription Factors CREB and C-Fos Play Key Roles in NCAM-Mediated Neuritogenesis in PC12-E2 Cells. *Journal of Neurochemistry* **79**(6):1149-60.

Johnson, C.P., Fujimoto, I., Perrin-Tricaud, C., Rutishauser, U., and Leckband, D. (2004): Mechanism of Homophilic Adhesion by the Neural Cell Adhesion Molecule: Use of Multiple Domains and Flexibility. *Proceedings of the National Academy of Sciences of the United States of America* **101**(18):6963-8.

Johnson, C.P., Fujimoto, I., Rutishauser, U., and Leckband, D.E. (2005): Direct Evidence That Neural Cell Adhesion Molecule (NCAM) Polysialylation Increases Intermembrane Repulsion and Abrogates Adhesion (Vol 280, Pg 137, 2005). *Journal of Biological Chemistry* **280**(24):23424.

Kadmon, G., Kowitz, A., Altevogt, P., and Schachner, M. (1990a): Functional Cooperation Between the Neural Adhesion Molecules L1 and N-Cam Is Carbohydrate Dependent. *Journal of Cell Biology* **110**(1):209-18.

Kadmon, G., Kowitz, A., Altevogt, P., and Schachner, M. (1990b): The Neural Cell-Adhesion Molecule N-Cam Enhances L1-Dependent Cell Cell-Interactions. *Journal of Cell Biology* **110**(1):193-208.

Kasper, C., Rasmussen, H., Kastrup, J.S., Ikemizu, S., Jones, E.Y., Berezin, V., Bock, E., and Larsen, I.K. (2000): Structural Basis of Cell-Cell Adhesion by NCAM. *Nature Structural Biology* **7**(5):389-93.

Kiselyov, V.V., Berezin, V., Maar, T.E., Soroka, V., Edvardsen, K., Schousboe, A., and Bock, E. (1997): The First Immunoglobulin-Like Neural Cell Adhesion Molecule (NCAM) Domain Is Involved in Double-Reciprocal Interaction With the Second Immunoglobulin-Like NCAM Domain and in Heparin Binding. *Journal of Biological Chemistry* **272**(15):10125-34.

Kiselyov, V.V., Skladchikova, G., Hinsby, A.M., Jensen, P.H., Kulahin, N., Soroka, V., Pedersen, N., Tsetlin, V., Poulsen, F.M., Berezin, V., and Bock, E. (2003): Structural Basis for a Direct Interaction Between FGFR1 and NCAM and Evidence for a Regulatory Role of ATP. *Structure* **11**(6):691-701.

Kitagawa, H. and Paulson, J.C. (1994): Differential Expression of 5 Sialyltransferase Genes in Human Tissues. *Journal of Biological Chemistry* **269**(27):17872-8.

Kitazume-Kawaguchi, S., Kabata, S., and Arita, M. (2001): Differential Biosynthesis of Polysialic or Disialic Acid Structure by ST8Sia II and ST8Sia IV. *Journal of Biological Chemistry* **276**(19):15696-703.

Kolkova, K., Novitskaya, V., Pedersen, N., Berezin, V., and Bock, E. (2000): Neural Cell Adhesion Molecule-Stimulated Neurite Outgrowth Depends on Activation of Protein Kinase C and the Ras-Mitogen-Activated Protein Kinase Pathway. *Journal of Neuroscience* **20**(6):2238-46.

Kolkova, K., Stensman, H., Berezin, V., Bock, E., and Larsson, C. (2005): Distinct Roles of PKC Isoforms in NCAM-Mediated Neurite Outgrowth. *Journal of Neurochemistry* **92**(4):886-94.

Kono, M., Ohyama, Y., Lee, Y.C., Hamamoto, T., Kojima, N., and Tsuji, S. (1997): Mouse Beta-Galactoside Alpha 2,3-Sialyltransferases: Comparison of in Vitro Substrate Specificities and Tissue Specific Expression. *Glycobiology* **7**(4):469-79.

Korshunova, I., Novitskaya, V., Kiryushko, D., Pedersen, N., Kolkova, K., Kropotova, E., Mosevitsky, M., Rayko, M., Morrow, J.S., Ginzburg, I., Berezin, V., and Bock, E. (2007): GAP-43 Regulates NCAM-180-Mediated Neurite Outgrowth. *Journal of Neurochemistry* **100**(6):1599-612.

Kramer, E.M., Klein, C., Koch, T., Boytinck, M., and Trotter, J. (1999): Compartmentation of Fyn Kinase With Glycosylphosphatidylinositol-Anchored Molecules in Oligodendrocytes Facilitates Kinase Activation During Myelination. *Journal of Biological Chemistry* **274**(41):29042-9.

Krishnamoorthy, L. and Mahal, L.K. (2009): Glycomic Analysis: an Array of Technologies. *ACS Chem. Biol.* **4**(9):715-32.

Lehembre, F., Yilmaz, M., Wicki, A., Schomber, T., Strittmatter, K., Ziegler, D., Kren, A., Went, P., Derksen, P.W.B., Berns, A., Jonkers, J., and Christofori, G. (2008): NCAM-Induced Focal Adhesion Assembly: a Functional Switch Upon Loss of E-Cadherin. *Embo Journal* **27**(19):2603-15.

Leshchyns'ka, I., Sytnyk, V., Morrow, J.S., and Schachner, M. (2003): Neural Cell Adhesion Molecule (NCAM) Association With PKCbeta2 Via BetaI Spectrin Is Implicated in NCAM-Mediated Neurite Outgrowth. *J. Cell Biol.* **161**(3):625-39.

Levine, Y.K. and Wilkins, M.H.F. (1971): Structure of Oriented Lipid Bilayers. *Nature-New Biology* **230**(11):69-&.

Liedtke, S., Geyer, H., Wuhrer, M., Geyer, R., Frank, G., Gerardy-Schahn, R., Zahringer, U., and Schachner, M. (2001): Characterization of N-Glycans From Mouse Brain Neural Cell Adhesion Molecule. *Glycobiology* **11**(5):373-84.

Lubec, G. (1986): Interactions of N-CAM With Heparin-Like Molecules. *Nature* **323**(6090):743-4.

Lundbaek, J.A., Andersen, O.S., Werge, T., and Nielsen, C. (2003): Cholesterol-Induced Protein Sorting: An Analysis of Energetic Feasibility. *Biophysical Journal* **84**(3):2080-9.

McGuire, E.J. and Binkley, S.B. (1964): The Structure And Chemistry Of Colominic Acid. *Biochemistry* **3**:247-51.

Mendiratta, S.S., Sekulic, N., Lavie, A., and Colley, K.J. (2005): Specific Amino Acids in the First Fibronectin Type III Repeat of the Neural Cell Adhesion Molecule Play a Role in Its Recognition and Polysialylation by the Polysialyltransferase ST8Sia IV/PST. *Journal of Biological Chemistry* **280**(37):32340-8.

Mendiratta, S.S., Sekulic, N., Hernandez-Guzman, F.G., Close, B.E., Lavie, A., and Colley, K.J. (2006): A Novel Alpha-Helix in the First Fibronectin Type III Repeat of the Neural Cell Adhesion Molecule Is Critical for N-Glycan Polysialylation. *Journal of Biological Chemistry* **281**(47):36052-9.

Milev, P., Maurel, P., Haring, M., Margolis, R.K., and Margolis, R.U. (1996): TAG-1/Axonin-1 Is a High-Affinity Ligand of Neurocan, Phosphacan/Protein-Tyrosine Phosphatase-Zeta/Beta, and N-CAM. *Journal of Biological Chemistry* **271**(26):15716-23.

Mouritsen, O.G. and Bloom, M. (1993): Models of Lipid-Protein Interactions in Membranes. *Annu. Rev. Biophys. Biomol. Struct.* **22**:145-71.

Muhlenhoff, M., Eckhardt, M., Bethe, A., Frosch, M., and Gerardy-Schahn, R. (1996a): Polysialylation of NCAM by a Single Enzyme. *Curr. Biol.* **6**(9):1188-91.

Muhlenhoff, M., Eckhardt, M., Bethe, A., Frosch, M., and Gerardy-Schahn, R. (1996b): Autocatalytic Polysialylation of Polysialyltransferase-1. *EMBO J.* **15**(24):6943-50.

Muhlenhoff, M., Eckhardt, M., and Gerardy-Schahn, R. (1998): Polysialic Acid: Three-Dimensional Structure, Biosynthesis and Function. *Curr. Opin. Struct. Biol.* **8**(5):558-64.

Muhlenhoff, M., Manegold, A., Windfuhr, M., Gotza, B., and Gerardy-Schahn, R. (2001): The Impact of N-Glycosylation on the Functions of Polysialyltransferases. *J. Biol. Chem.* **276**(36):34066-73.

Muhlenhoff, M., Oltmann-Norden, I., Weinhold, B., Hildebrandt, H., and Gerardy-Schahn, R. (2009): Brain Development Needs Sugar: the Role of Polysialic Acid in Controlling NCAM Functions. *Biol. Chem.* **390**(7):567-74.

Muller, D., Wang, C., Skibo, G., Toni, N., Cremer, H., Calaora, V., Rougon, G., and Kiss, J.Z. (1996): PSA-NCAM Is Required for Activity-Induced Synaptic Plasticity. *Neuron* **17**(3):413-22.

Muller, D., Djebbara-Hannas, Z., Jourdain, P., Vutskits, L., Durbec, P., Rougon, C., and Kiss, J.Z. (2000): Brain-Derived Neurotrophic Factor Restores Long-Term Potentiation in Polysialic Acid-Neural Cell Adhesion Molecule-Deficient Hippocampus. *Proceedings of the National Academy of Sciences of the United States of America* **97**(8):4315-20.

Munro, S. (1991): Sequences Within and Adjacent to the Transmembrane Segment of Alpha-2,6-Sialyltransferase Specify Golgi Retention. *Embo Journal* **10**(12):3577-88.

Munro, S. (1995a): A Comparison of the Transmembrane Domains of Golgi and Plasma-Membrane Proteins. *Biochemical Society Transactions* **23**(3):527-30.

Munro, S. (1995b): An Investigation of the Role of Transmembrane Domains in Golgi Protein Retention. *Embo Journal* **14**(19):4695-704.

Munster-Kuhnel, A.K., Tiralongo, J., Krapp, S., Weinhold, B., Ritz-Sedlacek, V., Jacob, U., and Gerardy-Schahn, R. (2004): Structure and Function of Vertebrate CMP-Sialic Acid Synthetases. *Glycobiology* **14**(10):43R-51R.

Najmabadi, H., Motazacker, M.M., Garshasbi, M., Kahrizi, K., Tzschach, A., Chen, W., Behjati, F., Hadavi, V., Nieh, S.E., Abedini, S.S., Vazifehmand, R., Firouzabadi, S.G., Jamali, P., Falah, M., Seifati, S.M., Gruters, A., Lenzner, S., Jensen, L.R., Ruschendorf, F., Kuss, A.W., and Ropers, H.H. (2007): Homozygosity Mapping in Consanguineous Families Reveals Extreme Heterogeneity of Non-Syndromic Autosomal Recessive Mental Retardation and Identifies 8 Novel Gene Loci. *Hum. Genet.* **121**(1):43-8.

Nakata, D., Zhang, L., and Troy, F.A. (2006): Molecular Basis for Polysialylation: A Novel Polybasic Polysialyltransferase Domain (PSTD) of 32 Amino Acids Unique to the Alpha 2,8-Polysialyltransferases Is Essential for Polysialylation. *Glycoconjugate Journal* **23**(5-6):423-36.

Nelson, R.W., Bates, P.A., and Rutishauser, U. (1995): Protein Determinants for Specific Polysialylation of the Neural Cell-Adhesion Molecule. *Journal of Biological Chemistry* **270**(29):17171-9.

Niethammer, P., Delling, M., Sytnyk, V., Dityatev, A., Fukami, K., and Schachner, M. (2002): Cosignaling of NCAM Via Lipid Rafts and the FGF Receptor Is Required for Neuritogenesis. *Journal of Cell Biology* **157**(3):521-32.

Nilsson, T., Lucocq, J.M., Mackay, D., and Warren, G. (1991): The Membrane Spanning Domain of Beta-1,4-Galactosyltransferase Specifies Transgolgi Localization. *Embo Journal* **10**(12):3567-75.

Oestreicher, A.B., De Graan, P.N., Gispen, W.H., Verhaagen, J., and Schrama, L.H. (1997): B-50, the Growth Associated Protein-43: Modulation of Cell Morphology and Communication in the Nervous System. *Prog. Neurobiol.* **53**(6):627-86.

Ong, S.H., Hadari, Y.R., Gotoh, N., Guy, G.R., Schlessinger, J., and Lax, I. (2001): Stimulation of Phosphatidylinositol 3-Kinase by Fibroblast Growth Factor Receptors Is Mediated by Coordinated Recruitment of Multiple Docking Proteins. *Proceedings of the National Academy of Sciences of the United States of America* **98**(11):6074-9.

Ono, K., Tomasiewicz, H., Magnuson, T., and Rutishauser, U. (1994): N-Cam Mutation Inhibits Tangential Neuronal Migration and Is Phenocopied by Enzymatic Removal of Polysialic Acid. *Neuron* **13**(3):595-609.

Orci, L., Montesano, R., Meda, P., Malaisselagae, F., Brown, D., Perrelet, A., and Vassalli, P. (1981): Heterogeneous Distribution of Filipin-Cholesterol Complexes Across the Cisternae of the Golgi-Apparatus. *Proceedings of the National Academy of Sciences of the United States of America-Biological Sciences* **78**(1):293-7.

Paratcha, G., Ledda, F., and Ibanez, C.F. (2003): The Neural Cell Adhesion Molecule NCAM Is an Alternative Signaling Receptor for GDNF Family Ligands. *Cell* **113**(7):867-79.

Phillips, M.L., Nudelman, E., Gaeta, F.C.A., Perez, M., Singhal, A.K., Hakomori, S.I., and Paulson, J.C. (1990): Elam-1 Mediates Cell-Adhesion by Recognition of A Carbohydrate Ligand, Sialyl-Lex. *Science* **250**(4984):1130-2.

Pollerberg, G.E., Schachner, M., and Davoust, J. (1986): Differentiation State-Dependent Surface Mobilities of 2 Forms of the Neural Cell-Adhesion Molecule. *Nature* **324**(6096):462-5.

Pollerberg, G.E., Burridge, K., Krebs, K.E., Goodman, S.R., and Schachner, M. (1987): The 180-Kd Component of the Neural Cell-Adhesion Molecule N-Cam Is Involved in Cell-Cell Contacts and Cytoskeleton-Membrane Interactions. *Cell and Tissue Research* **250**(1):227-36.

Polley, M.J., Phillips, M.L., Wayner, E., Nudelman, E., Singhal, A.K., Hakomori, S., and Paulson, J.C. (1991): CD62 and Endothelial Cell-Leukocyte Adhesion Molecule 1 (ELAM-1) Recognize the Same Carbohydrate Ligand, Sialyl-Lewis x. *Proc. Natl. Acad. Sci. U. S. A* **88**(14):6224-8.

Prag, S., Lepekhin, E.A., Kolkova, K., Hartmann-Petersen, R., Kawa, A., Walmod, P.S., Belman, V., Gallagher, H.C., Berezin, V., Bock, E., and Pedersen, N. (2002): NCAM Regulates Cell Motility. *Journal of Cell Science* **115**(2):283-92.

Probstmeier, R., Fahrig, T., Spiess, E., and Schachner, M. (1992): Interactions of the Neural Cell-Adhesion Molecule and the Myelin-Associated Glycoprotein With Collagen Type-I - Involvement in Fibrillogenesis. *Journal of Cell Biology* **116**(4):1063-70.

Rahmann, H. (1995): Brain Gangliosides and Memory Formation. *Behav. Brain Res.* **66**(1-2):105-16.

Ranheim, T.S., Edelman, G.M., and Cunningham, B.A. (1996): Hemophilic Adhesion Mediated by the Neural Cell Adhesion Molecule Involves Multiple Immunoglobulin Domains. *Proceedings of the National Academy of Sciences of the United States of America* **93**(9):4071-5.

Rao, Y., Wu, X.F., Gariepy, J., Rutishauser, U., and Siu, C.H. (1992): Identification of A Peptide Sequence Involved in Homophilic Binding in the Neural Cell-Adhesion Molecule Ncam. *Molecular Biology of the Cell* **3**:A216.

Rao, Y., Wu, X.F., Yip, P., Gariepy, J., and Siu, C.H. (1993): Structural Characterization of A Homophilic Binding-Site in the Neural Cell-Adhesion Molecule. *Journal of Biological Chemistry* **268**(27):20630-8.

Rao, Y., Zhao, X.N., and Siu, C.H. (1994): Mechanism of Homophilic Binding Mediated by the Neural Cell-Adhesion Molecule Ncam - Evidence for Isologous Interaction. *Journal of Biological Chemistry* **269**(44):27540-8.

Retzler, C., Gohring, W., and Rauch, U. (1996): Analysis of Neurocan Structures Interacting With the Neural Cell Adhesion Molecule N-CAM. *J. Biol. Chem.* **271**(44):27304-10.

Rockle, I., Seidenfaden, R., Weinhold, B., Muhlenhoff, M., Gerardy-Schahn, R., and Hildebrandt, H. (2008): Polysialic Acid Controls NCAM-Induced Differentiation of Neuronal Precursors into Calretinin-Positive Olfactory Bulb Interneurons. *Developmental Neurobiology* **68**(9):1170-84.

Ronn, L.C.B., Doherty, P., Holm, A., Berezin, V., and Bock, E. (2000): Neurite Outgrowth Induced by a Synthetic Peptide Ligand of Neural Cell Adhesion Molecule Requires Fibroblast Growth Factor Receptor Activation. *Journal of Neurochemistry* **75**(2):665-71.

Ropers, H.H. (2010): Genetics of Early Onset Cognitive Impairment. *Annual Review of Genomics and Human Genetics, Vol 11* **11**:161-87.

Rozakis-Adcock, M., McGlade, J., Mbamalu, G., Pelicci, G., Daly, R., Li, W., Batzer, A., Thomas, S., Brugge, J., Pelicci, P.G., and . (1992): Association of the Shc and Grb2/Sem5 SH2-Containing Proteins Is Implicated in Activation of the Ras Pathway by Tyrosine Kinases. *Nature* **360**(6405):689-92.

Rutishauser, U., Acheson, A., Hall, A.K., Mann, D.M., and Sunshine, J. (1988): The Neural Cell-Adhesion Molecule (Ncam) As A Regulator of Cell-Cell Interactions. *Science* **240**(4848):53-7.

Rutishauser, U. (2008): Polysialic Acid in the Plasticity of the Developing and Adult Vertebrate Nervous System. *Nat. Rev. Neurosci.* **9**(1):26-35.

Sadoul, R., Hirn, M., Deagostini-Bazin, H., Rougon, G., and Goridis, C. (1983): Adult and Embryonic Mouse Neural Cell Adhesion Molecules Have Different Binding Properties. *Nature* **304**(5924):347-9.

Saffell, J.L., Williams, E.J., Mason, I.J., Walsh, F.S., and Doherty, P. (1997): Expression of a Dominant Negative FGF Receptor Inhibits Axonal Growth and FGF Receptor Phosphorylation Stimulated by CAMs. *Neuron* **18**(2):231-42.

Scheidegger, E.P., Lackie, P.M., Papay, J., and Roth, J. (1994): In Vitro and in Vivo Growth of Clonal Sublines of Human Small Cell Lung Carcinoma Is Modulated by Polysialic Acid of the Neural Cell Adhesion Molecule. *Lab Invest* **70**(1):95-106.

Schmid, R.S., Graff, R.D., Schaller, M.D., Chen, S.Z., Schachner, M., Hemperly, J.J., and Maness, P.F. (1999): NCAM Stimulates the Ras-MAPK Pathway and CREB Phosphorylation in Neuronal Cells. *Journal of Neurobiology* **38**(4):542-58.

Schmitt-Ulms, G., Legname, G., Baldwin, M.A., Ball, H.L., Bradon, N., Bosque, P.J., Crossin, K.L., Edelman, G.M., DeArmond, S.J., Cohen, F.E., and Prusiner, S.B. (2001): Binding of Neural Cell Adhesion Molecules (N-CAMs) to the Cellular Prion Protein. *J. Mol. Biol.* **314**(5):1209-25.

Seidenfaden, R., Krauter, A., Schertzinger, F., Gerardy-Schahn, R., and Hildebrandt, H. (2003): Polysialic Acid Directs Tumor Cell Growth by Controlling Heterophilic Neural Cell Adhesion Molecule Interactions. *Molecular and Cellular Biology* **23**(16):5908-18.

Seki, T. and Rutishauser, U. (1998): Removal of Polysialic Acid Neural Cell Adhesion Molecule Induces Aberrant Mossy Fiber Innervation and Ectopic Synaptogenesis in the Hippocampus. *Journal of Neuroscience* **18**(10):3757-66.

Soroka, V., Kolkova, K., Kastrup, J.S., Diederichs, K., Breed, J., Kiselyov, V.V., Poulsen, F.M., Larsen, I.K., Welte, W., Berezin, V., Bock, E., and Kasper, C. (2003): Structure and Interactions of NCAM Ig1-2-3 Suggest a Novel Zipper Mechanism for Homophilic Adhesion. *Structure.* **11**(10):1291-301.

Sousa, V.L., Brito, C., Costa, T., Lanoix, J., Nilsson, T., and Costa, J. (2003): Importance of Cys, Gln, and Tyr From the Transmembrane Domain of Human Alpha 3/4 Fucosyltransferase III for Its Localization and Sorting in the Golgi of Baby Hamster Kidney Cells. *Journal of Biological Chemistry* **278**(9):7624-9.

Stagi, M., Fogel, A.I., and Biederer, T. (2010): SynCAM 1 Participates in Axo-Dendritic Contact Assembly and Shapes Neuronal Growth Cones. *Proceedings of the National Academy of Sciences of the United States of America* **107**(16):7568-73.

Storms, S.D., Kim, A.C., Tran, B.H.T., Cole, G.J., and Murray, B.A. (1996): NCAM-Mediated Adhesion of Transfected Cells to Agrin. *Cell Adhesion and Communication* **3**(6):497-509.

Suter, D.M., Errante, L.D., Belotserkovsky, V., and Forscher, P. (1998): The Ig Superfamily Cell Adhesion Molecule, ApCAM, Mediates Growth Cone Steering by Substrate-Cytoskeletal Coupling. *Journal of Cell Biology* **141**(1):227-40.

Suter, D.M. and Forscher, P. (2000): Substrate-Cytoskeletal Coupling As a Mechanism for the Regulation of Growth Cone Motility and Guidance. *Journal of Neurobiology* **44**(2):97-113.

Suzuki, M., Suzuki, M., Nakayama, J., Suzuki, A., Angata, K., Chen, S., Sakai, K., Hagihara, K., Yamaguchi, Y., and Fukuda, M. (2005): Polysialic Acid Facilitates Tumor Invasion by Glioma Cells. *Glycobiology* **15**(9):887-94.

Takashima, S. (2008): Characterization of Mouse Sialyltransferase Genes: Their Evolution and Diversity. *Bioscience Biotechnology and Biochemistry* **72**(5):1155-67.

Tanaka, F., Otake, Y., Nakagawa, T., Kawano, Y., Miyahara, R., Li, M., Yanagihara, K., Nakayama, J., Fujimoto, I., Ikenaka, K., and Wada, H. (2000): Expression of Polysialic Acid and STX, a Human Polysialyltransferase, Is Correlated With Tumor Progression in Non-Small Cell Lung Cancer. *Cancer Res.* **60**(11):3072-80.

Tang, B.L., Wong, S.H., Low, S.H., and Hong, W.J. (1992): The Transmembrane Domain of N-Glucosaminyltransferase-I Contains A Golgi Retention Signal. *Journal of Biological Chemistry* **267**(14):10122-6.

Teasdale, R.D., Dagostaro, G., and Gleeson, P.A. (1992): The Signal for Golgi Retention of Bovine-Beta-1,4-Galactosyltransferase Is in the Transmembrane Domain. *Journal of Biological Chemistry* **267**(6):4084-96.

Thomas, L.A., Akins, M.R., and Biederer, T. (2008): Expression and Adhesion Profiles of SynCAM Molecules Indicate Distinct Neuronal Functions. *Journal of Comparative Neurology* **510**(1):47-67.

Tomasiewicz, H., Ono, K., Yee, D., Thompson, C., Goridis, C., Rutishauser, U., and Magnuson, T. (1993): Genetic Deletion of a Neural Cell Adhesion Molecule Variant (N-CAM-180) Produces Distinct Defects in the Central Nervous System. *Neuron* **11**(6):1163-74.

Traving, C. and Schauer, R. (1998): Structure, Function and Metabolism of Sialic Acids. *Cell Mol. Life Sci.* **54**(12):1330-49.

Trouillas, J., Daniel, L., Guigard, M.P., Tong, S., Gouvernet, J., Jouanneau, E., Jan, M., Perrin, G., Fischer, G., Tabarin, A., Rougon, G.V., and Figarella-Branger, D. (2003): Polysialylated Neural Cell Adhesion Molecules Expressed in Human Pituitary Tumors and Related to Extrasellar Invasion. *Journal of Neurosurgery* **98**(5):1084-93.

Tu, L.N. and Banfield, D.K. (2010): Localization of Golgi-Resident Glycosyltransferases. *Cellular and Molecular Life Sciences* **67**(1):29-41.

Tyrrell, D., James, P., Rao, N., Foxall, C., Abbas, S., Dasgupta, F., Nashed, M., Hasegawa, A., Kiso, M., Asa, D., Kidd, J., and Brandley, B.K. (1991): Structural Requirements for the Carbohydrate Ligand of E-Selectin. *Proceedings of the National Academy of Sciences of the United States of America* **88**(22):10372-6.

van Meer, G. (1989): Lipid Traffic in Animal Cells. *Annu. Rev. Cell Biol.* **5**:247-75.

von der Ohe, M., Wheeler, S.F., Wuhrer, M., Harvey, D.J., Liedtke, S., Muhlenhoff, M., Gerardy-Schahn, R., Geyer, H., Dwek, R.A., Geyer, R., Wing, D.R., and Schachner, M.

(2002): Localization and Characterization of Polysialic Acid-Containing N-Linked Glycans From Bovine NCAM. *Glycobiology* **12**(1):47-63.

Varki, A. (1993): Biological Roles of Oligosaccharides: All of the Theories Are Correct. *Glycobiology* **3**(2):97-130.

Varki, N.M. and Varki, A. (2007): Diversity in Cell Surface Sialic Acid Presentations: Implications for Biology and Disease. *Laboratory Investigation* **87**(9):851-7.

Vutskits, L., Djebbara-Hannas, Z., Zhang, H., Paccaud, J.P., Durbec, P., Rougon, G., Muller, D., and Kiss, J.Z. (2001): PSA-NCAM Modulates BDNF-Dependent Survival and Differentiation of Cortical Neurons. *European Journal of Neuroscience* **13**(7):1391-402.

Wang, C., Rougon, G., and Kiss, J.Z. (1994): Requirement of Polysialic Acid for the Migration of the O-2A Glial Progenitor-Cell From Neurohypophyseal Explants. *Journal of Neuroscience* **14**(7):4446-57.

Wang, B., Yu, B., Karim, M., Hu, H., Sun, Y., McGreevy, P., Petocz, P., Held, S., and Brand-Miller, J. (2007): Dietary Sialic Acid Supplementation Improves Learning and Memory in Piglets. *Am. J. Clin. Nutr.* **85**(2):561-9.

Weinhold, B., Seidenfaden, R., Rockle, I., Muhlenhoff, M., Schertzinger, F., Conzelmann, S., Marth, J.D., Gerardy-Schahn, R., and Hildebrandt, H. (2005): Genetic Ablation of Polysialic Acid Causes Severe Neurodevelopmental Defects Rescued by Deletion of the Neural Cell Adhesion Molecule. *J. Biol. Chem.* **280**(52):42971-7.

Wieland, J.A., Gewirth, A.A., and Leckband, D.E. (2005): Single Molecule Adhesion Measurements Reveal Two Homophilic Neural Cell Adhesion Molecule Bonds With Mechanically Distinct Properties. *Journal of Biological Chemistry* **280**(49):41037-46.

Williams, E.J., Walsh, F.S., and Doherty, P. (1994): The Production of Arachidonic-Acid Can Account for Calcium-Channel Activation in the 2Nd Messenger Pathway Underlying Neurite Outgrowth Stimulated by Ncam, N-Cadherin, and L1. *Journal of Neurochemistry* **62**(3):1231-4.

Williams, E.J., Mittal, B., Walsh, F.S., and Doherty, P. (1995): A Ca2+/Calmodulin Kinase Inhibitor, Kn-62, Inhibits Neurite Outgrowth Stimulated by Cams and Fgf. *Molecular and Cellular Neuroscience* **6**(1):69-79.

Wong, S.H., Low, S.H., and Hong, W.J. (1992): The 17-Residue Transmembrane Domain of Beta-Galactoside Alpha-2,6-Sialyltransferase Is Sufficient for Golgi Retention. *Journal of Cell Biology* **117**(2):245-58.

Yabe, U., Sato, C., Matsuda, T., and Kitajima, K. (2003): Polysialic Acid in Human Milk - CD36 Is a New Member of Mammalian Polysialic Acid-Containing Glycoprotein. *Journal of Biological Chemistry* **278**(16):13875-80.

Yang, P.F., Major, D., and Rutishauser, U. (1994): Role of Charge and Hydration in Effects of Polysialic Acid on Molecular-Interactions on and Between Cell-Membranes. *Journal of Biological Chemistry* **269**(37):23039-44.

Zhang, H., Vutskits, L., Calaora, V., Durbec, P., and Kiss, J.Z. (2004): A Role for the Polysialic Acid - Neural Cell Adhesion Molecule in PDGF-Induced Chemotaxis of Oligodendrocyte Precursor Cells. *Journal of Cell Science* **117**(1):93-103.

Zuber, C., Lackie, P.M., Catterall, W.A., and Roth, J. (1992): Polysialic Acid Is Associated With Sodium-Channels and the Neural Cell-Adhesion Molecule N-Cam in Adult-Rat Brain. *Journal of Biological Chemistry* **267**(14):9965-71.

Abbreviations

Ala	Alanine
AMPA	α-amino-3-hydroxy-5-methyl-4-isoxazole propionic acid
Asn	Asparagine
Asp	Aspartic acid
AUC	Analytical ultracentrifugation
BDNF	neurotrophic factor
CD	Catalytic domain
CMP	Cytidine 5'-monophosphate
CNS	Central nervous system
CREB	cAMP-responsive-element-binding
EDTA	Ethylen-diamine-tetraacetic acid
EMBL	European Molecular Biology Lab
ER	Endoplasmic reticulum
ERAD	ER associated degradation
ERK	Extracellular signal regulated kinase
FAK	Focal adhesion kinase
FGF	Fibroblast growth factor
FGFR	Fibroblast growth factor receptor
FN domain	Fibronectin III like domain
GDNF	glial derived neurotrophic factor
GPI	Glycosylphosphatidylinositol
GT	Glycosyltransferase
hpi	hours post infection
HSPG	Heparan sulphate proteoglycan
ID	Intellectual disability
Ig domain	Immunoglobulin like domain
Kdn	2-keto-3-deoxy-D-glycero-D-galacto-nonulosonic acid
MAP kinase	Mitogen-activated protein kinase
MEK	MAP kinase kinase
mST8SiaII	murine ST8SiaII
NCAM	Neural cell adhesion molecule
Neu5Ac	5-N-acetylneuraminic acid
Neu5Gc	5-N-glycolylneuraminic acid
NMDA	N-methyl-D-aspartate
NSARID	Non-syndromic autosomal recessive intellectual disability
ob	small olfactory bulb
OCAM	Olfactory Cell Adhesion Molecule
PAGE	Polyacrylamide gel electrophoresis
Pax	Paxillin
PBR	Polybasic region
PDGF	platelet-derived growth factor
polySia	Polysialic acid
polyST	polysialyltransferase
PSTD	Polysialyltransferase domain
RMS	rostral migratory stream
SDS	Sodium dodecylsulphate
SEC	Size-exclusion chromatography
Sia	Sialic acid
SM III	Sialylmotif III

SM L   Sialylmotif L
SM S   Sialylmotif S
SM VS   Sialylmotif VS
ST   Sialyltransferase
SVZ   subventricular zone
SynCAM   Synaptic cell adhesion molecule
TCA   Trichloroacetic acid
TMD   Transmembrane domain
Tyr   Tyrosine
UPR   Unfolded protein response
wt   Wild-type
WB   Western Blot

Curriculum vitae

Personal Data

Home address

Albertstraße 8

30451 Hannover

Germany

Dienstanschrift

Medizinische Hochschule Hannover

Abteilung Zelluläre Chemie (OE 4330)

Carl-Neuberg-Straße 1

30625 Hannover

Germany

Email address

Eggers.Katinka@mh-hannover.de

Date and place of birth

Tübingen, 21.10.1982

Nationality

German

Education

School

1989-1990: Grundschule Dalumn, Sweden

1990-1992: Grundschule Bodenteich, Germany

1992-1994: Orientierungsstufe Bodenteich, Germany

1994-2001: Herzog-Ernst-Gymnasium Uelzen, Germany

Graduation

23.6.2001 Abitur at Herzog-Ernst-Gymnasium Uelzen

University

2001-2006: Studies in biochemistry (Diplom) at Gottfried Wilhelm Leibniz Universität Hannover and Medizinische Hochschule Hannover

Diploma Thesis

Mai 2006-November 2006: „Studien zur homogenen Darstellung und kinetischen Charakterisierung von Polysialyltransferasen" in the group of Prof. Dr. Rita Gerardy-Schahn, Abteilung Zelluläre Chemie, Medizinische Hochschule Hannover

Graduation

13.12.2006, Degree: Diplom-Biochemiker

Doctorial Thesis

2007-2011

Publications

Peer Reviewed Publication

Katinka Eggers, Timo Eichner, Jürgen Wönckhaus (2005): Mass spectrometric investigation of small silicate polyhedra in solution. *International Journal of Mass Spectrometry* 244:72-75

Sebastian P. Galuska, Manuela Rollenhagen, Moritz Kaup, **Katinka Eggers**, Imke Oltmann-Norden, Miriam Schiff, Maike Hartmann, Birgit Weinhold, Herbert Hildebrand, Rudolf Geyer, Martina Mühlenhoff, Hildegard Geyer (2010): Synaptic Cell Adhesion Molecule SynCAM 1 is a target for polysialylation in postnatal mouse brain. *PNAS* 107(22): 10250-10255

Submitted Manuscript

Katinka Eggers, Andrea Krauter, Sebastian Werneburg, Miriam Schiff, Matthias Scharenberg, Hannelore Burkhardt, Martina Mühlenhoff, Herbert Hildebrandt (2010): Polysialic acid controls NCAM signals at cell-cell contacts to regulate focal adhesion independant from FGF receptor activity. *Submitted to the Journal of Cell Science*

Manuscript in Preparation

Andreas Kuß, **Katinka Eggers**, Tim Hucho, Rita Gerardy-Schahn, *et al.*[1]: Defects in the ST3GAL3 gene cause a loss of function in the gene product, which leads to cognitive impairment in homozygous mutation carriers.

Oral Presentation

Katinka Eggers, Katharina Stummeyer, Martina Mühlenhoff, Rita Gerardy-Schahn: Studies towards understanding functional complex formation between the polyialyltransferase ST8SiaII and the Neutal Cell Adhesion Molecule NCAM. 20th Joint Glycobiology Meeting, 8-10th November 2009, Cologne, Germany.

---

[1] The final list of authors is not yet defined

Poster Presentations

Almut Günzel, Monika Marx, **Katinka Eggers**, Martin Bastmeyer, Katharina Stummeyer, Rita Gerardy-Schahn: Characterisation of ST8SiaII from zebrafish. 3rd international meeting polySia, 10-13th March, Bad Lauterberg, Germany.

Katinka Eggers, Almut Günzel, Rita Gerardy-Schahn, Katharina Stummeyer: Expression and purification of the polysialyltransferase ST8SiaII. 18th Joint Glycobiology Meeting, 4-6th November 2007, Lille Lesquin, France.

Katinka Eggers, Almut Günzel, Rita Gerardy-Schahn, Katharina Stummeyer: Recombinant production of the polysialyltransferase ST8SiaII: Activity and stability. Sialoglyco, 21-26th July 2008, Moscow-St. Petersburg, Russia.

Katinka Eggers, Katharina Stummeyer, Martina Mühlenhoff, Rita Gerardy-Schahn: Studies on the structural background of NCAM homophilic interaction and polysialylation by ST8SiaII. Sialoglyco, 21-26th August 2010, Potsdam, Germany.

Danksagung

Ganz besonders möchte ich mich bei Frau Prof. Dr. Rita Gerardy-Schahn für die Möglichkeit bedanken, diese Arbeit in ihrer Arbeitsgruppe anzufertigen, sowie für die Übernahme des Referats, die gute fachliche Betreuung und für die Möglichkeit, an zahlreichen internationalen Kongressen teilzunehmen.

Desweiteren möchte ich Herrn Prof. Dr. Andreas Kuß für die Übernahme des Co-Referats und für die gute Zusammenarbeit im ST3GalIII-Projekt danken.

Mein Dank gilt weiterhin Prof. Dr. Herbert Hildebrandt für die gute Betreuung und die gute Zusammenarbeit im NCAM-Signalling-Projekt, Frau Dr. Katharina Stummeyer für die anfängliche Betreuung meiner Doktorarbeit und Frau Dr. Martina Mühlenhoff für ihre fachliche Unterstützung bei den Experimenten zur Charakterisierung der ST3GalIII.

Für die gute Zusammenarbeit im NCAM-Signalling-Projekt möchte ich mich weiterhin bei Andrea Schertzinger, Hannelore Burkhardt, Sebastian Werneburg, Miriam Schiff und Matthias Scharenberg bedanken.

Frau Dr. Ute Curth danke ich für die gute Zusammenarbeit und fachliche Unterstützung bei der Durchführung und Auswertung der analytischen Ultrazentrifugations-Experimente.

Ganz herzlich möchte ich mich auch beim gesamten Labteam, vor allem bei Jana, Benni, Myri, Ela, Iris, Dave und Frieder für die gute Arbeitsathmosphäre, viel Schokolade und Unterstützung jeglicher Art bedanken.

Ein ganz besonderer Dank gilt Myri und Michelle für ihre Freundschaft und Unterstützung und meinen Eltern für ihre verlässliche Liebe und Unterstützung.